MONA OFFSHORE WIND PROJECT

Preliminary Environmental Information Report

Volume 5, annex 3.1: Underwater sound technical report


Image of an offshore wind farm

April 2023
FINAL

Document status

Version	Purpose of document	Authored by	Reviewed by	Approved by	Review date
Rev01	Draft for Client review	Seiche Ltd	RPS		07/09/22
Rev02	Addressing client comments	Seiche Ltd	RPS		13/10/22
Rev03	Addressing client comments	Seiche Ltd	RPS		08/12/22
Rev04	Final	Seiche Ltd	RPS	bpEnBW	24/01/22

Prepared by:	Prepared for:
RPS	**Mona Offshore Wind Ltd.**

Contents

Tables

Figures

Glossary

Term	Meaning
Amplitude	The maximum displacement of a point on a wave from equilibrium.
Dose-response relationship	Describes the magnitude of the response of an organism, as a function of exposure to a stimulus or stressor after a certain exposure time.
High order	Detonation of an unexploded ordnance as a clearance method.
Impulsive sound	Sound which is broadband, very brief with a high rise time and high peak level compared to the energy averaged sound level.
Kurtosis	A measure of sharpness of the peak of a frequency-distribution curve.
Low order	Use of techniques such as deflagration to clear UXOs without resulting in a high order explosion, leading to lower sound levels.
Noise	Unwanted sound.
Non impulsive (or continuous) sound	Sound which is either continuous or intermittent but without the characteristics described above for impulsive sound.
Particle motion	Movement of particles within the water or sediment.
Permanent threshold shift	Change (deterioration) in hearing of an animal which does not recover with time.
Propagation model	Computer model to predict how sound spreads away from a source of sound.
Sine wave	A waveform that represents periodic oscillations in which the amplitude of displacement at each point is proportional to the sine of the phase angle of the displacement and that is visualized as a sine curve.
Sound	Vibration of molecules in a liquid or gas.
Sound exposure level	Metric used to measure the cumulative sound energy to which a receiver is exposed.
Sound pressure	Measure of the resultant change in pressure due to vibration of particles in a fluid or gas.
Temporary threshold shift	Change (deterioration) in hearing of an animal which recovers after some time.

Acronyms

Acronym	Description
CPT	Cone Penetration Test
DOSITS	Discovery of Sound in the Sea
EIA	Environmental Impact Assessment
GEBCO	General Bathymetric Chart of the Oceans
HF	High frequency cetaceans
LAT	Lowest Astronomical Tide
LF	Low Frequency Cetaceans
MBES	Multi-Beam Echosounder
MDS	Maximum Design Scenario
OCW	Other Carnivores in Water
OSP	Offshore substation platform
PCW	Phocid Carnivores in Water
PM	Particle Motion
PTS	Permanent Threshold Shift
RL	Received Level
RMS	Root Mean Square
SBES	Single Beam Echosounder
SBP	Sub-Bottom Profiler
SEL	Sound Exposure Level
SL	Source Level
SPL	Sound Pressure Level
SSS	Sidescan Sonar
TL	Transmission Loss
TTS	Temporary Threshold Shift
UHRS	Ultra-High Resolution Seismic
UXO	Unexploded Ordnance
VFH	Very-high Frequency Cetaceans

Units

Unit	Description
%	Percentage
hrs	Hours
kg	Kilogramms
km^2	Square kilometres
μPa	Micro Pascal (10^{-6})
$μPa^2s$	Micro pascal squared second
dB	Decibel
Hz	Hertz

Unit	Description
kgm^{-3}	Kilograms per cubic metre
m	Metre
ms	Miliseconds
ms^{-1}	Metres per second
ms^{-2}	Metres per second squared
MW	Megawatt (10^{6})
nm/s	Nano metres per second (10^{-9})
s	Second

1 UNDERWATER SOUND TECHNICAL REPORT

1.1 Introduction

1.1.1.1 This underwater sound technical report presents the results of a desktop study undertaken by Seiche Ltd. considering the potential effects of underwater sound on the marine environment from the Mona Offshore Wind Project.

1.1.1.2 The location of the Mona Offshore Wind Project in the Irish Sea is illustrated in Figure 1.1. The planned activities at this site fall into four phases: pre-construction, construction, operations and maintenance, and decommissioning. Within each of these four phases, different underwater sound sources are identified. These sound sources are both continuous and intermittent in characteristics.

1.1.1.3 Sound is readily transmitted into the underwater environment and there is potential for the sound emissions from all phases of the Mona Offshore Wind Project to adversely affect marine mammals and fish. At a close range from a sound source with high sound levels, permanent or temporary hearing damage may occur to marine species, while at a very close range gross physical trauma is possible. At far ranges the introduction of any additional sound could potentially cause short-term behavioural changes, for example to the ability of species to communicate and to determine the presence of predators, food, underwater features, and obstructions (It should be noted that it is currently unclear whether/how close range or short term impacts may translate to long term population level impacts. This is an area of active research). This report provides an overview of the potential effects due to underwater sound from the proposed survey on the surrounding marine environment.

1.1.1.4 The primary purpose of this underwater sound technical report is to predict likely distances at which the onset of potential auditory injury (i.e. Permanent Threshold Shifts (PTS) in hearing) and behavioural effects on different marine fauna may occur when exposed to the different anthropogenic sounds that occur during different phases of the Mona Offshore Wind Project. The results from this underwater sound technical report have been used to inform the following chapters of the Preliminary Environmental Information Report (PEIR) Report in order to determine the potential impact of underwater sound on marine life:

- Volume 2, chapter 8: Fish and shellfish ecology
- Volume 2, chapter 9: Marine mammals
- Volume 2, chapter 11: Commercial fisheries.

1.1.1.5 Consequently, the sensitivity of species, magnitude of potential impact and significance of effect from underwater sound associated with the Mona Offshore Wind Project are addressed within the relevant chapters.

1.1.1.6 This technical report uses peer reviewed models to calculate the impact ranges to marine mammals and fish for each phase of the Mona Offshore Wind Project: pre-construction, construction, operations and maintenance and decommissioning. Key modelled sources include:

- Clearance of unexploded ordnance (UXO)
- Geophysical and geotechnical surveys
- Impact piling
- Vessels
- Operational wind turbines.

1.2 Study area

1.2.1.1 No separate study area has been outlined for underwater sound as this is defined by the receptors and discussed within the relevant topics listed in paragraph 1.1.1.4 above.

1.2.1.2 The modelled area is approximately 760km^2 and covers the Mona Array Area and an area extending to up to 120km from the boundaries north, south, east and west (except where cut off by land). The modelled area includes the waters around the north coast of Wales and Anglesey, the northwest coast of England, the Isle of Man and extends as far as the east coast of Ireland.

1.2.1.3 Bathymetry data used within the modelling was obtained from the General Bathymetric Chart of the Oceans (GEBCO). The GEBCO 2021 Grid, is a global terrain model for ocean and land, providing elevation data, in metres, on a 15 arc-second interval grid. It showed the water depth (Lowest Astronomical Tide (LAT)) within the Mona Array Area to range between 30m and 45m deep, with typical water depths within the area being approximately 40m.

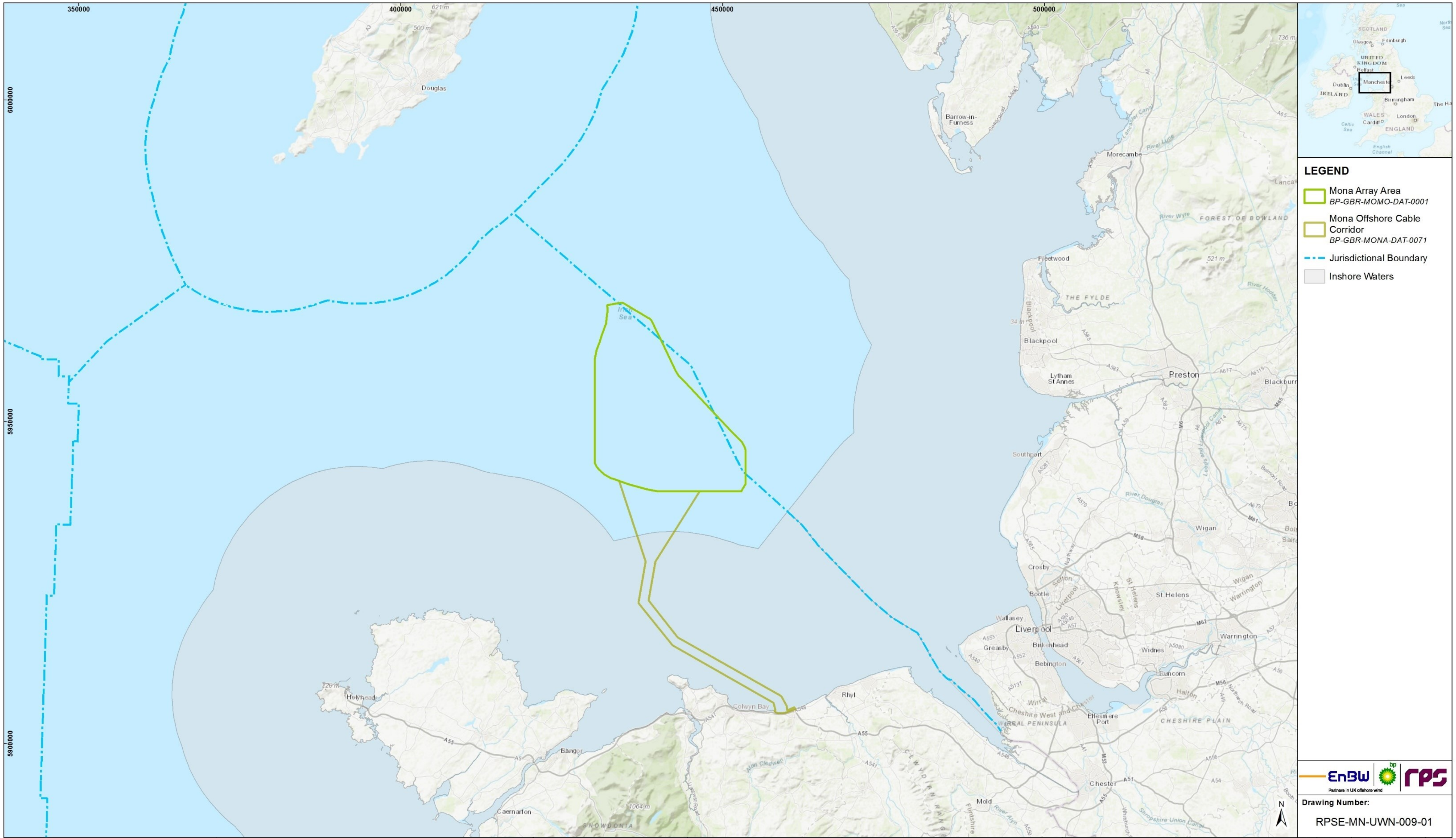

Project Name:	Drawing Title:	Scale	Geodetic Information:	Data Sources:	Service Layer Credits:
MONA OFFSHORE WIND PROJECT	LOCATION OF THE MONA OFFSHORE WIND PROJECT	0 1 2 4 6 8 10 nm; 0 2.5 5 10 15 km	Datum: ETRS 1989 Projection: ETRS 1989 UTM Zone 30N Scale@379mmx231mm: 1:600,000	Client	Sources: Esri, HERE, Garmin, Intermap, increment P Corp., GEBCO, USGS, FAO, NPS, NRCAN, GeoBase, IGN, Kadaster NL, Ordnance Survey, Esri Japan, METI, Esri China (Hong Kong), (c) OpenStreetMap contributors, and the GIS User Community

VER	DATE	DETAILS	BY	CHECK
00	11/10/22	Initial Issue	NA	ST
01	14/11/22	Revision	NA	ST

Figure 1.1: Location of the Mona Offshore Wind Project.

1.3 Consultation

1.3.1.1 A summary of the key issues raised during consultation activities undertaken to date specific to underwater sound is presented in Table 1.1 below.

Table 1.1: Summary of key consultation topics raised during consultation activities undertaken for the Mona Offshore Wind Project relevant to underwater sound.

Date	Consultee and type of response	Topics
June 2022	Mona EIA Scoping Opinion - JNCC	Fish swim speeds for exposure calculations should account for static fish, inclusion of 0m/s swim speed for all species. If there is an intent to use Acoustic Deterrent Devices, this should be included in the modelling. Agreement on representative modelling locations.
June 2022	Mona EIA Scoping Opinion - Natural England	Piling sequence as a mitigation option should be considered Is the cable laying sound representative? Is it dominated by the vessel sound? Agreement on the use of dose response to assess disturbance for marine mammals. Assessment of the impacts of operational wind turbine sounds is required. Agreement on representative modelling locations. Fish swim speeds for exposure calculations should account for static fish, inclusion of 0m/s swim speed for all species. Assessment of multiple piles installed in a 24-hour period is required.
June 2022	Mona EIA Scoping Opinion - National Resources Wales	Agreement on the choice of hearing weightings for marine mammals. Agreement on the use of dose response to assess disturbance for marine mammals. Consideration of Soft start and slow start, and whether the strike rate can be varied during these phases to reduce the impact. Need to model high order detonations of UXO. Fish swim speeds for exposure calculations should account for static fish, inclusion of 0m/s swim speed for all species.
June 2022	Mona EIA Scoping Opinion - The Planning Inspectorate	Agreement on the preferred method of UXO disposal. Consideration of the effects of particle motion on fish is necessary. Consideration of the impact on commercial fisheries. Effects of underwater sound due to jacket or monopile cutting and removal. Consideration of PTS, Temporary Threshold Shift (TTS) and disturbance ranges overlapping designated sites. Sound modelling should be undertaken for all phases of the Mona Offshore Wind Project. Consideration of concurrent piling scenarios should also be included. Fish swim speeds for exposure calculations should account for static fish, inclusion of 0m/s swim speed for all species. Consideration of the impact of geophysical surveys.
July 2022	Mona EIA Scoping Opinion - Marine Management Organisation	Consideration of impact on invertebrates. Fish swim speeds for exposure calculations should account for static fish, inclusion of 0m/s swim speed for all species. Question whether there is a requirement for multiple piling rigs and the number of piles installed per day, and how this will be assessed: will it be assumed that the animal will swim back into the area during breaks in piling? Agreement to the UXO thresholds (Sound Exposure Level (SEL) vs peak pressure).
July 2022	Evidence Plan Process Marine Mammal EWG2 – Natural England and JNCC	Agreement that auditory injury comprises Permanent Threshold Shifts (PTS), but a quantitative assessment of the Temporary Threshold Shift (TTS) impact ranges should be included. Activities associated with cable laying may also produce noise, such as trenching and rock placement. These activities should be given consideration in the underwater noise modelling. It should not be assumed that the noise from such activities will be contained within the noise from the vessels. Modelling of noise from operational wind turbines should be undertaken. Agreement on the underwater noise emissions modelling from deflagration: confirm that deflagration is the preferred method for UXO clearance, and high order should only be used as a last resort. Fish swim speeds for exposure calculations should account for static fish, inclusion of 0m/s swim speed for all species. Modelling a range of bathymetries is required.
November 2023	Evidence Plan Process Marine Mammal EWG3 – Natural England, Isle of Man government, Cefas, MMO, NRW and JNCC	Discussion on Marine Mammals and underwater sound. Due to the timing of the workshop ahead of publishing the PEIR, discussion outputs will be incorporated into the Environmental Statement.

1.4 Acoustic Concepts and Terminology

1.4.1.1 Sound travels through water as vibrations of the fluid particles in a series of pressure waves. These waves comprise a series of alternating compressions (positive pressure) and rarefactions (negative pressure). Because sound consists of variations in pressure, the unit for measuring sound is usually referenced to a unit of pressure, the Pascal (Pa). The decibel (dB) is a logarithmic ratio scale used to communicate the large range of acoustic pressures that can be perceived or detected, with a known pressure amplitude chosen as a reference value (i.e. 0dB). In the case of underwater sound, the reference value (Pref) is taken as 1µPa, whereas the airborne sound is usually referenced to a pressure of 20µPa. To convert from a sound pressure level referenced to 20µPa to one referenced to 1µPa, a factor of 20 log (20/1) i.e. 26dB has to be added to the former quantity. Thus 60dB re 20µPa is the same as 86dB re 1µPa, although differences in sound speeds and different densities mean that the decibel level difference in sound intensity is much more than the 26dB when converting pressure from air to water. All underwater sound pressure levels in this report are quantified in dB re 1µPa.

1.4.1.2 There are several descriptors used to characterise a sound wave. The difference between the lowest pressure variation (rarefaction) and the highest-pressure variation (compression) is called the peak to peak (or pk-pk) sound pressure level. The difference between the highest variation (either positive or negative) and the mean pressure is called the peak pressure level. Lastly, the Root Mean Square (rms) sound pressure level is used as a description of the average amplitude of the variations in pressure over a specific time window. Decibel values reported should always be quoted along with the P_{ref} value employed during calculations. For example, the measured Sound Pressure Level (SPL_{rms}) value of a pulse may be reported as 100dB re 1µPa. These descriptions are shown graphically in Figure 1.2.

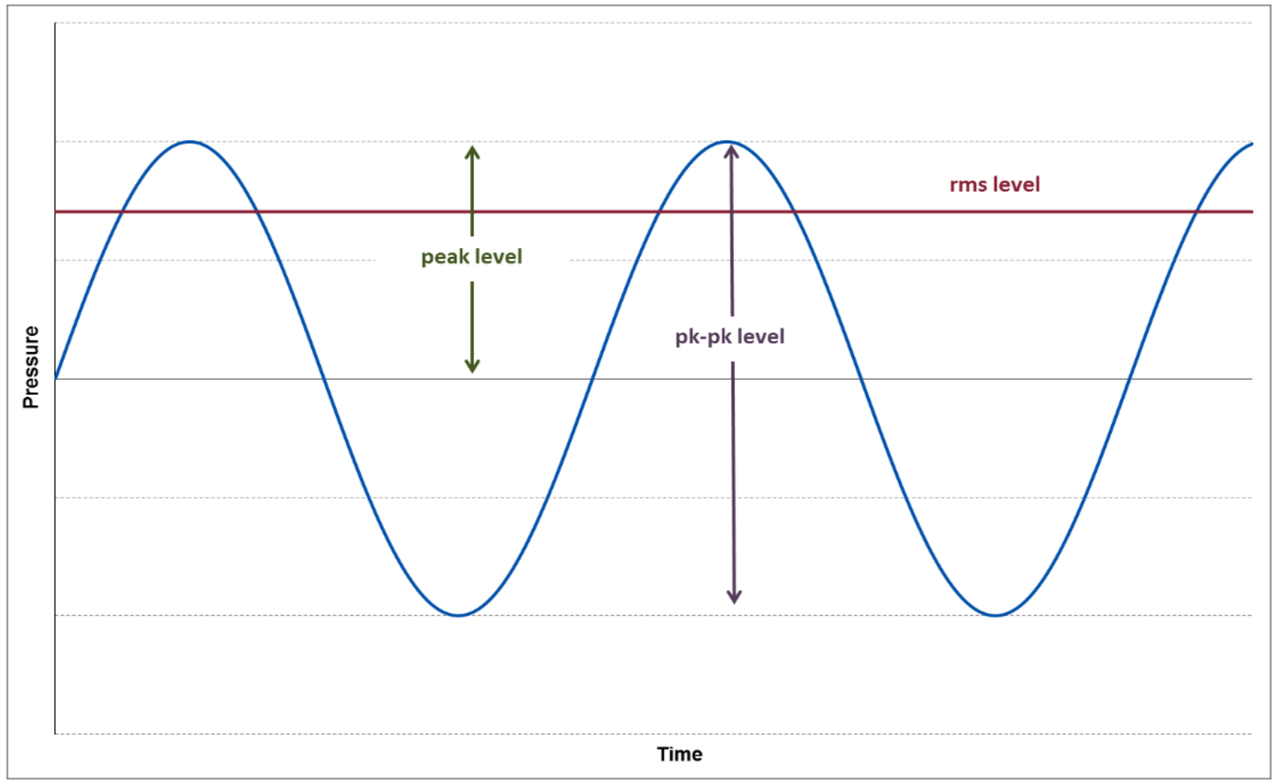

Figure 1.2: Graphical representation of acoustic wave descriptors.

1.4.1.3 The SPL_{rms} is defined as:

$$SPL_{rms} = 10log_{10}\left(\frac{1}{T}\int_{0}^{T}\left(\frac{p^2}{p_{ref}^2}\right)dt\right).$$

1.4.1.4 The magnitude of the rms sound pressure level for an impulsive sound (such as that from a seismic source array) will depend upon the integration time, T, used for the calculation (Madsen, 2005). It has become customary to utilise the T90 time period for calculating and reporting rms sound pressure levels[1]. This is the interval over which the cumulative energy curve rises from 5% to 95% of the total energy and therefore contains 90% of the sound energy.

1.4.1.5 Another useful measure of sound used in underwater acoustics is the SEL. This descriptor is used as a measure of the total sound energy of an event or a number of events (e.g. over the course of a day) and is normalised to one second. This allows the total acoustic energy contained in events lasting a different amount of time to be compared on a like for like basis[2]. The SEL is defined as:

$$SEL = 10log_{10}\left(\int_{0}^{T}\left(\frac{p^2(t)}{p_{ref}^2 t_{ref}}\right)dt\right).$$

1.4.1.6 The frequency, or pitch, of the sound is the rate at which the acoustic oscillations occur in the medium (air/ water) and is measured in cycles per second, or Hertz (Hz). When sound is measured in a way which approximates to how a human would perceive it using an A weighting- filter on a sound level meter, the resulting level is described in values of dBA. However, the hearing capability of marine species is not the same as humans, with marine mammals hearing over a wider range of frequencies and with a different sensitivity. It is therefore important to understand how an animal's hearing varies over its entire frequency range to assess the effects of anthropogenic sound on marine mammals. Consequently, use can be made of frequency weighting scales (M--weighting) to determine the level of the sound in comparison with the auditory response of the animal concerned. A comparison between the typical hearing response curves for fish, humans and marine mammals is shown in Figure 1.3[3].

1.4.1.7 **Third octave bands** - The broadband acoustic power (i.e. containing all the possible frequencies) emitted by a sound source, measured/modelled at a location within the Array Area is generally split into and reported in a series of frequency bands. In marine acoustics, the spectrum is generally reported in standard one-third octave band frequencies, where an octave represents a doubling in sound frequency[4].

1.4.1.8 **Source level (SL)** - The source level is the sound pressure level of an equivalent and infinitesimally small version of the source (known as point source) at a hypothetical distance of 1m from it. The source level is commonly used in combination with the transmission loss (TL) associated with the environment to obtain the received level (RL) at distances from (in the far field of) the source. The far field distance is chosen so that the behaviour of a distributed source[5] can be approximated to that of a point source. Source levels do not indicate the real sound pressure level at 1 m.

1.4.1.9 **TL** at a frequency of interest is defined as the loss of acoustic energy as the signal propagates from a hypothetical (point) source location to the chosen receiver location. The TL is dependent on water depth, source depth, receiver depth, frequency, geology, and environmental conditions. The TL values are generally evaluated using

[1] The integration time and T90 window are often not reported, particularly in some older studies, meaning that it is often difficult to compare reported rms sound pressure levels between studies.

[2] Historically, rms and peak SPL metrics were used for assessing potential effects of sound on marine life. However, SEL is increasingly being used as it allows exposure duration and the effect of exposure to multiple events to be considered.

[3] It is worth noting that hearing thresholds are sometimes shown as audiograms with sound level on the y axis rather than sensitivity, resulting in the graph shape being the inverse of the graph shown.

[4] There are two definitions for third octave bands, one using a base 2 and the other using base 10, also known as a decidecade. The frequency ratio corresponding to a decidecade is smaller than a one-third octave (base 2) by approximately 0.08% (ISO, 2017).

[5] A distributed source in this context refers to either a combination of two or more smaller sources, or a large source which cannot be treated as a point or monopole source.

an acoustic propagation model (various numerical methods exist) accounting for the above dependencies.

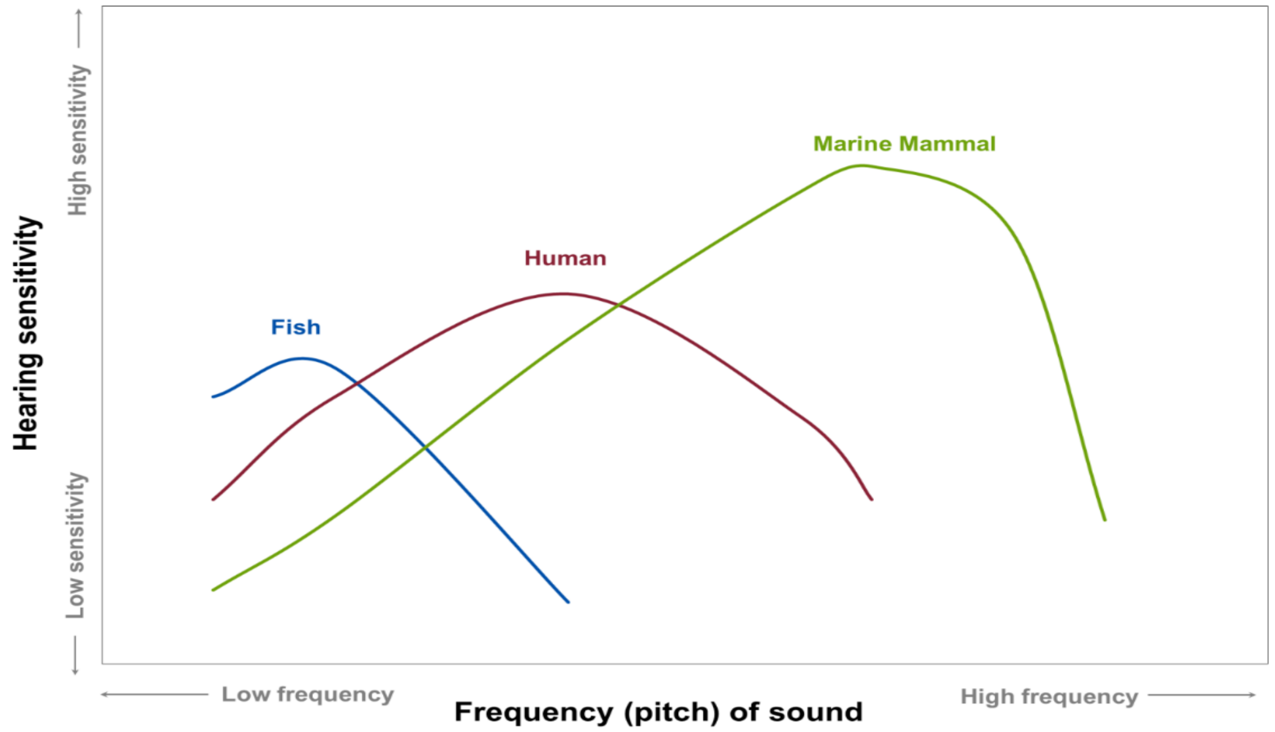

Figure 1.3: Comparison between hearing thresholds of different animals.

1.4.1.10 The RL is the sound level of the acoustic signal recorded (or modelled) at a given location, that corresponds to the acoustic pressure/ energy generated by a known active sound source. This considers the acoustic output of a source and is modified by propagation effects. This RL value is strongly dependant on the source, environmental properties, geological properties and measurement location/ depth. The RL is reported in dB either in rms or peak-to-peak SPL, and SEL metrics, within the relevant one-third octave band frequencies. The RL is related to the SL as:

$$RL = SL - TL$$

where TL is the transmission loss of the acoustic energy within the survey region.

1.4.1.11 The directional dependence of the source signature and the variation of TL with azimuthal direction α (which is strongly dependent on bathymetry) are generally combined and interpolated to report a 2-D plot of the RL around the chosen source point up to a chosen distance.

1.5 Acoustic Assessment Criteria

1.5.1 Introduction

1.5.1.1 Underwater sound has the potential to affect marine life in different ways depending on its sound level and characteristics. Richardson *et al.* (1995) defined four zones of sound influence which vary with distance from the source and level. These are:

- **The zone of audibility**: this is the area within which the animal can detect the sound. Audibility itself does not implicitly mean that the sound will affect the marine mammal
- **The zone of masking**: this is defined as the area within which sound can interfere with the detection of other sounds such as communication or echolocation clicks. This zone is very hard to estimate due to a paucity of data relating to how marine mammals detect sound in relation to masking levels[6] (for example, humans can hear tones well below the numeric value of the overall sound level)
- **The zone of responsiveness**: this is defined as the area within which the animal responds either behaviourally or physiologically. The zone of responsiveness is usually smaller than the zone of audibility because, as stated previously, audibility does not necessarily evoke a reaction
- **The zone of injury/ hearing loss**: this is the area where the sound level is high enough to cause tissue damage in the ear. This can be classified as either TTS or PTS. At even closer ranges, and for very high intensity sound sources (e.g. underwater explosions), physical trauma or even death are possible.

1.5.1.2 For this study, it is the zones of injury and disturbance (i.e. responsiveness) that are of concern (there is insufficient scientific evidence to properly evaluate masking). To determine the potential spatial range of injury and disturbance, a review has been undertaken of available evidence, including international guidance and scientific literature. The following sections summarise the relevant thresholds for onset of effects and describe the evidence base used to derive them.

1.5.2 Injury (physiological damage) to mammals

1.5.2.1 Sound propagation models can be constructed to allow the received sound level at different distances from the source to be calculated. To determine the consequence of these received levels on any marine mammals which might experience such sound emissions, it is necessary to relate the levels to known or estimated potential impact thresholds. The auditory injury (PTS/TTS) threshold criteria proposed by Southall *et al.* (2019) are based on a combination of un-weighted peak pressure levels and mammal hearing weighted SEL. The hearing weighting function is designed to represent the frequency characteristics (bandwidth and sound level) for each group within which acoustic signals can be perceived and therefore assumed have auditory effects. The categories include:

[6] The understanding of how masking occurs and what the implications may be for individual species and populations is an area of active research efforts.

- **Low Frequency (LF) cetaceans**: marine mammal species such as baleen whales (e.g. minke whale *Balaenoptera acutorostrata)*
- **High Frequency (HF) cetaceans**: marine mammal species such as dolphins, toothed whales, beaked whales and bottlenose whales (e.g. bottlenose dolphin *Tursiops truncates* and white-beaked dolphin *Lagenorhynchus albirostris*)
- **Very High Frequency (VHF) cetaceans**: marine mammal species such as true porpoises, river dolphins and pygmy/ dwarf sperm whales and some oceanic dolphins, generally with auditory centre frequencies above 100kHz) (e.g. harbour porpoise *Phocoena phocoena*)
- **Phocid Carnivores in Water (PCW)**: true seals (e.g. harbour seal *Phoca vitulina* and grey seal *Halichoreus grypus*); hearing in air is considered separately in the group PCA
- **Other Marine Carnivores in Water (OCW)**: including otariid pinnipeds (e.g. sea lions and fur seals), sea otters and polar bears; air hearing considered separately in the group Other Marine Carnivores in Air (OCA).

1.5.2.2 These weightings have therefore been used in this study and are shown in Figure 1.4.

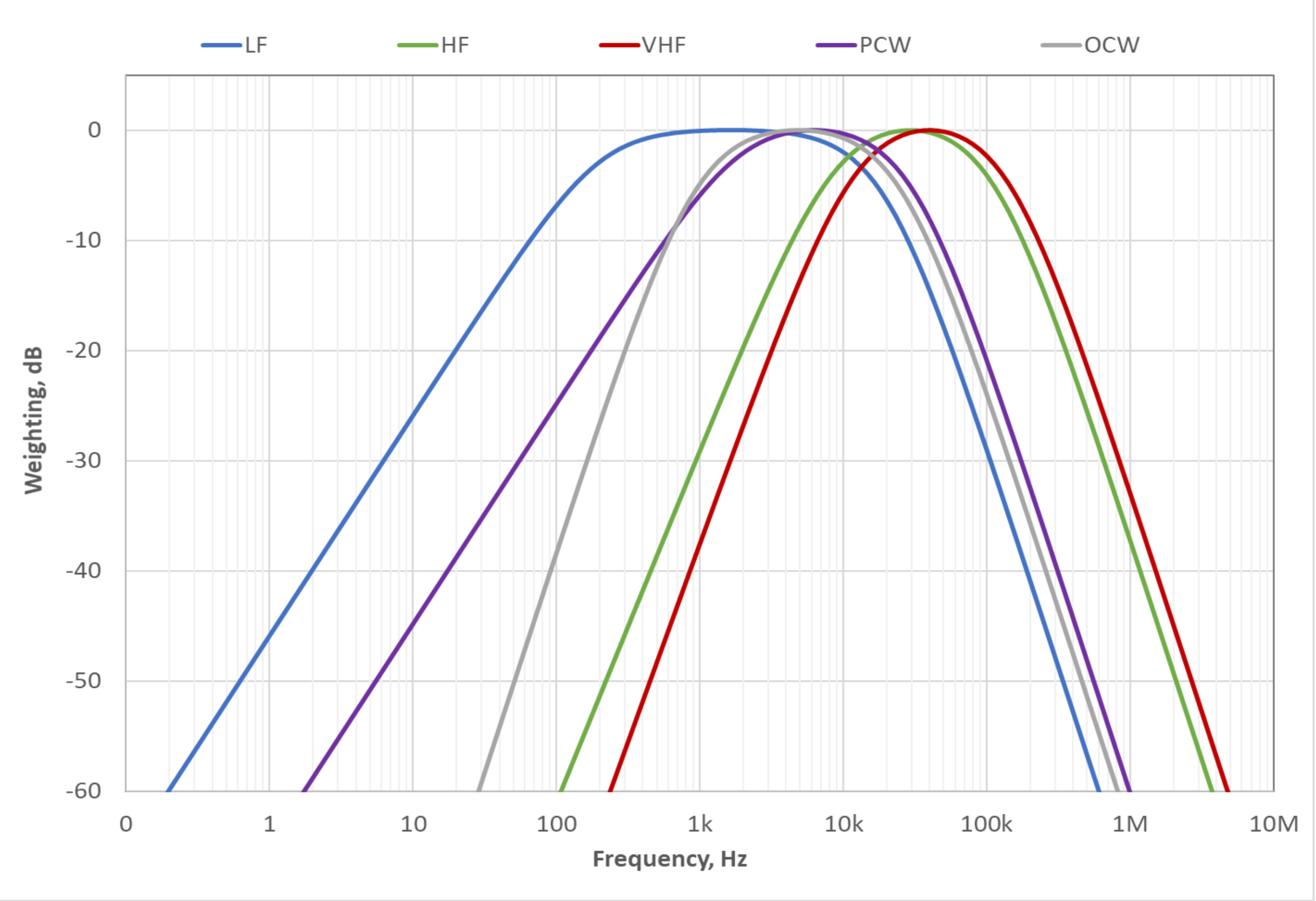

Figure 1.4: Hearing weighting functions for pinnipeds and cetaceans (Southall *et al.*, 2019).

1.5.2.3 Auditory injury criteria proposed in Southall *et al.* (2019) are for two different types of sound as follows:

- **Impulsive sounds** which are typically transient, brief (less than one second), broadband, and consist of high peak sound pressure with rapid rise time and rapid decay (ANSI, 1986 and 2005; NIOSH, 1998). This category includes sound sources such as seismic surveys, impact piling and underwater explosions; and
- **Non-impulsive sounds** which can be broadband, narrowband or tonal, brief or prolonged, continuous or intermittent and typically do not have a high peak sound pressure with rapid rise/ decay time that impulsive sounds do (ANSI, 1995; NIOSH, 1998). This category includes sound sources such as continuous running machinery, sonar, and vessels.

1.5.2.4 The criteria for impulsive and non-impulsive sound have been adopted for this study given the nature of the variety of sound source used during the various activities. The relevant criteria proposed by Southall *et al.* (2019) are as summarised in Table 1.2 and Table 1.3.

Table 1.2: Summary of PTS onset acoustic thresholds (Southall *et al.*, 2019; tables 6 and 7).

Hearing Group	Parameter	Impulsive	Non-impulsive
LF cetaceans	Peak, unweighted	219	-
	SEL, LF weighted	183	199
HF cetaceans	Peak, unweighted	230	-
	SEL, HF weighted	185	198
VHF cetaceans	Peak, unweighted	202	-
	SEL, VHF weighted	155	173
PCW	Peak, unweighted	218	-
	SEL, PCW weighted	185	201
OCW	Peak, unweighted	232	-
	SEL, OCW weighted	203	219

Table 1.3: Summary of TTS onset acoustic thresholds (Southall *et al.*, 2019; tables 6 and 7).

Hearing Group	Parameter	Impulsive	Non-impulsive
LF cetaceans	Peak, unweighted	213	-
	SEL, LF weighted	168	179
HF cetaceans	Peak, unweighted	224	-
	SEL, HF weighted	170	178
VHF cetaceans	Peak, unweighted	196	-
	SEL, VHF weighted	140	153
PCW	Peak, unweighted	212	-

Hearing Group	Parameter	Impulsive	Non-impulsive
	SEL, PCW weighted	170	181
OCW	Peak, unweighted	226	-
	SEL, OCW weighted	188	199

1.5.2.5 These updated marine mammal threshold criteria were published in March 2019 (Southall *et al.*, 2019). The paper utilised the same hearing weighting curves and thresholds as presented in the preceding regulations document National Marine Fisheries Service (NMFS) (2018) (and prior to that Southall *et al.* (2007)) with the main difference being the naming of the hearing groups and introduction of additional thresholds for animals not covered by NMFS (2018). A comparison between the two naming conventions is shown in Table 1.4.

1.5.2.6 For avoidance of doubt, the naming convention used in this report is based upon those set out in Southall *et al.* (2019). Consequently, this assessment utilises criteria which are applicable to both NMFS (2018) and Southall *et al.* (2019).

Table 1.4: Comparison of hearing group names between NMFS (2018) and Southall *et al.* (2019.).

NMFS (2018) hearing group name	Southall *et al.* (2019) hearing group name
Low-frequency cetaceans (LF)	LF
Mid-frequency cetaceans (MF)	HF
High-frequency cetaceans (HF)	VHF
Phocid pinnipeds in water (PW)	PCW

1.5.3 Disturbance to marine mammals

1.5.3.1 Beyond the area in which auditory injury may occur, effects on marine mammal behaviour is an important measure of potential impact. Non-trivial disturbance may occur when there is a risk of animals incurring sustained or chronic disruption of behaviour or when animals are displaced from an area, with subsequent redistribution being significantly different from that occurring due to natural variation.

1.5.3.2 To consider the possibility of disturbance resulting from the Mona Offshore Wind Project, it is necessary to consider:

- Whether or not a sound can be detected/heard by a receptor above background sound levels or level of acclimatisation above background levels
- The likelihood that the sound could cause non-trivial disturbance
- The likelihood that the sensitive receptors will be exposed to that sound
- Whether the number of animals exposed are likely to be significant at the population level

1.5.3.3 Assessing this is however a very difficult task due to the complex and variable nature of sound propagation, the variability of documented animal responses to similar levels of sound, and the availability of population estimates and regional density estimates for all marine mammal species. Behavioural responses are widely recognised as being highly variable and context specific (Southall *et al.*, 2007; 2019; 2021). Assessing the severity of such impacts and development of probability-based response functions continues to be an area of ongoing scientific research interest (Graham *et al.,* 2019; Harris *et al.,* 2018; Southall *et al.,* 2021).

1.5.3.4 Southall *et al.* (2007) recommended that the only currently feasible way to assess whether a specific sound could cause disturbance is to compare the circumstances of the situation with empirical studies. Joint Nature Conservation Committee (JNCC) guidance in the UK (JNCC, 2010) indicates that a score of five or more on the Southall *et al.* (2007) behavioural response severity scale could be significant. The more severe the response on the scale, the lower the amount of time that the animals will tolerate it before there could be adverse consequences to life functions, which would constitute a disturbance. The severity scale was revised in Southall et al. (2021), which included splitting severity assessment methods on captive studies from assessments on field studies. Behavioural responses related to field studies included impacts to survival, reproduction and foraging.

1.5.3.5 Southall *et al.* (2007) and (2021) both present a summary of observed behavioural responses for various mammal groups exposed to different types of sound: continuous (non-pulsed) or impulsive (single or multiple pulsed).

1.5.3.6 Disturbance to marine mammals is discussed in more detail in volume 2, chapter 9: Marine mammals of the PEIR.

1.5.4 Continuous (non-pulsed, non-impulsive) sound

1.5.4.1 For non-pulsed sound (e.g. drilled piles, vessels etc.), the lowest sound pressure level at which a score of five or more on the Southall *et al.* (2007) behavioural response severity scale occurs for low frequency cetaceans is 90dB to 100dB re 1µPa (rms). However, this relates to a study involving only migrating grey whales. A study for minke whale showed a response score of three at a received level of 100dB to 110dB re 1µPa (rms), with no higher severity score encountered for this species. For mid frequency cetaceans, a response score of eight was encountered at a received level of 90dB to 100dB re 1µPa (rms), but this was for one mammal (a sperm whale *Physeter macrocephalus*) and might not be applicable for the species likely to be encountered in the vicinity of the Mona Offshore Wind Project. For Atlantic white-beaked dolphin *Lagenorhynchus albirostris*, a response score of three was encountered for received levels of 110 to 120dB re 1µPa (rms), with no higher severity score encountered. For high frequency cetaceans such as bottlenose dolphins *Tursiops truncatus*, a number of individual responses with a response score of six are noted ranging from 80dB re 1µPa (rms) and upwards. There is a significant increase in the number of mammals responding at a response score of six once the received sound pressure level is greater than 140dB re 1µPa (rms).

1.5.4.2 It is worth noting that the above sound pressure levels are based on the rms sound pressure level metric, which was historically often reported in such studies. More recent studies often use other metrics such as the SEL and care must be taken not to directly compare sound levels quoted using different parameters. See section 1.4 for a discussion of these different metrics.

1.5.4.3 The NMFS (2005) guidance sets the marine mammal level B harassment threshold (analogous to disturbance) for continuous sound at 120dB re 1µPa (rms). This threshold is based on studies by Malme *et al.* (1984) which investigate the effects of sound from the offshore petroleum industry on migrating gray whale behaviour offshore Alaska. This value sits approximately mid-way between the range of values identified in Southall *et al.* (2007) for continuous sound but is lower than the value at which the majority of marine mammals responded at a response score of six (i.e. once the received rms sound pressure level is greater than 140dB re 1µPa). Considering the paucity and high level variation of data relating to onset of behavioural effects due to continuous sound, any ranges predicted using this number are likely to be probabilistic and potentially over precautionary.

1.5.4.4 It is worth nothing that the distinction between impulsive and non-impulsive sound was removed from Southall et al. (2021) as "some source types, such as airguns, may produce impulsive sounds near the source and non-impulsive sounds at greater ranges (see Southall, 2021)". However, Southall et al. (2021) does not present thresholds for assessing disturbance, therefore the thresholds discussed above have been adopted.

1.5.5 Impulsive (pulsed) sound

1.5.5.1 Southall *et al.* (2007) presents a summary of observed behavioural responses due to multiple pulsed sound, although the data is primarily based on responses to seismic exploration activities (rather than for piling). Although these datasets contain much relevant data for LF cetaceans, there is less data for MF or HF cetaceans within the document. Low frequency cetaceans, other than bow-head whales, were typically observed to respond significantly at a received level of 140dB to 160dB re 1µPa (rms). Behavioural changes at these levels during multiple pulses may have included visible startle response, extended cessation or modification of vocal behaviour, brief cessation of reproductive behaviour or brief/minor separation of females and dependent offspring. The data available for MF cetaceans indicate that some significant response was observed at a SPL of 120dB to 130dB re 1µPa (rms), although the majority of cetaceans in this category did not display behaviours of this severity until exposed to a level of 170dB to 180dB re 1µPa (rms). Furthermore, other MF cetaceans within the same study were observed to have no behavioural response even when exposed to a level of 170dB to 180dB re 1µPa (rms).

1.5.5.2 A more recent study is described in Graham *et al.* (2019). Empirical evidence from piling at the Beatrice Offshore Wind Farm (Moray Firth, Scotland) was used to derive a dose-response curve for harbour porpoise[7]. The unweighted single pulse SEL contours were plotted in 5dB increments and applied the dose-response curve to estimate the number of animals that would be disturbed by piling within each stepped contour. The study shows a 100% probability of disturbance at an (un-weighted) SEL of 180dB re 1µPa^{2}s, 50% at 155dB re 1µPa^{2}s and dropping to approximately 0% at an SEL of 120dB re 1µPa^{2}s. This approach to understanding the behavioural effects from piling has been applied at other UK offshore wind farms (for example Seagreen Alpha/Bravo Environmental Statement Chapter 10 Marine Mammals (Seagreen Wind Energy, 2018), Hornsea Three Environmental Statement volume 2 chapter 4 Marine Mammals (Orsted, 2020) and Awel y Mor Environmental Statement volume 2, chapter 7: Marine Mammals ((RWE, 2022)). Similar stepped/probability based threshold criteria have been used on other studies such as for assessing the response of marine mammals to geophysical activities (e.g. Southall *et al*., 2017).

1.5.5.3 According to Southall *et al.* (2007) there is a general paucity of data relating to the effects of sound on pinnipeds in particular. One study using ringed *Pusa hispida*, bearded *Erignathus barbatus* and spotted *Phoca largha* seals (Harris *et al*., 2001) found onset of a significant response at a received sound pressure level of 160dB to 170dB re 1µPa (rms), although larger numbers of animals showed no response at sound levels of up to 180dB re 1µPa (rms). It is only at much higher sound pressure levels in the range of 190dB to 200dB re 1µPa (rms) that significant numbers of seals were found to exhibit a significant response. For non-pulsed sound, one study elicited a significant response on a single harbour seal at a received level of 100dB to 110dB re 1µPa (rms), although other studies found no response or non-significant reactions occurred at much higher received levels of up to 140dB re 1µPa (rms). No data are available for higher sound levels and the low number of animals observed in the various studies means that it is difficult to make any firm conclusions from these studies.

1.5.5.4 Southall *et al.* (2007) also notes that, due to the uncertainty over whether HF cetaceans may perceive certain sounds and due to paucity of data, it was not possible to present any data on responses of HF cetaceans. However, Lucke *et al.* (2009) showed a single harbour porpoise consistently showed aversive behavioural reactions to pulsed sound at received SPL above 174dB re 1µPa (peak-to-peak) or a SEL of 145dB re 1µPa^{2}s, equivalent to an estimated 8rms sound pressure level of 166dB re 1µPa.

1.5.5.5 There is much intra-category and perhaps intra-species variability in behavioural response. As such, a conservative approach should be taken to ensure that the most sensitive marine mammals remain protected.

1.5.5.6 The High Energy Seismic Survey (HESS) workshop on the effects of seismic (i.e. pulsed) sound on marine mammals (HESS, 1997) concluded that mild behavioural disturbance would most likely occur at rms sound levels greater than 140dB re 1µPa (rms). This workshop drew on studies by Richardson (1995) but recognised that there was some degree of variability in reactions between different studies and mammal groups. Consequently, for the purposes of this study, a precautionary level of 140dB re 1µPa (rms) is used to indicate the onset of low-level marine mammal disturbance effects for all mammal groups for impulsive sound.

1.5.5.7 Disturbance of marine mammals due to impulsive sound from piling activity has been assessed quantitatively by considering the proportional response of individuals exposed to decreasing sound levels with increasing distance from the sound source. Empirical evidence from piling studies at the Beatrice Offshore Wind Farm (Moray Firth, Scotland) (Graham *et al*., 2019) and Horns Rev offshore wind farm (Brandt *et al*., 2011) demonstrated that the probability of occurrence of harbour porpoise (measured as porpoise positive minutes) increased exponentially moving further away from the source. Graham *et al.* (2019) showed a 100% probability of disturbance at an (un-weighted) SEL of 180dB re 1µPa^{2}s, 50% at 155dB re 1µPa^{2}s and dropping to

[7] Dose-response relationships describe the magnitude of the response of an organism, as a function of exposure to a stimulus or stressor after a certain exposure time.

8 Based on an analysis of the time history graph in Lucke et al. (2007), the T90 period is estimated to be approximately 8 ms, resulting in a correction of 21dB applied to the SEL to derive the rms_{T90} sound pressure level. However, the T90 was not directly reported in the paper.

approximately 0% at an SEL of 120dB re 1μPa²s and the data were subsequently used to develop a dose-response curve. The assessment of behavioural response and disturbance is presented in the Marine Mammals chapter (volume 2, chapter 9: Marine Mammals of the PEIR).

1.5.5.8 Similarly, a telemetry study undertaken by Russell *et al.* (2016) investigating the behaviour of tagged harbour seals during pile driving at the Lincs offshore wind farm in the Wash found that there was a proportional response at different received sound levels. Dividing the study area into a 5km x 5km grid, the authors modelled SEL_{ss} levels and matched these to corresponding densities of harbour seals in the same grids during periods of non-piling versus piling to show change in usage. The study found that there was a significant decrease during piling activities at predicted received SEL levels of between 142 and 151dB re 1μPa²s.

1.5.5.9 The approach to be employed for the Mona Offshore Wind Project is therefore to plot unweighted single pulse SEL contours in 5dB increments and apply the appropriate dose-response curve to estimate the number of animals that would be disturbed by sound from the piling within each stepped contour. For cetaceans, the dose-response curve will be applied from the Beatrice data (Graham *et al.,* 2019) whilst for pinnipeds the dose-response curve will be applied using Russell *et al.* (2016) (Figure 1.5 and Figure 1.6 below).

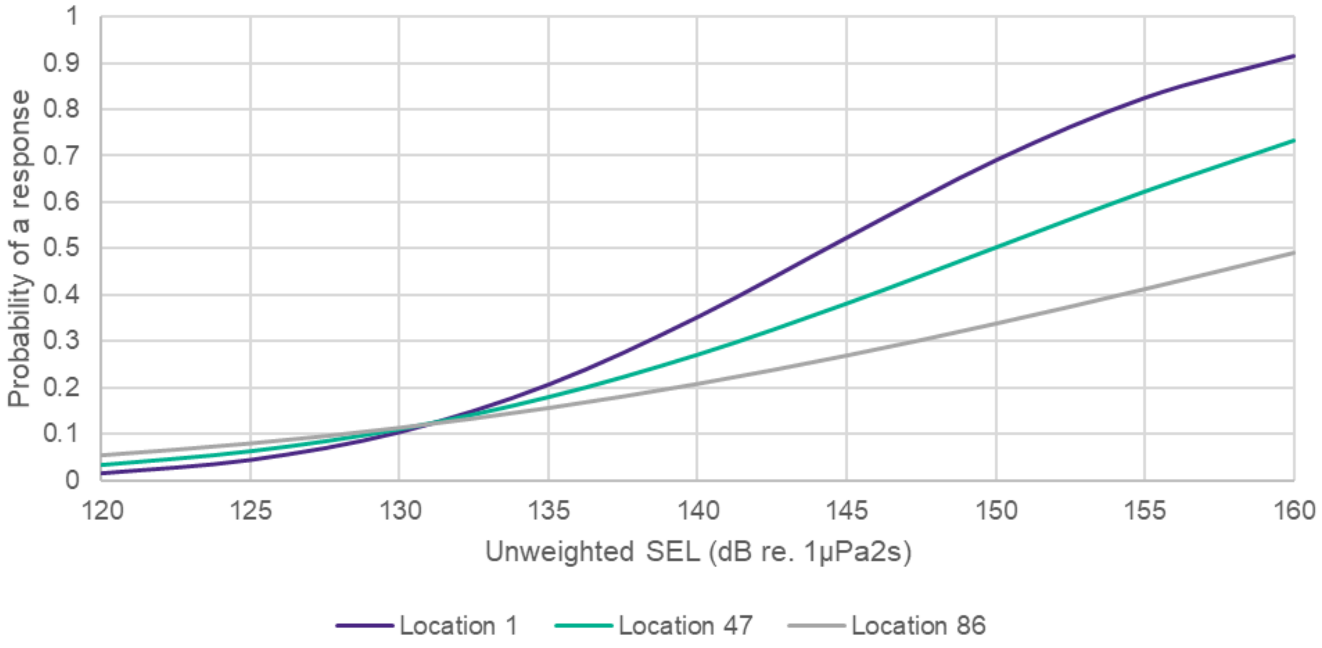

Figure 1.5: The Probability of a Harbour Porpoise Response (24h) in Relation to the Partial Contribution of Unweighted Received Single-Pulse SEL for the First Location Piled (Purple Line), the Middle Location (green line) and the Final Location Piled (Blue Line). Reproduced with Permission from Graham *et al.* (2019).

1.5.5.10 This is an accepted approach to assessing potential behavioural effects of sound from piling and has been applied at other UK offshore windfarms (for example Seagreen Alpha/ Bravo, Awel y Mor and Hornsea Three).

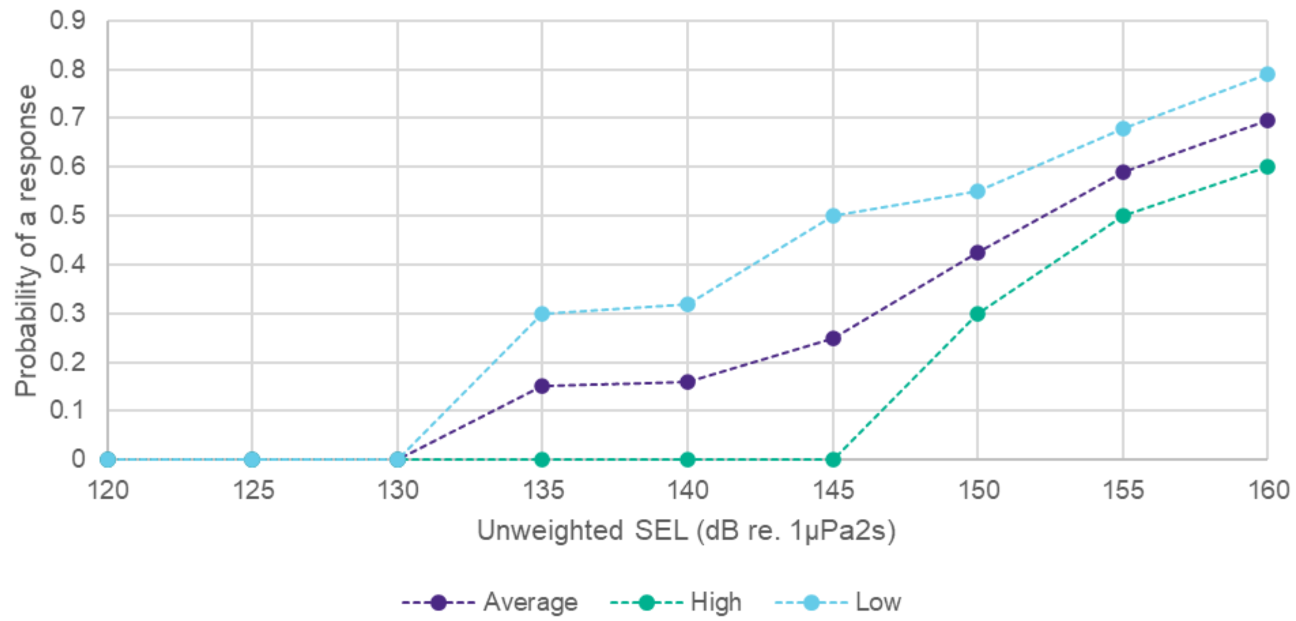

Figure 1.6: The Probability of Response for Seals due to Piling in Relation to Unweighted Received Single-Pulse SEL at 5dB Increments. Adapted from Russell *et al.* (2016).

1.5.5.11 For impulsive sound sources other than piling (e.g. UXO clearance, some geotechnical and geophysical surveys), this assessment adopts the NMFS (2005) Level B harassment threshold of 160dB re 1μPa (rms) for impulsive sound. Level B Harassment is defined by NMFS (2005) as having the potential to disturb a marine mammal or marine mammal stock in the wild by causing disruption of behavioural patterns, including, but not limited to, migration, breathing, nursing, breeding, feeding, or sheltering but which does not have the potential to injure a marine mammal or marine mammal stock in the wild. This is similar to the JNCC (2010) description of non-trivial disturbance and has therefore been used as the basis for onset of behavioural change in the assessment.

1.5.5.12 For assessing the severity of behavioural response, the distinction between impulsive and non-impulsive sound was removed from Southall *et al.* (2021) as "*some source types, such as airguns, may produce impulsive sounds near the source and non-impulsive sounds at greater ranges (see Southall, 2021)*". Southall *et al.* (2021) instead assigns categories to various sources based on the operational characteristics and applies revised severity assessments to selected studies in each category. For example, Table 7 within that paper details a number of observational studies of marine mammals and their responses to piling, with an indication of severity of response and in some cases a received level. However, Southall *et al.* (2021) does not present thresholds for assessing disturbance, therefore the thresholds discussed above have been adopted for this study. The assessment of disturbance and behavioural response is presented in full in the Marine Mammals chapter (Volume 2, chapter 9: Marine Mammals of the PEIR).

1.5.5.13 It is important to understand that exposure to sound levels in excess of the behavioural change threshold stated above does not necessarily imply that the sound will result in significant disturbance. As noted previously, it is also necessary to assess the likelihood that the sensitive receptors will be exposed to that sound and whether the numbers exposed are likely to be significant at the population level.

Table 1.5: Disturbance criteria for marine mammals used in this study.

Effect	Non-Impulsive Threshold	Impulsive Threshold (Other than Piling)	Impulsive Threshold (Piling)
Mild disturbance (all marine mammals)	-	140dB re 1μPa (rms)	Based on SEL 5dB contours
Strong disturbance (all marine mammals)	120dB re 1μPa (rms)	160dB re 1μPa (rms)	Based on SEL 5dB contours

1.5.5.14 It should be borne in mind that there is a considerable degree of uncertainty and variability in the onset of disturbance and therefore any disturbance ranges should be treated as potentially over precautionary. Exceedance of a threshold does not mean that there is a 100% chance of disturbance occurring or indeed that any such disturbance would be significant. Another important consideration is that the majority of sound produced by project activities, with the exception of operational wind turbine sound, will be either temporary or transitory, as opposed to permanent and fixed. These important considerations are not taken into account in the sound modelling but will be assessed in the relevant marine ecology topic chapters.

Injury and disturbance to fish

1.5.5.15 For fish, the most relevant criteria for injury effects are considered to be those contained in the Sound Exposure Guidelines for Fishes and Sea Turtles (Popper *et al.* 2014). These guidelines broadly group fish into the following categories based on their anatomy and the available information on hearing of other fish species with comparable anatomies:

- Group 1: fishes with no swim bladder or other gas chamber (e.g. elasmobranchs, flatfishes and lampreys). These species are less susceptible to barotrauma and are only sensitive to particle motion, not sound pressure. Basking sharks, which do not have a swim bladder, also fall into this hearing group
- Group 2: fishes with swim bladders but the swim bladder does not play a role in hearing (e.g. salmonids). These species are susceptible to barotrauma, although hearing only involves particle motion, not sound pressure
- Group 3: Fishes with swim bladders that are close, but not connected, to the ear (e.g. gadoids and eels). These fishes are sensitive to both particle motion and sound pressure and show a more extended frequency range than Groups 1 and 2, extending to about 500Hz
- Group 4: Fishes that have special structures mechanically linking the swim bladder to the ear (e.g. clupeids such as herring, sprat and shads). These fishes are sensitive primarily to sound pressure, although they also detect particle motion. These species have a wider frequency range, extending to several kHz and generally show higher sensitivity to sound pressure than fishes in Groups 1, 2 and 3
- Sea turtles: There is limited information on auditory criteria for sea turtles and the effect of impulsive sound is therefore inferred from documented effects to other vertebrates. Bone conducted hearing is the most likely mechanism for auditory reception in sea turtles and, since high frequencies are attenuated by bone, the range of hearing are limited to low frequencies only. For leatherback turtle the hearing range has been recorded as between 50 and 1,200Hz with maximum sensitivity between 100 and 400Hz
- Fish eggs and larvae: separated due to greater vulnerability and reduced mobility. Very few peer-reviewed studies report on the response of eggs and larvae to anthropogenic sound.

1.5.5.16 The guidelines set out criteria for injury effects due to different sources of sound. Those relevant to the Mona Offshore Wind Project are considered to be those for impulsive piling sources only, as non-impulsive sources were not considered to be a key potential impact and therefore were screened out of the guidance[9]. The criteria include a range of indices including SEL, rms and peak SPLs. Where insufficient data exist to determine a quantitative guideline value, the risk is categorised in relative terms as “high”, “moderate” or “low” at three distances from the source: “near” (i.e. in the tens of metres), “intermediate” (i.e. in the hundreds of metres) or “far” (i.e. in the thousands of metres). It should be noted that these qualitative criteria cannot differentiate between exposures to different sound levels and therefore all sources of sound, no matter how loud, would theoretically elicit the same assessment result. However, because the qualitative risks are generally qualified as “low”, with the exception of a moderate risk at “near” range (i.e. within tens of metres) for some types of hearing groups and impairment effects, this is not considered to be a significant issue with respect to determining the potential effect of sound on fish.

1.5.5.17 The injury threshold criteria used in this underwater sound assessment for impulsive piling are given in Table 1.6. In the table, both peak and SEL criteria are unweighted. Physiological effects relating to injury criteria are described below (Popper *et al.*, 2014; Popper and Hawkins, 2016):

- **Mortality and potential mortal injury**: either immediate mortality or tissue and/or physiological damage that is sufficiently severe (e.g. a barotrauma) that death occurs sometime later due to decreased fitness. Mortality has a direct effect upon animal populations, especially if it affects individuals close to maturity
- **Recoverable injury**: Tissue and other physical damage or physiological effects, that are recoverable but which may place animals at lower levels of fitness, may render them more open to predation, impaired feeding and growth, or lack of breeding success, until recovery takes place
- **TTS**: Short term changes in hearing sensitivity may, or may not, reduce fitness and survival. Impairment of hearing may affect the ability of animals to capture prey and avoid predators, and also cause deterioration in communication between individuals; affecting growth, survival, and reproductive success. After termination of a sound that causes TTS, normal hearing ability returns over a period that is variable, depending on many factors, including the intensity and duration of sound exposure.

9 Guideline exposure criteria for seismic surveys, continuous sound and naval sonar are also presented though are not applicable to the Mona Offshore Wind Project.

Table 1.6: Criteria for onset of injury to fish and sea turtles due to impulsive piling (Popper *et al.*, 2014).

Type of Animal	Parameter	Mortality and Potential Mortal Injury	Recoverable Injury	TTS
Group 1 Fish: no swim bladder (particle motion detection)	SEL, dB re 1μPa^{2}s	>219	>216	>>186
	Peak, dB re 1μPa	>213	>213	-
Group 2 Fish: where swim bladder is not involved in hearing (particle motion detection)	SEL, dB re 1μPa^{2}s	210	203	>186
	Peak, dB re 1μPa	>207	>207	-
Groups 3 and 4 Fish: where swim bladder is involved in hearing (primarily pressure detection)	SEL, dB re 1μPa^{2}s	207	203	186
	Peak, dB re 1μPa	>207	>207	-
Sea turtles	SEL, dB re 1μPa^{2}s	210	(Near) High (Intermediate) Low (Far) Low	(Near) High (Intermediate) Low (Far) Low
	Peak, dB re 1μPa	>207		
Eggs and larvae	SEL, dB re 1μPa^{2}s	>210	(Near) Moderate (Intermediate) Low (Far) Low	(Near) Moderate (Intermediate) Low (Far) Low
	Peak, dB re 1μPa	>207		

1.5.5.18 The criteria used in this underwater sound assessment for non-impulsive piling and other continuous sound sources, such as vessels, are given in Table 1.7. The only numerical criteria for these sources are for recoverable injury and TTS for Groups 3 and 4 Fish.

Table 1.7: Criteria for onset of injury to fish and sea turtles due to non-impulsive sound (Popper *et al.*, 2014).

Type of Animal	Mortality and Potential Mortal Injury	Recoverable Injury	TTS
Group 1 Fish: no swim bladder (particle motion detection)	(Near) Low (Intermediate) Low (Far) Low	(Near) Low (Intermediate) Low (Far) Low	(Near) Moderate (Intermediate) Low (Far) Low
Group 2 Fish: where swim bladder is not involved in hearing (particle motion detection)	(Near) Low (Intermediate) Low (Far) Low	(Near) Low (Intermediate) Low (Far) Low	(Near) Moderate (Intermediate) Low (Far) Low
Groups 3 and 4 Fish: where swim bladder is involved in hearing (primarily pressure detection)	(Near) Low (Intermediate) Low (Far) Low	170dB re 1μPa (rms) for 48 hours	158dB re 1μPa (rms) for 12 hours
Sea turtles	(Near) Low (Intermediate) Low (Far) Low	(Near) Low (Intermediate) Low (Far) Low	(Near) Moderate (Intermediate) Low (Far) Low
Eggs and larvae	(Near) Low (Intermediate) Low (Far) Low	(Near) Low (Intermediate) Low (Far) Low	(Near) Low (Intermediate) Low (Far) Low

1.5.5.19 The criteria used in this underwater sound assessment for explosives are given in Table 1.8.

Table 1.8: Criteria for injury to fish due to explosives (Popper *et al.*, 2014).

Type of Animal	Parameter	Mortality and Potential Mortal Injury	Recoverable Injury	TTS
Group 1 Fish: no swim bladder (particle motion detection)	Peak, dB re 1μPa	229 - 234	(Near) High (Intermediate) Low (Far) Low	(Near) High (Intermediate) Moderate (Far) Low
Group 2 Fish: where swim bladder is not involved in hearing (particle motion detection)	Peak, dB re 1μPa	229 - 234	(Near) High (Intermediate) High (Far) Low	(Near) High (Intermediate) Moderate (Far) Low
Group 3 and 4 Fish: where swim bladder is involved in hearing (primarily pressure detection)	Peak, dB re 1μPa	229 - 234	(Near) High (Intermediate) High (Far) Low	(Near) High (Intermediate) High (Far) Low

1.5.5.20 It should be noted that there are no thresholds in Popper *et al.* (2014) in relation to sound from high frequency sonar (>10 kHz). This is because the hearing range of fish species falls well below the frequency range of high frequency sonar systems. Consequently, the effects of sound from high frequency sonar surveys on fish has not been conducted as part of this study, due to the frequency of the source being beyond the range of hearing and also due to the lack of any suitable thresholds.

1.5.5.21 Behavioural reaction of fish to sound has been found to vary between species based on their hearing sensitivity. Typically, fish sense sound via particle motion in the inner ear which is detected from sound-induced motions in the fish's body (see section 1.10 for further details on particle motion). The detection of sound pressure is restricted to those fish which have air filled swim bladders; however, particle motion (induced by sound) can be detected by fish without swim bladders[10].

1.5.5.22 Highly sensitive species such as herring have elaborate specialisations of their auditory apparatus, known as an otic bulla – a gas filled sphere, connected to the swim bladder, which enhances hearing ability. The gas filled swim bladder in species such as cod and salmon may be involved in their hearing capabilities, so although there is no direct link to the inner ear, these species are able to detect lower sound frequencies and as such are considered to be of medium sensitivity to sound. Flat fish and elasmobranchs have no swim bladders and as such are considered to be relatively less sensitive to sound pressure.

1.5.5.23 The most recent criteria for disturbance are considered to be those contained in Popper *et al.* (2014) which set out qualitative criteria for disturbance due to different sources of sound. The risk of behavioural effects is categorised in relative terms as "high", "moderate" or "low" at three distances from the source: "near" (i.e. in the tens of metres), "intermediate" (i.e. in the hundreds of metres) or "far" (i.e. in the thousands of metres), as shown in Table 1.9.

Table 1.9: Criteria for onset of behavioural effects in fish and sea turtles for impulsive and non-impulsive sound (Popper *et al.*, 2014).

Type of Animal	Relative Risk of Behavioural Effects		
	Impulsive Piling	Explosives	Non-Impulsive Sound
Group 1 Fish: no swim bladder (particle motion detection)	(Near) High (Intermediate) Moderate (Far) Low	(Near) High (Intermediate) Moderate (Far) Low	(Near) Moderate (Intermediate) Moderate (Far) Low
Group 2 Fish: where swim bladder is not involved in hearing (particle motion detection)	(Near) High (Intermediate) Moderate (Far) Low	(Near) High (Intermediate) High (Far) Low	(Near) Moderate (Intermediate) Moderate (Far) Low
Groups 3 and 4 Fish: where swim bladder is involved in hearing (primarily pressure detection)	(Near) High (Intermediate) High (Far) Moderate	(Near) High (Intermediate) High (Far) Low	(Near) High (Intermediate) Moderate (Far) Low
Sea turtles	(Near) High (Intermediate) Moderate (Far) Low	(Near) High (Intermediate) High (Far) Low	(Near) High (Intermediate) Moderate (Far) Low
Eggs and larvae	(Near) Moderate (Intermediate) Low (Far) Low	(Near) High (Intermediate) Low (Far) Low	(Near) Moderate (Intermediate) Moderate (Far) Low

10 It should be noted that the presence of a swim bladder does not necessarily mean that the fish can detect pressure. Some fish have swim bladders that are not involved in the hearing mechanism and can only detect particle motion.

1.5.5.24 It is important to note that the Popper *et al.* (2014) criteria for disturbance due to sound are qualitative rather than quantitative. Consequently, a source of sound of a particular type (e.g. piling) would be predicted to result in the same potential impact, no matter the level of sound produced or the propagation characteristics.

1.5.5.25 Therefore, the criteria presented in the Washington State Department of Transport Biological Assessment Preparation for Transport Projects Advanced Training Manual (WSDOT, 2011) are also used in this assessment for predicting the distances at which behavioural effects may occur due to sound from impulsive piling. The manual suggests an un-weighted sound pressure level of 150dB re 1µPa (rms) as the criterion for onset of behavioural effects, based on work by (Hastings, 2002). Sound pressure levels in excess of 150dB re 1µPa (rms) are expected to cause temporary behavioural changes, such as elicitation of a startle response, disruption of feeding, or avoidance of an area. The document notes that levels exceeding this threshold are not expected to cause direct permanent injury but may indirectly affect the individual fish (such as by impairing predator detection). It is important to note that this threshold is for onset of potential effects, and not necessarily an 'adverse effect' threshold.

Use of impulsive sound thresholds at large ranges

1.5.5.26 For any sound of a given amplitude and frequency content, impulsive sound has a greater potential to cause auditory injury than a similar magnitude non-impulsive sound (B. L. Southall *et al.,* 2007; 2019; 2021; NMFS, 2018; von Benda-Beckmann *et al.,* 2022). For highly impulsive sounds such as those generated by impact piling, UXO detonations and seismic source arrays, the interaction with the seafloor and the water column is complex. In these cases, due to a combination of dispersion (i.e., where the waveform elongates), multiple reflections from the sea surface and seafloor and molecular absorption of high frequency energy, the sound is unlikely to still be impulsive in character once it has propagated some distance (Hastie *et al.*, 2019; Martin *et al.*, 2020; B. L. Southall *et al.*, 2019; Southall, 2021). This transition in the acoustic characteristics therefore has implications with respect to which threshold values should be used (impulsive vs. non impulsive criteria) and, consequently, the distances at which potential injury effects may occur.

1.5.5.27 This acoustic wave elongation effect is particularly pronounced at larger ranges of several kilometres and, in particular, it is considered highly unlikely that predicted permanent threshold shift (PTS) or temporary threshold shift (TTS) ranges for impulsive sound which are found to be in the tens of kilometres are realistic (Southall, 2021). However, the precise range at which the transition from impulsive to non-impulsive sound occurs is difficult to define precisely, not least because the transition also depends on the response of the marine mammals' ear. Consequently, there is currently no consensus as to the range at which this transition occurs or indeed the measure of impulsivity which can be used to determine which threshold should be applied (Southall, 2021) although evidence for impact pile driving and seismic source arrays does indicate that some measures of impulsivity change markedly within 10km of the source (Hastie *et al.*, 2019). Additionally, the draft NMFS (2018) guidance suggested 3km as a transition range, but this was removed from the final document.

1.5.5.28 This is an area of ongoing research and there are a number of potential methods for determining the cross-over point being investigated, such as the kurtosis metric, and the loss of high frequency energy from the spectrum (above 10kHz, e.g. Southall, 2021). In the meantime it is considered that any predicted injury ranges in the tens of kilometres are almost certainly an overly precautionary interpretation of existing criteria (Southall, 2021).

1.5.5.29 Because disturbance ranges are likely to extend beyond the range at which injury (PTS or TTS) could occur, this transition from impulsive to continuous sound is likely to be even more important (e.g. Southall *et al.,* 2021). For example, where dose response relationships have been derived based on exposure to impulsive sounds, particularly where these have been derived based on experiments relatively close to the impulsive source, then extrapolation of the dose-response relationship to larger ranges could be misleading. This is particularly true where the dose response relationship has been derived using parameters such as unweighted single pulse SEL or rms(T90) SPL, which does not take into account the characteristics (e.g. frequency content of impulsivity) of the sound. Consequently, great caution should be used when interpreting potential disturbance ranges in the order of tens of kilometres, which should be considered alongside an understanding of potential background sound levels in order to understand the distances at which sounds related to an impulsive source may be detected.

1.6 Baseline

1.6.1.1 Background or “ambient” underwater sound is created by several natural sources, such as rain, breaking waves, wind at the surface, seismic sound, biological sound and thermal sound. Anthropogenic sounds related to the Mona Offshore Wind Project activities can be either impulsive (pulsed) such as impact piling, or non-impulsive (continuous) such as ship engines, and the magnitude of the impact on marine life will depend heavily on these characteristics. Biological sources include marine mammals (using sound to communicate, build up an image of their environment and detect prey and predators) as well as certain fish and shrimp. Anthropogenic sources of sound in the marine environment include fishing boats, ships (non-impulsive), marine construction, seismic surveys and leisure activities (all could be either impulsive or non-impulsive), all of which add to ambient background sound. Other anthropogenic sound within the vicinity of the Mona Offshore Wind Project will arise primarily from shipping, the offshore oil and gas industry, subsea geophysical and geotechnical surveys, and the offshore renewables industry. Underwater acoustic measurements of operational sound were undertaken in and around the Ormonde Wind Farm in June 2012 (Nedwell *et al.*, 2012). The results reported that there was an increase in sound levels between 0 and 50kHz at a water depth of 30m around individual wind turbines. The sound was continuous in nature, and the increase was detectable to a maximum range of approximately 1km. Beyond this range, the underwater sound level was consistent with the ambient underwater sound in the region (Nedwell *et al.*, 2012).

1.6.1.2 Historically, research relating to both physiological effects and behavioural disturbance of sound on marine receptors has typically been based on determining the absolute sound level for the onset of that effect (whether presented as a single onset threshold or a dose-response/ probabilistic function). Consequently, the available numerical criteria for assessing the effects of sound on marine mammals, fish and shellfish, tend to be based on the absolute sound level criteria, rather than the difference between the baseline sound level and the sound being assessed (Southall *et al.*, 2019).

1.6.1.3 Baseline or background sound levels vary significantly depending on multiple factors, such as seasonal variations and different sea states. Lack of long term measurements/sound data is a widely recognised gap in knowledge in relation to general soundscape and potential effects of human activities on marine life. Understanding the baseline sound level could therefore be valuable in enabling future studies to assess long term effects related to continuous sound levels over time in addition to activity specific effects such as masking impacts. However, the value of establishing the precise baseline sound level is limited in relation to the current assessment methods due to the lack of available evidence-based studies on the effects of sound relative to background levels on marine receptors.

1.7 Source Sound Levels

1.7.1 General

1.7.1.1 Underwater sound source level is usually quantified using a decibel (dB) scale with values generally referenced to 1µPa pressure amplitude as if measured at a distance of 1m from a hypothetical, infinitesimally small point source (sometimes referred to as the Source Level). This quantity is often referred to as an equivalent monopole source level. In practice, it is not usually possible to measure sound at 1m from a large structure, which, in reality, is more akin to a distributed sound source, but the source level metric allows comparisons and reporting of different source sound emissions on a like-for-like basis. As well as a standard input parameter for sound propagation models. In reality, for a large sound source such as a monopile, seismic source array or vessel, the source level value at this conceptual point at 1m from the (theoretical, infinitesimally small) acoustic centre does not exist. Furthermore, the energy is distributed across the source and does not all emanate from this imagined acoustic centre point. Therefore, the stated sound pressure level at 1m does not occur at any point in space for these large sources. In the acoustic near field (i.e. close to the source), the sound pressure level will be significantly lower than the value predicted by the Source Level.

1.7.1.2 A wealth of experimental data and literature-based information is available for quantifying the sound emission from different construction operations. This information, which allows us to predict with a good degree of accuracy the sound generated by a source at discrete frequencies in one-third octave bands, will be employed to characterise their acoustic emission in the underwater environment. Sections 1.7.2 to 1.7.7 detail the types of sound sources present during different construction activities, their potential signatures in different frequency bands, and acoustic levels.

1.7.2 Types of sound sources

1.7.2.1 The sound sources and activities which were investigated during the underwater sound technical report are summarised in Table 1.10.

Table 1.10: Summary of sound sources and activities included in the underwater sound assessment.

Phase	Source/Activity
Pre-Construction	Geophysical site investigation activities including: • Multi-Beam Echo-Sounder (MBES) • Sidescan Sonar (SSS) • Single Beam Echosounder (SBES) • Sub-Bottom Profilers (SBP) • Ultra-High Resolution Seismic (UHRS). Geotechnical site investigation activities including: • Drilling of boreholes • Cone Penetration Tests (CPTs) • Vibrocores. Use of geophysical/geotechnical survey vessels. Clearance of unexploded ordnance (UXOs) including potential use of low-order and low-yield techniques as well as possible high order detonation.
Construction	Impact driven or drilled piled monopile and jacket foundations for wind turbine and Offshore Substation Platforms (OSPs). Vessels used for a range of construction activities including e.g. boulder clearance, sand wave clearance, drilling and trenching. Range of construction vessels including: • Main installation and support vessels • Tug/Anchor handlers • Cable lay installation and support vessels • Guard vessels • Survey vessels (e.g. for geophysical or geotechnical surveys) • Seabed preparation vessels for boulder removal, grapnel, pre-sweep/ levelling • Crew transfer vessels • Scour protection installation vessels • Cable protection installation vessels.
Operational and maintenance	Operational sound from wind turbines. Operational and maintenance vessels, including: • Crew transfer vessels/workboats • Jack-up vessels • Cable repair vessels • Excavators or backhoe dredger.
Decommissioning	Vessels for a range of decommissioning activities, assumed as per vessel activity described for construction phase.

1.7.2.2 The above sources for each project phase are considered in more detail in the following sections.

1.7.3 Pre-construction phase

Geophysical surveys

1.7.3.1 Several sonar like survey source types will potentially be used for the pre-construction site investigation geophysical surveys. During the survey a transmitter emits an acoustic signal directly toward the seabed (or alongside, at an angle to the seabed, in the case of side scan techniques). The equipment likely to be used can typically work at a range of signal frequencies, depending on the distance to the bottom and the required resolution. The signal is highly directional and acts as a beam, with the energy narrowly concentrated within a few degrees of the direction in which it is aimed. The signal is emitted in pulses, the length of which can be varied as per the survey requirements. The assumed pulse rate, pulse width and beam width used in the assessment are based on a review of typical units used in other similar surveys. It should be noted that sonar like survey sources are classed as non-impulsive sound because they generally comprise a single (or multiple discrete) frequency (e.g. a sine wave or swept sine wave) as opposed to a broadband signal with high kurtosis, high peak pressures and rapid rise times.

1.7.3.2 The characteristics assumed for each device modelled in this assessment are summarised in Table 1.11. For the purpose of potential impacts, these sources are considered to be continuous (non-impulsive).

Table 1.11: Typical Sonar based survey equipment parameters used in assessment.

Survey Type	Frequency (kHz)	Source Level, (dB re 1µPa re 1m) (rms)	Pulse Rate, s^{-1}	Pulse Width (ms)	Beam Width
MBES	200 - 500	180 - 240	10	0.3 - 1.5	1 - 10°
SSS	200 - 700	216 - 228	3 - 15	0.1	Horizontal 0.2 - 1.5° Vertical 40 - 55°
SBES	20 - 400	180 - 240	10	0.3 - 1.5	1 - 10°
SBP (pinger and chirp)	0.2 - 14 (chirp) 2 - 7 (pinger)	200 - 240 chirp 200 - 235 pinger	4	1.5	2°

1.7.3.3 The assumed pulse rate has been used to calculate the SEL, which is normalised to one second, from the rms sound pressure level. Directivity corrections were calculated based on the transducer dimensions and ping frequency and taken from manufacturer's datasheets. It is important to note that directivity will vary significantly with frequency, but that these directivity values have been used in line with the modelling assumptions stated above.

1.7.3.4 Unlike the sonar like survey sources, the UHRS source is likely to utilise a sparker, which produces an impulsive, broadband source signal. The parameters used in the underwater sound modelling are summarised in Table 1.12.

Table 1.12: Typical UHRS survey equipment parameters used in assessment.

Source	Peak Frequency (kHz)	Source Level (dB re 1µPa re 1m) (peak)	Source SEL (dB re 1µPa²s re 1m)	Source Level (dB re 1µPa re 1m) (rms)	T90 (ms)
Ultra-high-resolution seismic (sparker)	0.05 - 4	219	182	170-200	0.7

Geotechnical surveys

1.7.3.5 Source sound data for the proposed Cone Penetration Testing (CPTs) was reported by Erbe and McPherson (2017). In this report, the SEL measurements at two different sites in Western Australia at a measured distance of 10m were presented. The signature is generally broadband in nature with levels measured generally 20dB above the baseline sound levels. The report also mentions other paths for acoustic energy including direct air to water transmission and other multipath directions, which implied that measured sound level is strongly dependant on depth and range from the source. The third octave band SEL levels from the CPT extracted are presented in Table 1.13.

Table 1.13: CPT source levels in different third octave band frequencies (SEL metric) used for the assessment (Erbe and McPherson, 2017).

SEL (dB re 1µPa²s)	Third Octave Band Centre Frequency (kHz)									
	0.016	0.0315	0.063	0.125	0.25	0.5	1	2	4	8
189	173	173	164	163	172	177	180	182	184	182

1.7.3.6 Seismic CPT sound is classified as impulsive at source since it has a rapid rise time and a high peak sound pressure level of 220dB re 1µPa (pk), compared to a SEL of 189dB re 1µPa²s.

1.7.3.7 The seismic CPT test is typically conducted at various depths for each location every three to five minutes with between 10 and 20 strikes per depth.

1.7.3.8 It should be noted that if non-seismic CPT were to be used, the sound would be considered non-impulsive if it produced any sound at all, and therefore the assessment of seismic CPT is considered precautionary.

1.7.3.9 Measurements of a vibro-core test (Reiser *et al.*, 2011) show underwater source sound pressure levels of approximately 187dB re 1µPa re 1m (rms). The SEL has been calculated based on a one hour sample time which, it is understood, is the typical maximum time required for each sample. The vessel would then move on to the next location and take the next sample with approximately one-hour break between each operation. The vibro-core sound is considered to be continuous (non-impulsive).

Table 1.14: Vibro-core source levels used in the assessment.

Parameter	Source Level	Unit
SEL (unweighted) – based on one-hour operation for single core sample	223	dB re 1µPa²s re 1m
RMS T90	187	dB re 1µPa re 1m
Peak	190	dB re 1µPa re 1m

1.7.3.10 The frequency spectral shape for vibro-coring is presented in Figure 1.7.

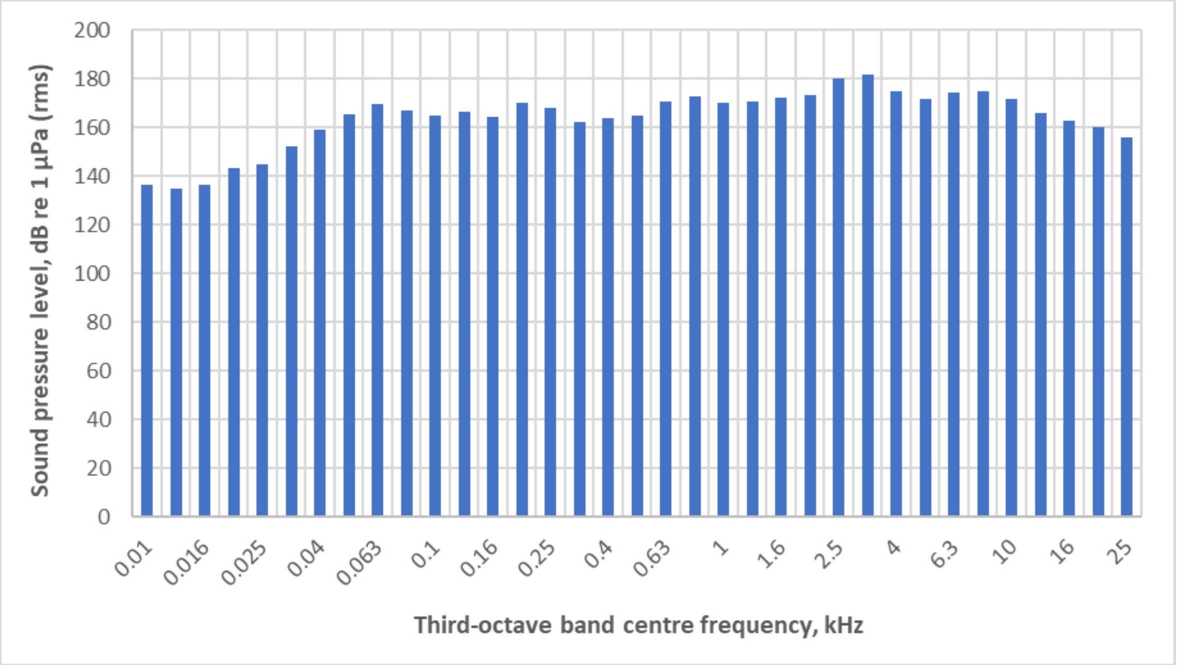

Figure 1.7: Frequency spectral shape used for vibro-coring.

1.7.3.11 Source levels for borehole drilling ahead of standard penetration testing was reported in Erbe and McPherson (2017), with source levels of 142dB to 145dB re 1µPa re 1m (rms). A set of one third octave band levels, calculated from the spectrum presented in the paper are shown in Figure 1.8.

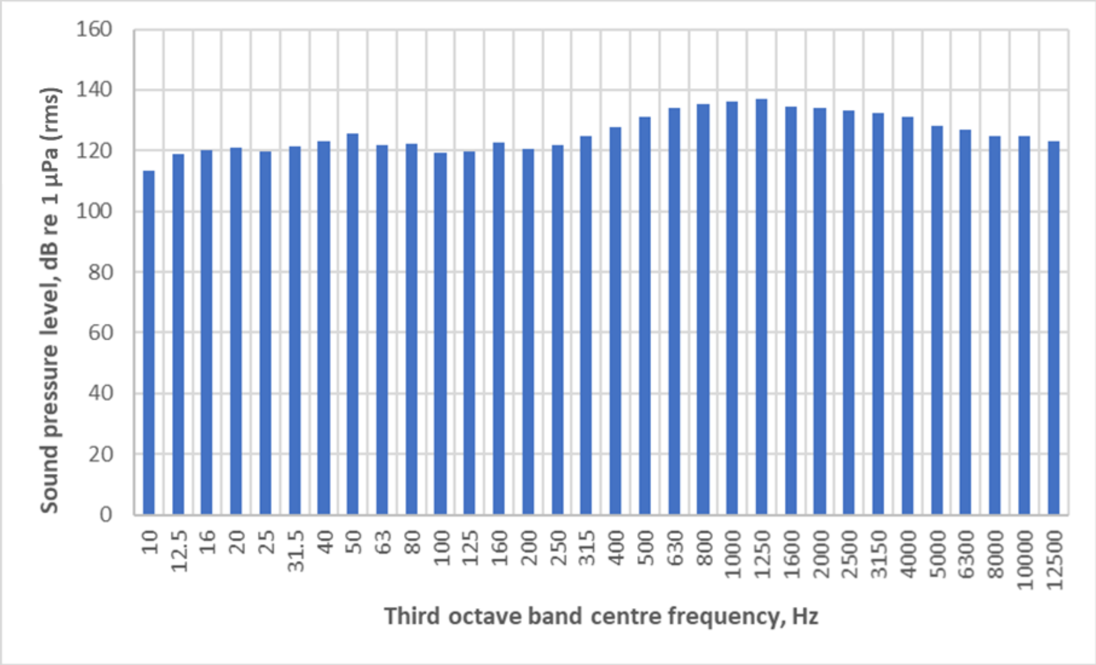

Figure 1.8: Borehole drilling source level spectrum shape used in the assessment.

1.7.3.12 As for other non-impulsive sources, impact assessment criteria is the SEL metric for a receptor moving away from the source.

UXO clearance

1.7.3.13 The precise details and locations of potential UXOs is unknown at this time. For the purposes of this assessment, it has been assumed that the Maximum Design Scenario (MDS) will be clearance of UXO with a Net Explosive Quantity (NEQ) of 907kg cleared by either low order or high order techniques. Low order techniques are not always possible and are dependent upon the individual situations surrounding each UXO.

1.7.3.14 There are a number of low-order and low-yield techniques available for the clearance of UXO, with the development of new techniques being a subject of ongoing research. For example, one such technique (deflagration) uses a single charge of 30g to 80g NEQ which is placed in close proximity to the UXO to target a specific entry point. When detonated, a shaped charge penetrates the casing of the UXO to introduce a small, clinical plasma jet into the main explosive filling. The intention is to excite the explosive molecules within the main filling to generate enough pressure to burst the UXO casing, producing a deflagration of the main filling and neutralising the UXO.

1.7.3.15 Recent controlled experiments showed low-order deflagration to result in a substantial reduction in acoustic output over traditional high order methods, with SPL_{pk} and SEL being typically significantly lower for the deflagration of the same size munition, and with the acoustic output being proportional to the size of the shaped charge, rather than the size of the UXO itself (Robinson *et al.*, 2020). Using this low order deflagration method, the probability of a low order outcome is high; however, there is a small inherent risk with these clearance methods that the UXO will detonate or deflagrate violently resulting in higher sound level emissions.

1.7.3.16 It is possible that there will be residual explosive material remaining on the seabed following the use of low order techniques for unexploded ordnance disposal. In this case, and only for debris of sufficient size to be a risk to fishing activities, recovery will be performed which includes the potential use of a small (500g) 'clearing shot'.

1.7.3.17 Alternatively, a low-yield clearance technique could be utilised for UXOs utilising two 750g donor charges, or four 750g donor charges in the case of German ground mines.

1.7.3.18 As a last resort, if it is not possible to carry out low-order or low-yield clearance techniques, it may be necessary to carry out a high order detonation of the UXO. These are likely to range between 25kg to 907kg, with the most common UXO size likely to be in the order of 130kg.

1.7.3.19 The underwater sound modelling has been undertaken exemplarily for a range of charge configurations as set out in Table 1.15.

Table 1.15: Details of UXO and their relevant charge sizes employed for modelling.

Charge Size (kg NEQ)	Notes/Assumptions
Low-order and low-yield donor charge configurations	
0.08kg	Maximum size of donor charge used for low-order technique.
0.5kg	Maximum size of clearing shot to neutralise any residual explosive material.
2 x 0.75kg	Charge configuration for low-yield technique for most UXO.
4 x 0.75kg	Maximum charge configuration for low-yield technique (for German ground mines).
High-order donor charge options	
1.2kg	Most common donor charge for high-order UXO disposal.
3.5kg	Single barracuda blast-fragmentation charge for high-order disposal.
Potential UXOs (high-order disposal)	
25kg	Smallest potential UXO size.
130kg	Most common/likely (based on estimated number of devices) UXO size.
907kg	Maximum estimated UXO size.

1.7.3.20 The source levels for UXO are included within the terms for propagation modelling and are described in section 1.8.5.

1.7.4 Construction phase

Impact piling

1.7.4.1 The sound generated and radiated by a monopile as it is driven into the ground is complex, due to the many components which make up the generation and radiation mechanisms. Larger pile sizes can require a higher energy in order to drive them into the seabed. Different seabed and underlying substrate types can require use of different installation techniques including varying the hammer energies and the number of hammer strikes. In addition, the seabed characteristics can affect how sound propagates from the monopile through the sub-surface geology, thus fundamentally affecting the acoustic field around the activity. The type of hammer method used (i.e. the force-impulse characteristics) can also affect the sound emission characteristics.

1.7.4.2 A useful measure of sound used in underwater acoustics is the Sound Exposure Level, or SEL. This descriptor is used as a measure of the total sound energy of an event or a number of events (e.g., over the course of a day) and is normalised to one second. This allows the total acoustic energy contained in events lasting a different amount of time to be compared on a like for like basis. For impulsive sounds it has become customary to utilise the T90 time period for calculating and reporting rms sound pressure levels. This is the interval over which the cumulative energy curve rises from 5% to 95% of the total energy and therefore contains 90% of the sound energy.

1.7.4.3 It is common practice for sound modelling studies for UK offshore wind farms to estimate source levels for piling based on existing measurements of other similar piles, extrapolation of data or assumptions about the percentage of the hammer energy which is emitted into the water as sound. Such methods are useful for estimating source levels for piling for pile sizes, installation methodologies and hammer energies that are similar to those for which measurement data already exist. However, potentially widescale errors could occur by extrapolating these measurement data well beyond the scale of the operations for which they were intended.

1.7.4.4 For the Mona Offshore Wind Project, it is proposed to use monopiles which are of a significantly larger diameter than those for which any real-world measurement data is publicly available (e.g. potential monopile foundations of up to 16m diameter). Consequently, it is considered that the use of existing empirical data for smaller monopile dimensions would not be a suitably robust method to use for estimating the source level for impact piling for the Mona Offshore Wind Project.

Pile source modelling method

1.7.4.5 The source sound modelling methodology for piling has used a finite element (FE) model that was set up for a representative location of the site, applying the pile design and the surrounding soil conditions. The FE model allows for a detailed calculation of the excitation force due to the hammer, the resulting pile and soil reactions as well as the nearfield sound propagation in the water column. The general modelling approach exhibits a number of feasible simplifications, such as the reduction to a 2-dimensional rotational-symmetric problem, partly homogenised soil parameters, etc. and has been thoroughly validated within multiple measurement campaigns (Lippert *et al.* 2016; von Pein *et al.* 2017; 2019; 2021).

1.7.4.6 The methodology is capable of taking into account a number of variables including:

- Monopile geometries (e.g. diameter, wall thickness, profile)
- Water depth at the pile locations and surrounding bathymetry
- Sound velocity profiles in the soil at the pile locations (definition of s-wave and p-wave velocities and density for each soil layer)
- Specification of the type of impact hammer, the connecting devices between hammer and pile (like anvil, anvil ring, follower, etc), and the energy level
- Hammer type and energy, including velocity and force time profiles to describe the excitation by the hammer impact acting at the pile head.

1.7.4.7 The detailed pile source modelling report is provided in Appendix A. A summary of the resulting source levels is shown in Table 1.16.

Table 1.16: Summary of source modelling results for piles.

Case	Type	Diameter (top/bottom)	Penetration case	Hammer energy, kJ	SEL @ 750m, dB re 1µPa	SPL_{pk} @ 750m, dB re 1µPa^{2}s	Source SEL re 1m, dB re 1µPa^{2}s
Mona Offshore Wind Project, case C3-50	Mono	12/16	50% penetration	5500	184	202	226
Mona Offshore Wind Project, case C3-100	Mono	12/16	final penetration	5500	183	203	225
Mona Offshore Wind Project, case D3-50	Pin	5.5	pile head flush with sea surface	3700	180	201	221
Mona Offshore Wind Project, case D3-100	Pin	5.5	final penetration	3700	170	189	213

1.7.4.8 In addition to the modelled hammer energy scenarios, an estimation of the effect on the sound levels when changing the hammer energy in the range between minimum and maximum hammer energy has been performed based on a linear scaling law.

1.7.4.9 The spectral distribution of the source SELs for impact piling have been based on the detailed pile source level study (Appendix A). For frequencies above 2 kHz, these have been supplemented from the reference spectrum provided in De Jong and Ainslie (2008). The resulting spectrum shapes are reproduced in Figure 1.9.

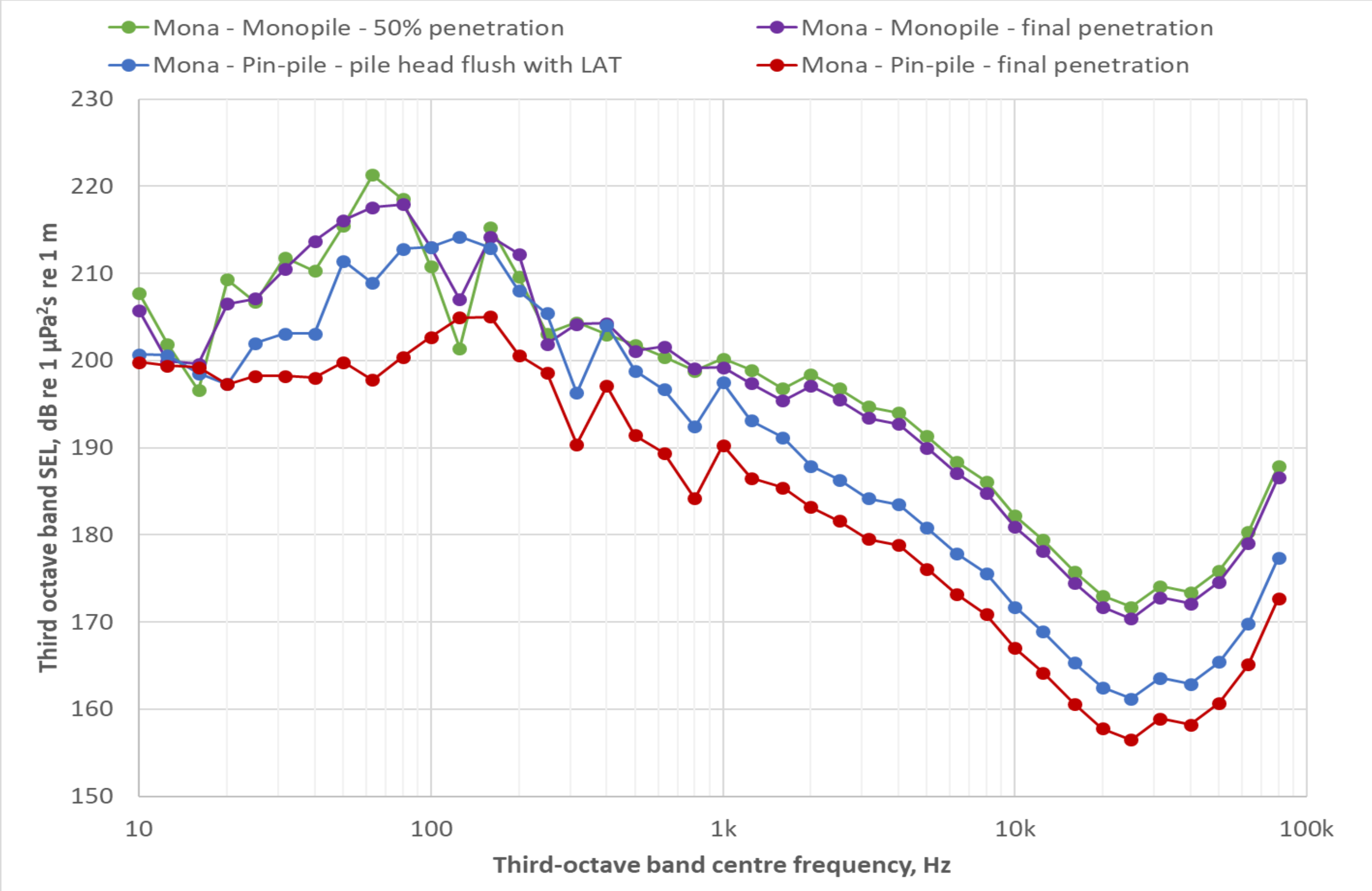

Figure 1.9: Impact piling source frequency distribution used in the assessment.

1.7.4.10 The impact piling scenarios that have been modelled for the Mona Offshore Wind Project are:

- Wind turbine foundations (Monopile) MDS 24MW turbines (largest turbine) using an absolute maximum hammer energy of 5,500 kJ for the longest possible duration (up to 9.5 hours) (see Table 1.17)
- Wind turbine foundations (Piled Jacket) MDS 24MW (see Table 1.18) using a maximum hammer energy of 2,800 kJ for a duration of up to 6.5 hours
- OSP Foundations (Monopile and Jacket) MDS – using a maximum hammer energy and durations defined above for wind turbine foundations.

Table 1.17: Impact piling schedule used in assessment - wind turbine and OSP foundations (MDS for monopiles).

Activity / stage	Duration, minutes	Hammer Energy, kJ	Strike Rate (strikes per minute)	Number of strikes	Notes/description
Initiation	10	550	0.67	7	Slow start to allow for alignment etc., 1 strike every 90 seconds
Soft start	20	550	10	200	Soft start at low hammer energy
Ramp up	20	550 to 5,000	15	300	Ramp up in hammer energy after soft start period
Full power piling	520	5,500	40	20,800	Hard driving using maximum hammer energy
Total piling duration, mins	570				
Total piling duration, hours	9.5				
Total no. of strikes	21,307				

Table 1.18: Impact piling schedule used in assessment – wind turbine and OSP foundations (MDS for pin-piles).

Activity/stage	Duration, minutes	Hammer Energy, kJ	Strike Rate (strikes per minute)	Number of strikes	Notes/description
Initiation	10	300	0.67	7	Slow start to allow for alignment etc., 1 strike every 90 seconds
Soft start	20	300	10	200	Soft start at low hammer energy
Ramp up	20	300 to 2,500	15	300	Ramp up in hammer energy after soft start period
Full power piling	331	2,800	40	13,240	Hard driving using maximum hammer energy
Total piling duration, mins	381				
Total piling duration, hours	6hrs 21 minutes				
Total no. of strikes	13,747				

1.7.4.11 The piling of wind turbine foundations described in Table 1.18 was also modelled with the inclusion of an Acoustic Deterrent Device (ADD) before commencement of piling. Use of an ADD was modelled for a duration of 30 minutes prior to commencement of piling, all other stages of piling remained the same, and the ADD itself was assumed to not contribute towards any animal injury effects (Boisseau et al. 2021). This effectively allows the animal 30 minutes to move away from the sound source before the start of piling. It should be noted that the use of an ADD decreases the effective cumulative SEL PTS and TTS range because the animal can move further from the pile before being exposed to piling sound. In the case of peak PTS and TTS thresholds (i.e. potential for instantaneous auditory injury) the potential radius at which the threshold could be exceeded remains the same, although it is possible that the animal will swim outside the injury range before piling commences, effectively reducing the peak SPL injury range to zero.

Drilled piles

1.7.4.12 For drilled piling, source sound levels have been based on pile drilling for the Oyster 800 project (Kongsberg, 2011). The hydraulic rock breaking source sound levels are based on those measured by Lawrence (2016). The source levels used in the assessment are summarised in Table 1.19.

1.7.4.13 Rotary drilling is non-impulsive in character and therefore the non-impulsive injury and behavioural thresholds have been adopted for the assessment.

Table 1.19: Drilled pile sound source levels used in assessment (un-weighted).

Parameter	Source Level at 1m
SEL per second of operation @ 1m, dB re 1µPa²s	163
Peak sound pressure level @ 1m, dB re 1µPa	166
rmsT90 sound pressure level @ 1m, dB re 1µPa	163

1.7.4.14 The other sound source potentially active during the construction phase are related to cable installation (i.e. trenching and cable laying activities), and their related operations such as the jack-up rigs. The SEL based source levels are presented in Table 1.20.

Table 1.20: SEL based source levels for other sources.

Sources	Data Source	RMS (dB re 1µPa)	Frequency (Hz)											
			16	31.5	63	125	250	500	1k	2k	4k	8k	16k	31.5k
Cable laying	Wyatt (2008)	180	168	166	166	165	162	157	153	155	138	131	125	161
Cable trenching /cutting	Nedwell *et al.* (2003)	178	135	135	148	161	167	169	167	162	157	148	142	141
Jack up rig	Nedwell and Edwards (2004)	163	120	132	141	148	148	152	149	143	148	152	145	139

Vessels

1.7.4.15 Use of vessels is addressed in section 1.7.7 for all phases of the Mona Offshore Wind Project.

1.7.5 Operational and maintenance phase

Operational sound from turbines

1.7.5.1 Underwater sound from the operational wind turbine generators has been estimated based on the methodology presented in Tougaard *et al.* (2020). The paper provides an empirical relationship between wind turbine power, wind speed and distance from the wind turbine in order to estimate the received sound level. The received sound level is estimated using the formula:

$$L_{eq} = C + \alpha\, log_{10}\left(\frac{distance}{100\ m}\right) + \beta\, log_{10}\left(\frac{wind\ speed}{10\ m/s}\right) + \gamma\, log_{10}\left(\frac{turbine\ size}{1\ MW}\right)$$

where α = 23.7dB/decade, β = 18.5dB/decade, γ = 13.6dB/decade and C = 109dB re 1µPa (rms).

1.7.5.2 Calculations were performed for the maximum potential wind turbine size using a 10 m/s wind speed (Volume 1, chapter 3: Project Description of the PEIR). The 10m/s wind speed assumption is considered reasonable because it is representative of the average annual wind speeds in the Mona Array Area. It should be noted that during periods of higher wind speeds the sound level produced by the wind turbines will increase, although it is likely that the ambient sound levels will also increase due to higher wind speeds and wave conditions during these periods, which may result in additional masking of wind turbine sounds.

1.7.5.3 A reference spectrum based on that reported by Pangerc *et al.* (2016) was used for the calculation of hearing weighted SELs (which in turn were based on a static animal assumption for simplicity of calculation).

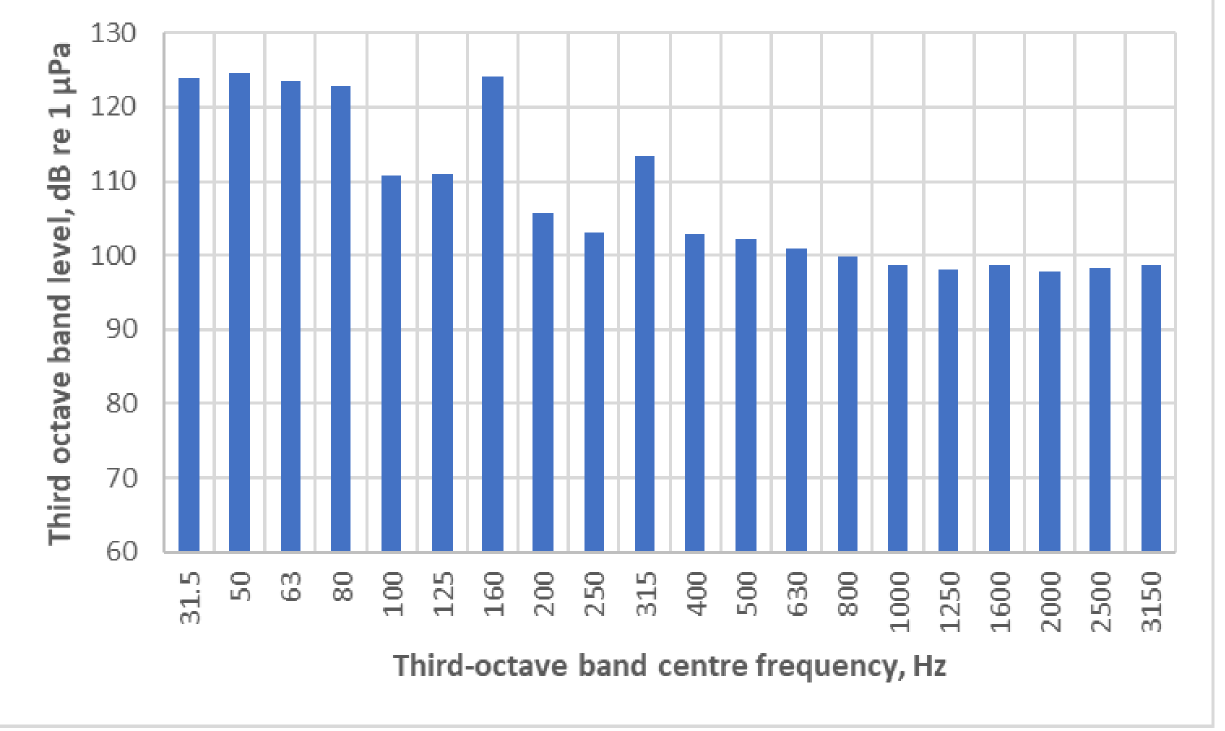

Figure 1.10: Operational wind turbine frequency distribution used in the assessment.

Geophysical surveys

1.7.5.4 Routine geophysical surveys will be similar to the geophysical surveys already discussed for the pre-construction phase (see section 1.7.3).

Routine operational and maintenance

1.7.5.5 There are very few activities during the operational and maintenance phase that generate significant amounts of underwater sound. The source level for the general operations carried out in the operational and maintenance phase such as the jet cutting operation, which is considered to be the activity with the highest sound level, is presented in Table 1.21.

Table 1.21: SEL based octave band levels used for different operations in this phase.

Source	SEL Broadband Level	Frequency (kHz)											
		0.016	0.0315	0.063	0.125	0.25	0.5	1	2	4	8	16	31.5
Jet cutting	195	167	170	173	176	179	182	185	185	181	175	166	157

Vessels

1.7.5.6 The potential for vessel use to create underwater sound is presented in section 1.7.7 for all phases of the Mona Offshore Wind Project.

1.7.6 Decommissioning phase

Vessels

1.7.6.1 As agreed with stakeholders during the pre-Application consultation phase, only the potential impact of sound from vessel activity has been scoped into the underwater sound assessment for the decommissioning phase of the Mona Offshore Wind Project. It should be noted that cavitation from the vessels themselves is likely to dominate the soundscape for other decommissioning activities (e.g. removal of subsea structures). The potential impact of vessels sound emissions is addressed in section 1.7.7 for all phases of the Mona Offshore Wind Project.

1.7.7 Vessels (all phases)

1.7.7.1 The sound emissions from the types of vessels that may be used for the Mona Offshore Wind Project are quantified in Table 1.22, based on a review of publicly available data. Sound from the vessels themselves (e.g. propeller, thrusters and sonar (if used)) primarily dominates the emission level, hence sound from activities such as seabed preparation, trenching and rock placement (if required) have not been included separately.

1.7.7.2 In Table 1.22, a correction of +3dB has been applied to the rms sound pressure level to estimate the likely peak sound pressure level. SELs have been estimated for each source based on 24 hours continuous operation, although it is important to note that it is highly unlikely that any marine mammal or fish would stay at a stationary location or within a fixed radius of a vessel (or any other sound source) for 24 hours. Consequently, the acoustic modelling has been undertaken based on an animal swimming away from the source (or the source moving away from an animal). Source sound levels for vessels depend on the vessel size and speed as well as propeller design and other factors. There can be considerable variation in sound magnitude and character between vessels even within the same class. Therefore, source data for the Mona Offshore Wind Project has been based on MDS assumptions (i.e. using sound data toward the higher end of the scale for the relevant class of ship as a proxy). In the case of the cable laying vessel, no publicly available information was available for a similar vessel and therefore measurements on a suction dredger using Dynamic Positioning (DP) thrusters was used as a proxy. This is considered an appropriate proxy because it is a similar size of vessel using dynamic positioning and therefore likely to have a similar acoustic footprint.

Table 1.22: Source sound data for construction, installation and operation vessels.

Item	Description/ Assumptions	Data Source	Source SPL at 1m		
			RMS (dB re 1μPa)	Peak (dB re 1μPa)	SEL(24h) (dB re 1μPa²s)
Sandwave clearance	'Gerardus Mercator' trailer hopper suction dredger using dynamic positioning (DP) as proxy	Wyatt *et al.* (2020)	180	183	229
Boulder clearance, floating crane vessel	Back-hoe dredger used as proxy	Nedwell *et al.* (2008)	163	166	212
Main Installation Vessels (Jack-up Barge/DP vessel)	'Gerardus Mercator' trailer hopper suction dredger using DP as proxy	Wyatt *et al.* (2020)	180	183	229
Jack up rig/jack up vessel	Jack up rig	Evans (1996)	163	166	212
Tug/Anchor Handlers	Tug used as proxy	Richardson (1995)	172	175	221
Cable Installation Vessels	'Gerardus Mercator' trailer hopper suction dredger using DP as proxy	Wyatt *et al.* (2020)	180	183	229
Rock Placement Vessels	'Gerardus Mercator' trailer hopper suction dredger using DP as proxy	Wyatt *et al.* (2020)	180	183	229
Guard Vessels	Tug used as proxy	Richardson (1995)	172	175	221

Item	Description/ Assumptions	Data Source	Source SPL at 1m		
			RMS (dB re 1µPa)	Peak (dB re 1µPa)	SEL(24h) (dB re 1µPa^{2}s)
Survey Vessels	Offshore support vessel used as proxy	McCauley (1998)	179	182	228
Crew Transfer Vessels, Service Operation Vessels	Offshore support vessel used as proxy	McCauley (1998)	179	182	228
Scour/Cable Protection/Seabed Preparation/Installation Vessels	Offshore support vessel used as proxy	McCauley (1998)	179	182	228

1.8 Propagation Modelling

1.8.1 Propagation of sound underwater

1.8.1.1 As the distance from the sound source increases the level of received or recorded sound reduces, primarily due to the spreading of the sound energy with distance, in combination with attenuation due to absorption of sound energy by molecules in the water. This latter mechanism is more important for higher frequency sound than for lower frequencies.

1.8.1.2 The way that the sound spreads (geometrical divergence) will depend upon several factors such as water column depth, pressure, temperature gradients, salinity as well as water surface and bottom (i.e., seabed) conditions. Thus, even for a given locality, there are temporal variations to the way that sound will propagate. However, in simple terms, the sound energy may spread out in a spherical pattern (close to the source) or a cylindrical pattern (much further from the source), although other factors mean that decay in sound energy may be somewhere between these two simplistic cases. The distance at which cylindrical spreading dominates is highly dependent on water depth. Sound propagation in shallow water depths will be dominated by cylindrical spreading as opposed to spherical spreading.

1.8.1.3 In acoustically shallow waters[11] in particular, the propagation mechanism is influenced by multiple interactions with the seabed and the water surface (Lurton, 2002; Etter, 2013; Urick, 1983; Brekhovskikh and Lysanov, 2014; Kinsler *et al.*, 1999). Whereas in deeper waters, the sound will propagate further without encountering the surface or bottom of the sea (seabed)

1.8.1.4 At the sea surface, the majority of the sound is reflected into the water due to the difference in acoustic impedance (i.e. product of sound speed and density) between air and water. However, the scattering of sound at the surface of the sea can be an important factor in the propagation of sound. In an ideal case (i.e. for a perfectly smooth sea surface), the majority of sound energy will be reflected into the sea. However, for rough seas, much of the sound energy is scattered (e.g. Eckart, 1953; Fortuin, 1970; Marsh, Schulkin, and Kneale, 1961; Urick and Hoover, 1956). Scattering can also occur due to bubbles near the surface such as those generated by wind or fish or due to suspended solids in the water such as particulates and marine life. Scattering is more pronounced for higher frequencies than for low frequencies and is dependent on the sea state (i.e. wave height). However, the various factors affecting this mechanism are complex.

1.8.1.5 Because surface scattering results in differences in reflected sound, its effect will be more important at longer ranges from the sound source and in acoustically shallow water (i.e. where there are multiple reflections between the source and receiver). The degree of scattering will depend upon the sea state/ wind speed, water depth, frequency of the sound, temperature gradient, grazing angle and range from source. It should be noted that variations in propagation due to scattering will vary temporally within an area primarily due to different sea-states/ wind speeds at different times. However, over shorter ranges (e.g. several hundred meters or less) the sound will experience fewer reflections and so the effect of scattering should not be significant.

1.8.1.6 When sound waves encounter the seabed, the amount of sound reflected will depend on the geoacoustic properties of the bottom (e.g. grain size, porosity, density, sound speed, absorption coefficient and roughness) as well as the grazing angle and frequency of the sound (Cole, 1965; Hamilton, 1970; Mackenzie, 1960; McKinney and Anderson, 1964; Etter, 2013; Lurton, 2002; Urick, 1983). Thus, seabeds comprising primarily mud or other acoustically soft sediments will reflect less sound than acoustically harder bottoms such as rock or sand. This will also depend on the profile of the bottom (e.g. the depth of the sediment layer and how the geoacoustic properties vary with depth below the seafloor). The effect is less pronounced at low frequencies (a few kHz and below). A scattering effect (similar to that which occurs at the surface) also occurs at the seabed (Essen, 1994; Greaves and Stephen, 2003; McKinney and Anderson, 1964; Kuo, 1992), particularly on rough substrates (e.g. pebbles).

1.8.1.7 The waveguide effect should also be considered, which defines the shallow water columns that do not allow the propagation of low frequency sound (Urick, 1983; Etter, 2013). The cut-off frequency of the lowest mode in a channel can be calculated based on the water depth and knowledge of the sediment geoacoustic properties but, for example, the cut-off frequency as a function of water depth (based on the equations set out in Urick, 1983) is shown in Figure 1.11 for a range of seabed types. Any sound below this frequency will not propagate far due to energy losses through multiple reflections.

[11] Acoustically, shallow water conditions exist whenever the propagation is characterised by multiple reflections with both the sea surface and bottom (Etter, 2013).Consequently, the depth at which water can be classified as acoustically deep or shallow depends upon numerous factors including the sound speed gradient, water depth, frequency of the sound and distance between the source and receiver.

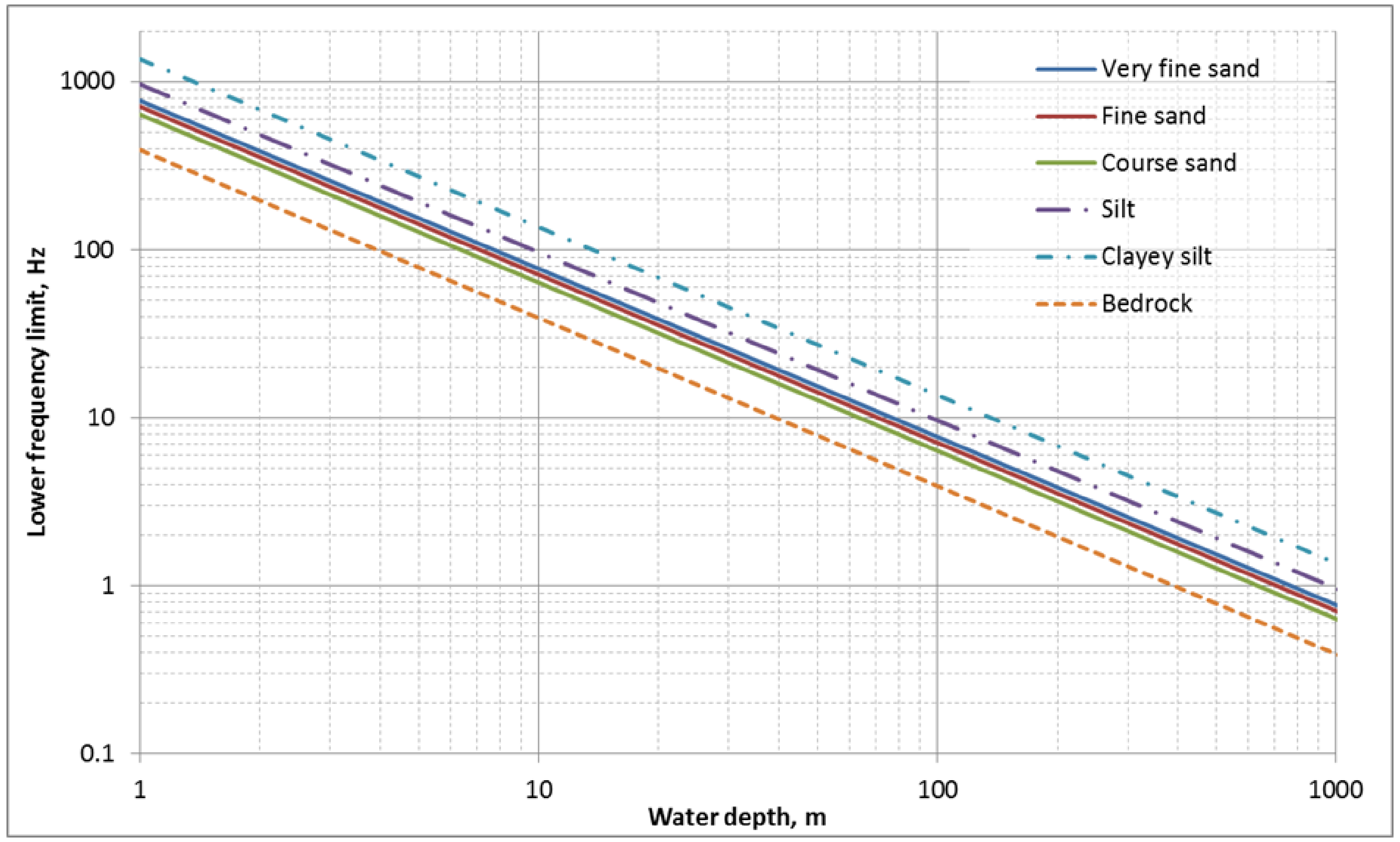

Figure 1.11: Lower cut-off frequency as a function of depth for a range of seabed types

1.8.1.8 Changes in the water temperature and the hydrostatic pressure with depth mean that the speed of sound varies throughout the water column. This can lead to significant variations in sound propagation and can also lead to sound channels, particularly for high-frequency sound (Lurton 2002). Sound can propagate in a duct-like manner within these channels, effectively focussing the sound, and conversely, they can also lead to shadow zones. The frequency at which this occurs depends on the characteristics of the sound channel and since the temperature gradient can vary throughout the year there will be potential variation in sound propagation depending on the season.

1.8.1.9 Sound energy is also absorbed due to interactions at the molecular level converting the acoustic energy into heat (Urick 1983). This is another frequency-dependent effect with higher frequencies experiencing much higher losses than lower frequencies.

1.8.2 Modelling approach

1.8.2.1 There are several methods available for modelling the propagation of sound between a source and receiver ranging from very simple models which simply assume spreading effects according to a 10 log (R) or 20 log (R) relationship (as discussed above, and where R is the range from source) to full acoustic models (e.g. ray tracing, normal mode, parabolic equation, wavenumber integration and energy flux models). In addition, semi-empirical models are available, whose complexity and accuracy are somewhere in between these two extremes.

1.8.2.2 In choosing the correct propagation model to employ, it is important to ensure that it is fit for purpose and produces results with a suitable degree of accuracy for the application in question, taking into account the context, as detailed in “Monitoring Guidance for Underwater Noise in European Seas Part III”, NPL Guidance, (Dekeling *et al.*, 2014) and in Farcas *et al.* (2016). Thus, in some situations (e.g. low risk of auditory injury due to underwater sound, where range dependent bathymetry is not an issue, i.e. for non-impulsive sound) a simple (N log R) model might be sufficient, particularly where other uncertainties (such as uncertainties in source level or the impact thresholds) outweigh the uncertainties due to modelling. On the other hand, some situations (e.g. very high source levels, impulsive sound, complex source and propagation path characteristics, highly sensitive receivers, and low uncertainties in assessment criteria) warrant a more complex modelling methodology.

1.8.2.3 The first step in choosing a propagation model is therefore to examine these various factors, such as:

- Balancing of errors/uncertainties
- Range dependant bathymetry
- Frequency dependence
- Source characteristics.

1.8.2.4 For the sound field model, relevant survey parameters were chosen based on a combination of data provided by the Applicant combined with the information gathered from the publicly available literature. These parameters were fed into an appropriate propagation model routine, in this case the Weston Energy Flux model (for more information see Weston, 1971; 1980a; 1980b), suited to the region and the frequencies of interest. The frequency-dependent loss of acoustic energy with distance (TL) values were then evaluated along different transects around the chosen source points. The frequencies of interest in the present study are from 20Hz to 1,000 kHz (1 MHz), with different sound sources operating in different frequency bands. These frequencies overlap with the hearing sensitivities (as per Figure 1.4) of some of the marine mammals that are likely to be present in the Mona Array Area.

Table 1.23: Regions of transmission loss derived by Weston (1971).

Region	Transmission Loss	Range of validity
Spherical	$TL = 10\log_{10}[R^2]$	$R < \frac{H_a}{2\theta_c}$
Channelling	$TL = 10\log_{10}\left[\frac{RH_aH_b}{2H_c\theta_c}\right]$	$\frac{H_a}{2\theta_c} < R < \frac{6.8H_a}{\alpha\theta_c^{\,2}}$
Mode stripping	$TL = 10\log_{10}\left[\frac{RH_aH_b}{5.22}\left(\alpha\int_0^R\frac{dR}{H^3}\right)^{1/2}\right]$	$\frac{6.8H_a}{\alpha\theta_c^{\,2}} < R < \frac{27k^2H_a^{\,3}}{(2\pi)^2\alpha}$
Single mode	$TL = 10\log_{10}\left[\frac{RH_aH_b}{\lambda}\right] + \frac{\lambda^2\alpha}{8}\int_0^R\frac{dR}{H^3}$	$R > \frac{27k^2H_a^{\,3}}{(2\pi)^2\alpha}$

1.8.2.5 The propagation loss is calculated using one for the four formulae detailed in the table above, depending on the distance of the receiver location from the source, and related to the frequency and the seafloor conditions such as depth and its composition.

1.8.2.6 In Table 1.23, H_a is the depth at the source, H_b is the depth at the receiver, H_c is the minimum depth along the bathymetry profile (between the source and the receiver), θ_c is the critical grazing angle (related to the speed of sound in both seawater and the seafloor material), λ and k are the wavelength and wavenumber as usual, and α is the seabed reflection loss gradient, empirically derived to be 12.4dB/rad in Weston (1971).

1.8.2.7 The spherical spreading region exists in the immediate vicinity of the source, which is followed by a region where the propagation follows a cylindrical spread out until the grazing angle is equal to the critical grazing angle θ_c. Above the critical grazing angle in the mode stripping region an additional loss factor is introduced which is due to seafloor reflection loss, where higher modes are attenuated faster due to their larger grazing angles. In the final region, the single-mode region, all modes but the lowest have been fully attenuated.

1.8.2.8 For estimation of propagation loss of acoustic energy at different distances away from the sound source location (in different directions), the following steps were considered:

- The bathymetry information around this chosen source points were extracted from the GEBCO database up to 120km (where possible, for example where not interrupted by land) in 72 different transects
- A geoacoustic model of the different seafloor layers in the survey region was calculated
- A calibrated Weston Energy model was employed to estimate the TL matrices for different frequencies of interest (from 25Hz to 80kHz) along the 72 different transects
- The calculated source level values were combined with the TL results to achieve a frequency and range dependant RL of acoustic energy around the chosen source position
- The TTS and PTS potential impact distances for different marine mammal groups were calculated using relevant metrics and weighting functions (from Southall *et al.*, 2019) and by employing a simplistic animal movement model (directly away from the sound source) where appropriate
- The Weston model was calibrated against the results of the hybrid FE/ PE model in order to ensure consistency. A further calibration was performed against the AcTUP PE and NM models.

1.8.2.9 The propagation and sound exposure calculations were conducted over a range of locations representing different geoacoustic conditions, water column depths and proximities to receptors to determine the likely range for injury and disturbance. The choice of locations was based on the extremities of the Project area and proximity to the various Special Areas of Conservation (SACs). The modelling points chosen are as follows:

- Southwest boundary to assess potential impact on the North Anglesey Marine harbour porpoise SAC to the west as well as herring spawning off east coast of Isle of Man and grey seals at Calf of Man
- Southeast boundary of the array to capture the other main water depth and also allow for assessment of potential impact on the seals at Hilbre Point
- North/ northwest boundary of the Mona Array Area to capture herring spawning off east coast of Isle of Man and grey seals at Calf of Man.

1.8.2.10 These points are shown in Figure 1.12, along with an example of the modelling transects or “spokes” used in the sound propagation modelling.

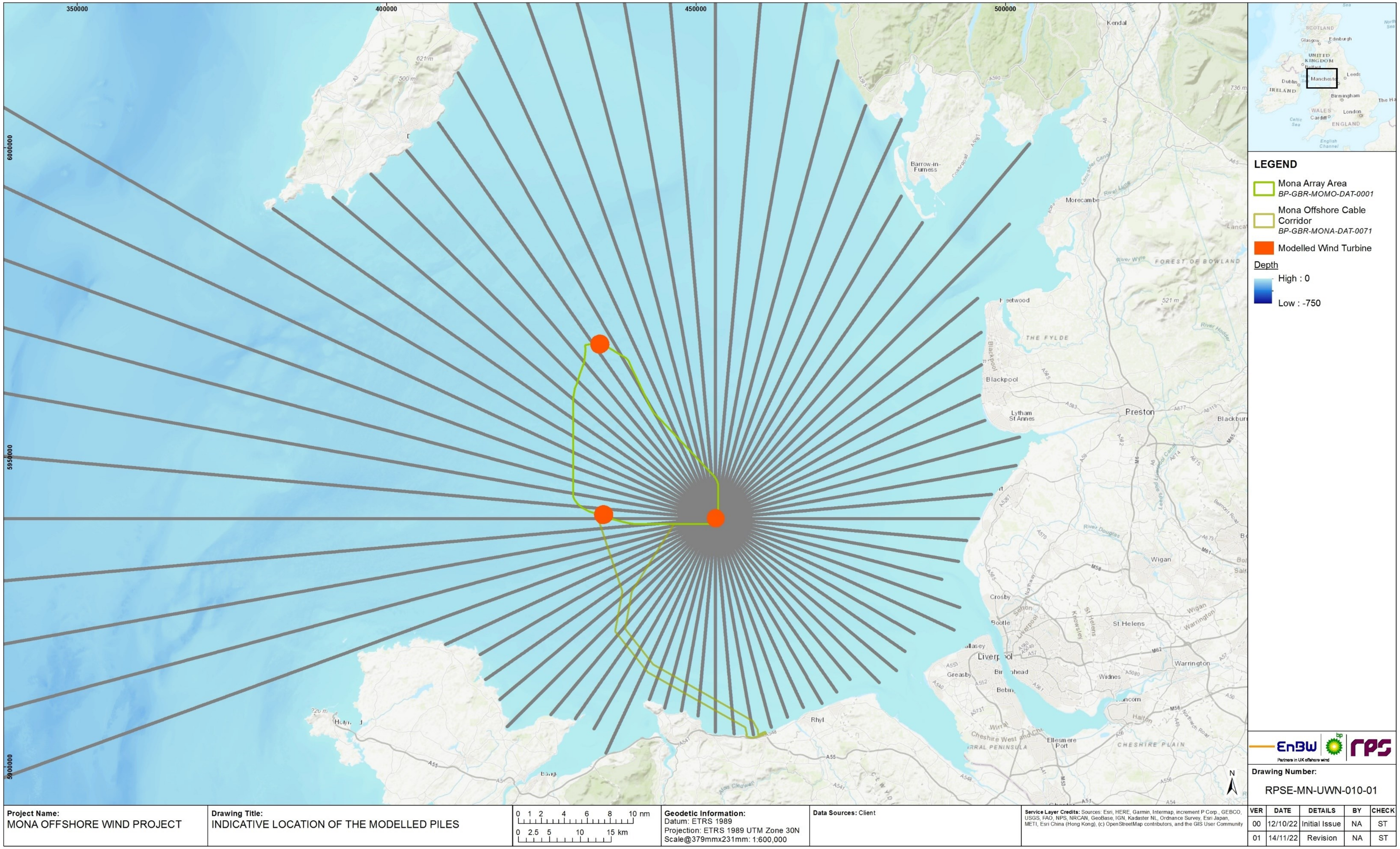

Figure 1.12: Indicative location of the modelled piles (red circles) in the Mona Offshore Wind Project, general bathymetry depth (darker is deeper water), and an example of the different transects employed for the study radiating out from one of the modelled source locations.

1.8.2.11 It should be noted that sound levels (and associated range of effects) will vary depending on actual conditions at the time (day-to-day and season-to-season) and that the model predicts a typical MDS. Considering factors such as animal behaviour and habituation, any injury and disturbance ranges should be viewed as indicative and probabilistic ranges to assist in understanding potential impacts on marine life rather than lines either side of which a potential impact will or will not occur.

1.8.2.12 The Weston energy flux propagation model used for this assessment has been calibrated against a range of other propagation models showing good agreement (typically within +/- 1dB to a range of 2.5km). The acoustical properties of different layers employed in the propagation modelling are presented in Table 1.24. This data is evaluated using recommendations by Hamilton (1980; 1978) based on the geological layers present in the survey region and the acoustic properties of the water column. Due to the relatively shallow nature of the area, only a single speed of sound in the water column was considered.

Table 1.24: Acoustical properties of the water layer and sediment used for propagation modelling calibration and pile source modelling.

Depth below sea floor [m]	Soil/Rock	Soil unit weight [kN/m^3]	Wave velocity		Attenuation coeff		Density [kg/m^3]
			V_p [m/s]	V_s [m/s]	α_p [dB/λ_p]	α_s [dB/λ_s]	
0	Water		1,493				1,000
0 - 1	Sand	20.5	1,806	124	0.8	2.5	2,090
1 - 2	Sand	20.5	1,825	154	0.8	2.5	2,090
2 - 3	Clay	22.9	1,515	127	0.2	1	2,334
8 - 13	Mercia Mudstone (weathered)	20.5	2,044	633	0.1	0.1	2,090
13 - 33	Mercia Mudstone	22.5	2,836	1,250	0.1	0.1	2,294
33 - 75	Sherwood Sandstone	21	3,933	3,067	0.1	0.2	2,246
75-200	Sherwood Sandstone	21	4,020	3,134	0.1	0.2	2,265
200-300	Sherwood Sandstone	21	4,123	3,215	0.1	0.2	2,288
300-400	Sherwood Sandstone	21	4,217	3,288	0.1	0.2	2,308
400-500	Sherwood Sandstone	21	4,300	3,353	0.1	0.2	2,326
500-600	Sherwood Sandstone	21	4,375	3,412	0.1	0.2	2,341
600-700	Sherwood Sandstone	21	4,445	3,466	0.1	0.2	2,356
700-800	Sherwood Sandstone	21	4,510	3,516	0.1	0.2	2,370
800-900	Sherwood Sandstone	21	4,571	3,564	0.1	0.2	2,382
900-1,000	Sherwood Sandstone	21	4,630	3,611	0.1	0.2	2,394
1,000+	Halfspace (Sandstone)	21	4,660	3,634	0.1	0.2	2,400

1.8.2.13 The level of detail presented in terms of sound modelling needs to be considered in relation to the level of uncertainty for animal injury and disturbance thresholds. Uncertainty in the sound level predictions will be higher over larger propagation distances (i.e. in relation to disturbance thresholds) and much lower over shorter distances (i.e. in relation to injury thresholds). Nevertheless, it is considered that the uncertainty in animal injury and disturbance thresholds is likely to be higher than uncertainty in sound predictions. This is further compounded by differences in individual animal response, sensitivity, and behaviour. It would therefore be wholly misleading to present any injury or disturbance ranges as a hard and fast distance beyond which no effect can occur, and it would be equally misleading to present any sound modelling results in such a way.

1.8.3 Batch processing

1.8.3.1 To improve the performance and reduce the time taken to process and evaluate multiple TL calculations required for this study, Seiche Ltd's proprietary software was employed. This software iteratively evaluates the propagation modelling routine for the specified number of azimuthal bearings radiating from a source point, providing a fan of range-dependent TL curves departing from the sound source for each given frequency and receiver depth. In-house routines are then employed to interpolate the TL values across transects, to give an estimate of the sound field for the whole area around the source point.

1.8.3.2 Once the TL values were evaluated at the source points, in all azimuthal directions, and at all frequencies of interest for various sources, the results were then coupled with the corresponding SL values in third octave frequency bands. The combination of SL with TL data provided us with the third octave band RL at each point in the receiver grid (i.e. at each modelled range, depth, and azimuth of the receiver).

1.8.3.3 The received levels were evaluated for the SPL_{pk}, SPL_{rms} or SEL metric, for each source type, source location, and azimuthal transect to produce the associated 2-D maps. The broadband RL were then calculated for these metrics and from the third octave band results. The set of simulated RL transects were circularly interpolated to generate the broadband 2-D RL maps centred around each source point.

1.8.3.4 For impact piling, the far-field received peak sound pressure level was calculated from SEL values via the empirical fitting between pile driving SEL and peak SPL data, given in Lippert *et al.* (2015), as:

$$SPL_{pk} = 1.43 \times SEL - 44.0 .$$

1.8.3.5 RMS sound pressure levels were calculated assuming a typical T90 pulse duration for impact piling (i.e. the period that contains 90% of the total cumulative sound energy) of 100ms. It should be noted that in reality the rms T90 period will increase significantly with distance which means that any ranges based on rms sound pressure levels at ranges of more than a few kilometres are likely to be significant over estimates and should therefore be treated as highly conservative.

1.8.4 Exposure calculations

1.8.4.1 As well as calculating the un-weighted sound levels at various distances from different source, it is also necessary to calculate the received acoustic signal in terms of the SEL metric (where necessary and possible) for a marine mammal using the relevant hearing weighting functions. For different operations related sound sources, the numerical SEL value is equal to the SPL rms value integrated over a one second window as the sources are continuous and non-impulsive. These SEL values are employed for calculation of cSEL (cumulative SEL) metric for different marine mammal groups to assess potential impact ranges.

1.8.4.2 Simplified exposure modelling could assume that the animal is either static and at a fixed distance away from the sound source, or that the animal is swimming at a constant speed in a perpendicular direction away from a sound source. For fixed receiver calculations, it has generally been assumed (in literature) that an animal will stay at a known distance from the sound source for a period of 24 hours. As the animal does not move, the sound will be constant over the integration period of 24 hours (assuming the source does not change its operational characteristics over this time). This, however, would give an unrealistic level of exposure, as the animals are highly unlikely to remain stationary when exposed to loud sound, and are therefore expected to swim away from the source. The approximation used in these calculations, therefore, is that the animals move directly away from the source. Nevertheless, in the case of fish exposure calculations have also been undertaken based on a static receiver assumption.

1.8.4.3 It should be noted that the sound exposure calculations are based on the simplistic assumption that the sound source is active continuously (or intermittently based on source activation timings) over a 24 hour period. The real world situation is more complex. The SEL calculations presented in this study do not take any breaks in activity into account, such as repositioning of the piling vessel.

1.8.4.4 Furthermore, the sound criteria described in the Southall *et al.* (2019) guidelines assume that the animal does not recover hearing between periods of activity. It is likely that both the intervals between operations could allow some recovery from temporary hearing threshold shifts for animals exposed to the sound (von Benda-Beckmann *et al.* 2022) and, therefore, the assessment of sound exposure level is conservative.

1.8.4.5 In order to carry out the moving marine mammal calculation, it has been assumed that a mammal will swim away from the sound source at the onset of activities. For impulsive sounds of piledriving the calculation considers each pulse to be established separately resulting in a series of discrete SEL values of decreasing magnitude (see Figure 1.13).

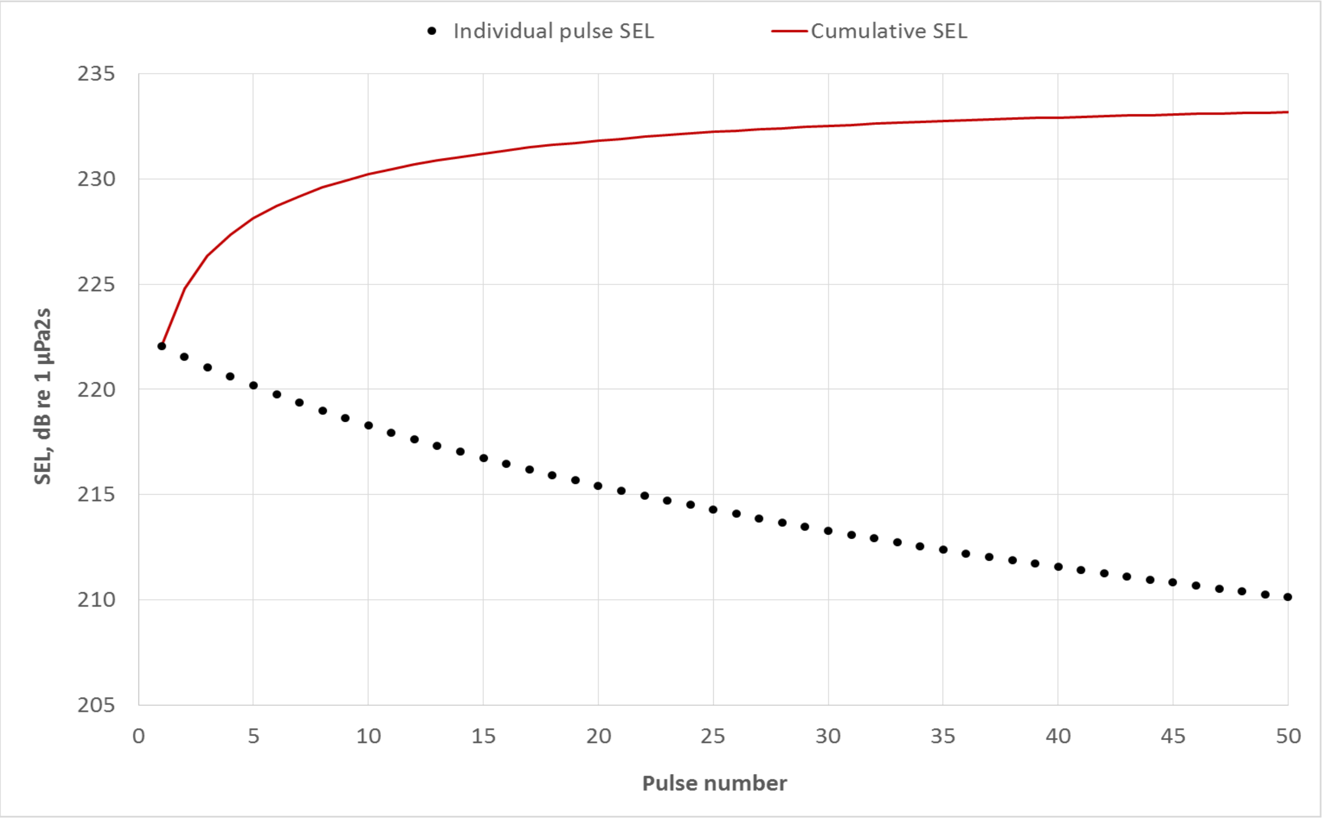

Figure 1.13: A comparison of discrete SEL per pulse, and cumulative SEL values.

1.8.4.6 As an animal swims away from the sound source, the sound it experiences will become progressively lower (more attenuated); the cumulative SEL is derived by logarithmically adding the SEL to which the mammal is exposed as it travels away from the source. This calculation was used to estimate the approximate minimum start distance for an animal in order for it not to be exposed to sufficient sound energy to result in the onset of potential auditory injury. It should be noted that the sound exposure calculations are based on the simplistic assumption that the animal will continue to swim away at a fairly constant relative speed. The real-world situation is more complex, and the animal is likely to move in a more complex manner.

1.8.4.7 The assumed swim speeds for animals likely to be present across the Mona Offshore Wind Project are set out in Table 1.25.

Table 1.25: Assessment swim speeds of marine mammals and fish that are likely to occur within the Irish Sea for the purpose of exposure modelling.

[a] As a sensitivity check, exposure modelling has also been performed for stationary fish.

Species	Hearing group	Swim speed (m/s)	Source reference
Harbour seal *Phoca vitulina*	Phocid Carnivores in Water (PCW)	1.8	Thompson *et al.* (2015)
Grey seal *Halichoerus grypus*	Phocid Carnivores in Water (PCW)	1.8	Thompson *et al.* (2015)
Harbour porpoise *Phocoena phocoena*	Very High Frequency (VHF)	1.5	Otani *et al.* (2000)

Species	Hearing group	Swim speed (m/s)	Source reference
Minke whale *Balaenoptera acutorostrata*	Low Frequency (LF)	2.3	Boisseau *et al.* (2021)
Bottlenose dolphin *Tursiops truncatus*	High Frequency (HF)	1.52	Bailey *et al.* (2010)
White-beaked dolphin *Lagenorhynchus albirostris*	High Frequency (HF)	1.52	Bailey *et al.* (2010)
Short beaked common dolphin *Delphinus delphis*	High Frequency (HF)	1.52	Bailey *et al.* (2010)
Risso's dolphin *Grampus griseus*	High Frequency (HF)	1.52	Bailey *et al.* (2010)
Basking shark *Cetorhinus maximus*	Group 1 fish	1.0	Sims *et al.* (2000)
All fish hearing groups[a] (excluding basking sharks)	Group 1 to 4 fish	0 and 0.5[a]	Popper *et al.* (2014)

1.8.4.8 As an additional sensitivity analysis, modelling was carried out for fish assuming a swim speed of 0m/s (i.e. stationary).

1.8.4.9 To perform the cumulative exposure calculation, the first step is to parameterise the m-weighted sound exposure levels (or unweighted in the case of fish) for single strikes of a given energy via the 95th percentile line of best fit against the calculated received levels from the model. This function is then used to predict the exposure level for each strike in the planned hammer schedule (periods of slow start, ramp up and full power).

1.8.4.10 In addition to the single-source pile driving, simplified situations of simultaneous monopile driving from two piling rigs have been considered. The response has been approximated as moving directly away from the point on a line equidistant between the two sources. For simplicity, the sources are considered to be omnidirectional and the piling schedules (soft start, ramp up, etc) are synchronised, entering each stage of the schedule at the same time.

1.8.5 UXO sound modelling

High order detonation

1.8.5.1 Acoustic modelling for UXO clearance has been undertaken using the methodology described in Soloway and Dahl (2014). The equation provides a simple relationship between distance from an explosion and the weight of the charge (or equivalent TNT weight) but does not take into account bottom topography or sediment characteristics.

$$P_{peak} = 52.4 \times 10^6 \left(\frac{R}{W^{1/3}}\right)^{-1.13}$$

1.8.5.2 Where *W* is the equivalent TNT charge weight and *R* is the distance from source to receiver.

1.8.5.3 Since the charge is assumed to be freely standing in mid-water, unlike a UXO which would be resting on the seabed and could potentially be buried, degraded or subject to other significant attenuation, this estimation of the source level can be considered conservative.

1.8.5.4 According to Soloway and Dahl (2014), the SEL can be estimated by the following equation:

$$SEL = 6.14 \times log_{10}\left(W^{1/3}\left(\frac{R}{W^{1/3}}\right)^{-2.12}\right) + 219$$

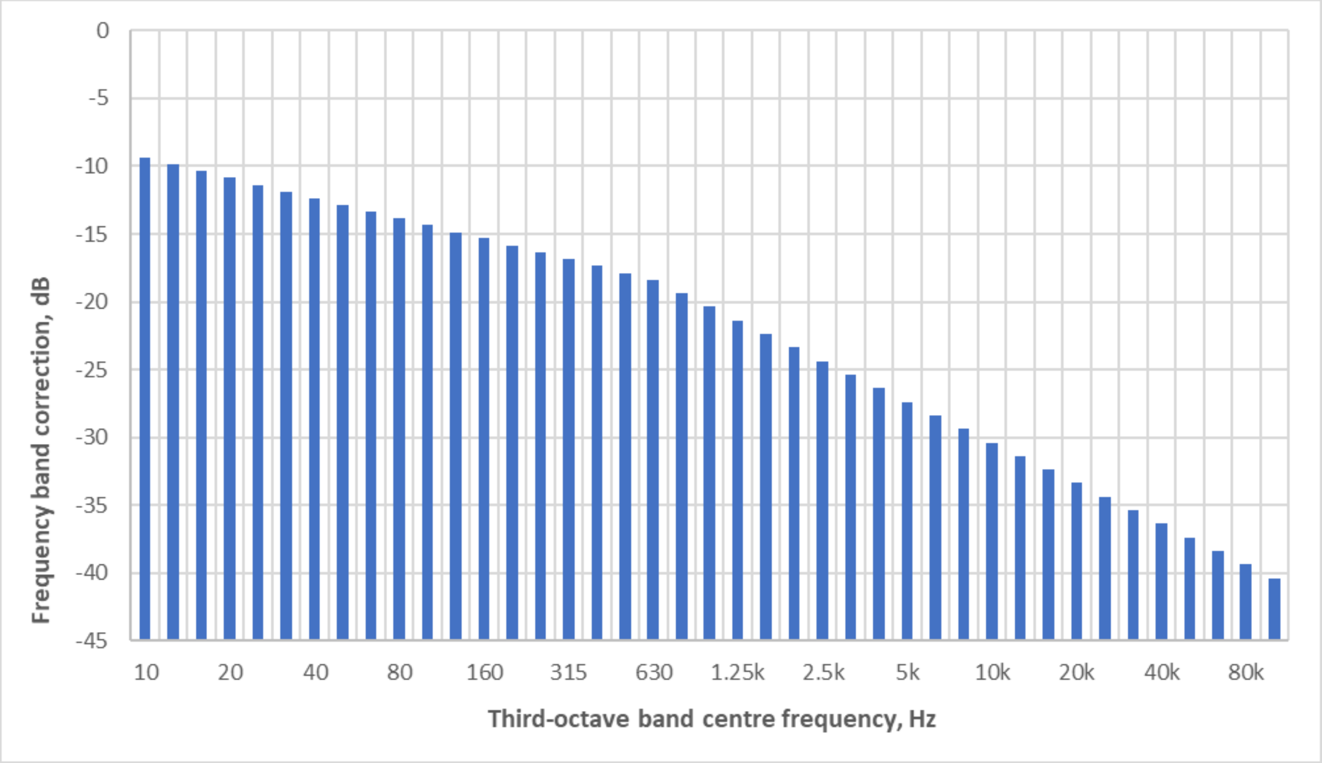

Figure 1.14: Assumed explosive spectrum shape used to estimate hearing weighting corrections to SEL.

1.8.5.5 In order to compare to the marine mammal hearing weighted thresholds, it is necessary to apply the frequency dependent weighting functions at each distance from the source. This was accomplished by determining a transfer function between unweighted and weighted SEL values at various distances based on an assumed spectrum shape (see Figure 1.14) and taking into account molecular absorption at various ranges. Furthermore, because there is potential for more than one UXO clearance event per day (a maximum of two per day is assumed) then it is also necessary to take this into account in the exposure calculation.

Low order techniques

1.8.5.6 According to Robinson *et al.* (2020), low order deflagration (a specific method of low order UXO clearance) results in a much lower amplitude of peak sound pressure than high order detonations. The study concluded that peak sound pressure during deflagration is due only to the size of the shaped charge used to initiate deflagration and, consequently, that the acoustic output can be predicted for deflagration as long as the size of the shaped charge is known.

1.8.5.7 Acoustic modelling for low order techniques (such as deflagration) has therefore been based on the methodology described above for high order detonations, using a smaller donor charge size.

1.9 Sound Modelling Results

1.9.1 Pre-construction phase

1.9.1.1 The estimated ranges for auditory injury to marine mammals due to various proposed activities undertaken during the pre-construction site investigation surveying phase of the operations are presented in this section. These include geophysical and geotechnical survey activities, UXO clearance and supported vessel activities.

1.9.1.2 The potential ranges presented for injury and behavioural response are not a hard and fast 'line' where an impact will occur on one side and not on the other. Potential impact is more probabilistic than that; dose dependency in PTS onset, individual variations and uncertainties regarding behavioural response and swim speed/direction all mean that it is much more complex than drawing a contour around a location. These ranges are designed to provide an understandable way in which a wider audience can appreciate the potential spatial extent of the impact.

Geophysical and Geotechnical surveys

1.9.1.3 Geophysical surveying includes many sonar like sound sources operations and the resulting injury and disturbance ranges for marine mammals are presented in Table 1.26, based on a comparison to the non-impulsive thresholds set out in Southall *et al.* (2019). Table 1.27 presents the results for geotechnical investigations. CPT distances are based on a comparison to the Southall *et al.* (2019) thresholds for impulsive sound (with the distances presented in brackets for peak SPL thresholds) whereas borehole drilling and vibro-core results are compared against the non-impulsive thresholds. Borehole drilling source levels were reported as 142dB to 145dB re 1µPa rms at 1 m, indicating little to no disturbance.

1.9.1.4 The potential impact distances from these operations vary based on their frequencies of operation and source levels and are rounded to the nearest 5 m. It should be noted that, for the sonar like survey sources, many of the injury ranges are limited to approximately 65m as this is the approximate water depth in the area. Sonar like systems have very strong directivity which effectively means that there is only potential for injury when a marine mammal is directly underneath the sound source. Once the animal moves outside of the main beam, there is significantly reduced potential for injury. The same is true in many cases for TTS where an animal is only exposed to enough energy to cause TTS when inside the direct beam of the sonar like source. For this reason, many of the TTS and PTS ranges are similar (i.e. limited by the depth of the water). Disturbance thresholds are as shown in Table 1.5 for impulsive and non-impulsive sources respectively.

Table 1.26: Potential Impact Ranges (m) for Marine Mammals During the Various Geophysical Investigation Activities Based on Comparison to Southall *et al.* (2019) SEL Thresholds.

N/E- Not Exceeded

*Non-impulsive threshold

**Impulsive threshold

Source	Potential Impact Range (m)										
	LF		HF		VHF		PCW		OCW		All
	TTS	PTS	TTS	PTS	TTS	PTS	TTS	PTS	TTS	PTS	Disturbance
MBES*	40	12	45	41	175	68	40	25	3	2	830
SSS*	29	2	29	2	46	41	37	6	5	N/E	310
SBES*	40	12	40	12	175	68	40	25	3	2	830
SBP (chirp/ pinger)*	76	40	76	40	2,300	254	81	40	40	38	17,300
UHRS (sparker)**	30	N/E	N/E	N/E	48	11	6	N/E	N/E	N/E	637m (mild) 95m (strong)

Table 1.27: Potential Impact Ranges for Geotechnical Site Investigation Activities Based on Comparison to Southall *et al.* (2019) SEL Thresholds (Comparison to Ranges for Peak SPL Where Threshold was Exceeded Shown in Brackets).

N/E- Not Exceeded

*Non-impulsive threshold

**Impulsive threshold

Source	Potential Impact Range (m)										
	LF		HF		VHF		PCW		OCW		All
	TTS	PTS	TTS	PTS	TTS	PTS	TTS	PTS	TTS	PTS	Disturbance
Borehole drilling*	N/E	N/E	N/E	N/E	<15	N/E	N/E	N/E	N/E	N/E	1.47km (strong)
Cone penetration testing**	117	4	9	N/E	950 (30)	55 (14)	39	N/E	N/E	N/E	1.35km (mild) 158m (strong)
Vibro-coring*	<10	N/E	<20	N/E	11,020	79	<10	N/E	N/E	N/E	31km

Vessels

1.9.1.5 The potential impact ranges for vessels are included in section 1.9.4, which summarises the vessel modelling results for all phases of the Mona Offshore Wind Project.

UXO clearance

1.9.1.6 The predicted injury ranges for low order disposal are presented in Table 1.28, for high order donor charges in Table 1.29 and for high order detonation of UXOs in Table 1.30. All UXO injury and disturbance ranges are based on a comparison to the relevant impulsive sound thresholds as set out in Section 1.5.5.

1.9.1.7 It should be noted that, due to a combination of dispersion (i.e. where the waveform elongates), multiple reflections from the sea surface and seabed and molecular absorption of high frequency energy, the sound is unlikely to still be impulsive in character once it has propagated more than a few kilometres. Consequently, great caution should be used when interpreting any results with predicted injury ranges in the order of tens of kilometres. Furthermore, the modelling assumes that the UXO acts like a charge suspended in open water whereas in reality it is likely to be partially buried in the sediment. In addition, it is possible that the explosive material will have deteriorated over time meaning that the predicted sound levels are likely to be over-estimated. In combination, these factors mean that the results should be treated as precautionary potential impact ranges which are likely to be significantly lower than predicted.

Table 1.28: Potential Impact Ranges for Low Order and Low Yield UXO Clearance Activities.

	PTS range, m		TTS range, m	
	SPL	**SEL**	**SPL**	**SEL**
0.08kg low-order donor charge				
LF	122	47	224	655
HF	40	2	73	23
VHF	685	190	1,265	1,500
PCW	135	9	247	124
OCW	32	N/E	60	5
Fish (lower range)	44			
Fish (upper range)	27			
0.5kg clearing shot				
LF	223	115	411	1,585
HF	73	4	134	56
VHF	1,265	421	2,325	2,465
PCW	247	22	455	301
OCW	60	N/E	110	13
Fish (lower range)	81			
Fish (upper range)	49			
2 x 0.75kg low-yield charge				
LF	322	196	593	2,665
HF	105	7	194	95
VHF	1,820	650	3,350	3,120
PCW	357	38	660	504
OCW	86	2	158	23
Fish (lower range)	117			
Fish (upper range)	70			
4 x 0.75kg low-yield charge				
LF	406	275	750	3,670
HF	133	10	244	131
VHF	2,290	840	4,220	3,600
PCW	449	53	830	695
OCW	108	2	199	32
Fish (lower range)	147			
Fish (upper range)	88			

Table 1.29: Potential Impact Ranges for Donor Charges used in High Order UXO Clearance Activities.

	PTS range, m		TTS range, m	
	SPL	**SEL**	**SPL**	**SEL**
1.2kg donor charge for high-order UXO disposal				
LF	299	176	551	2,400
HF	98	6	180	85
VHF	1,690	596	3,110	2,795
PCW	331	34	610	454
OCW	80	1	147	21
Fish (lower range)	108			
Fish (upper range)	65			
3.5kg donor blast-fragmentation charge for high-order UXO disposal				
LF	427	297	790	3,940
HF	140	10	257	141
VHF	2,415	885	4,445	3,715
PCW	473	57	875	745
OCW	114	2	209	35
Fish (lower range)	154			

	PTS range, m		TTS range, m	
Fish (upper range)	93			

Table 1.30: Potential Impact Ranges for High Order Clearance of UXOs.

	PTS range, m		TTS range, m	
	SPL	SEL	SPL	SEL
25kg UXO – high order explosion				
LF	825	775	1,515	9,325
HF	268	27	494	343
VHF	4,645	1,645	8,555	5,290
PCW	910	147	1,680	1,760
OCW	219	6	403	90
Fish (lower range)	297			
Fish (upper range)	179			
130kg UXO – high order explosion				
LF	1,425	1,705	2,625	17,755
HF	464	61	855	680
VHF	8,045	2,520	14,825	6,830
PCW	1,580	323	2,905	3,360
OCW	379	15	700	200
Fish (lower range)	514			
Fish (upper range)	309			
907kg UXO – high order explosion				
LF	2,720	4,215	5,015	34,365
HF	890	151	1,635	1,380
VHF	15,370	3,820	28,320	8,925
PCW	3,015	800	5,550	6,470
OCW	725	37	1,335	501
Fish (lower range)	985			
Fish (upper range)	590			

1.9.2 Construction phase

Impact piling

1.9.2.1 The impact piling scenarios modelled were as follows:

- Single piling rig – Monopile wind turbine foundations and OSP (5,500kJ)
- Single piling rig – Pin pile wind turbine foundations and OSP (2,800kJ)
- Two rigs concurrent piling – Monopile wind turbine foundations
- Two rigs concurrent piling – Pin pile wind turbine foundations
- Two rigs consecutive piling – Monopile wind turbine foundations
- Two rigs consecutive piling – Pin pile wind turbine foundations.

1.9.2.2 All cases are presented both with and without the use of 30 minutes of ADD prior to installation.

1.9.2.3 There is a possibility that during the piling operations it will be necessary for two pile installation vessels to operate concurrently. For the concurrent piling scenarios, two separate maximum adverse case assumptions were identified, as follows:

- Separation distance of 1km (the minimum distance between foundations) as a maximum adverse scenario for injury; and
- Separation distance of up to 35km as a maximum adverse scenario for disturbance.

1.9.2.4 The reason the MDS separation distances for injury and disturbance differ is that the scenario which results in the greatest potential for injury is when two rigs are operating in close proximity, meaning that the animal is exposed to sound from both rigs at relatively high levels. Conversely, the maximum area of disturbance occurs when both rigs are operating at a further distance apart in the Mona Array Area and their disturbance ranges are just overlapping. For the latter case, the MDS is not necessarily the greatest possible separation distance and piles at the northern, southeast and southwest boundaries were chosen as representative as the combined maximum adverse scenario in terms of separation distance and bathymetry.

1.9.2.5 All impact piling injury ranges are based on a comparison to the relevant impulsive sound thresholds as set out in section 1.5. Disturbance effects are presented in volume 2, chapter 9: Marine mammals of the PEIR using the dose-response approach described in Section 1.5.5.

1.9.2.6 The injury ranges for peak sound pressure are based on both the sound from the first strike a receptor may experience at the closest point during each phase of the pile installation, as well as for the maximum hammer energy over the entire installation.

1.9.2.7 It should be noted that peak sound pressure is a time domain parameter and do not necessarily add together to produce higher received peak sound pressure levels. Even if two piling hammers were to strike their piles synchronously (i.e. to the exact millisecond) the sound waves will arrive at different locations at different times. Consequently, the peak pressure ranges for simultaneous piling do not differ from the peak injury ranges identified for single rigs.

1.9.2.8 During impact piling the interaction with the seabed and the water column is complex. In these cases, a combination of dispersion (i.e. where the waveform shape elongates), and multiple reflections from the sea surface and bottom and molecular absorption of high frequency energy, the sound will lose its impulsive shape after some distance (generally in order of several kilometres).

1.9.2.9 A recent article by Southall (2021) discusses this aspect in detail, and notes that *"…when onset criteria levels were applied to relatively high-intensity impulsive sources (e.g. pile driving), TTS onset was predicted in some instances at ranges of tens of kilometers from the sources. In reality, acoustic propagation over such ranges transforms impulsive characteristics in time and frequency (see Hastie et al., 2019; Amaral et al., 2020; Martin et al., 2020). Changes to received signals include less rapid signal onset, longer total duration, reduced crest factor, reduced kurtosis, and narrower bandwidth (reduced high-frequency content). A better means of accounting for these changes can avoid overly precautionary conclusions, although how to do so is proving vexing"*. The point is reenforced later in the discussion which points out that *"…it should be recognized that the use of impulsive exposure criteria for receivers at greater ranges (tens of kilometers) is almost certainly an overly precautionary interpretation of existing criteria"*. (See discussion in section 1.5).

1.9.2.10 Consequently, great caution should be used when interpreting any results with predicted injury ranges in the order of tens of kilometres.

Single piling rig

1.9.2.11 Distances are presented at which sound levels decrease to below PTS/TTS threshold values in terms of cumulative SEL and peak sound pressure level. It should be noted that the potential PTS/TTS ranges reduce significantly with the use of ADD because it is assumed that an animal swims away from the area for 30 minutes before being exposed to sound from piling, therefore significantly reducing its cumulative SEL for any given start range.

1.9.2.12 Distances are presented in Table 1.31 to Table 1.35 for monopile installation and Table 1.36 to Table 1.41 for pin pile installation.

Table 1.31: Marine Mammal Injury Ranges for Single Monopile Installation Based on the Cumulative SEL Metric (N/E – threshold not exceeded).

Species/Group	Threshold (Weighted SEL)	Range (m)	
		No ADD	30 min ADD
LF	PTS - 183dB re 1µPa²s	3,870	N/E
	TTS - 168dB re 1µPa²s	65,400	61,260
HF	PTS - 185dB re 1µPa²s	N/E	N/E
	TTS - 170dB re 1µPa²s	N/E	N/E
VHF	PTS - 155dB re 1µPa²s	2,150	N/E
	TTS - 140dB re 1µPa²s	38,700	36,260
PCW	PTS - 185dB re 1µPa²s	N/E	N/E
	TTS - 170dB re 1µPa²s	20,200	17,040
OCW	PTS - 203dB re 1µPa²s	N/E	N/E
	TTS - 188dB re 1µPa²s	N/E	N/E

Table 1.32: Marine Mammal Injury Ranges for Single Monopile Installation Based on the Peak SPL Metric (N/E – threshold not exceeded).

Species/Group	Threshold (Unweighted Peak)	Range (m)	
		First Strike	Max
LF	PTS - 219dB re 1µPa (pk)	88	263
	TTS - 213dB re 1µPa (pk)	140	420
HF	PTS - 230dB re 1µPa (pk)	37	111
	TTS - 224dB re 1µPa (pk)	59	178
VHF	PTS - 202dB re 1µPa (pk)	330	990
	TTS - 196dB re 1µPa (pk)	528	1,581
PCW	PTS - 218dB re 1µPa (pk)	95	284
	TTS - 212dB re 1µPa (pk)	151	454
OCW	PTS - 232dB re 1µ Pa (pk)	32	95
	TTS - 226dB re 1µPa (pk)	51	152

Table 1.33: Fish Injury Ranges for Single Monopile Installation Based on the Cumulative SEL Metric for Moving Fish (N/E – threshold not exceeded).

Hearing Group	Response	Threshold (SEL, dB re 1µPa²s)	Range (m)
Group 1 Fish: No swim bladder (particle motion detection) – [basking shark ranges shown in square brackets].	Mortality	219	N/E
	Recoverable injury	216	N/E
	TTS	186	18,100 [12,300]
Group 2 Fish: Swim bladder not involved in hearing (particle motion detection)	Mortality	210	N/E
	Recoverable injury	203	67
	TTS	186	18,100
Group 3 and 4 Fish: Swim bladder involved in hearing (primarily pressure detection)	Mortality	207	N/E
	Recoverable injury	203	67
	TTS	186	18,100
Sea turtles	Mortality	210	N/E
Fish eggs and larvae (static)	Mortality	210	2,090

Table 1.34: Fish Injury Ranges for Single Monopile Installation Based on the Cumulative SEL Metric for Static Fish (N/E – threshold not exceeded).

Hearing Group	Response	Threshold (SEL, dB re 1µPa²s)	Range (m)
Group 1 Fish: No swim bladder (particle motion detection)	Mortality	219	780
	Recoverable injury	216	1,085
	TTS	186	26,240
Group 2 Fish: Swim bladder not involved in hearing (particle motion detection)	Mortality	210	2,090
	Recoverable injury	203	4,440
	TTS	186	26,240
Group 3 and 4 Fish: Swim bladder involved in hearing (primarily pressure detection)	Mortality	207	2,880
	Recoverable injury	203	4,440
	TTS	186	26,240
Sea turtles	Mortality	210	2,090
Fish eggs and larvae	Mortality	210	2,090

Table 1.35: Fish Injury Ranges for Single Monopile Installation Based on the Peak SPL Metric (N/E – threshold not exceeded).

Hearing Group	Response	Threshold (SPL_{pk}, dB re 1µPa)	Range (m)	
			First Strike	Max
Group 1 Fish: No swim bladder (particle motion detection)	Mortality	213	140	420
	Recoverable injury	213	140	420
Group 2 Fish: Swim bladder not involved in hearing (particle motion detection)	Mortality	207	224	670
	Recoverable injury	207	224	670
Group 3 and 4 Fish: Swim bladder involved in hearing (primarily pressure detection)	Mortality	207	224	670
	Recoverable injury	207	224	670
Sea turtles	Mortality	207	224	670
Fish eggs and larvae	Mortality	207	224	670

Table 1.36: Marine Mammal Injury Ranges for Single Pin Pile Installation Based on the Cumulative SEL Metric (N/E – threshold not exceeded).

Species/Group	Threshold (Weighted SEL)	Range (m)	
		No ADD	30 min ADD
LF	PTS - 183dB re 1µPa²s	61	N/E
	TTS - 168dB re 1µPa²s	39,260	35,160
HF	PTS - 185dB re 1µPa²s	N/E	N/E
	TTS - 170dB re 1µPa²s	N/E	N/E
VHF	PTS - 155dB re 1µPa²s	N/E	N/E
	TTS - 140dB re 1µPa²s	7,140	4,445
PCW	PTS - 185dB re 1µPa²s	N/E	N/E
	TTS - 170dB re 1µPa²s	2,441	N/E
OCW	PTS - 203dB re 1µPa²s	N/E	N/E
	TTS - 188dB re 1µPa²s	N/E	N/E

Table 1.37: Marine Mammal Injury Ranges for Single Pin Pile Installation Based on the Peak SPL Metric (N/E – threshold not exceeded).

Species/Group	Threshold (Unweighted Peak)	Range (m)	
		First Strike	Max
LF	PTS - 219dB re 1µPa (pk)	47	148
	TTS - 213dB re 1µPa (pk)	78	244
HF	PTS - 230dB re 1µPa (pk)	19	59
	TTS - 224dB re 1µPa (pk)	31	98
VHF	PTS - 202dB re 1µPa (pk)	196	610
	TTS - 196dB re 1µPa (pk)	322	1,005
PCW	PTS - 218dB re 1µPa (pk)	52	161
	TTS - 212dB re 1µPa (pk)	85	265
OCW	PTS - 232dB re 1µ Pa (pk)	16	50
	TTS - 226dB re 1µPa (pk)	26	83

Table 1.38: Fish Injury Ranges for Single Pin Pile Installation Based on the Cumulative SEL Metric for Moving Fish (N/E – threshold not exceeded).

Hearing Group	Response	Threshold (SEL, dB re 1μPa²s)	Range (m)
Group 1 Fish: No swim bladder (particle motion detection) – [*basking shark ranges shown in square brackets*].	Mortality	219	N/E
	Recoverable injury	216	N/E
	TTS	186	8,400 [5,240]
Group 2 Fish: Swim bladder not involved in hearing (particle motion detection)	Mortality	210	N/E
	Recoverable injury	203	N/E
	TTS	186	8,400
Group 3 and 4 Fish: Swim bladder involved in hearing (primarily pressure detection)	Mortality	207	N/E
	Recoverable injury	203	N/E
	TTS	186	8,400
Sea turtles	Mortality	210	N/E
Fish eggs and larvae (static)	Mortality	210	765

Table 1.39: Fish Injury Ranges for Single Pin Pile Installation Based on the Cumulative SEL Metric for Static Fish (N/E – threshold not exceeded).

Hearing Group	Response	Threshold (SEL, dB re 1μPa²s)	Range (m)
Group 1 Fish: No swim bladder (particle motion detection)	Mortality	219	266
	Recoverable injury	216	376
	TTS	186	12,340
Group 2 Fish: Swim bladder not involved in hearing (particle motion detection)	Mortality	210	765
	Recoverable injury	203	1,730
	TTS	186	12,340
Group 3 and 4 Fish: Swim bladder involved in hearing (primarily pressure detection)	Mortality	207	1,090
	Recoverable injury	203	1,730
	TTS	186	12,340
Sea turtles	Mortality	210	765
Fish eggs and larvae	Mortality	210	765

Table 1.40: Fish Injury Ranges for Single Pin Pile Installation Based on the Peak SPL Metric (N/E – threshold not exceeded).

Hearing Group	Response	Threshold (SPL_{pk}, dB re 1μPa)	Range (m)	
			First Strike	Max
Group 1 Fish: No swim bladder (particle motion detection)	Mortality	213	78	244
	Recoverable injury	213	78	244
Group 2 Fish: Swim bladder not involved in hearing (particle motion detection)	Mortality	207	129	402
	Recoverable injury	207	129	402
Group 3 and 4 Fish: Swim bladder involved in hearing (primarily pressure detection)	Mortality	207	129	402
	Recoverable injury	207	129	402
Sea turtles	Mortality	207	129	402
Fish eggs and larvae	Mortality	207	129	402

Table 1.41: Fish Disturbance Ranges for Single Pile Installation Based on the 150dB re 1μPa (rms) Contour

Range (m)	
Monopile	**Pin Pile**
39,770	31,435

Concurrent piling

1.9.2.13 Construction may occur utilising two pile installation vessels operating concurrently. The potential cumulative SEL injury ranges for marine mammals and fish due to impact pile driving of monopiles and pin piles are modelled as following the same piling plans with all phases starting at the same time. For injury the MDS is considered to be that of two adjacent piles, separated by a distance of 1km due to the maximal overlap of sound propagation contours leading to the maximum generated sound levels. Conversely, for disturbance the maximum separation between two piling locations would lead to the larger area ensonified at any one time and therefore the greatest disturbance.

- Injury ranges are presented in terms of cumulative SEL metric in Table 1.42 to Table 1.44 for monopile installation and Table 1.45 to Table 1.47 for pin piles. The peak metric will remain the same as the single installation case. As noted previously, disturbance effects are covered in volume 2, chapter 9: Marine mammals of the PEIR using the dose-response approach described in Section 1.5.5.

Table 1.42: Marine Mammal Injury Ranges for Concurrent Monopile Installation Based on the Cumulative SEL Metric (N/E – threshold not exceeded).

Species/Group	Threshold (Weighted SEL)	Range (m)	
		No ADD	30 min ADD
LF	PTS - 183dB re 1µPa²s	5,470	1,315
	TTS - 168dB re 1µPa²s	70,300	66,200
HF	PTS - 185dB re 1µPa²s	N/E	N/E
	TTS - 170dB re 1µPa²s	N/E	N/E
VHF	PTS - 155dB re 1µPa²s	3,330	745
	TTS - 140dB re 1µPa²s	42,500	39,800
PCW	PTS - 185dB re 1µPa²s	N/E	N/E
	TTS - 170dB re 1µPa²s	24,400	21,200
OCW	PTS - 203dB re 1µPa²s	N/E	N/E
	TTS - 188dB re 1µPa²s	N/E	N/E

Table 1.43: Fish Injury Ranges for Concurrent Monopile Installation Based on the Cumulative SEL Metric for Fish Moving Away (N/E – threshold not exceeded).

Hearing Group	Response	Threshold (SEL, dB re 1µPa²s)	Range (m)
Group 1 Fish: No swim bladder (particle motion detection) – [basking shark ranges shown in square brackets].	Mortality	219	N/E
	Recoverable injury	216	N/E
	TTS	186	19,780 [13,640]
Group 2 Fish: Swim bladder not involved in hearing (particle motion detection)	Mortality	210	N/E
	Recoverable injury	203	160
	TTS	186	19,780
Group 3 and 4 Fish: Swim bladder involved in hearing (primarily pressure detection)	Mortality	207	N/E
	Recoverable injury	203	160
	TTS	186	19,780
Sea turtles	Mortality	210	N/E
Fish eggs and larvae (static)	Mortality	210	2,230

Table 1.44: Fish Injury Ranges for Concurrent Monopile Installation Based on the Cumulative SEL Metric for Static Fish (N/E – threshold not exceeded).

Hearing Group	Response	Threshold (SEL, dB re 1µPa²s)	Range (m)
Group 1 Fish: No swim bladder (particle motion detection)	Mortality	219	835
	Recoverable injury	216	1,160
	TTS	186	27,580
Group 2 Fish: Swim bladder not involved in hearing (particle motion detection)	Mortality	210	2,230
	Recoverable injury	203	4,720
	TTS	186	27,580
Group 3 and 4 Fish: Swim bladder involved in hearing (primarily pressure detection)	Mortality	207	3,080
	Recoverable injury	203	4,720
	TTS	186	27,580
Sea turtles	Mortality	210	2,230
Fish eggs and larvae	Mortality	210	2,230

Table 1.45: Marine Mammal Injury Ranges for Concurrent Pin Pile Installation Based on the Cumulative SEL Metric (N/E – threshold not exceeded).

Species/Group	Threshold (Weighted SEL)	Range (m)	
		No ADD	30 min ADD
LF	PTS - 183dB re 1µPa2s	160	N/E
	TTS - 168dB re 1µPa2s	42,660	38,860
HF	PTS - 185dB re 1µPa2s	N/E	N/E
	TTS - 170dB re 1µPa2s	N/E	N/E
VHF	PTS - 155dB re 1µPa2s	N/E	N/E
	TTS - 140dB re 1µPa2s	8,860	6,160
PCW	PTS - 185dB re 1µPa2s	N/E	N/E
	TTS - 170dB re 1µPa2s	4,205	951
OCW	PTS - 203dB re 1µPa2s	N/E	N/E
	TTS - 188dB re 1µPa2s	N/E	N/E

Table 1.46: Fish Injury Ranges for Concurrent Pin Pile Installation Based on the Cumulative SEL Metric for Fish Moving Away (N/E – threshold not exceeded).

Hearing Group	Response	Threshold (SEL, dB re 1µPa²s)	Range (m)
Group 1 Fish: No swim bladder (particle motion detection) – [basking shark ranges shown in square brackets].	Mortality	219	N/E
	Recoverable injury	216	N/E
	TTS	186	9,160 [5,840]
Group 2 Fish: Swim bladder not involved in hearing (particle motion detection)	Mortality	210	N/E
	Recoverable injury	203	N/E
	TTS	186	9,160
Group 3 and 4 Fish: Swim bladder involved in hearing (primarily pressure detection)	Mortality	207	N/E
	Recoverable injury	203	N/E
	TTS	186	9,160
Sea turtles	Mortality	210	N/E
Fish eggs and larvae (static)	Mortality	210	820

Table 1.47: Fish Injury Ranges for Concurrent Pin Pile Installation Based on the Cumulative SEL Metric for Static Fish (N/E – threshold not exceeded).

Hearing Group	Response	Threshold (SEL, dB re 1µPa²s)	Range (m)
Group 1 Fish: No swim bladder (particle motion detection)	Mortality	219	266
	Recoverable injury	216	376
	TTS	186	13,040
Group 2 Fish: Swim bladder not involved in hearing (particle motion detection)	Mortality	210	765
	Recoverable injury	203	1,730
	TTS	186	13,040
Group 3 and 4 Fish: Swim bladder involved in hearing (primarily pressure detection)	Mortality	207	1,090
	Recoverable injury	203	1,730
	TTS	186	13,040
Sea turtles	Mortality	210	820
Fish eggs and larvae	Mortality	210	820

Consecutive piling

1.9.2.14 There is a possibility that during pile installation multiple piles will need to be installed in a single 24 hour period. The potential cumulative SEL injury ranges for marine mammals due to impact pile driving of monopiles and pin piles are modelled as following the same piling schedules. For injury the MDS is considered to be that of two adjacent piles, separated by a distance of 1km due to the maximal overlap of sound propagation contours leading to the maximum generated sound levels. It is assumed that the marine receptor will swim away from the pile installation and not return to the area within the 24 hour period. If it is assumed that the animal returns to the area the resulting injury ranges will be the same as for concurrent piling.

1.9.2.15 The results for consecutive piling are shown in Table 1.48 to Table 1.50 for monopile installation and Table 1.51 to Table 1.53 for pin piles.

Table 1.48: Marine Mammal Injury Ranges for Consecutive Monopile Installation Based on the Cumulative SEL Metric (N/E – threshold not exceeded).

Species/Group	Threshold (Weighted SEL)	Range (m)	
		No ADD	30 min ADD
LF	PTS - 183dB re 1µPa²s	4,065	N/E
	TTS - 168dB re 1µPa²s	68,720	64,620
HF	PTS - 185dB re 1µPa²s	N/E	N/E
	TTS - 170dB re 1µPa²s	N/E	N/E
VHF	PTS - 155dB re 1µPa²s	2,225	N/E
	TTS - 140dB re 1µPa²s	40,460	37,760
PCW	PTS - 185dB re 1µPa²s	N/E	N/E
	TTS - 170dB re 1µPa²s	21,580	18,340
OCW	PTS - 203dB re 1µPa²s	N/E	N/E
	TTS - 188dB re 1µPa²s	N/E	N/E

Table 1.49: Fish Injury Ranges for Consecutive Monopile Installation Based on the Cumulative SEL Metric for Fish Moving Away (N/E – threshold not exceeded).

Hearing Group	Response	Threshold (SEL, dB re 1µPa²s)	Range (m)
Group 1 Fish: No swim bladder (particle motion detection) – [basking shark ranges shown in square brackets].	Mortality	219	N/E
	Recoverable injury	216	N/E
	TTS	186	22,600 [13,800]
Group 2 Fish: Swim bladder not involved in hearing (particle motion detection)	Mortality	210	N/E
	Recoverable injury	203	72
	TTS	186	22,600

Hearing Group	Response	Threshold (SEL, dB re 1µPa²s)	Range (m)
Group 3 and 4 Fish: Swim bladder involved in hearing (primarily pressure detection)	Mortality	207	N/E
	Recoverable injury	203	72
	TTS	186	22,600
Sea turtles	Mortality	210	N/E
Fish eggs and larvae (static)	Mortality	210	3,300

Table 1.50: Fish Injury Ranges for Consecutive Monopile Installation Based on the Cumulative SEL Metric for Static Fish (N/E – threshold not exceeded).

Hearing Group	Response	Threshold (SEL, dB re 1µPa²s)	Range (m)
Group 1 Fish: No swim bladder (particle motion detection)	Mortality	219	1,240
	Recoverable injury	216	1,720
	TTS	186	39,480
Group 2 Fish: Swim bladder not involved in hearing (particle motion detection)	Mortality	210	3,300
	Recoverable injury	203	6,9800
	TTS	186	39,200
Group 3 and 4 Fish: Swim bladder involved in hearing (primarily pressure detection)	Mortality	207	4,580
	Recoverable injury	203	6,980
	TTS	186	39,200
Sea turtles	Mortality	210	3,300
Fish eggs and larvae	Mortality	210	3,300

Table 1.51: Marine Mammal Injury Ranges for Consecutive Pin Pile Installation Based on the Cumulative SEL Metric (N/E – threshold not exceeded).

Species/Group	Threshold (Weighted SEL)	Range (m)	
		No ADD	30 min ADD
LF	PTS - 183dB re 1µPa²s	63	N/E
	TTS - 168dB re 1µPa²s	40,460	36,260
HF	PTS - 185dB re 1µPa²s	N/E	N/E
	TTS - 170dB re 1µPa²s	N/E	N/E
VHF	PTS - 155dB re 1µPa²s	N/E	N/E
	TTS - 140dB re 1µPa²s	7,360	4,660

Species/Group	Threshold (Weighted SEL)	Range (m)	
		No ADD	30 min ADD
PCW	PTS - 185dB re 1µPa²s	N/E	N/E
	TTS - 170dB re 1µPa²s	2,581	N/E
OCW	PTS - 203dB re 1µPa²s	N/E	N/E
	TTS - 188dB re 1µPa²s	N/E	N/E

Table 1.52: Fish Injury Ranges for Consecutive Pin Pile Installation Based on the Cumulative SEL Metric for Fish Moving Away (N/E – threshold not exceeded).

Hearing Group	Response	Threshold (SEL, dB re 1µPa2s)	Range (m)
Group 1 Fish: No swim bladder (particle motion detection) – [basking shark ranges shown in square brackets].	Mortality	219	N/E
	Recoverable injury	216	N/E
	TTS	186	9,400 [5,540]
Group 2 Fish: Swim bladder not involved in hearing (particle motion detection)	Mortality	210	N/E
	Recoverable injury	203	N/E
	TTS	186	9,400
Group 3 and 4 Fish: Swim bladder involved in hearing (primarily pressure detection)	Mortality	207	N/E
	Recoverable injury	203	N/E
	TTS	186	9,400
Sea turtles	Mortality	210	N/E
Fish eggs and larvae (static)	Mortality	210	1,040

Table 1.53: Fish Injury Ranges for Consecutive Pin Pile Installation Based on the Cumulative SEL Metric for Static Fish (N/E – threshold not exceeded).

Hearing Group	Response	Threshold (SEL, dB re 1µPa²s)	Range (m)
Group 1 Fish: No swim bladder (particle motion detection)	Mortality	219	351
	Recoverable injury	216	505
	TTS	186	17,540
Group 2 Fish: Swim bladder not involved in hearing (particle motion detection)	Mortality	210	1,040
	Recoverable injury	203	2,400
	TTS	186	17,540

Hearing Group	Response	Threshold (SEL, dB re 1µPa²s)	Range (m)
Group 3 and 4 Fish: Swim bladder involved in hearing (primarily pressure detection)	Mortality	207	1,480
	Recoverable injury	203	2,400
	TTS	186	17,540
Sea turtles	Mortality	210	1,040
Fish eggs and larvae	Mortality	210	1,040

Drilled piling

1.9.2.16 The potential impact ranges for drilled piling are small (or not exceeded) for all marine mammal species groups, due to the low broadband SEL levels expected from these operations, at 160dB re 1µPa²s (see Table 1.54). The behavioural threshold range for all marine mammal groups is also reported.

Table 1.54: Potential Impact Ranges (m) for Marine Mammal Exposed to Drilled Piling

Source	Potential Impact Ranges (m)										
	LF		HF		VHF		PCW		OCW		All
	TTS	PTS	TTS	PTS	TTS	PTS	TTS	PTS	TTS	PTS	Behaviour
Drilled piling	N/E	N/E	N/E	N/E	<15	N/E	N/E	N/E	N/E	N/E	1,477

1.9.2.17 The ranges for recoverable injury and TTS for Group 3 and 4 Fish are presented in Table 1.55 based on the thresholds contained in Popper *et al.* (2014). Note that the guidance only states numerical thresholds for Group 3 and 4 Fish. It should be noted that fish would need to be exposed within these potential impact ranges for a period of 48 hours continuously in the case of recoverable injury and 12 hours continuously in the case of TTS for the effect to occur. It is therefore considered that these ranges are highly precautionary, and injury is unlikely to occur in reality.

Table 1.55: Median Potential Impact Ranges (m) for Group 3 and 4 Fish Exposed to Drilled Piling

Source	Recoverable Injury	TTS
	170dB rms for 48hrs	158dB for 12hrs
Drilled piling	<10	<10

Other operations

1.9.2.18 The potential impact ranges from other construction related activities (such as cable trenching, cable laying and supporting jack-up rigs) on different marine mammal groups are presented in Table 1.56. The potential impact ranges for fish are presented in Table 1.57.

Table 1.56: Potential Impact Ranges (m) for Marine Mammals During other Construction Related Operations.

Source	Potential Impact Ranges (m)										
	LF		HF		VHF		PCW		OCW		All
	TTS	PTS	TTS	PTS	TTS	PTS	TTS	PTS	TTS	PTS	Disturbance
Cable trenching	N/E	N/E	N/E	N/E	5,200	<10	N/E	N/E	N/E	N/E	19km
Cable laying	N/E	N/E	N/E	N/E	1,600	N/E	N/E	N/E	N/E	N/E	8km
Jack-up rig	N/E	N/E	N/E	N/E	N/E	N/E	N/E	N/E	N/E	N/E	<10 m

Table 1.57: Median Potential Impact Ranges (m) for Group 3 and 4 Fish Exposed to Other Construction Related Operations.

Source	Injury Zone Radius (m)	
	Recoverable Injury	TTS
	170dB rms for 48hrs	158dB rms for 12hrs
Cable trenching	< 10m	34
Cable laying	< 15	63
Jack-up rig	N/E	N/E

Vessels

1.9.2.19 The potential impact ranges for vessels are included in section 1.9.4, which summarises the vessel modelling results for all phases of the Mona Offshore Wind Project.

1.9.3 Operational and maintenance phase

Operational wind turbines

1.9.3.1 Unweighted rms sound contours for operational sound from wind turbines is shown in Figure 1.15, based on an indicative layout for the largest (i.e. highest power rating) wind turbines.

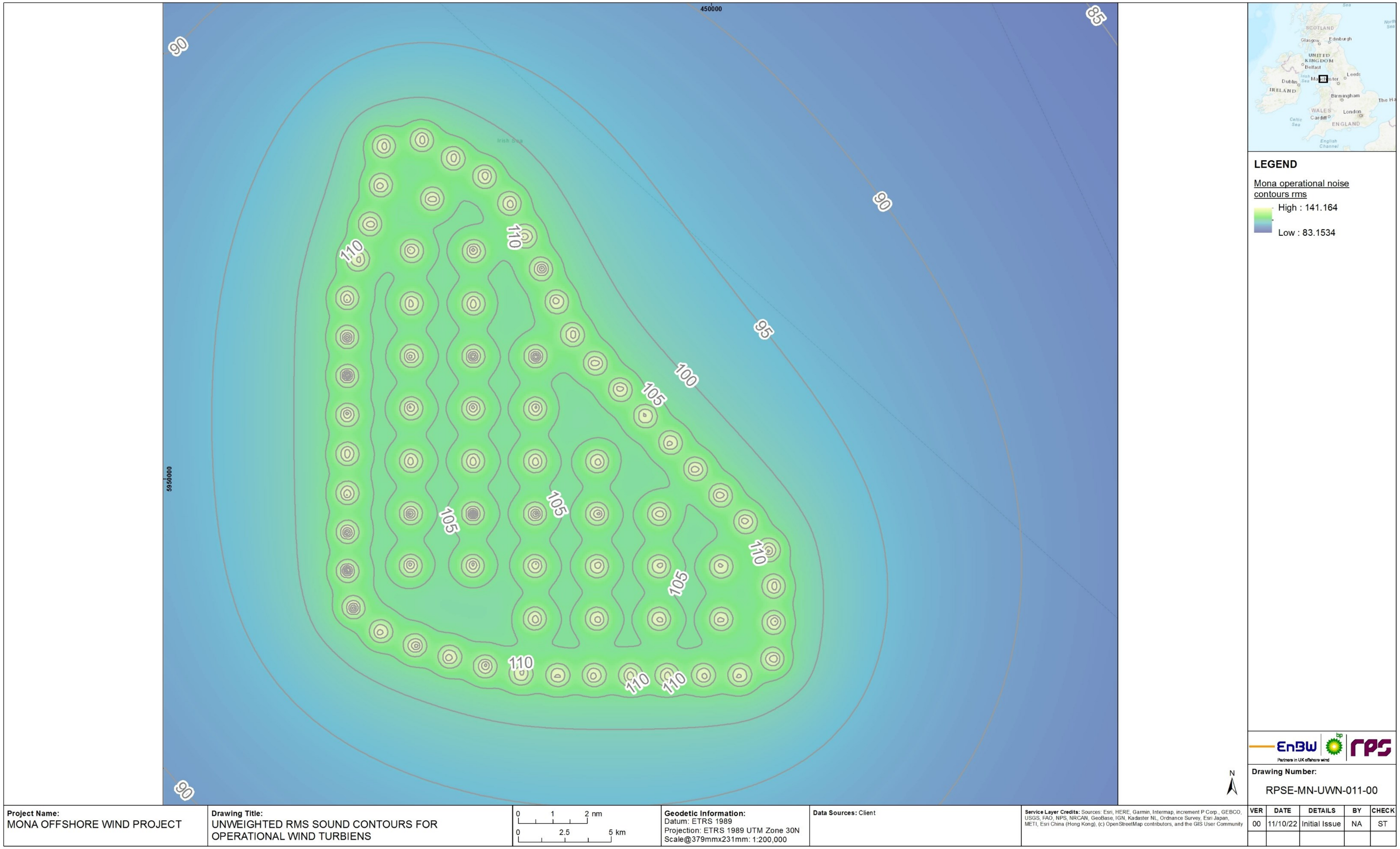

Figure 1.15: Unweighted rms sound contours for operational wind turbines, dB re 1µPa (rms) for an indicative wind turbine layout.

1.9.3.2 Potential disturbance to marine mammals could occur within approximately 160m of each wind turbine, based on the sound contour plot 120dB re 1µPa (rms) contours.

1.9.3.3 The calculated injury ranges for marine mammals, based on 24 hours exposure for a static animal, are shown in Table 1.58. The results show that a LF cetacean would need to remain within 5m of an operational turbine for a period of 24 hours or more in order to reach the PTS threshold, which is considered highly unlikely to occur. It can therefore be concluded that the risk of injury to marine mammals due to operational wind turbines is negligible.

Table 1.58: Potential injury radii for marine mammals due to operational wind turbines sound (static animals 24 hour exposure).

	PTS threshold, dB re 1µPa^{2}s	PTS range, m	TTS threshold, dB re 1µPa^{2}s	TTS range, m
LF cetaceans	199	5	179	39
HF cetaceans	198	N/E	178	N/E
VHF cetaceans	173	N/E	153	8
PCW	201	N/E	181	7
OCW	219	N/E	199	N/E

1.9.3.4 The potential distances at which recoverable injury and TTS could occur to fish due to operational wind turbines is shown in Table 1.59. The recoverable injury threshold is not exceeded and the TTS threshold is exceeded within 5m of a wind turbine , assuming that it acts as an infinitesimally small point source. In reality, this sound level does not exist for a large, distributed, source such as a wind turbine (i.e. the sound is spread out over the area around the entire foundation) and therefore it is considered highly unlikely that TTS will occur, even if a fish was to spend 12 hours in the immediate vicinity of a wind turbine.

Table 1.59: Potential Impact Ranges (m) for Groups 3 and 4 Fish due to operational wind turbines.

Source	Injury Zone Radius (m)	
	Recoverable Injury	TTS
	170dB rms for 48hrs	158dB rms for 12hrs
Operational wind turbines	N/E	5

Maintenance sources

1.9.3.5 The potential impact ranges for the maintenance sound source are reported in Table 1.60 and Table 1.61 below.

Table 1.60: Potential Impact Ranges (m) for Marine Mammal Groups from other Maintenance Operations.

Source	Potential Impact Range (m)										
	LF		HF		VHF		PCW		OCW		All
	TTS	PTS	TTS	PTS	TTS	PTS	TTS	PTS	TTS	PTS	Disturbance
Jet cutting	103	N/E	375	N/E	63,640	2,390	63	N/E	N/E	N/E	>100km

Table 1.61: Potential Impact Ranges (m) for Groups 3 and 4 Fish from other Maintenance Operations.

Source	Injury Zone Radius (m)	
	Recoverable Injury	TTS
	170dB rms for 48hrs	158dB rms for 12hrs
Jet cutting	89	630

Vessels

1.9.3.6 The potential impact ranges for vessels are included in section 1.9.4, which summarises the vessel modelling results for all phases of the Mona Offshore Wind Project.

1.9.4 Vessels and other continuous sounds (all phases)

1.9.4.1 Estimated ranges for injury to marine mammals due to the continuous sound sources (vessels) during different phases of the construction and operations are presented below.

1.9.4.2 It should be borne in mind that there is a considerable degree of uncertainty and variability in the onset of disturbance and therefore any disturbance ranges should be treated as potentially over precautionary. Another important consideration is that vessels and construction sound will be temporary and transitory, as opposed to permanent and fixed. In this respect, construction sound is unlikely to differ significantly from vessel traffic already in the area.

1.9.4.3 The estimated median ranges for onset of TTS or PTS for different marine mammal groups exposure to different sound characteristics of different vessel traffic are shown in Table 1.62. The exposure metrics for different marine mammal and flee speeds (as detailed in section 1.8.4) were employed.

Table 1.62: Estimated PTS and TTS Ranges from Different Vessels for Marine Mammals.

Source/ Vessel	Range (m)										
	LF		HF		VHF		PCW		OCW		All
	TTS	PTS	TTS	PTS	TTS	PTS	TTS	PTS	TTS	PTS	Disturbance
Sandwave clearance	N/E	N/E	N/E	N/E	1,600	N/E	N/E	N/E	N/E	N/E	8km
Boulder clearance	N/E	N/E	N/E	N/E	<15	N/E	N/E	N/E	N/E	N/E	1km
Installation vessel, construction vessel (DP)	N/E	N/E	N/E	N/E	1,600	N/E	N/E	N/E	N/E	N/E	8km
Jack up rig	N/E	N/E	N/E	N/E	N/E	N/E	N/E	N/E	N/E	N/E	<10m
Tug/ anchor handlers	N/E	N/E	N/E	N/E	645	N/E	N/E	N/E	N/E	N/E	6.5km
Rock placement vessel and cable installation vessels	N/E	N/E	N/E	N/E	1,600	N/E	N/E	N/E	N/E	N/E	8km
Guard vessels	N/E	N/E	N/E	N/E	645	N/E	N/E	N/E	N/E	N/E	6.5km
Survey vessel and support vessels	N/E	N/E	N/E	N/E	6,800	N/E	N/E	N/E	N/E	N/E	22km
Crew transfer vessel	N/E	N/E	N/E	N/E	6,800	N/E	N/E	N/E	N/E	N/E	22km
Scour/ Cable Protection/ Seabed Preparation/Installation Vessels	N/E	N/E	N/E	N/E	6,800	N/E	N/E	N/E	N/E	N/E	22km

1.9.4.4 The ranges for recoverable injury and TTS for Groups 3 and 4 Fish are presented in Table 1.63 based on the thresholds contained in Popper et al. (2014). It should be noted that fish would need to be exposed within these potential impact ranges for a period of 48 hours continuously in the case of recoverable injury and 12 hours continuously in the case of TTS for the effect to occur. It is therefore considered that these ranges are highly precautionary, and injury is unlikely to occur in reality.

Table 1.63: Estimated Recoverable Injury and TTS Ranges from Vessels for Groups 3 and 4 Fish.

Source/Vessel	Injury Zone Radius (m)	
	Recoverable Injury	TTS
	170dB rms for 48hrs	158dB rms for 12hrs
Sandwave clearance	< 15	63
Boulder clearance	N/E	< 10
Installation vessel, construction vessel (DP)	< 15	63
Jack up rig	N/E	N/E
Tug/anchor handlers	< 10	15
Rock placement vessel and cable installation vessels	< 15	63
Guard vessels	< 10	15
Survey vessel and support vessels	<15	65
Crew transfer vessel	<15	65
Scour/Cable Protection/Seabed Preparation/Installation Vessels	< 10	41

1.10 Particle Motion

1.10.1 Introduction

1.10.1.1 This Underwater Sound Technical Report, provides an analysis of the effects of sound on marine life. However, there are uncertainties in relation to the presence of compression and interface waves at the water/ ground substrate boundary during piling, and the potential effect on fish and invertebrates. Although the risk of injury to fish with and without swim bladders is addressed through the use of SEL and peak pressure thresholds (Popper *et al.*, 2014), it is possible that some fish are only sensitive to particle motion. These fish could experience high levels of particle motion in close proximity to piling. However, the Popper *et al.* (2014) paper primarily addresses high amplitude sounds and high dynamic pressure, rather than particle motion.

1.10.1.2 The majority of measurements during piling for offshore wind farms are undertaken using hydrophones in the water column which includes contributions from both direct radiated sound from the pile into the water, as well as ground-borne radiated sound, and there are uncertainties with respect to how effectively the ground borne energy couples into the sea. If measurements were taken in an evanescent (non-propagating) field then high particle motion would not be reflected in the associated dynamic pressure measurements, particularly if those measurements were taken in shallow water and the energy is below the cut-off frequency. Consequently, it is possible that the effects on benthic fauna close to the pile could be under-estimated, particularly for species primarily sensitive to vibration of the seafloor sediment.

1.10.1.3 To put this issue into perspective, under section 5.1 entitled “Death or Injury”, Popper *et al.* (2014) states that “extreme levels of particle motion arising from various impulsive sources may also have the potential to injure tissues, although this has yet to be demonstrated for any source”. It would therefore appear that there is currently a lack of criteria for (or detailed measurements of) particle motion during piling operations for this issue to be currently assessed. Thus, in terms of potential damage to fish, volume 2, chapter 8: Fish and shellfish of the PEIR has addressed the impact as far as is practicable with the existing state of knowledge, based primarily on exposure to sound pressure.

1.10.1.4 The purpose of this chapter is to provide an overview of the acoustic aspects of particle motion. Potential effects on marine life are dealt with in the marine ecology topic chapters of the PEIR.

1.10.2 Overview of particle motion

1.10.2.1 Particle motion is defined as the motion of an infinitesimally small part of the medium relative to the rest of the medium, that is caused by a sound wave (Popper *et al.,* 2014). Unlike the pressure variation caused by the wave, which is a scalar quantity and therefore has no direction, the particle motion is a three-dimensional vector quantity (i.e. directional). Particle motion can be described by the velocity, acceleration, and displacement of the particle. These are related by the following equations (Nedelec *et al.,* 2016):

$$a = u \times 2\pi f$$

$$\xi = \frac{u}{2\pi f}$$

where a = acceleration (ms^{-2}), u = particle velocity (ms^{-1}), 2πf = angular frequency, and ξ = displacement (m).

1.10.2.2 Particle motion can also be related to measured sound pressure and can be approximated from the sound pressure in simplified circumstances such as a plane wave. For a plane wave, or a wave for which a plane wave is a good approximation of its behaviour (a wave in the free-field), the following relationship holds:

$$u = \frac{P}{\rho c}$$

where P = acoustic pressure (Pa), ρ = density of the water (kgm^{-3}), and c = sound speed (ms^{-1}). The quantity ρc is also known as the characteristic acoustic impedance.

1.10.2.3 The following relationship holds true for the near field of a point source. The source must be far from any boundaries that could lead to the wave not propagating due to cut off frequency, or reflections that could interfere with the propagation of the wave:

$$\xi = \frac{p}{2\pi f \rho c}\left[1 + \left(\frac{\lambda}{2\pi r}\right)^2\right]^{1/2}$$

where r = distance to sound source (m). All other symbols are consistent throughout the equations presented here.

1.10.2.4 A plane wave is a wave that can be considered to have a flat wavefront. This generally occurs far from both the source of the wave and any sources of reflected waves. The term 'far' is relative to the wavelength of the sound and the size of the source as both will change the distance at which the wave can be considered a plane wave. In shallow coastal and sea-shelf habitats these far-field conditions are not often met at the acoustic frequencies relevant to fish and invertebrates. This means that there is usually not a reliable way to derive particle motion from sound pressure measurement in these habitats. Technically a relationship between particle motion and sound pressure can be derived for more complicated wavefronts (e.g. by assuming that the wavefront has an idealised geometry). However, this is not necessarily reliable, and, in most cases where plane waves cannot be assumed, the only reliable solution is to measure directly (Nedelec *et al.*, 2016).

1.10.2.5 In those situations where it is appropriate to assume that waves generated by a monopole are plane waves (i.e. in the acoustic far field), it is possible to approximate the magnitude of the particle motion. It is important to understand where it is appropriate to make these assumptions. Spherical spreading occurs when sound propagates from a source without any interference and the applicability of the plane wave assumption is based on the frequency of interest and the waveguide (i.e. the duct formed by the surface and bottom of the water column), which encapsulates the water depth, distance to source, source type, and the sound speed in water and sediment. The values that are key for this assumption are the wavelength of the lowest frequency of interest (λ) and the cut off frequency (f_0) based on the waveguide. These values can be calculated from the following equations (Nedelec *et al.*, 2021):

$$\lambda = \frac{c_w}{f}$$

$$f_0 = \frac{c_w}{4D\sqrt{1 - \left(\frac{c_w}{c_b}\right)^2}}$$

Where f_0 is the cut off frequency, *D* is the water depth, c_w is the sound speed in water, and c_b is the sound speed in sediment.

1.10.2.6 If the distance to the sound source is greater than one wavelength and the lowest frequency is greater than the cut off frequency, then it is possible to estimate the magnitude of the particle motion from a Sound Pressure Level (SPL) measurement. However, it must be noted that this only applies to a travelling plane wave and as such the signal to noise ratio must be high enough to consider other sounds negligible (Nedelec *et al.,* 2021).

1.10.2.7 It should also be borne in mind that sound produced from piling is, in reality, not a monopole source. The pile acts as a line source throughout the water column and in the sediment and produces a complex Mach wavefront. Consequently, the above simplifications may not be appropriate to assess the particle motion produced by piling.

1.10.3 Hearing in fish and invertebrates

1.10.3.1 All fish, and many invertebrates, detect the particle motion (PM) of a sound wave with mechanosensory organs such as the inner ear, statocyst or lateral line (Nedelec *et al.,* 2021). The ability to hear their surroundings gives fish, and many invertebrates, an abundance of information about their environment. This ability is unaffected by light levels and is omnidirectional, allowing for the most abundant information about the environment. Of all the senses that fish, and many invertebrates, use to assess their surroundings, hearing is the most versatile in a marine environment. In particular, their hearing is able to give rapid feedback with relatively long distance 3-D information (Popper and Hawkins, 2019).

1.10.3.2 The detection of sound and characterisation of the immediate soundscape is something that is key to the way that fish and many vertebrates live. This ability allows them to detect the direction of predators, and subsequently avoid them, or detect prey and move towards them. Furthermore, this ability can be used to recognise others within their own species and select a mate. Although not all fishes, or invertebrates, produce sound for communication, they are all known to use it for awareness of their surroundings. As such any interference with this ability could impact the survival of the fish (Popper and Hawkins, 2019).

1.10.3.3 There have been several studies into the hearing capabilities of fish and invertebrates. However, very few of them have used conditions that are truly representative of the environment that they would encounter in open water. This is due to tank conditions or methodologies used to observe them in an offshore environment. Furthermore, few of these studies have focussed on particle motion specifically (Popper and Hawkins, 2019).

1.10.3.4 Taking this into account it is possible to establish a reasonable assumption for hearing range of various species. Most fish appear to be able to detect sound that falls between 10Hz and 500Hz. If the fish or invertebrates are capable of detecting sound pressure then they may be able to detect sounds at higher frequencies up to approximately 1kHz or more. There are also a small number of fish that are capable of hearing between 3Hz and 4kHz due to various specialisations that they have (Popper and Hawkins, 2019). The values presented here are the upper and lower estimates of each range, there is a degree of variability in each of the values. This is in part due to the complexity of the sound field in a tank or enclosure (Popper *et al.,* 2019). Likewise, invertebrates are also typically sensitive to lower frequencies (Nedelec *et al.,* 2016).

1.10.4 Effects of sound and particle motion

1.10.4.1 Potential effects of sound and particle motion on fishes and invertebrates can be summarised as follows (Popper *et al.,* 2014; Popper and Hawkins, 2018; Nedelec *et al.*, 2016):

- Death and Injury
- Exposure to very high amplitude sounds can cause injury and death in fish and other marine life. In addition, the effect of sudden pressure changes (barotrauma) must be considered
  - Barotrauma is the tissue injury that is caused by a sudden change in pressure resulting in a shock wave effect (e.g. primarily caused by explosions, as opposed to non-shock wave propagation as is typically caused by impulsive piling). Rapid pressure changes can cause the gases in blood to come out of solution and can cause rapid movement in the swim bladder. This can damage other organs and even rupture the swim bladder
  - Sudden changes in pressure (such as that from impulsive sounds) are more likely to cause damage than gradual ones
  - Extreme levels of particle motion may have the potential to cause tissue damage, but this has not been proven yet (Popper *et al.,* 2014).
- Effects on Hearing
  - Hearing loss can be permanent or temporary (Permanent Threshold Shift (PTS) and Temporary Threshold Shift (TTS)) with PTS being caused by damage to the tissue in the auditory pathway (including the swim bladder)
  - TTS results from temporary damage to the hairs in the inner ear or to the auditory nerves. In fish (unlike in mammals) the hairs of the inner ear are constantly added and replaced if damaged. Therefore, loss of hearing due to damage to these hairs may be mitigated over time in fishes
  - While experiencing TTS, fish may have a decrease in fitness in terms of communication, detecting predators or prey, and/or assessing their environment
  - Masking is an impairment with respect to the relevant sound sources normally detected within the soundscape. The consequences of masking are not fully understood for fish and sea turtles. It is likely that higher levels of masking occur with a higher sound level from the masker.
- Effects on Behaviour
  - It is possible that anthropogenic sound will have a detrimental effect on the communication of species between conspecifics, it may also hinder their identification of predator and prey
  - There have been a variety of behavioural reactions observed from fish, including changes in swimming patterns and startle reactions
  - These reactions may habituate over repeated exposure to the sound.
  - There has been very limited research carried out to date in relation to the effects of particle motion on marine invertebrates (Popper and Hawkins, 2018). However, they are expected to have the same types of effect even if the severity is unclear.

1.10.4.2 Popper *et al.* (2014) categorised fish species into the following identifiable groups:

- Fishes with no swim bladder or other gas chamber. These fish are less susceptible to barotrauma and only detect particle motion, however, some barotrauma may occur from exposure to sound pressure
- Fish with swim bladders in which hearing does not involve the swim bladder or some other gas volume. These species again only detect particle motion; however, they are susceptible to barotrauma due to the presence of the swim bladder
- Fish in which the swim bladder (or other gas volume) is involved in hearing. These species detect sound pressure as well as particle motion and are susceptible to barotrauma. The frequency sensitivity range of this group is higher than the other groups due to the ability to detect the pressure component of the sound signal as well as the particle motion
- Sea turtles
- Fish eggs and larvae.

1.10.4.3 These groups are known to be able to detect particle motion. However, it is also likely that marine invertebrates are able to detect particle motion (Popper and Hawkins, 2018; Discovery of Sound in the Sea (DOSITS)). Furthermore, some marine invertebrates can detect the vibrations directly from the substrate. This makes them susceptible not only to the particle motion in the water but also the rolling waves, and associated particle motion, in the substrate. It has been observed that benthic marine invertebrates respond directly to anthropogenic sound that has been generated in the substrate or very close to its surface (Hawkins *et al.*, 2021; Aimon *et al.*, 2021). This is particularly important for construction processes like piling that generate a large amount of sound into the substrate. The repercussions of this is that offshore construction activity may affect the benthic habitat, and many benthic invertebrates have a key role in how the substrate is structured. Considerable disturbance of these creatures for a prolonged period could affect habitat quality in addition to any potential impacts associated with sound pressure. It has also been suggested that some species use the sound that travels through the substrate to communicate or to find food sources, loud sounds that mask these sounds could make it difficult for them to operate normally (Popper and Hawkins, 2018).

1.10.4.4 There have been several studies into the hearing abilities of fish for a relatively small number of species. From these studies, the upper limit of detection for particle motion was found to be between 200Hz and 400Hz and the lower limit was 0.1Hz (Sigray and Anderson, 2011). It is considered likely that all teleost fish have a similar extent of ability to detect particle motion (Radford *et al.*, 2012). Elasmobranchs are also considered to have a similar range of detection for particle motion. For piling, specifically, it is currently considered that most fish would be able to detect particle motion from 750m away (Thomsen *et al.,* 2015). Marine invertebrates are generally not considered to be sensitive to the pressure wave component of sound as they lack an air-filled space in their bodies. Research still needs to be carried out to understand the hearing capabilities of marine invertebrates. The research that has been undertaken so far has primarily focused on crustaceans and molluscs. A need has been identified to develop species specific audiograms to improve the understanding of the detection thresholds.

1.10.4.5 Hammar *et al.* (2014) discussed the impact of the Kattegat offshore wind farm (offshore Sweden) on Atlantic cod *Gadus morhua* in the region. Estimates of operational sound were predicted as 150dB re 1µPa (rms) at 1m for the 6MW turbines and 250dB re 1µPa (rms) for the pile driving based on measurements on the Burbo Bank offshore wind farm taken by Parvin and Nedwell (2006). Using these estimates Hammar *et al.* (2014) established that developed Atlantic cod were likely to suffer physical injury within several hundred meters of pile driving. However, studies have shown that fish often group around operational wind turbines (Sigray and Andersson, 2011; Engås *et al.*, 1995; Wahlberg and Westerberg, 2005). This suggests that operational sound is not enough to cause them to vacate the area, however it is not clear if it results in higher stress levels in fish in the area.

1.10.5 Potential range of effects due to particle motion at the Mona Offshore Wind Project

1.10.5.1 Due to the current state of understanding and existing (validated) modelling methodologies it is not considered feasible at this time to provide a quantitative assessment of the effects of particle motion on marine life for the Mona Offshore Wind Project.

1.10.5.2 Predicting the levels of particle motion from anthropogenic sound sources is difficult. There is a small amount of measured data available on which to base such predictions and some of these data are not necessarily applicable to full scale industrial procedures such as installation of wind turbine foundations. The measurements that do exist mostly come from small scale tank testing. Some of this testing has been conducted in flooded dock style locations with small scale piles. Other recordings have used play-back speakers to generate a simulated piling sound (Roberts *et al.,* 2016; Ceraulo *et al.,* 2016). There is some debate about the validity of comparing measurements from tank tests or from playback speakers to full scale piling operations, as the way that particles move within a tank or smaller scale system is different to the full scale in the open ocean. Furthermore, the way that a speaker will agitate the particles is different to that of a cylindrical pile with an exposed length in the water column and sediment. However, there is one commonality between all measurements so far: the particle motion attenuates rapidly close to the source and more slowly further from it (Mueller-Blenkle *et al.*, 2010).

1.10.5.3 One such experiment was studied by Ceraulo *et al.* (2016), which consisted of measurements during piling at several locations within a flooded dock that incorporated a simulated seabed layer (approximately 3.5m thick). This allowed the piling to be measured from different ranges. Through this experiment it was found that the sound propagation was close to cylindrical in nature. The levels of particle motion were found to be 102dB re 1nm/s at a distance of 2m from the pile and this dropped to 86dB re 1nm/s at 30m. There was an interesting observation that the pressure wave appeared to have a cut off frequency at 400Hz for shallow water and 300Hz for deep water, although the particle motion does not share this cut off. The study was able to confirm that there is a roughly linear relation between particle motion and pressure although it also found that the particle motion levels were higher than expected.

1.10.5.4 An added complication in predicting particle motion is the propagation of sound through the substrate. This is particularly prominent in piling operations as the pile being driven into the ground will generate considerable waves through the substrate. This particle motion can impact the benthic species in the area due to behavioural reactions and potential injury. This has been identified as an area that requires more research and should be monitored alongside particle motion within the water column itself. Furthermore, the waves passing through the substrate can add to those in the water column, making the sound field in the water more complex (Mueller-Blenkle *et al.*, 2010).

1.10.5.5 A study by Thomsen *et al.* (2015) investigated particle motion around the installation of piles at offshore wind sites. The study found that higher hammer energies elicited higher levels of particle motion and that particle motion levels at 750m from the pile were higher than baseline ambient levels throughout the frequency spectrum, except at very low frequencies. Thomsen *et al.* (2015) showed that with mitigation (a bubble curtain) turned on however, particle motion levels reduced considerably. It should be noted that the range cited of 750m was likely due to the regulatory requirement for monitoring at 750m from a pile and this number is therefore somewhat arbitrary in terms of the potential range of effect for particle motion (i.e. it is the most common measurement range for sound pressure rather than being the range over which particle motion effects were thought likely to occur).

1.10.5.6 Nevertheless, the study concluded that, for most fish, particle motion levels at 750m are high enough to be detected during pile driving of even a mitigated pile. However, for elasmobranchs, the study concluded that detectability of mitigated piles is likely restricted to relatively short ranges from the source depending on the ambient sound in the area. For invertebrates the study concluded that there is even less information on how they perceive particle motion, but the Thomsen *et al.* (2015) study would indicate that some invertebrates should be able to detect the piling sound at a distance of 750m, whether mitigated or not.

1.10.5.7 Taking the above into consideration, it is thought likely that particle motion will be detectable for many fish and invertebrates within the order of 750m from piling at the Mona Offshore Wind Project, although it is not feasible to quantify this further at this stage. Furthermore, it is not possible at this time to determine whether the detection of sound by these species at this range is likely to result in an effect, such as behavioural disturbance or injury. Likewise, it is not possible at this time to define the requirements for, or potential effectiveness of, mitigation for particle motion. However, it is likely that potential injury due to particle motion will be confined to a smaller range than disturbance and detectability. Ultimately, until such a time as considerably more data become available, both in terms of measured particle motion during full scale piling and effects on marine life, it is considered that the assessment of effects as set out in this report represents a robust assessment based on the current state of knowledge.

1.11 Conclusions

1.11.1.1 Acoustic modelling has been undertaken to determine distances at which potential effects on marine mammals, fish, and sea turtles may occur due to sound from piling activities associated with construction of the Mona Offshore Wind Project. The results are summarised in Table 1.64 which shows the maximum injury range for each group of mammals, fish, and sea turtles, for individual and concurrent piling (the MDS of cumulative SEL or peak). The potential PTS impact range is typically dominated by nearest pile, so these ranges do not change for single or concurrent pile driving (except for LF cetaceans where the sound propagates further).

1.11.1.2 It should be noted that the highest distance value for the dual metric PTS threshold range (i.e. for exceedance of either the cumulative SEL of peak SPL, whichever is the highest) is shown in the table. Distance values marked with an asterisk (*) denote where the highest value is as a result of the cumulative SEL metric, and in all other cases it is the result of the peak SPL.

Table 1.64: Summary of Maximum PTS Injury Ranges for Marine Mammals, and Mortality for Fish and Turtles due to Impact Piling of Monopiles and Pin-piles Based on Highest Range of Peak Pressure or SEL without the use of ADD (N/E = Threshold Not Exceeded).

* – Cumulative SEL has the greatest range

Species Group	Range (m)			
	Single Piling (Monopile)	Single Piling (Pin pile)	Concurrent Piling (Monopile)	Concurrent Piling (Pin pile)
Marine Mammals				
Low frequency cetacean	3,870*	61*	5,470*	160*
High frequency cetacean	37	31	37	31
Very high frequency cetacean	2,150*	322	3,330*	322
Phocid carnivores	95	85	95	85
Other carnivores	32	26	32	26
Fish, Eggs/Larvae, Turtles (moving away)				
Group 1 Fish: no swim bladder	140	78	140	78
Group 2 Fish: where swim bladder is not involved in hearing	224	129	224	129
Group 3 to 4 Fish: where swim bladder is involved in hearing	224	129	224	129
Sea turtles	224	129	224	129
Eggs and larvae	224	129	224	129

Table 1.65 Summary of Maximum PTS Injury Ranges for Marine Mammals due to Impact Piling of Monopiles and Pin-piles Based on Highest Range of Peak Pressure or SEL including the use of ADD (N/E = Threshold Not Exceeded).

* – Cumulative SEL has the greatest range

Species Group	Range (m)			
	Single Piling (Monopile)	Single Piling (Pin pile)	Concurrent Piling (Monopile)	Concurrent Piling (Pin pile)
Marine Mammals				
Low frequency cetacean	88	47	1,315*	47
High frequency cetacean	37	19	37	19
Very high frequency cetacean	330	196	745*	196
Phocid carnivores	95	52	95	52
Other carnivores	32	16	32	16

1.11.1.3 In all but the LF and VHF cetacean cases, the PTS ranges are more influenced by peak SPL metric, which mean that the exposure distances are the same for single as for concurrent piling. Consecutive piling has not been included in the summary as the ranges are low compared with the concurrent case, therefore concurrent piling is concluded to result in the largest ranges.

1.11.1.4 Underwater sound emissions from the wind turbines, pre-construction activities, other relevant operational sounds, and vessels during the operational and maintenance phase are unlikely to be at a level sufficient to cause injury to marine mammals, fish, or sea turtles. Discussion of disturbance to marine mammals is provided within Volume 2, chapter 9: Marine mammals of the PEIR.

1.11.1.5 The use of ADD means that no cumulative SEL PTS injury thresholds are exceeded for marine mammals for the single or consecutive piling scenarios, and the injury ranges result only from the peak. The cumulative SEL PTS thresholds for LF and VHF cetaceans are exceeded in the concurrent piling scenario.

1.12 References

HESS. (1997) ‘Summary of Recommendations Made by the Expert Panel at the HESS Workshop on the Effects of Seismic Sound on Marine Mammals’. (1997) In . Pepperdine University, Malibu, California.

Aimon, Cassandre, Stephen D. Simpson, Richard A. Hazelwood, Rick Bruintjes, and Mauricio A. Urbina. (2021) ‘Anthropogenic Underwater Vibrations Are Sensed and Stressful for the Shore Crab Carcinus Maenas’. Environmental Pollution 285: 117148.

ANSI. (1986) ‘S12.7-1986 Method for Measurement of Impulse Noise’.

ANSI. (1995) ‘ANSI S3.20-1995 Bioacoustical Terminology’. American National Standards Institute.

ANSI. (2005) ‘ANSI S1.13-2005 Measurement of Sound Pressure Levels in Air’. American National Standards Institute.

Bailey, Helen, Bridget Senior, Dave Simmons, Jan Rusin, Gordon Picken, and Paul M. Thompson. (2010) ‘Assessing Underwater Noise Levels during Pile-Driving at an Offshore Windfarm and Its Potential Effects on Marine Mammals’. Marine Pollution Bulletin 60 (6): 888–97.

Benda-Beckmann, A. M. von, D. R. Ketten, F. P. A. Lam, C. A. F. de Jong, R. A. J. Müller, and R. A. Kastelein. (2022) ‘Evaluation of Kurtosis-Corrected Sound Exposure Level as a Metric for Predicting Onset of Hearing Threshold Shifts in Harbor Porpoises (Phocoena Phocoena)’. The Journal of the Acoustical Society of America 152 (1): 295–301.

Boisseau, Oliver, Tessa McGarry, Simon Stephenson, Ross Compton, Anna-Christina Cucknell, Conor Ryan, Richard McLanaghan, and Anna Moscrop. (2021) ‘Minke Whales Balaenoptera Acutorostrata Avoid a 15 KHz Acoustic Deterrent Device (ADD)’. Marine Ecology Progress Series 667: 191–206.

Brandt, Miriam J., Ansgar Diederichs, Klaus Betke, and Georg Nehls. (2011) ‘Responses of Harbour Porpoises to Pile Driving at the Horns Rev II Offshore Wind Farm in the Danish North Sea’. Marine Ecology Progress Series 421: 205–16.

Brekhovskikh, Leonid Maksimovich, and I͡Uriĭ Lysanov. (2003) Fundamentals of Ocean Acoustics.

Ceraulo, Maria, Rick Bruintjes, Thomas Benson, Kate Rossington, Almo Farina, and Giuseppa Buscaino. (2016) ‘Relationships of Sound Pressure and Particle Velocity during Pile Driving in a Flooded Dock’. In Proceedings of Meetings on Acoustics 4ENAL, 27:040007. Acoustical Society of America.

Cole, B. F. (1965) ‘Marine Sediment Attenuation and Ocean-Bottom-Reflected Sound’. The Journal of the Acoustical Society of America 38 (2): 291–97.

Dekeling, R. P. A., M. L. Tasker, A. J. Van der Graaf, M. A. Ainslie, M. H. Andersson, M. André, J. F. Borsani, K. Brensing, M. Castellote, and D. Cronin. (2014) ‘Monitoring Guidance for Underwater Noise in European Seas, Part II: Monitoring Guidance Specifications. A Guidance Document within the Common Implementation Strategy for the Marine Strategy Framework Directive by MSFD Technical Subgroup on Underwater Noise.’

Eckart, Carl. (1953) ‘The Scattering of Sound from the Sea Surface’. The Journal of the Acoustical Society of America 25 (3): 566–70.

Engås, Arill, Ole Arve Misund, Aud Vold Soldal, Berit Horvei, and Arne Solstad. (1995) ‘Reactions of Penned Herring and Cod to Playback of Original, Frequency-Filtered and Time-Smoothed Vessel Sound’. Fisheries Research 22 (3–4): 243–54.

Erbe, C., and McPherson, C. (2017). "Underwater noise from geotechnical drilling and standard penetration testing.". The Journal of the Acoustical Society of America 142, no. 3 (2017): EL281-EL285.

Essen, H.-H. (1994) ‘Scattering from a Rough Sedimental Seafloor Containing Shear and Layering’. The Journal of the Acoustical Society of America 95 (3): 1299–1310.

Etter, Paul C. (2013) Underwater Acoustic Modeling and Simulation. CRC Press.

Farcas, Adrian, Paul M. Thompson, and Nathan D. Merchant. (2016) ‘Underwater Noise Modelling for Environmental Impact Assessment’. Environmental Impact Assessment Review 57: 114–22.

Fortuin, Leonard. (1970) ‘Survey of Literature on Reflection and Scattering of Sound Waves at the Sea Surface’. The Journal of the Acoustical Society of America 47 (5B): 1209–28.

Graham, Isla M., Enrico Pirotta, Nathan D. Merchant, Adrian Farcas, Tim R. Barton, Barbara Cheney, Gordon D. Hastie, and Paul M. Thompson. (2017) ‘Responses of Bottlenose Dolphins and Harbor Porpoises to Impact and Vibration Piling Noise during Harbor Construction’. Ecosphere 8 (5): e01793.

Graham, Isla M., Nathan D. Merchant, Adrian Farcas, Tim R. Barton, Barbara Cheney, Saliza Bono, and Paul M. Thompson. (2019) ‘Harbour Porpoise Responses to Pile-Driving Diminish over Time’. Royal Society Open Science 6 (6): 190335.

Greaves, Robert J., and Ralph A. Stephen. (2003) ‘The Influence of Large-Scale Seafloor Slope and Average Bottom Sound Speed on Low-Grazing-Angle Monostatic Acoustic Scattering’. The Journal of the Acoustical Society of America 113 (5): 2548–61.

Hamilton, Edwin L. (1970) ‘Reflection Coefficients and Bottom Losses at Normal Incidence Computed from Pacific Sediment Properties’. Geophysics 35 (6): 995–1004.

Hamilton, Edwin L. (1978) ‘Sound Velocity–Density Relations in Sea-Floor Sediments and Rocks’. The Journal of the Acoustical Society of America 63 (2): 366–77.

Hamilton, Edwin L. (1980) ‘Geoacoustic Modeling of the Sea Floor’. The Journal of the Acoustical Society of America 68 (5): 1313–40.

Hammar, Linus, Andreas Wikström, and Sverker Molander. (2014) ‘Assessing Ecological Risks of Offshore Wind Power on Kattegat Cod’. Renewable Energy 66: 414–24.

Harris, CM, Thomas, L, Falcone, EA, et al. (2018) Marine mammals and sonar: Dose–response studies, the risk-disturbance hypothesis and the role of exposure context. J Appl Ecol. 2018; 55: 396– 404.

Harris, R.E., Miller, G.W. and Richardson, W.J. (2001). Seal Responses to Airgun Sounds During Summer Seismic Surveys in the Alaskan Beaufort Sea. Marine Mammal Science, 17(4):795-812. Society for Marine Mammalogy.

Hastie, Gordon, Nathan D. Merchant, Thomas Götz, Debbie JF Russell, Paul Thompson, and Vincent M. Janik. (2019) ‘Effects of Impulsive Noise on Marine Mammals: Investigating Range-Dependent Risk’. Ecological Applications 29 (5): e01906.

Hastings, M. C. (2002) ‘Clarification of the Meaning of Sound Pressure Levels & the Known Effects of Sound on Fish’. White Paper.

Hawkins, Anthony D., Richard A. Hazelwood, Arthur N. Popper, and Patrick C. Macey. (2021) ‘Substrate Vibrations and Their Potential Effects upon Fishes and Invertebrates’. The Journal of the Acoustical Society of America 149 (4): 2782–90.

ISO (2017). ISO 18405:2017(en) Underwater Acoustics - Terminology

JNCC (2010) Statutory nature conservation agency protocol for minimising the risk of injury to marine mammals from piling noise. Available online at: https://data.jncc.gov.uk/data/31662b6a-19ed-4918-9fab-8fbcff752046/JNCC-CNCB-Piling-protocol-August2010-Web.pdf. Accessed: January 2022

Kinsler, Lawrence E., Austin R. Frey, Alan B. Coppens, and James V. Sanders. (1999) 'Fundamentals of Acoustics'. Fundamentals of Acoustics, 4th Edition, by Lawrence E. Kinsler, Austin R. Frey, Alan B. Coppens, James V. Sanders, Pp. 560. ISBN 0-471-84789-5. Wiley-VCH, December 1999. 1.

Kongsberg. (2011) 'Measurement of Underwater Noise during Installation of 2.4MW Oyster Array at EMEC Wave Test Site, Billia Croo, Orkney'. 250121-TR-0001. Kongsberg.

Kuo, Edward YT. (1992) 'Acoustic Wave Scattering from Two Solid Boundaries at the Ocean Bottom: Reflection Loss'. Oceanic Engineering, IEEE Journal Of 17 (1): 159–70.

Lawrence, B. (2016) 'Underwater Noise Measurements – Rock Breaking at Acheron Head'.

Lippert, T., Galindo-Romero, M., Gavrilov, A.N., and von Estorff, O. (2015). "Empirical Estimation of Peak Pressure Level from Sound Exposure Level. Part II: Offshore Impact Pile Driving Noise". The Journal of the Acoustical Society of America 138 (3)

Lippert, Stephan, Marten Nijhof, Tristan Lippert, Daniel Wilkes, Alexander Gavrilov, Kristof Heitmann, Marcel Ruhnau, Otto von Estorff, Alexandra Schäfke, and Ingo Schäfer. (2016) 'COMPILE—A Generic Benchmark Case for Predictions of Marine Pile-Driving Noise'. IEEE Journal of Oceanic Engineering 41 (4): 1061–71.

Lucke, Klaus, Ursula Siebert, Paul A. Lepper, and Marie-Anne Blanchet. (2009) 'Temporary Shift in Masked Hearing Thresholds in a Harbor Porpoise (Phocoena Phocoena) after Exposure to Seismic Airgun Stimuli'. The Journal of the Acoustical Society of America 125 (6): 4060–70.

Lurton, Xavier. (2002) An Introduction to Underwater Acoustics: Principles and Applications. Springer Science & Business Media.

Mackenzie, K. V. (1960) 'Reflection of Sound from Coastal Bottoms'. The Journal of the Acoustical Society of America 32 (2): 221–31.

Madsen, P. T. (2005) 'Marine Mammals and Noise: Problems with Root Mean Square Sound Pressure Levels for Transients'. The Journal of the Acoustical Society of America 117: 3952.

Malme, C. I., Miles, P. R., Clark, C. W., Tyack, P., & Bird, J. E. (1984). Investigations of the potential effects of underwater noise from petroleum-industry activities on migrating gray-whale behavior. Phase 2: January 1984 migration (No. PB-86-218377/XAB; BBN-5586). Bolt, Beranek and Newman, Inc., Cambridge, MA (USA).

Marsh, H. Wysor, M. Schulkin, and S. G. Kneale. (1961) 'Scattering of Underwater Sound by the Sea Surface'. The Journal of the Acoustical Society of America 33 (3): 334–40.

Martin, S. Bruce, Klaus Lucke, and David R. Barclay. (2020) 'Techniques for Distinguishing between Impulsive and Non-Impulsive Sound in the Context of Regulating Sound Exposure for Marine Mammals'. The Journal of the Acoustical Society of America 147 (4): 2159–76.

McCauley, Rob. 1998. 'Radiated Underwater Noise Measured From the Drilling Rig Ocean General, Rig Tenders Pacific Ariki and Pacific Frontier, Fishing Vessel Reef Venture and Natural Sources in the Timor Sea, Northern Australia'. C98-20. Centre for Marine Science and Technology, Curtin University of Technology.

McKinney, C. Mo, and C. D. Anderson. (1964) 'Measurements of Backscattering of Sound from the Ocean Bottom'. The Journal of The Acoustical Society of America 36 (1): 158–63.

Mueller-Blenkle, Christina, Peter K. McGregor, Andrew B. Gill, Mathias H. Andersson, Julian Metcalfe, Victoria Bendall, Peter Sigray, Daniel Wood, and Frank Thomsen. (2010) 'Effects of Pile Driving Noise on the Behaviour of Marine Fish'. COWRIE technical report. 31st March 2010. Ref: Fish 06-08.

Nedelec, Sophie L., James Campbell, Andrew N. Radford, Stephen D. Simpson, and Nathan D. Merchant. (2016) 'Particle Motion: The Missing Link in Underwater Acoustic Ecology'. Methods in Ecology and Evolution 7 (7): 836–42.

Nedelec, Sophie L., Michael A. Ainslie, M. Andersson, C. Sei-Him, M. B. Halvorsen, M. Linné, B. Martin, A. Nöjd, S. P. Robinson, and S. D. Simpson. (2021) 'Best Practice Guide for Underwater Particle Motion Measurement for Biological Applications'. Technical Report, University of Exeter, IOGP Marine Sound and Life Joint Industry Programme.

Nedwell, J.R., Collett, A.G., Barham, R.J., Mason, T.I., Bird, H.V. (2012) Measurement and Assessment of Underwater Noise during Ormonde Offshore Wind Farm's Operational Phase, Subacoustech Report No. E354R0104.

Nedwell, J. R., and B. Edwards. (2004) 'A Review of Measurements of Underwater Man-Made Noise Carried out by Subacoustech Ltd, 1993 - 2003'. 534R0109. Subacoustech Ltd.

Nedwell, J., J. Langworthy, and D. Howell. (2003) 'Assessment of Sub-Sea Acoustic Noise and Vibration from Offshore Wind Turbines and Its Impact on Marine Wildlife; Initial Measurements of Underwater Noise during Construction of Offshore Windfarms, and Comparison with Background Noise'. Subacoustech Report Ref: 544R0423, Published by COWRIE.

Nedwell, J. R., Parvin, S. J., Brooker, A. G. & Lambert, D. R. (2008). Modelling and measurement of underwater noise associated with the proposed Port of Southampton capital dredge and redevelopment of berths 201/202 and assessment of the disturbance to salmon. 05 December 2008. Subacoustech Report No. 805R0444. Subacoustech.

NIOSH. (1998) 'Criteria for a Recommended Standard: Occupational Noise Exposure.' National Institute for Occupational Safety and Health.

NMFS. (2005) 'Scoping Report for NMFS EIS for the National Acoustic Guidelines on Marine Mammals'. National Marine Fisheries Service.

NMFS. (2018) '2018 Revision to: Technical Guidance for Assessing the Effects of Anthropogenic Sound on Marine Mammal Hearing (Version 2.0)'. NOAA Technical Memorandum NMFS-OPR-59. National Oceanic and Atmospheric Administration.

Orsted. 2020. Volume 2 Chapter 4 Marine Mammals. Available: https://infrastructure.planninginspectorate.gov.uk/projects/eastern/hornsea-project-three-offshore-wind-farm/?ipcsection=docs&stage=app&filter1=Environmental+Statement Accessed October 2022

Otani, Seiji, Yasuhiko Naito, Akiko Kato, and Akito Kawamura. (2000) 'Diving Behavior And Swimming Speed of a Free-Ranging Harbor Porpoise, Phocoena Phocoena'. Marine Mammal Science 16 (4): 811–14.

Pangerc, Tanja, Peter D. Theobald, Lian S. Wang, Stephen P. Robinson, and Paul A. Lepper. (2016) 'Measurement and Characterisation of Radiated Underwater Sound from a 3.6MW Monopile Wind Turbine'. The Journal of the Acoustical Society of America 140 (4): 2913–22.

Parvin, S. J., and J. R. Nedwell. (2006) ‘Underwater Noise Survey during Impact Piling to Construct the Burbo Bank Offshore Wind Farm’. Subacoustech Ltd, 5.

Pein, Jonas von, Elin Klages, Stephan Lippert, and Otto von Estorff. (2019) ‘A Hybrid Model for the 3D Computation of Pile Driving Noise’. In OCEANS 2019-Marseille, 1–6. IEEE.

Pein, Jonas von, Stephan Lippert, and Otto von Estorff. (2017) ‘A 3D Far-Field Model for Underwater Pile Driving Noise’. In 4th Underwater Acoustics Conference and Exhibition (UACE 2017), Skiathos, Greece.

Pein, Jonas von, Stephan Lippert, and Otto von Estorff. (2021) ‘Validation of a Finite Element Modelling Approach for Mitigated and Unmitigated Pile Driving Noise Prognosis’. The Journal of the Acoustical Society of America 149 (3): 1737–48.

Popper, A.N. and Hawkins, A.D. (2016). The Effects of Noise on Acquatic Life, II. Springer Science+Business Media. New York, NY.

Popper, Arthur N., and Anthony D. Hawkins. (2018) ‘The Importance of Particle Motion to Fishes and Invertebrates’. The Journal of the Acoustical Society of America 143 (1): 470–88.

Popper, Arthur N., and Anthony D. Hawkins. (2019) ‘An Overview of Fish Bioacoustics and the Impacts of Anthropogenic Sounds on Fishes’. Journal of Fish Biology 94 (5): 692–713.

Popper, Arthur N., Anthony D. Hawkins, Olav Sand, and Joseph A. Sisneros. (2019) ‘Examining the Hearing Abilities of Fishes’. The Journal of the Acoustical Society of America 146 (2): 948–55.

Popper, Arthur N., Anthony D. Hawkins, Richard R. Fay, David A. Mann, Soraya Bartol, Thomas J. Carlson, Sheryl Coombs, *et al.* (2014) ASA S3/SC1.4 TR-2014 Sound Exposure Guidelines for Fishes and Sea Turtles: A Technical Report Prepared by ANSI-Accredited Standards Committee S3/SC1 and Registered with ANSI. Springer.

Radford, Craig A., John C. Montgomery, Paul Caiger, and Dennis M. Higgs. (2012) ‘Pressure and Particle Motion Detection Thresholds in Fish: A Re-Examination of Salient Auditory Cues in Teleosts’. Journal of Experimental Biology 215 (19): 3429–35.

Reiser, Craig, Dale Funk, Robert Rodrigues, and David Hannay. (2011) Marine Mammal Monitoring and Mitigation During Marine Geophysical Surveys by Shell Offshore, Inc. in the Alaskan Chukchi and Beaufort Seas, July-October 2010: 90-Day Report. LGL Alaska Research Associates.

Richardson, William John, Denis H. Thomson, Charles R. Greene, Jr., and Charles I. Malme. (1995) Marine Mammals and Noise. Academic Press.

Richardson, William John. (1995) Marine Mammals and Noise. San Diego, Calif. ; Toronto: Academic Press.

Roberts, Louise, Harry R. Harding, Irene Voellmy, Rick Bruintjes, Steven D. Simpson, Andrew N. Radford, Thomas Breithaupt, and Michael Elliott. (2016) ‘Exposure of Benthic Invertebrates to Sediment Vibration: From Laboratory Experiments to Outdoor Simulated Pile-Driving’. In Proceedings of Meetings on Acoustics 4ENAL, 27:010029. Acoustical Society of America.

Robinson, Stephen P., Lian Wang, Sei-Him Cheong, Paul A. Lepper, Francesca Marubini, and John P. Hartley. (2020) ‘Underwater Acoustic Characterisation of Unexploded Ordnance Disposal Using Deflagration’. Marine Pollution Bulletin 160: 111646.

Russell, Debbie JF, Gordon D. Hastie, David Thompson, Vincent M. Janik, Philip S. Hammond, Lindesay AS Scott-Hayward, Jason Matthiopoulos, Esther L. Jones, and Bernie J. McConnell. (2016) ‘Avoidance of Wind Farms by Harbour Seals Is Limited to Pile Driving Activities’. Journal of Applied Ecology 53 (6): 1642–52.

RWE. (2022). Awel y Môr Offshore Wind Farm Category 6: Environmental Statement. Volume 2, Chapter 7: Marine Mammals. Date: April 2022 Revision: B

Seagreen Wind Energy. 2018. Chapter 10 Marine Mammals. Available: https://marine.gov.scot/sites/default/files/chapter_10_marine_mammals.pdf Accessed October 2022

Sigray, Peter, and Mathias H. Andersson. (2011) ‘Particle Motion Measured at an Operational Wind Turbine in Relation to Hearing Sensitivity in Fish’. The Journal of the Acoustical Society of America 130 (1): 200–207.

Sigray, P., Linné, M., Andersson, M.H., Nöjd, A., Persson, L.K.G., Gill, A.B. and Thomsen, F. (2022). Particle motion observed during offshore wind turbine piling operation. Marine Pollution Bulletin 180: 113734.

Sims, David W., Colin D. Speedie, and Adrian M. Fox. (2000) ‘Movements and Growth of a Female Basking Shark Re-Sighted after a Three Year Period’. Journal of the Marine Biological Association of the United Kingdom 80 (6): 1141–42.

Soloway, Alexander G., and Peter H. Dahl. (2014) ‘Peak Sound Pressure and Sound Exposure Level from Underwater Explosions in Shallow Water’. The Journal of the Acoustical Society of America 136 (3): EL218–23.

Southall, B. (2021) ‘Evolutions in Marine Mammal Noise Exposure Criteria’. Acoustics Today 17 (2).

Southall, B. L., Nowacek, D. P., Bowles, A. E., Senigaglia, V., Bejder, L., & Tyack, P. L. (2021). Marine Mammal Noise Exposure Criteria: Assessing the Severity of Marine Mammal Behavioral Responses to Human Noise. Aquatic Mammals, 47(5), 421-464.Southall, Brandon L., Ann E. Bowles, William T. Ellison, James J. Finneran, Roger L. Gentry, Charles R. Greene Jr, David Kastak, *et al.* (2007) ‘Marine Mammal Noise-Exposure Criteria: Initial Scientific Recommendations’. Aquatic Mammals 33 (4): 411–521.

Southall, B., D. Tollit, C. Clark, and W. Ellison. (2017) ‘Application of an Adapted, Relativistic Risk Assessment Framework to Evaluate Modeled Marine Mammal Noise Exposures Resulting from Gulf of Mexico OCS Proposed Geological and Geophysical Activities (Programmatic DEIS): Final Draft Report.’

Southall, Brandon L., James J. Finneran, Colleen Reichmuth, Paul E. Nachtigall, Darlene R. Ketten, Ann E. Bowles, William T. Ellison, Douglas P. Nowacek, and Peter L. Tyack. (2019) ‘Marine Mammal Noise Exposure Criteria: Updated Scientific Recommendations for Residual Hearing Effects’. Aquatic Mammals 45 (2): 125–232.

Thompson, D., A. Brownlow, J. Onoufriou, and S. Moss. (2015) ‘Collision Risk and Impact Study: Field Tests of Turbine Blade-Seal Carcass Collisions’. Report to Scottish Government MR 7 (3): 1–16.

Thomsen, F., A. Gill, M. Kosecka, M. Andersson, M. Andre, S. Degraer, T. Folegot, J. Gabriel, A. Judd, and T. Neumann. (2015) ‘MaRVEN–Environmental Impacts of Noise, Vibrations and Electromagnetic Emissions from Marine Renewable Energy’. Final Study Report, Brussels, Belgium.

Tougaard, Jakob, Line Hermannsen, and Peter T. Madsen. (2020) ‘How Loud Is the Underwater Noise from Operating Offshore Wind Turbines?’ The Journal of the Acoustical Society of America 148 (5): 2885–93.

Urick, Robert J. (1983) Principles of Underwater Sound. McGraw-Hill.

Urick, Robert J., and Robert M. Hoover. (1956) ‘Backscattering of Sound from the Sea Surface: Its Measurement, Causes, and Application to the Prediction of Reverberation Levels’. The Journal of the Acoustical Society of America 28 (6): 1038–42.

Wahlberg, Magnus, and Håkan Westerberg. (2005) ‘Hearing in Fish and Their Reactions to Sounds from Offshore Wind Farms’. Marine Ecology Progress Series 288: 295–309.

Weston, D. E. (1971) ‘Intensity-Range Relations in Oceanographic Acoustics’. Journal of Sound and Vibration 18 (2): 271–87.

Weston, D. E. (1980a) ‘Acoustic Flux Formulas for Range-Dependent Ocean Ducts’. The Journal of the Acoustical Society of America 68 (1): 269–81.

Weston, D. E. (1980b) ‘Acoustic Flux Methods for Oceanic Guided Waves’. The Journal of the Acoustical Society of America 68 (1): 287–96.

WSDOT. (2011) ‘Biological Assessment Preparation for Transport Projects - Advanced Training Manual’. Washington State Department of Transport.

Wyatt, R., Jiménez-Arranz, G., Banda, N., and Cook, S. (2020) ‘Review on Existing Data on Underwater Sounds Produced by the Oil and Gas Industry - A Report Prepared by Seiche Ltd for the Joint Industry Programme (JIP) on E&P Sound and Marine Life’. P783. Seiche Ltd.

Wyatt, R. (2008) ‘Joint Industry Programme on Sound and Marine Life - Review of Existing Data on Underwater Sounds Produced by the Oil and Gas Industry’.

Appendix A: Pile Driving Study

Prediction of the underwater sound emission during construction of the Morgan and Mona Offshore Wind Projects

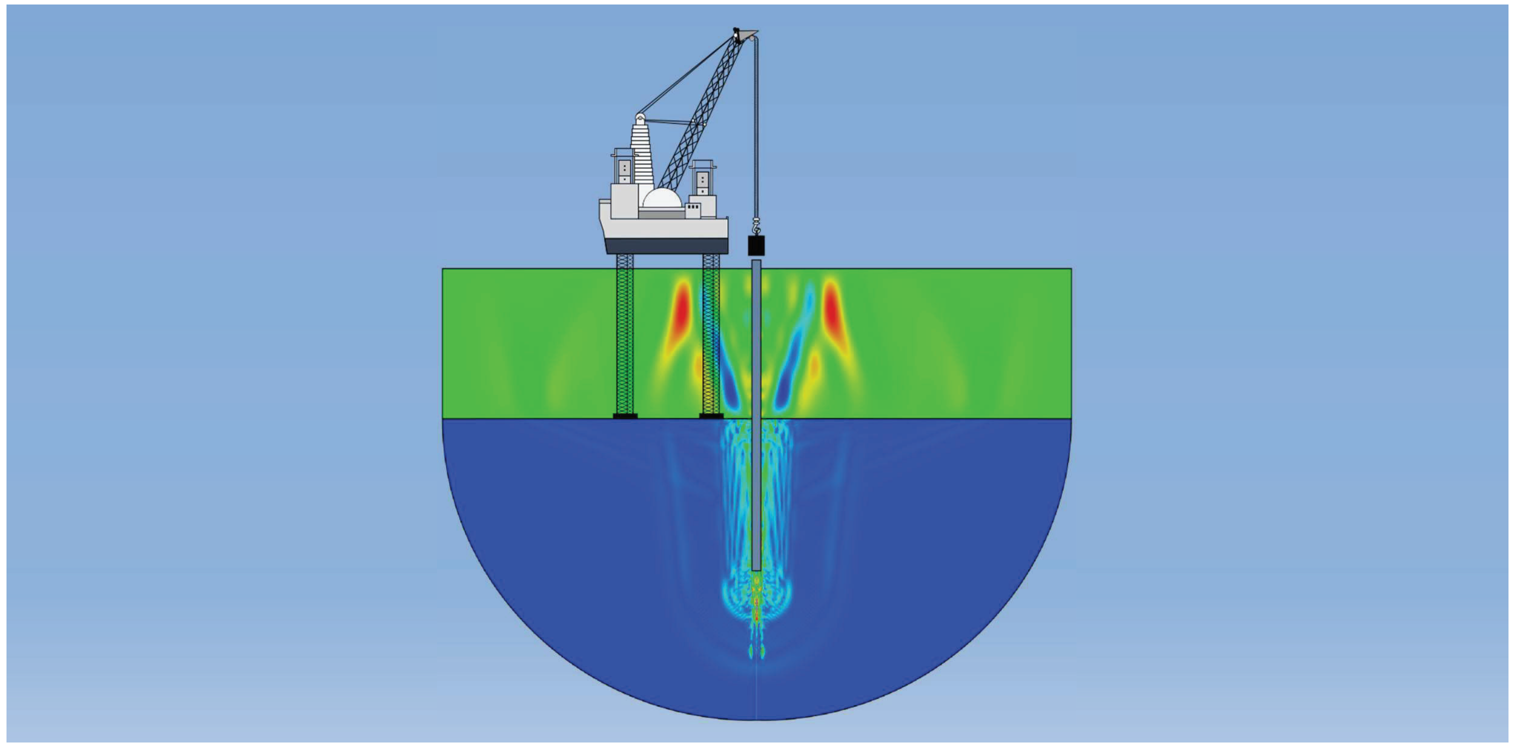

Ordering party: Seiche Ltd
Bradworthy Industrial Estate, Langdon Road
Bradworthy, Devon, EX22 7SF, United Kingdom

Editor: Novicos GmbH
Veritaskai 8, 21079 Hamburg, Germany
Dr. S. Lippert, Dr. N. Rehbein, J. von Pein
lippert@novicos.de

Report number: 22-121-128-01-02 (Rev. 02)
Hamburg, September 01, 2022

92 pages incl. front page and appendix

Report no. 22-121-128-01-02 (Rev. 02)

Table of contents

1. Introduction

1.1 Motivation

During construction of the proposed Morgan and Mona Offshore Wind Projects, located in the Irish Sea approximately 30km off the coast between Liverpool and the Isle of Man, the installation of steel piles with an impact hammer is intended. The effect of underwater sound on marine life due to offshore pile driving has gained increasing importance within recent years [1,2]. Therefore, the pile driving related sound levels need to be taken into consideration as part of the environmental impact assessment. Within this study, a prediction of the underwater sound emission during installation of the monopile and jacket foundations has been performed.

1.2 Scope of work

Due to the large pile diameters and hammer energies proposed in the PEIR PDE for the Morgan and Mona Offshore Wind Projects foundations, extrapolation of pile source levels from existing datasets would likely result in gross errors in the estimation of the sound emissions. Consequently, *Seiche Ltd* has commissioned *Novicos GmbH* to undertake additional modelling in order to provide a more scientific basis for source level calculations.

The scope of this study is to:

- Build an underwater sound model to predict the sound exposure levels (L_E) and the peak sound pressure levels (L_{peak}) at a control location of 750 m from the pile (Chap. 2); and
- Predict corresponding spectral source levels

This study covers several preliminary monopile and pin pile (jacket foundation) designs for both a typical Morgan and a typical Mona location. Depending on the pile design, different hammer options have been considered. The calculations are carried out using comprehensive numerical models (Chap. 3), which are based on the specific input parameters of the project/site as provided by the client (Chap. 4).

In the following parts of the study, the resulting L_E and L_{peak} levels from the investigations for the different settings are illustrated (Chap. 5 to Chap. 8). Finally, remarks regarding the uncertainty of the predictions (Chap. 9) and a summary of the modelling study results (Chap. 10) are given.

2. Fundamentals

Within this report, all sound pressure levels stated in decibel [dB] refer to a reference pressure of 1µPa, which is commonly used in the frame of underwater acoustics.

The following relevant sound levels and terminology will be used [3,4]:

Peak pressure level (L_{peak}):

The L_{peak} is a measure of the occurring peak values of the sound pressure.

$$L_{peak} = 20 \cdot \log\left(\frac{|p_{peak}|}{p_0}\right) \quad (1)$$

Here, the p_{peak} represents the maximum positive or negative sound pressure, while p_0 is the reference pressure of 1µPa.

Often, the L_{peak} is also referred to as *SPL* or SPL_{peak}.

Sound exposure level (L_E):

The L_E of a hammer strike is a measure for the energy equivalent continuous sound level of a continuous sound signal of length 1s.

$$L_E = 10 \cdot \log\left(\frac{1}{T_0}\int_{T_1}^{T_2} \frac{p(t)^2}{p_0^2} dt\right) \quad (2)$$

Here, T_0 represents the reference period of 1s, while T_1 and T_2 mark the starting as well as the end time of the averaging. The time-dependent pressure development within the averaging period is referred to as *p(t)*, while p_0 again stands for the reference pressure of 1µPa, resulting in a reference unit of dB re 1 µPa^{2}s.

A common synonym for the L_E is the term *SEL*.

3. General model configuration

The finite element method (FEM) is used to model the sound generation and propagation due to the pile driving. The FEM is a mathematical discretization method for differential equations (DE), which transfers the DE into a system of linear equations and thus numerically approximates their solution. The FEM technique is widely applied in numerous areas of physics including structural dynamics and acoustics. It is especially suitable to solve coupled problems, e.g. vibro-acoustic problems, such as offshore pile driving (*von Estorff et al.* [5] and *Lippert et al.* [6]).

To predict the sound emission into the water column related to the pile driving, an approach has been chosen that splits the calculation into two dedicated steps, which are based on different models. This ensures for a high precision along with tolerable calculation times.

In a first step, the pile excitation force due to the hammer impact is determined in a separate pre-calculation applying a FEM model, which takes the pile, the impact hammer, the anvil as well as the contact parameters between the different components into account at a very high level of detail. The approach is based on the method described in *Heitmann et al.* [7,8]. In contrast to common approximation procedures, which are often used to estimate the excitation force (e.g. *Deeks and Randolph* [9]), a far more detailed description of the excitation force acting on the pile head is possible. Among others, the model not only explicitly takes into account the geometry and mass of the ram weight, but also the geometry and mass of the anvil and possible further components between hammer and pile. The contact parameters, which significantly influence the characteristics of the excitation force, have been specifically derived for offshore pile driving. Due to this approach, it is possible to model not only the general characteristics of the forcing function, but also its high-frequent signal contents, which is an important prerequisite for accurately determining the resulting hydrosound emission. In this particular case, the axial excitation signals for the different hammer settings that have been considered within the frame of this study were calculated by the piling company IQIP and have been provided by the client as an input to the study (see Chap. 4.2 for details).

The pile head excitation signal is then used as an initial boundary condition for a separate FEM propagation model, which consists of the pile as well as the surrounding soil and water. This allows a substitution of the coupling between the pile and the impact hammer in the second model by replacing it with the corresponding pile head excitation. The general setup of the acoustic propagation model, for example its two-dimensional rotational symmetry, is based on the work of *Reinhall and Dahl* [10]. For the discretisation, a mesh size is chosen that allows the calculation to be carried out for frequencies up to 2kHz. Especially when considering large pile diameters, as is the case for the piles modelled in this study, a restriction of the frequency range is legitimate, since most of the energy transferred into the water column and soil occurs significantly low-frequent at around 100Hz.

For the present model, the approach has been modified and extended in various ways, to enable for an accurate prediction of the underwater noise emission related to the pile driving. Therefore, the soil is not represented as an equivalent fluid but instead by linear-elastic elements. Besides the propagation of the occurring pressure waves, the model also includes the seismic shear waves. Since the linear-elastic modelling does not reproduce energy losses related to plastic deformation due to the pile-soil interaction, corresponding Rayleigh damping parameters for the embedded part of the pile, which take into account these losses, have been determined according to *Heitmann et al.* [11]. The approach is based on an extended Wave Equation Analysis of Pile Driving (WEAP) code, in which an additional implementation of the radial displacements has been added to the conventional WEAP scheme [11].

The coupling between the pile and the soil is then realized by a special contact (see *Milatz et al.* [12]), which allows for a precise modelling of the energy transmission from the pile into the soil.

Infinite wave propagation at the edges of the computational domain is assured by defining non-reflecting boundary conditions at the outer soil boundaries as well as on the outer lateral water boundary (see Chap. 4.4 and 4.5). These boundary conditions ensure a reflection-free propagation of the pile driving induced waves out of the domain.

The approaches and procedures that the calculation model is based on have been validated within the frame of profound offshore measurement campaigns and allow for a reliable prediction of the pile driving noise emission into the water column. The modelling approach used by Novicos corresponds to the latest procedure that has been successfully developed within the frame of the BORA project [14]. In addition to the wind farms BARD Offshore 1 (tripiles) and Global Tech I (tripods), the BORA models have been validated during construction of the monopiles at the wind farm Borkum Riffgrund 01. All three wind farms are located in the German North Sea at water depths between 20m and 40m. Altogether, the numerical models were able to reproduce the measured sound levels with high accuracy. The fundamental applicability of the model in case of large pile diameters has been proven on the basis of a monopile at the wind farm Borkum Riffgrund 01 (calculated SEL at 750m: 175.0dB; averaged SEL measured at three positions along the 750m circumference: 174.1dB), see *Heitmann et al.* [15]. Regarding BARD Offshore 1, the same modelling approach was able to achieve a comparable accuracy (calculated SEL at 750m: 177.6dB; SEL measured at three positions along the 750m circumference: 177/180/179dB), see *Heitmann et al.* [16]. Also in the special case of submerged piles, the noise levels could be predicted with similar accuracy. Among others, corresponding results from validation have been published for tripod installation at Global Tech I in the final report of the BORA project [14] and for the skirt piles of the jacket structure of the BorWin3 converter platform in *Lippert et al.* [17], where it has been shown that the numerical model is capable of accurately reflecting the effect of the decreasing free pile length in the water column on the noise levels. Thus, the model is validated for a variety of boundary conditions regarding pile diameter and water depth. Within Novicos, the modelling approach is continuously developed further with the experience from several finished and ongoing offshore projects. Detailed information regarding the modelling as well as the validation can be found in the final report of the BORA project [14], in *Heitmann et al.* [7,8,15,16], in *Lippert et al.* [17], in *Heitmann* [18], in *Lippert and von Estorff* [19], and in *von Pein et al.* [20].

In addition to the previously described FE model, a separate numerical propagation model based on parabolic equations (PE) has been used for the back-calculation of equivalent sound pressure levels and pressure time series at a (virtual) distance of 1m from the pile centre. The applied PE model is capable of both 2D and 3D computations

for pile driving noise. It is based on the split-step Padé technique and can be used for forward and backward 2D computations, see *Collins and Westwood* [21] and *Collins* [22]. The specific setup of the PE model is described in detail in *von Pein et al.* [23]. The necessary starting field for the PE computations is derived by the transformation of the pressure time series from the FE model into the frequency domain at a certain coupling range and the scaling by the inverse of the Hankel function of the first kind according to *Jensen et al.* [24]. Thereby, the soil within the PE model is considered as a fluid, so that only longitudinal waves are taken into account and the effect of shear waves is not included. Despite the neglected shear waves, however, the soil model (layering, longitudinal wave speed, and density) and all other characteristics of the propagation path, like e.g. the consideration of a perfectly reflecting sea surface by a zero boundary condition, are identical to the FE model.

4. Relevant modelling parameters

4.1 Pile

The pile design has a fundamental influence on the dynamic behaviour of the pile and its direct interaction with the impact hammer as well as with the surrounding media. Thus, it essentially determines the sound radiation characteristics of the pile.

For the prediction at hand, all in all six FEM models have been generated, whereby three preliminary monopile designs as well as three preliminary pin pile designs as specified by the client have been included [25]. The models consider the following pile dimensions and penetration depths:

Monopile design 1 (lower case)

- Pile type: Monopile
- Pile length *L* [m]: 104.30
- Pile diameter top / bottom [m]: 11.00 / 12.00
- Wall thickness over length *L* [mm]: *- see Appendix C -*
- Requested penetration depths [m]: 25.00 (mid penetration)
50.00 (final penetration)

Monopile design 2 (mid case)

- Pile type: Monopile
- Pile length *L* [m]: 114.30
- Pile diameter top / bottom [m]: 12.00 / 13.00
- Wall thickness over length *L* [mm]: *- see Appendix C -*
- Requested penetration depths [m]: 30.00 (mid penetration)
60.00 (final penetration)

Monopile design 3 (upper case)

- Pile type: Monopile

- Pile length *L* [m]: 114.30
- Pile diameter top / bottom [m]: 12.00 / 16.00
- Wall thickness over length *L* [mm]: *- see Appendix C -*
- Requested penetration depths [m]: 30.00 (mid penetration)
60.00 (final penetration)

Pin pile design 1 (lower case)

- Pile type: Pin pile
- Pile length *L* [m]: 60.47
- Pile diameter [m]: 3.32
- Wall thickness over length *L* [mm]: 85
- Requested penetration depths [m]: 17.47 (flush with sea surface Mona)
20.47 (flush with sea surface Morgan)
55.00 (final penetration)

Pin pile design 2 (mid case)

- Pile type: Pin pile
- Pile length *L* [m]: 60.47
- Pile diameter [m]: 4.00
- Wall thickness over length *L* [mm]: 85
- Requested penetration depths [m]: 17.47 (flush with sea surface Mona)
20.47 (flush with sea surface Morgan)
55.00 (final penetration)

Pin pile design 3 (upper case)

- Pile type: Pin pile
- Pile length *L* [m]: 80.47
- Pile diameter [m]: 5.50
- Wall thickness over length *L* [mm]: 85

- Requested penetration depths [m]: 37.47 (flush with sea surface Mona)
  40.47 (flush with sea surface Morgan)
  75.00 (final penetration)

For the monopiles, 50% and 100% of final penetration depth have been considered. For the pin piles, however, two characteristic stages during the pile driving of sub-merged piles are taken into account:

- The penetration at which the top of the pile is flush with the sea surface; and
- The final penetration depth, at which the top of the pile is maximum submerged below the sea surface.

4.2 Impact hammer

The choice of the impact hammer has an important influence on the pile head force. The duration of the impulse and its derivative, hence the frequency content of the pile head force due to the hammer impact, are primarily driven by the design of the impact hammer and of the components connecting hammer and pile (e.g. anvil, follower).

For the prediction at hand, an IQIP S-5500 hammer has been considered for the three monopile designs. For the pin pile designs, however, an IQIP S-3000 was applied for the lower and mid case, while an IQIP S-4000 has been used for the upper case. The corresponding excitation signals on the head of the different piles were computed by IQIP and have been provided to Novicos by the client [26-31].

All in all, the following cases have been requested:

Case A (Morgan monopile foundation):

Case A1-100:

- Pile design: Monopile design 1 (lower case)
- Site conditions: Morgan soil layering, water depth 40m
- Hammer: IQIP S-5500
- Hammer energy [kJ]: 4500

- Penetration depth [m]: 50.00 (final penetration, 100%)

Case A2-100:

- Pile design: Monopile design 2 (mid case)
- Site conditions: Morgan soil layering, water depth 40m
- Hammer: IQIP S-5500
- Hammer energy [kJ]: 4700
- Penetration depth [m]: 60.00 (final penetration, 100%)

Case A3-100:

- Pile design: Monopile design 3 (upper case)
- Site conditions: Morgan soil layering, water depth 40m
- Hammer: IQIP S-5500
- Hammer energy [kJ]: 5500
- Penetration depth [m]: 60.00 (final penetration, 100%)

Case A3-50:

- Pile design: Monopile design 3 (upper case)
- Site conditions: Morgan soil layering, water depth 40m
- Hammer: IQIP S-5500
- Hammer energy [kJ]: 5500
- Penetration depth [m]: 30.00 (mid penetration, 50%)

Case B (Morgan pin pile foundation):

Case B1-100:

- Pile design: Pin pile design 1 (lower case)

- Site conditions: Morgan soil layering, water depth 40m
- Hammer: IQIP S-3000
- Hammer energy [kJ]: 1900
- Penetration depth [m]: 55.00 (final penetration, 100%)

Case B2-100:

- Pile design: Pin pile design 2 (mid case)
- Site conditions: Morgan soil layering, water depth 40m
- Hammer: IQIP S-3000
- Hammer energy [kJ]: 2100
- Penetration depth [m]: 55.00 (final penetration, 100%)

Case B3-100:

- Pile design: Pin pile design 3 (upper case)
- Site conditions: Morgan soil layering, water depth 40m
- Hammer: IQIP S-4000
- Hammer energy [kJ]: 3700
- Penetration depth [m]: 75.00 (final penetration, 100%)

Case B3-54:

- Pile design: Pin pile design 3 (upper case)
- Site conditions: Morgan soil layering, water depth 40m
- Hammer: IQIP S-4000
- Hammer energy [kJ]: 3700
- Penetration depth [m]: 40.47 (pile head flush with LAT Morgan, 54%)

Case C (Mona monopile foundation):

Case C3-100:

- Pile design: Monopile design 3 (upper case)
- Site conditions: Mona soil layering, water depth 43m
- Hammer: IQIP S-5500
- Hammer energy [kJ]: 5500
- Penetration depth [m]: 60.00 (final penetration, 100%)

Case C3-50:

- Pile design: Monopile design 3 (upper case)
- Site conditions: Mona soil layering, water depth 43m
- Hammer: IQIP S-5500
- Hammer energy [kJ]: 5500
- Penetration depth [m]: 30.00 (mid penetration, 50%)

Case D (Mona pin pile foundation):

Case D3-100:

- Pile design: Pin pile design 3 (upper case)
- Site conditions: Mona soil layering, water depth 43m
- Hammer: IQIP S-4000
- Hammer energy [kJ]: 3700
- Penetration depth [m]: 75.00 (final penetration, 100%)

Case D3-50:

- Pile design: Pin pile design 3 (upper case)

- Site conditions: Mona soil layering, water depth 43m
- Hammer: IQIP S-4000
- Hammer energy [kJ]: 3700
- Penetration depth [m]: 37.47 (pile head flush with LAT Mona, 50%)

4.3 Secondary noise mitigation

For this study, secondary noise mitigation measures have not been considered.

4.4 Water column

The site is assumed to show generally well-mixed salt water conditions. For a frequency range up to 2kHz, dominant sound channels are not to be expected, so that a layering within the water column need not be considered. Thus, the sea water is represented by a homogenous fluid with constant temperature and salinity over water depth. Due to the comparatively shallow water depth, an influence of the increasing hydrostatic pressure over depth on the propagation speed of acoustic waves is negligible, so that the speed of sound is assumed constant in the water column. At the interface between water and air, a perfectly reflecting surface is considered. The lateral borders of the water column are constrained with a non-reflecting boundary condition to ensure a reflection-free propagation of the acoustic waves.

Note that all computations have been performed at a fixed water depth. The resulting noise levels may differ for sea levels other than that depth, e.g. due to tides or variations between different pile locations.

With these considerations, the water column features the following parameters, that have been provided by the client [32]:

- Density of the sea water [kg/m^3]: 1000
- Speed of sound in the sea water [m/s]: 1493
- Water depth [m]: 40.00 (Morgan)
  43.00 (Mona)

4.5 Soil

The derivation of a representative soil model and the corresponding acoustical soil layering for the two Morgan and Mona locations has been performed by the client based on the geophysical and geotechnical information that is available for the sites. The soil scenarios which have been provided by the client [32] and which are used within the scope of this prognosis are shown in the following tables, where Δz is the layer thickness, v_p the longitudinal wave speed, and v_s the transversal wave speed. Both the lateral boundaries and the boundary at the bottom of the simulation domain have been covered with a non-reflecting boundary condition to ensure a reflection-free propagation of the soil waves.

For both locations, each a setting with a low and with a high soil damping scenario has been considered when executing the different computational cases.

Table 1: Acoustical soil layering for the **Morgan site (Y1DP1).**

Type	Δz [m]	v_p [m/s]	v_s [m/s]	ρ [kg/m³]
Sand	1	1806	124	2090
Sand	1	1825	154	2090
Sand	1	1836	174	2090
Sand	1	1843	190	2090
Sand	1	1850	202	2090
Sand	3	1859	222	2090
Sand	2	1868	242	2090
Clay	5	1515	127	2334
Carboniferous sandstone	61 *	3933	2105	2243
Carboniferous sandstone	Half space	4020	3134	2265

* Note: Thickness of layer has been increased by 1m to avoid numerical issues due to final penetration of pin pile design 3 (upper case), which is 75m.

Table 2: Acoustical soil layering for the **Mona site (Y2DP2).**

Type	Δz [m]	v_p [m/s]	v_s [m/s]	ρ [kg/m³]
Sand	1	1806	124	2090
Sand	1	1825	154	2090
Clay	6	1515	127	2334
Mercia mudstone (weathered)	5	2044	633	2090
Mercia mudstone	20	2836	1250	2294
Sherwood sandstone	43 *	3933	3067	2246
Sherwood sandstone	Half space	4020	3134	2265

* Note: Thickness of layer has been increased by 1m to avoid numerical issues due to final penetration of pin pile design 3 (upper case), which is 75m.

5. Results for case A (Morgan monopile foundation)

Note: All resultant values given in this chapter are evaluated for a reference height above the seabed of 2m.

Within this Chapter, both the sound exposure levels L_E as well as the peak pressure levels L_{peak} that have been derived by using the FE models for case A are summarized. The investigations are based on the combinations of pile, soil, and hammer excitation as defined in Chap. 4. In a first step, the cases A1-100 (lower case design), A2-100 (mid case design), and A3-100 (upper case design) have been executed, which all consider final penetration depth. Based on these results, the upper case has been identified as the worst case of the three monopile designs with respect to noise emission. Therefore, an intermediate stage of 50% of the final penetration depth has only been computed for case A3-50.

In addition to the computations with the FE model, virtual source levels at a distance of 1m to the pile axis have been derived by back-calculation of equivalent sound pressure levels and pressure time series using the PE models for the cases A3-50 and A3-100. The corresponding results have been provided to the client in Excel format.

5.1 Sound exposure level L_E

The development of the predicted sound exposure levels L_E in a distance up to 1km to the pile is depicted in Figure 1 to Figure 4. A more detailed view of the range between 650m and 850m is shown in Figure 5 to Figure 8. The corresponding frequency content of the signals is given in Figure 9 to Figure 12.

Due to the specific characteristics of the wave guide and corresponding interference effects, the logarithmic decay of the levels with range is only met as a general trend. In practice (both in measurement and simulation), a more or less pronounced oscillation about the decay curve is observed, with dedicated minima and maxima (see Figure 1 to Figure 4). These oscillations contribute significantly to the high variability of the

monitored underwater noise levels, as an exact deployment of the measuring devices at a certain distance to the pile within a few meters is not possible under offshore conditions.

At 750m distance to the pile and 2m above the sea floor, the $L_{E,mean}$ levels (arithmetic mean in the range of 650m to 850m) result to 180.8dB/180.1dB (case A1-100), 181.3dB/180.5dB (case A2-100), 183.5dB/183.0dB (case A3-50), and 182.9dB/182.1dB (case A3-100) for the low and the high soil damping scenario, respectively. The variations of the L_E in the range of ±100m around the arithmetic mean levels $L_{E,mean}$ for the 750m position are up to about -2dB/+1dB (see Figure 5 to Figure 8).

A compilation of the predicted levels can be found in Appendix A. An estimation of the effect on the noise levels when changing the hammer energy can be obtained according to Appendix B.

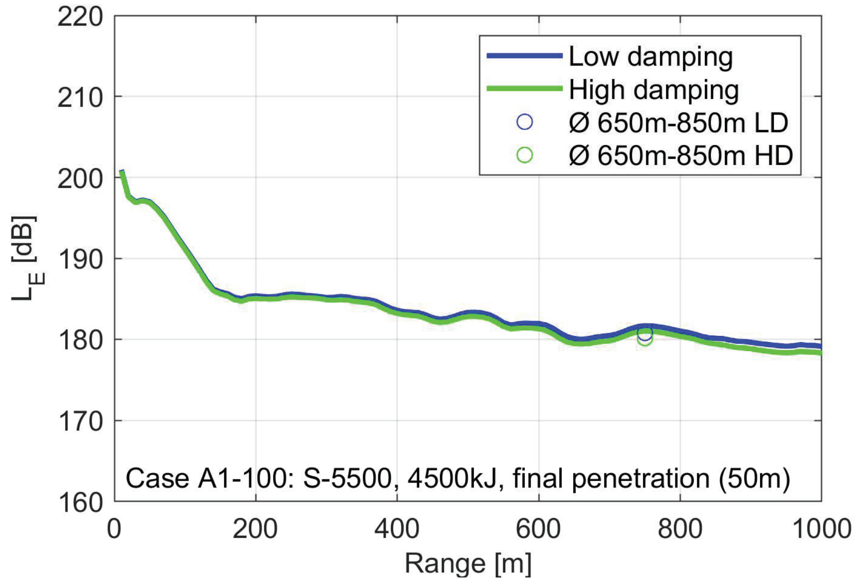

Figure 1: Predicted ***L_E* for case A1-100** in the range up to 1km from the pile for the low and the high soil damping scenario, respectively. **Morgan lower case** monopile design 11m/12m, **IQIP S-5500**, hammer energy 4500kJ, **final penetration depth (50m)**, no secondary noise mitigation.

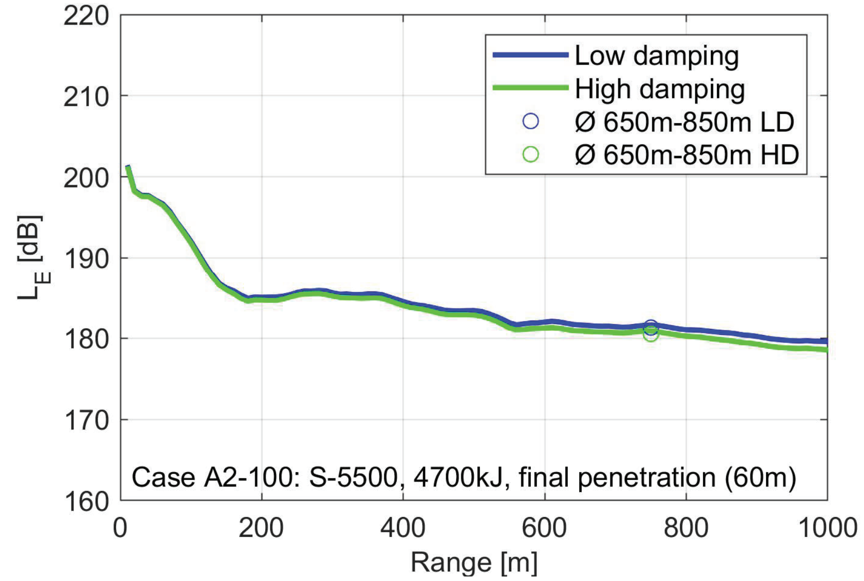

Figure 2: Predicted ***L_E* for case A2-100** in the range up to 1km from the pile for the low and the high soil damping scenario, respectively. **Morgan mid case** monopile design 12m/13m, **IQIP S-5500**, hammer energy 4700kJ, **final penetration depth (60m)**, no secondary noise mitigation.

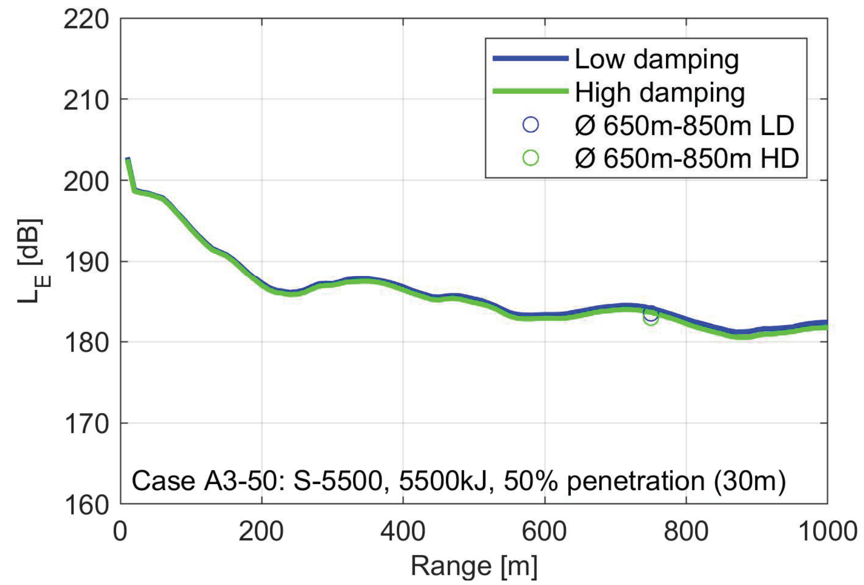

Figure 3: Predicted ***L_E* for case A3-50** in the range up to 1km from the pile for the low and the high soil damping scenario, respectively. **Morgan upper case** monopile design 12m/16m, **IQIP S-5500**, hammer energy 5500kJ, **mid penetration depth (30m)**, no secondary noise mitigation.

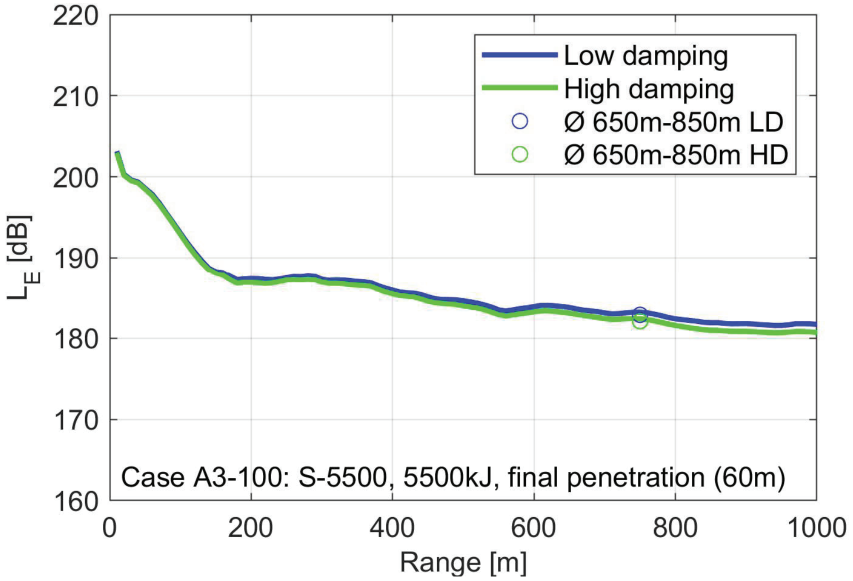

Figure 4: Predicted ***L_E* for case A3-100** in the range up to 1km from the pile for the low and the high soil damping scenario, respectively. **Morgan upper case** monopile design 12m/16m, **IQIP S-5500**, hammer energy 5500kJ, **final penetration depth (60m)**, no secondary noise mitigation.

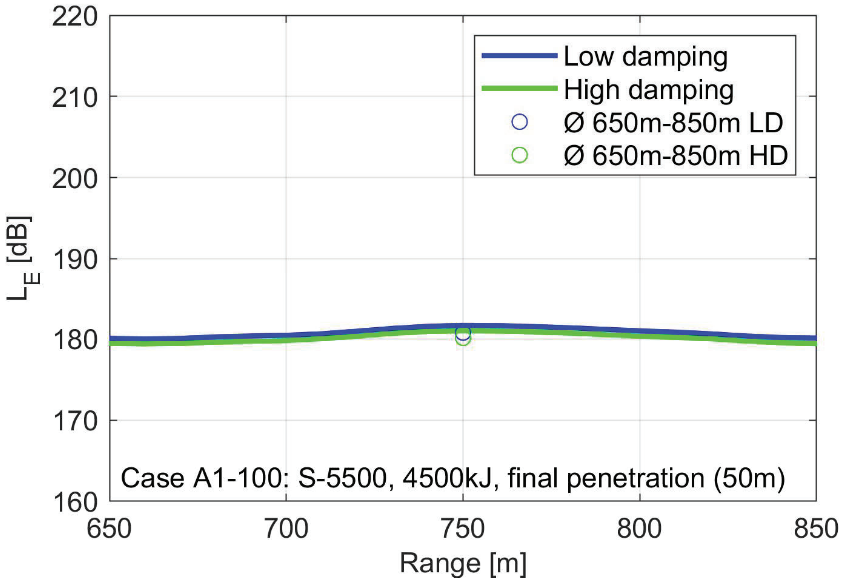

Figure 5: Variation of the predicted ***L_E* for case A1-100** in the range 650m to 850m from the pile for the low and the high soil damping scenario, respectively. **Morgan lower case** monopile design 11m/12m, **IQIP S-5500**, hammer energy 4500kJ, **final penetration depth (50m)**, no secondary noise mitigation.

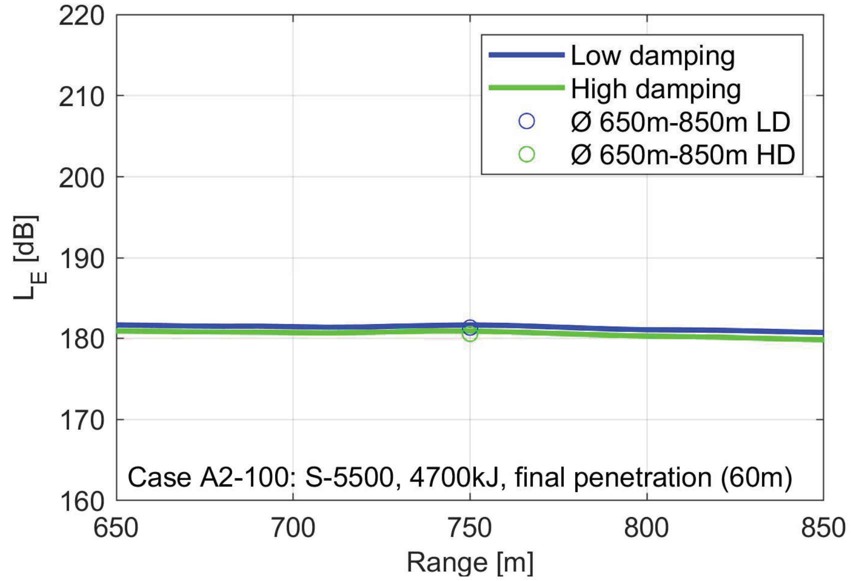

Figure 6: Variation of the predicted ***L_E* for case A2-100** in the range 650m to 850m from the pile for the low and the high soil damping scenario, respectively. **Morgan mid case** monopile design 12m/13m, **IQIP S-5500**, hammer energy 4700kJ, **final penetration depth (60m)**, no secondary noise mitigation.

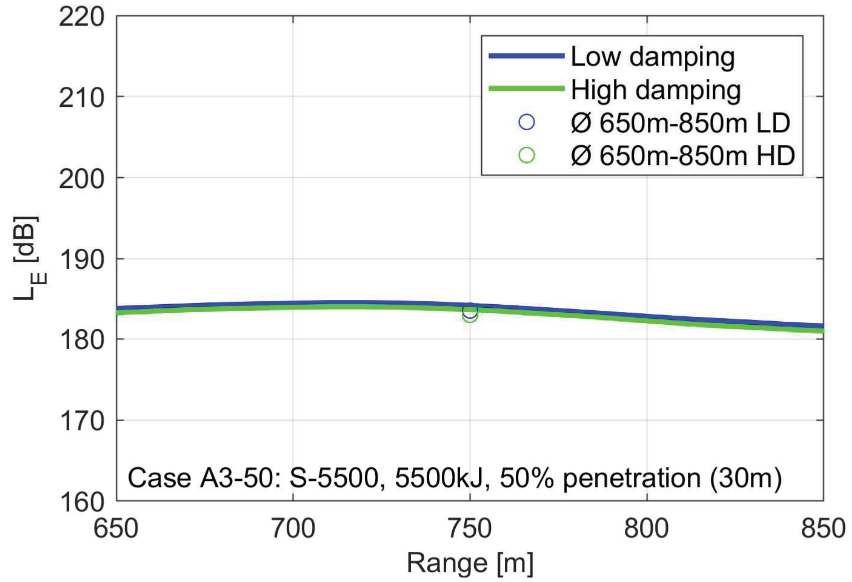

Figure 7: Variation of the predicted ***L_E* for case A3-50** in the range 650m to 850m from the pile for the low and the high soil damping scenario, respectively. **Morgan upper case** monopile design 12m/16m, **IQIP S-5500**, hammer energy 5500kJ, **mid penetration depth (30m)**, no secondary noise mitigation.

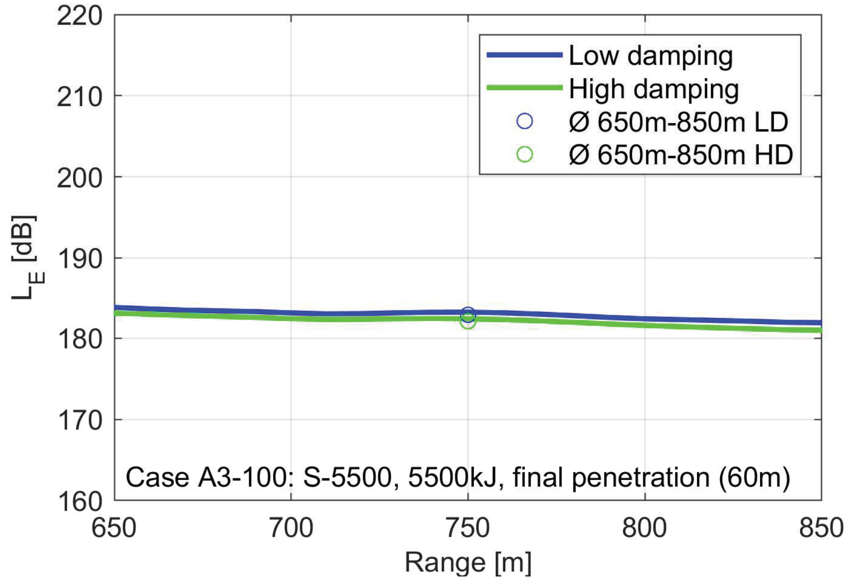

Figure 8: Variation of the predicted ***L_E* for case A3-100** in the range 650m to 850m from the pile for the low and the high soil damping scenario, respectively. **Morgan upper case** monopile design 12m/16m, **IQIP S-5500**, hammer energy 5500kJ, **final penetration depth (60m)**, no secondary noise mitigation.

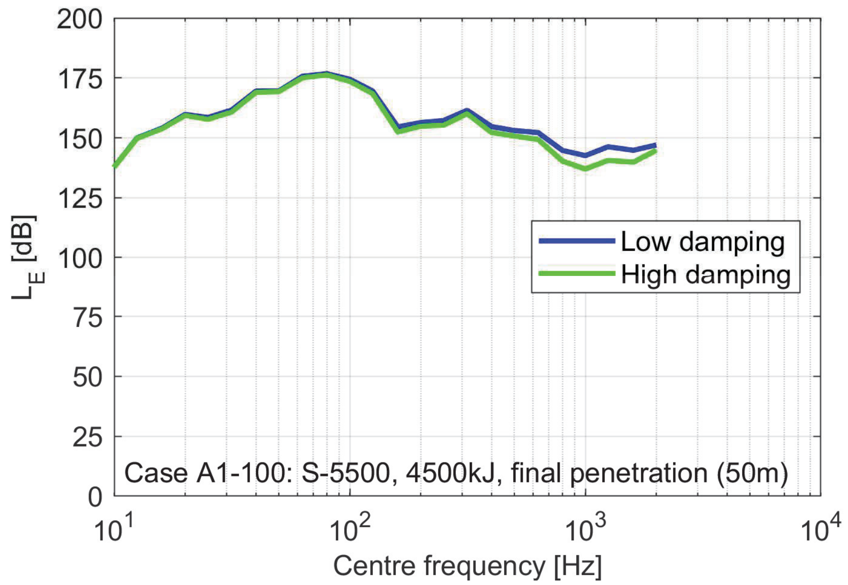

Figure 9: Predicted **spectral *L_E* for case A1-100** at 750m from the pile for the low and the high soil damping scenario, respectively. **Morgan lower case** monopile design 11m/12m, **IQIP S-5500**, hammer energy 4500kJ, **final penetration depth (50m)**, no secondary noise mitigation.

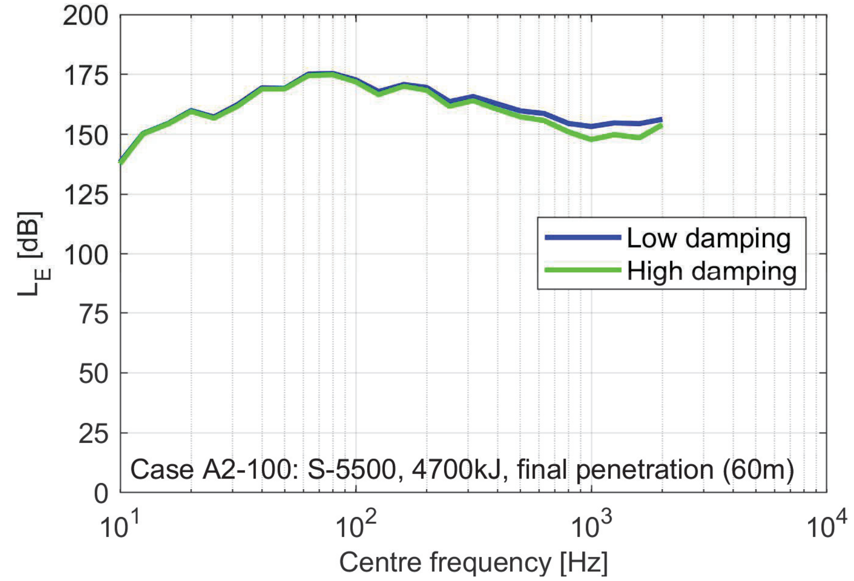

Figure 10: Predicted **spectral *L_E* for case A2-100** at 750m from the pile for the low and the high soil damping scenario, respectively. **Morgan mid case** monopile design 12m/13m, **IQIP S-5500**, hammer energy 4700kJ, **final penetration depth (60m)**, no secondary noise mitigation.

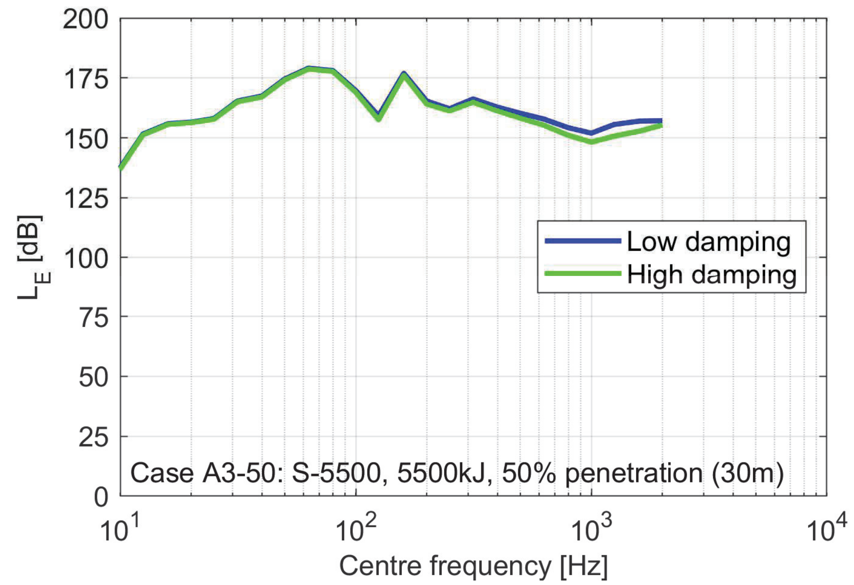

Figure 11: Predicted **spectral *L_E* for case A3-50** at 750m from the pile for the low and the high soil damping scenario, respectively. **Morgan upper case** monopile design 12m/16m, **IQIP S-5500**, hammer energy 5500kJ, **mid penetration depth (30m)**, no secondary noise mitigation.

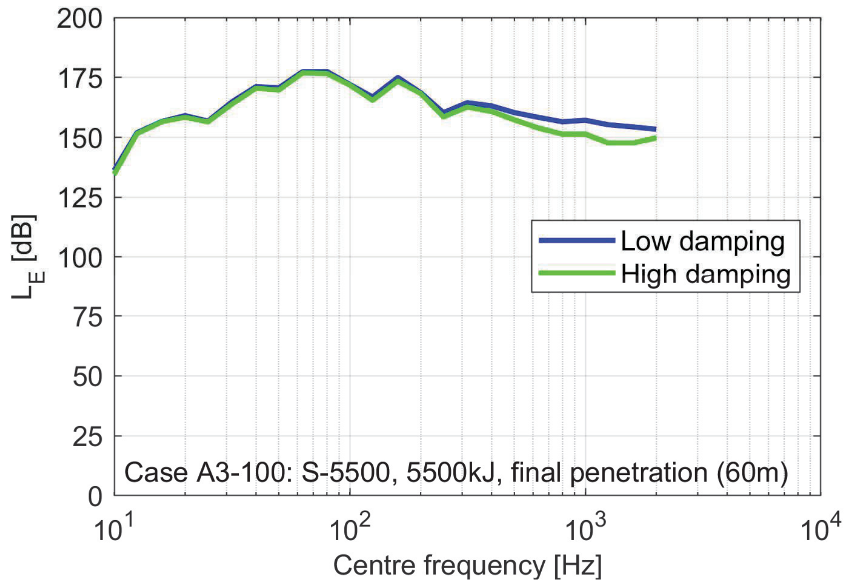

Figure 12: Predicted **spectral L_E for case A3-100** at 750m from the pile for the low and the high soil damping scenario, respectively. **Morgan upper case** monopile design 12m/16m, **IQIP S-5500**, hammer energy 5500kJ, **final penetration depth (60m)**, no secondary noise mitigation.

5.2 Peak pressure level L_{peak}

For the peak pressure level L_{peak}, similar conclusions can be drawn. The corresponding results for the range up to 1km and the area between 650m to 850m can be found in Figure 13 to Figure 16 and in Figure 17 to Figure 20, respectively.

At 750m distance from the pile and 2m above the sea floor, the $L_{peak,mean}$ levels (arithmetic mean in the range of 650m to 850m) yield values of 199.2dB/198.6dB (case A1-100), 201.4dB/200.6dB (case A2-100), 201.8dB/201.2dB (case A3-50), and 201.6dB/
200.9dB (case A3-100) for the low and the high soil damping scenario, respectively. The variations of the L_{peak} in the range of ±100m around the arithmetic mean levels $L_{peak,mean}$ for the 750m position are up to about -4dB/+3dB (see Figure 17 to Figure 20).

Again, the predicted levels are compiled in Appendix A. An estimation of the effect on the noise levels when changing the hammer energy can be found in Appendix B.

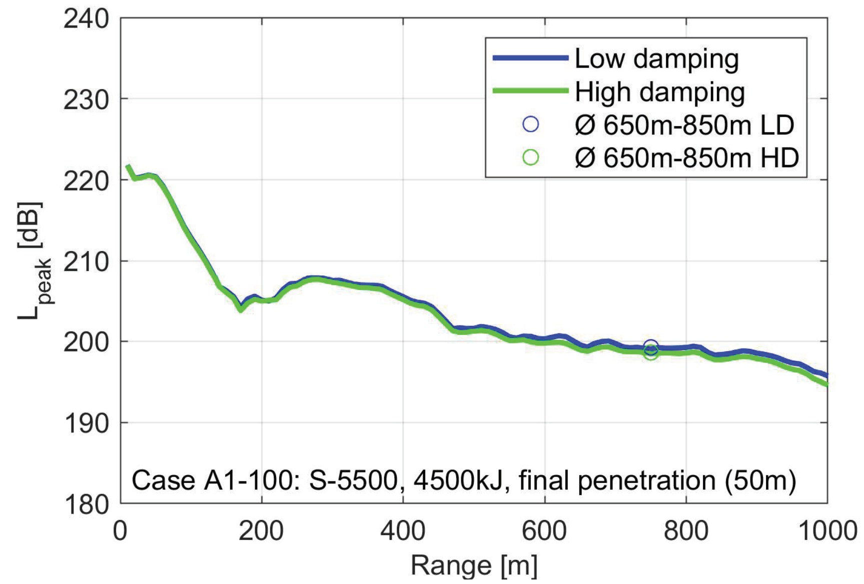

Figure 13: Predicted L_{peak} **for case A1-100** in the range up to 1km from the pile for the low and the high soil damping scenario, respectively. **Morgan lower case** monopile design 11m/12m, **IQIP S-5500**, hammer energy 4500kJ, **final penetration depth (50m)**, no secondary noise mitigation.

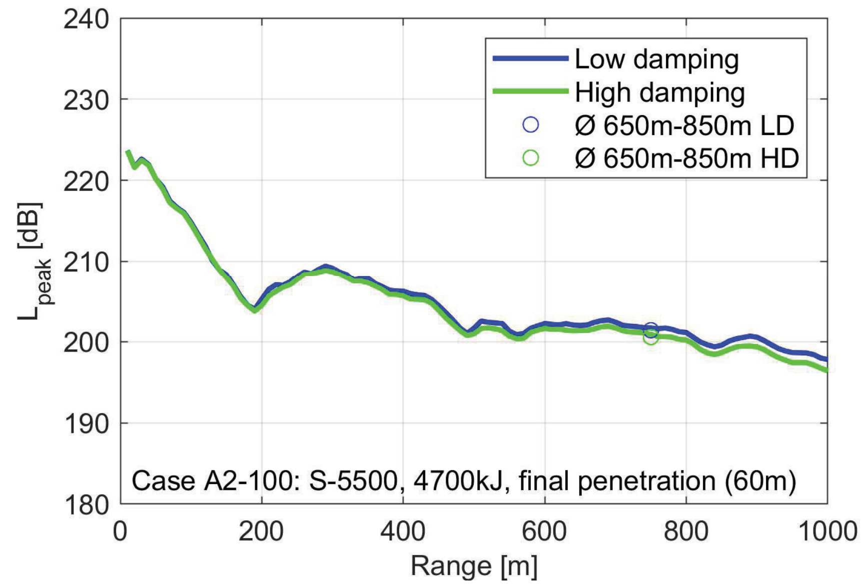

Figure 14: Predicted L_{peak} **for case A2-100** in the range up to 1km from the pile for the low and the high soil damping scenario, respectively. **Morgan mid case** monopile design 12m/13m, **IQIP S-5500**, hammer energy 4700kJ, **final penetration depth (60m)**, no secondary noise mitigation.

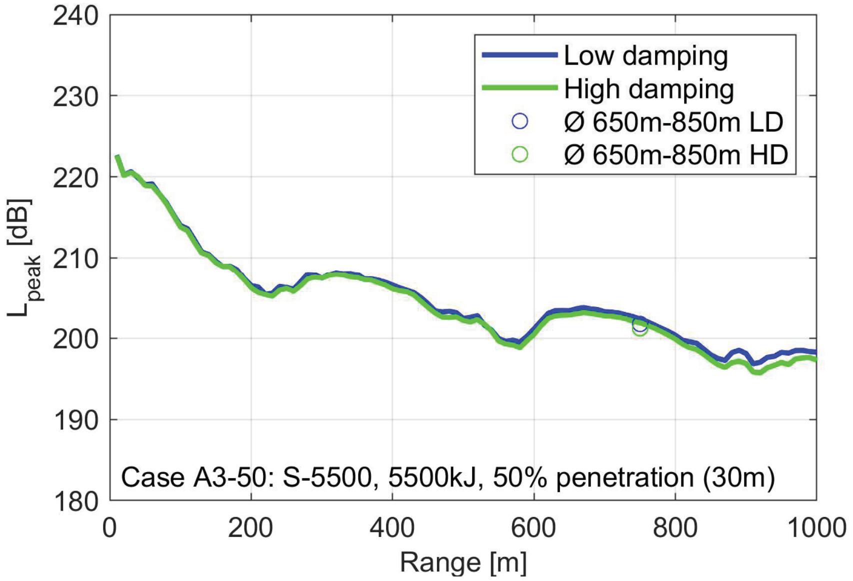

Figure 15: Predicted ***L_{peak}* for case A3-50** in the range up to 1km from the pile for the low and the high soil damping scenario, respectively. **Morgan upper case** monopile design 12m/16m, **IQIP S-5500**, hammer energy 5500kJ, **mid penetration depth (30m)**, no secondary noise mitigation.

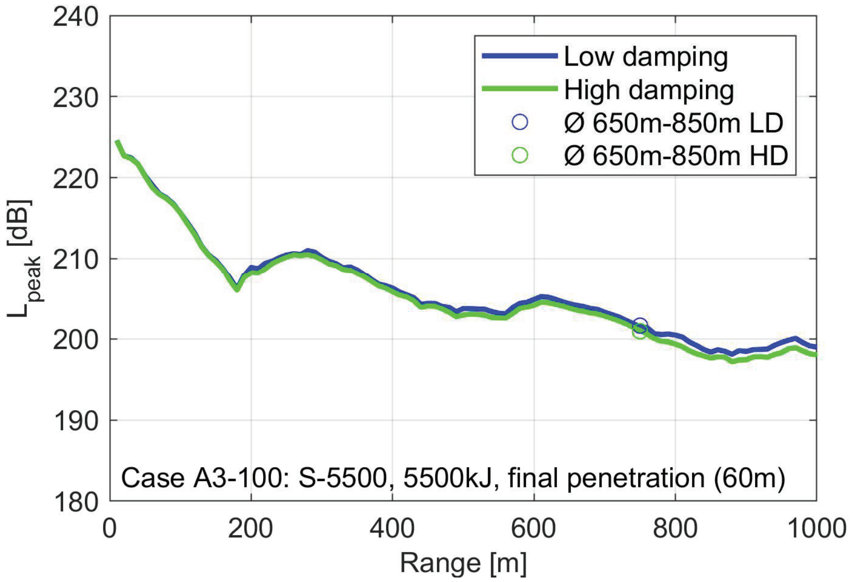

Figure 16: Predicted ***L_{peak}* for case A3-100** in the range up to 1km from the pile for the low and the high soil damping scenario, respectively. **Morgan upper case** monopile design 12m/16m, **IQIP S-5500**, hammer energy 5500kJ, **final penetration depth (60m)**, no secondary noise mitigation.

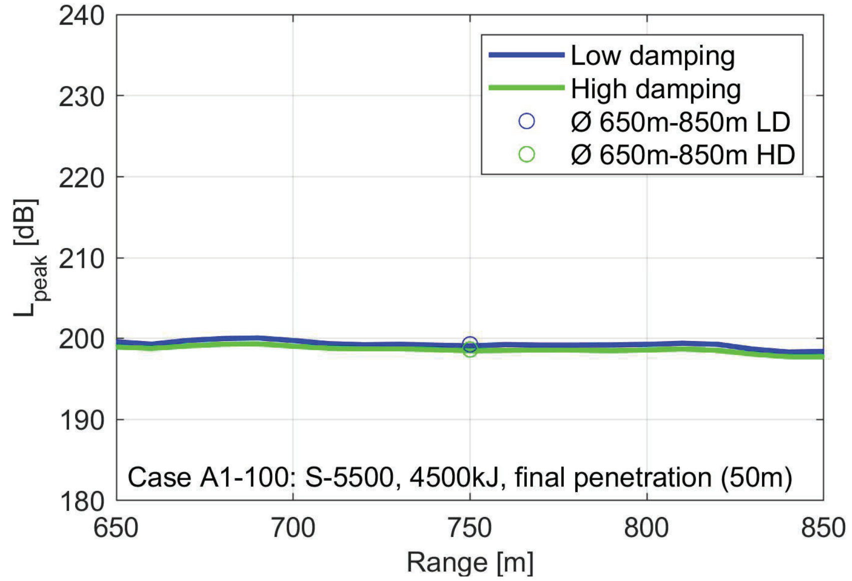

Figure 17: Variation of the predicted ***L_{peak}* for case A1-100** in the range 650m to 850m from the pile for the low and the high soil damping scenario, respectively. **Morgan lower case** monopile design 11m/12m, **IQIP S-5500**, hammer energy 4500kJ, **final penetration depth (50m)**, no secondary noise mitigation.

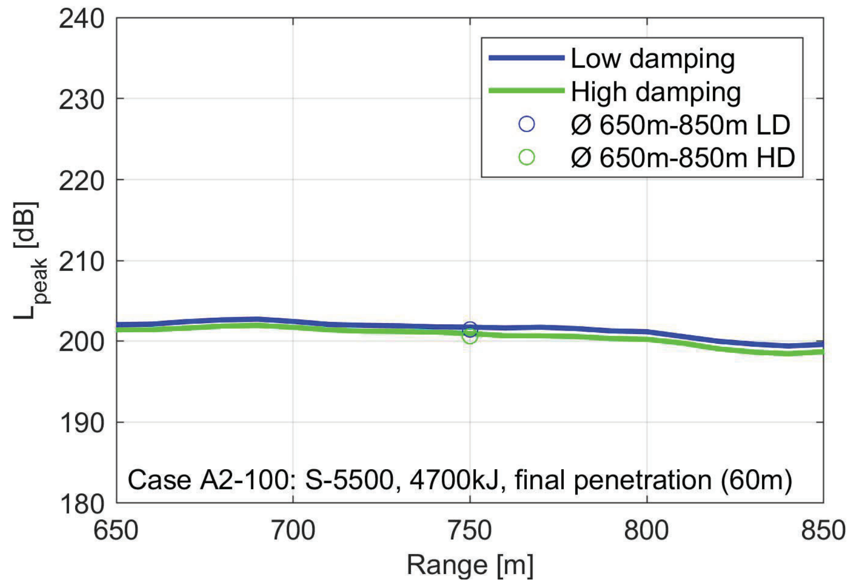

Figure 18: Variation of the predicted ***L_{peak}* for case A2-100** in the range 650m to 850m from the pile for the low and the high soil damping scenario, respectively. **Morgan mid case** monopile design 12m/13m, **IQIP S-5500**, hammer energy 4700kJ, **final penetration depth (60m)**, no secondary noise mitigation.

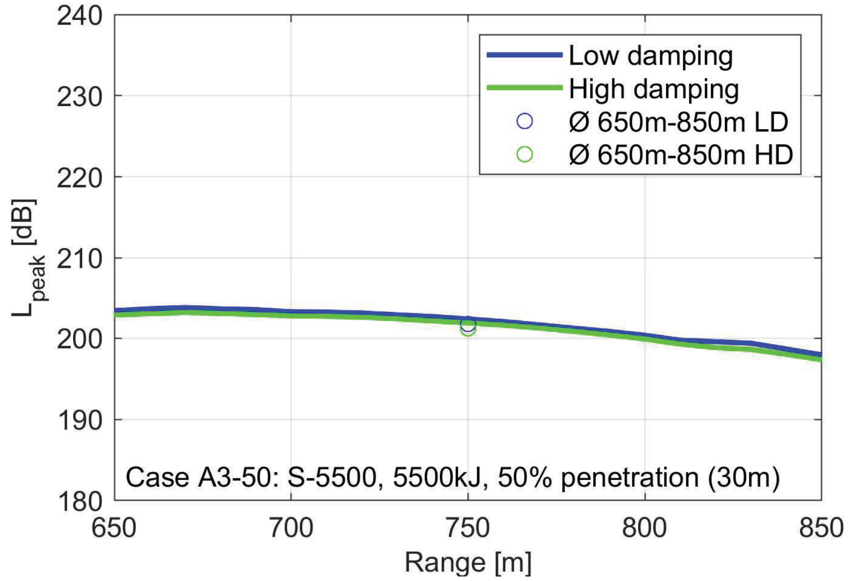

Figure 19: Variation of the predicted L_{peak} **for case A3-50** in the range 650m to 850m from the pile for the low and the high soil damping scenario, respectively. **Morgan upper case** monopile design 12m/16m, **IQIP S-5500**, hammer energy 5500kJ, **mid penetration depth (30m)**, no secondary noise mitigation.

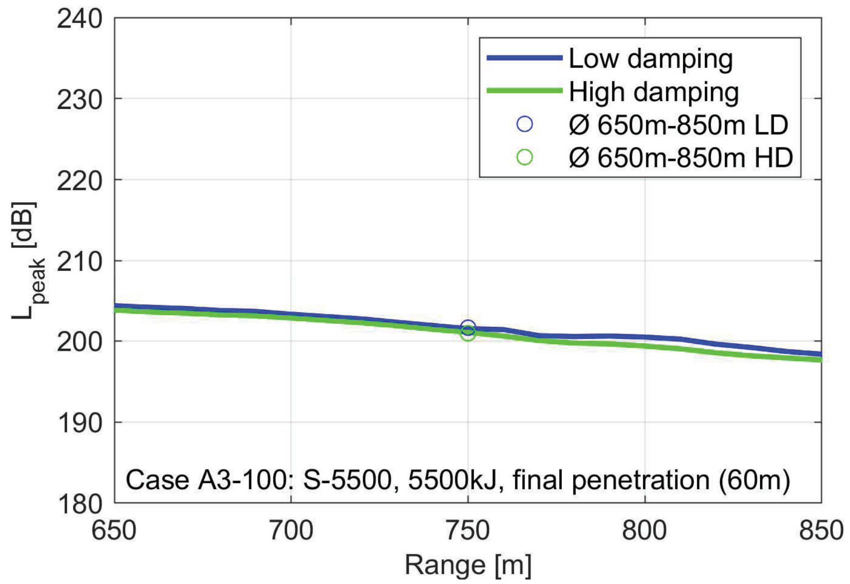

Figure 20: Variation of the predicted L_{peak} **for case A3-100** in the range 650m to 850m from the pile for the low and the high soil damping scenario, respectively. **Morgan upper case** monopile design 12m/16m, **IQIP S-5500**, hammer energy 5500kJ, **final penetration depth (60m)**, no secondary noise mitigation.

Report no. 22-121-128-01-02 (Rev. 02)

6. Results for case B (Morgan pin pile foundation)

Note: All resultant values given in this chapter are evaluated for a reference height above the seabed of 2m.

Within this Chapter, both the sound exposure levels L_E as well as the peak pressure levels L_{peak} that have been derived by using the FE models for case B are summarized. The investigations are based on the combinations of pile, soil, and hammer excitation as defined in Chap. 4. In a first step, the cases B1-100 (lower case design), B2-100 (mid case design), and B3-100 (upper case design) have been executed, which all consider final penetration depth. Based on these results, the upper case has been identified as the worst case of the three pin pile designs with respect to noise emission. Therefore, an intermediate stage of 54% of the final penetration depth, where the pile top is flush with the sea surface, has only been computed for case B3-54.

In addition to the computations with the FE model, virtual source levels at a distance of 1m to the pile axis have been derived by back-calculation of equivalent sound pressure levels and pressure time series using the PE models for the cases B3-54 and B3-100. The corresponding results have been provided to the client in Excel format.

6.1 Sound exposure level L_E

The development of the predicted sound exposure levels L_E in a distance up to 1km to the pile is depicted in Figure 21 to Figure 24. A more detailed view of the range between 650m and 850m is shown in Figure 25 to Figure 28. The corresponding frequency content of the signals is given in Figure 29 to Figure 32.

Due to the specific characteristics of the wave guide and corresponding interference effects, the logarithmic decay of the levels with range is only met as a general trend. In practice (both in measurement and simulation), a more or less pronounced oscillation about the decay curve is observed, with dedicated minima and maxima (see Figure 21 to Figure 24). These oscillations contribute significantly to the high variability of the

monitored underwater noise levels, as an exact deployment of the measuring devices at a certain distance to the pile within a few meters is not possible under offshore conditions.

In 750m distance to the pile and 2m above the sea floor, the $L_{E,mean}$ levels (arithmetic mean in the range of 650m to 850m) result to 165.0dB/163.6dB (case B1-100), 165.9dB/164.6dB (case B2-100), 180.2dB/179.4dB (case B3-54), and 170.5dB/ 169.4dB (case B3-100) for the low and the high soil damping scenario, respectively. The variations of the L_E in the range of ±100m around the arithmetic mean levels $L_{E,mean}$ for the 750m position are up to about -1dB/+1.5dB (see Figure 25 to Figure 28).

A compilation of the predicted levels can be found in Appendix A. An estimation of the effect on the noise levels when changing the hammer energy can be obtained according to Appendix B.

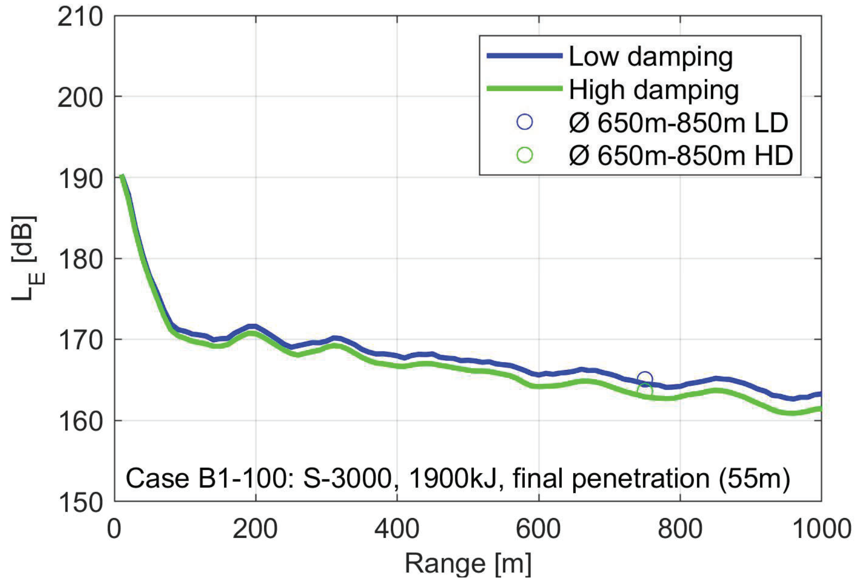

Figure 21: Predicted ***L_E* for case B1-100** in the range up to 1km from the pile for the low and the high soil damping scenario, respectively. **Morgan lower case** pin pile design 3.32m, **IQIP S-3000**, hammer energy 1900kJ, **final penetration depth (55m)**, no secondary noise mitigation.

Report no. 22-121-128-01-02 (Rev. 02)

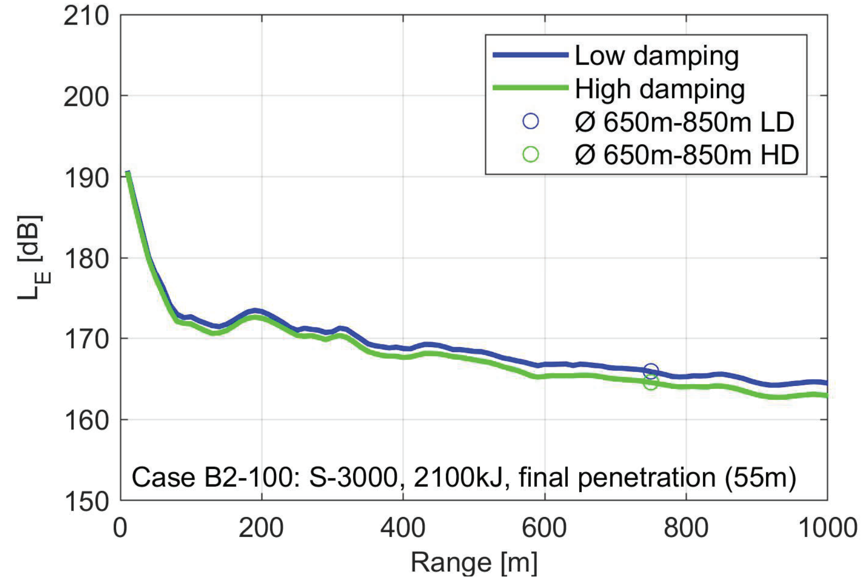

Figure 22: Predicted ***L_E* for case B2-100** in the range up to 1km from the pile for the low and the high soil damping scenario, respectively. **Morgan mid case** pin pile design 4m, **IQIP S-3000**, hammer energy 2100kJ, **final penetration depth (55m)**, no secondary noise mitigation.

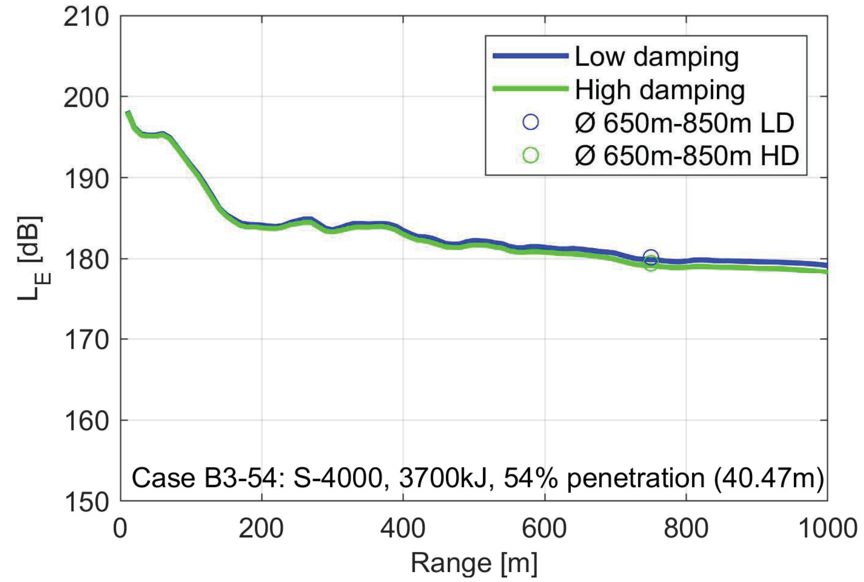

Figure 23: Predicted ***L_E* for case B3-54** in the range up to 1km from the pile for the low and the high soil damping scenario, respectively. **Morgan upper case** pin pile design 5.5m, **IQIP S-4000**, hammer energy 3700kJ, **pile top flush with sea surface (40.47m)**, no secondary noise mitigation.

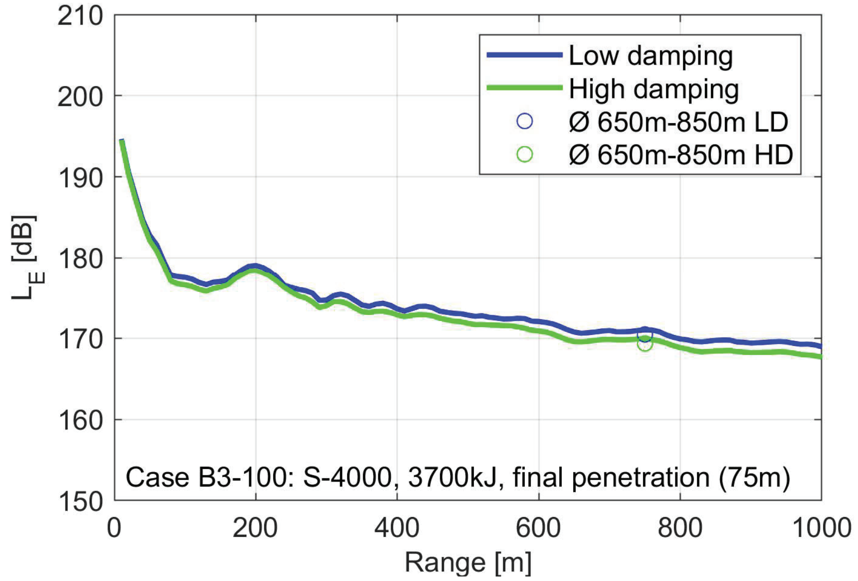

Figure 24: Predicted ***L_E* for case B3-100** in the range up to 1km from the pile for the low and the high soil damping scenario, respectively. **Morgan upper case** pin pile design 5.5m, **IQIP S-4000**, hammer energy 3700kJ, **final penetration depth (75m)**, no secondary noise mitigation.

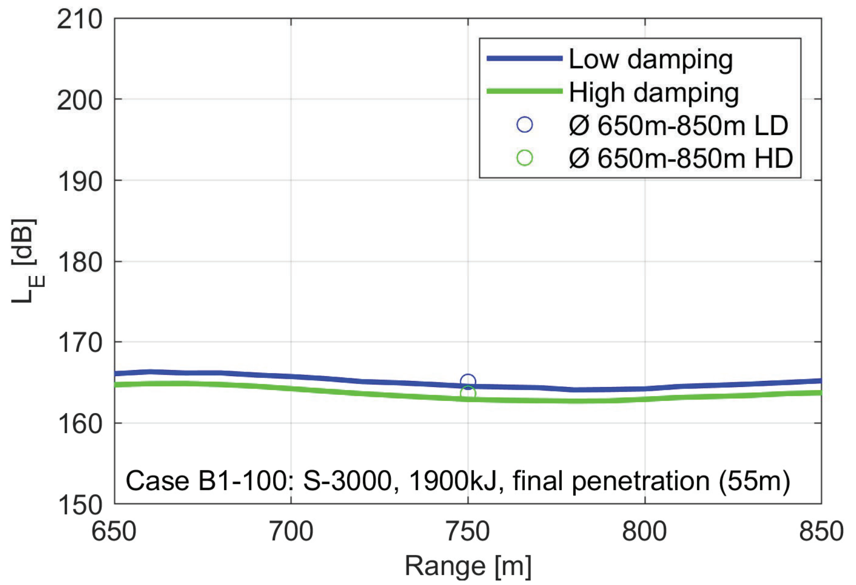

Figure 25: Variation of the predicted ***L_E* for case B1-100** in the range 650m to 850m from the pile for the low and the high soil damping scenario, respectively. **Morgan lower case** pin pile design 3.32m, **IQIP S-3000**, hammer energy 1900kJ, **final penetration depth (55m)**, no secondary noise mitigation.

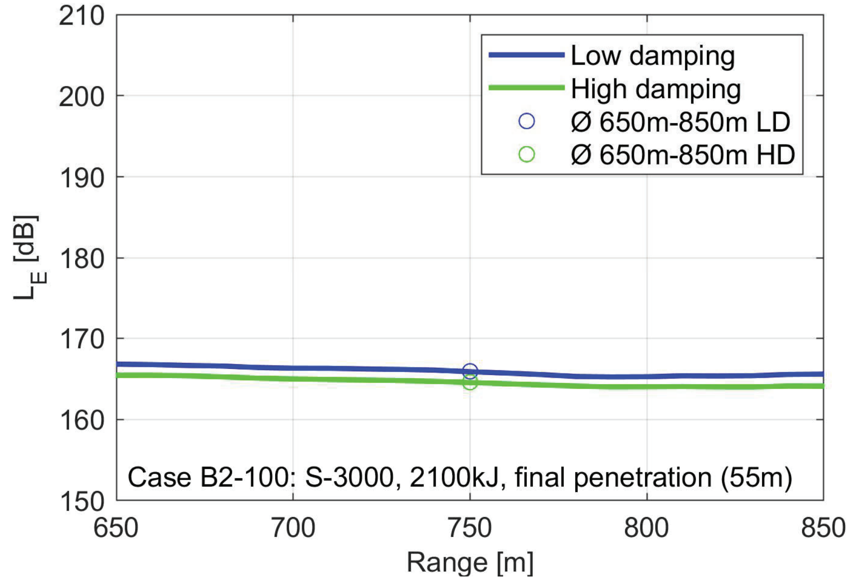

Figure 26: Variation of the predicted ***L_E* for case B2-100** in the range 650m to 850m from the pile for the low and the high soil damping scenario, respectively. **Morgan mid case** pin pile design 4m, **IQIP S-3000**, hammer energy 2100kJ, **final penetration depth (55m)**, no secondary noise mitigation.

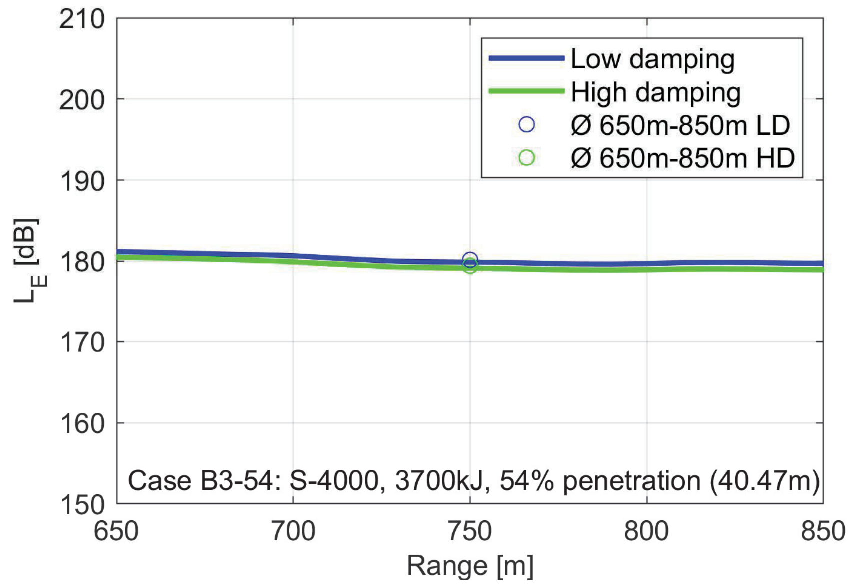

Figure 27: Variation of the predicted ***L_E* for case B3-54** in the range 650m to 850m from the pile for the low and the high soil damping scenario, respectively. **Morgan upper case** pin pile design 5.5m, **IQIP S-4000**, hammer energy 3700kJ, **pile top flush with sea surface (40.47m)**, no sec. noise mitigation.

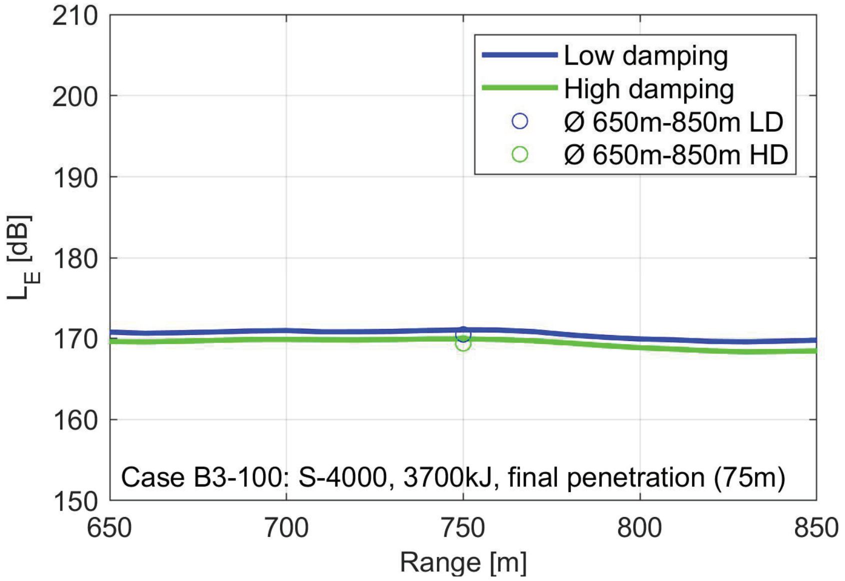

Figure 28: Variation of the predicted **L_E for case B3-100** in the range 650m to 850m from the pile for the low and the high soil damping scenario, respectively. **Morgan upper case** pin pile design 5.5m, **IQIP S-4000**, hammer energy 3700kJ, **final penetration depth (75m)**, no secondary noise mitigation.

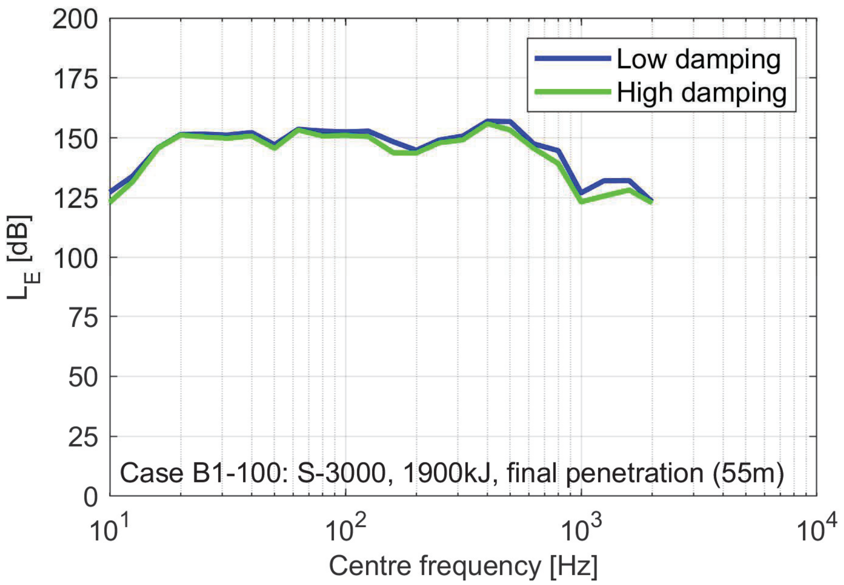

Figure 29: Predicted **spectral L_E for case B1-100** at 750m from the pile for the low and the high soil damping scenario, respectively. **Morgan lower case** pin pile design 3.32m, **IQIP S-3000**, hammer energy 1900kJ, **final penetration depth (55m)**, no secondary noise mitigation.

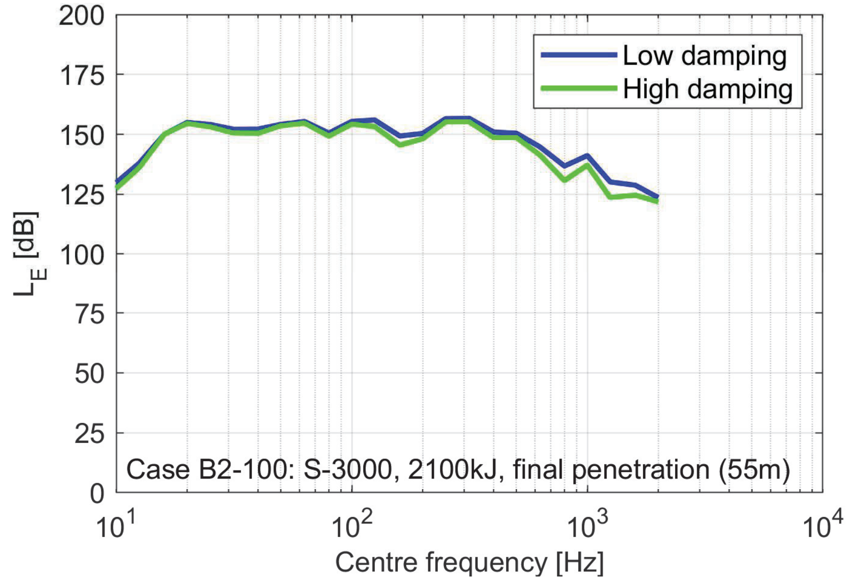

Figure 30: Predicted **spectral L_E for case B2-100** at 750m from the pile for the low and the high soil damping scenario, respectively. **Morgan mid case** pin pile design 4m, **IQIP S-3000**, hammer energy 2100kJ, **final penetration depth (55m)**, no secondary noise mitigation.

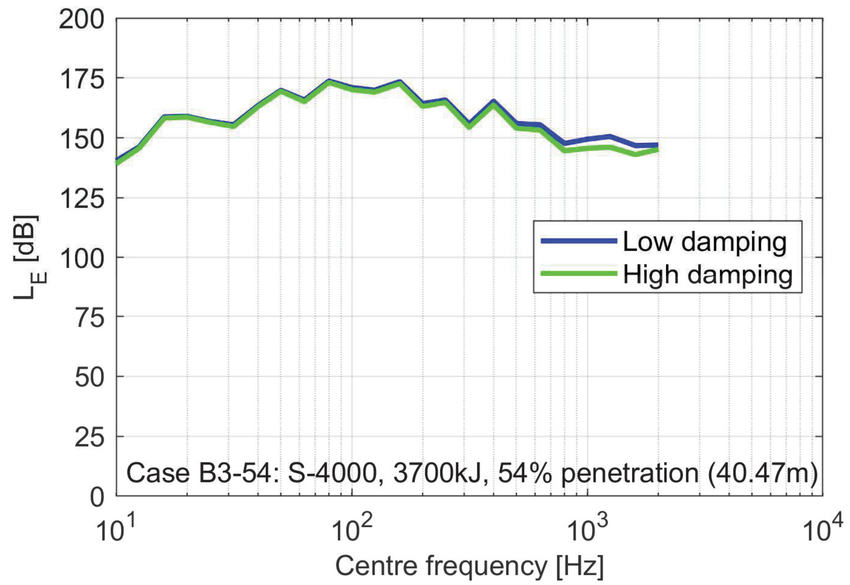

Figure 31: Predicted **spectral L_E for case B3-54** at 750m from the pile for the low and the high soil damping scenario, respectively. **Morgan upper case** pin pile design 5.5m, **IQIP S-4000**, hammer energy 3700kJ, **pile top flush with sea surface (40.47m)**, no secondary noise mitigation.

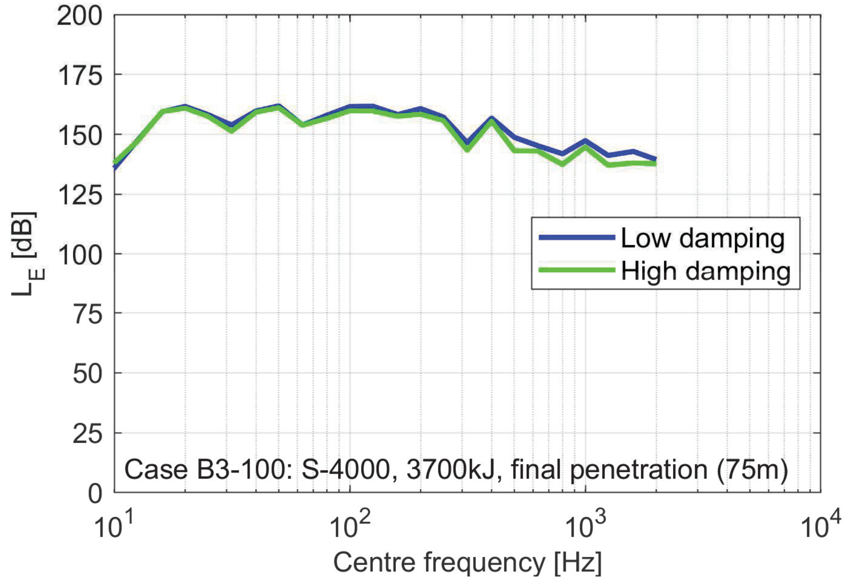

Figure 32: Predicted **spectral L_E for case B3-100** at 750m from the pile for the low and the high soil damping scenario, respectively. **Morgan upper case** pin pile design 5.5m, **IQIP S-4000**, hammer energy 3700kJ, **final penetration depth (75m)**, no secondary noise mitigation.

6.2 Peak pressure level L_{peak}

For the peak pressure level L_{peak}, similar conclusions can be drawn. The corresponding results for the range up to 1km and the area between 650m to 850m can be found in Figure 33 to Figure 36 and in Figure 37 to Figure 40, respectively.

In 750m distance to the pile and 2m above the sea floor, the $L_{peak,mean}$ levels (arithmetic mean in the range of 650m to 850m) yield values of 186.5dB/185.2dB (case B1-100), 184.4dB/183.2dB (case B2-100), 201.2dB/200.6dB (case B3-54), and 189.0dB/188.0dB (case B3-100) for the low and the high soil damping scenario, respectively. The variations of the L_{peak} in the range of ±100m around the arithmetic mean levels $L_{peak,mean}$ for the 750m position are up to about ±3dB (see Figure 37 to Figure 40).

Again, the predicted levels are compiled in Appendix A. An estimation of the effect on the noise levels when changing the hammer energy can be found in Appendix B.

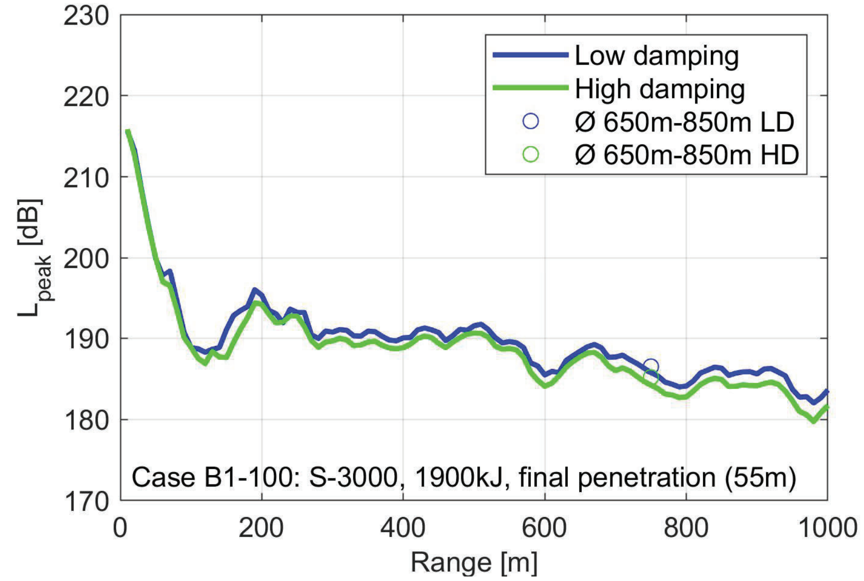

Figure 33: Predicted **L_{peak} for case B1-100** in the range up to 1km from the pile for the low and the high soil damping scenario, respectively. **Morgan lower case** pin pile design 3.32m, **IQIP S-3000**, hammer energy 1900kJ, **final penetration depth (55m)**, no secondary noise mitigation.

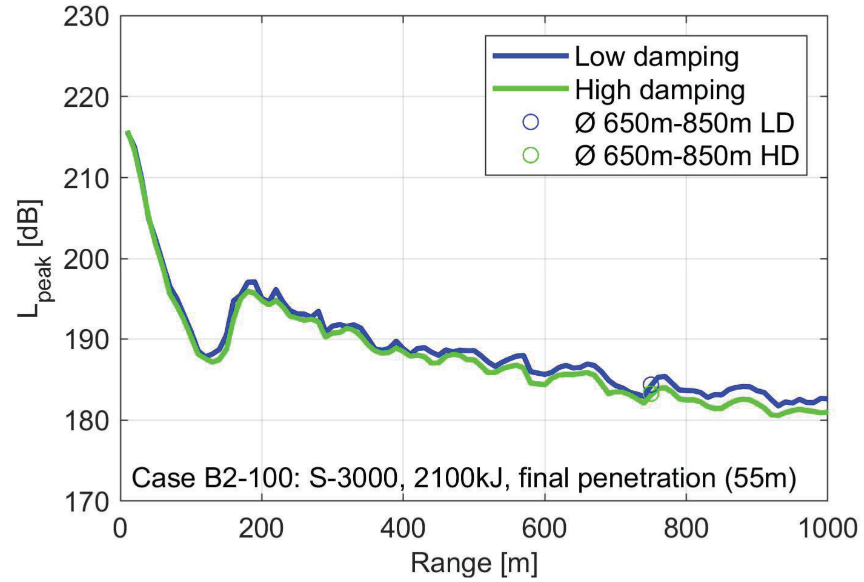

Figure 34: Predicted **L_{peak} for case B2-100** in the range up to 1km from the pile for the low and the high soil damping scenario, respectively. **Morgan mid case** pin pile design 4m, **IQIP S-3000**, hammer energy 2100kJ, **final penetration depth (55m)**, no secondary noise mitigation.

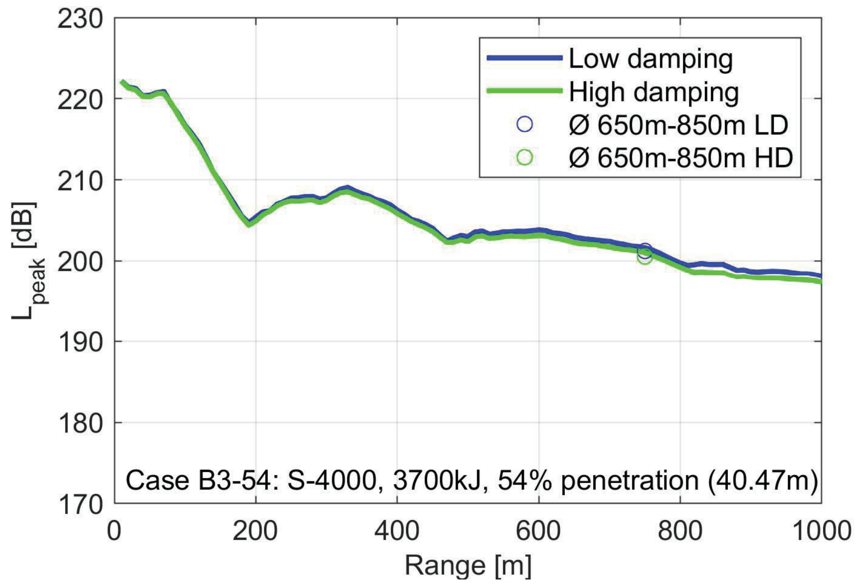

Figure 35: Predicted ***L_{peak}* for case B3-54** in the range up to 1km from the pile for the low and the high soil damping scenario, respectively. **Morgan upper case** pin pile design 5.5m, **IQIP S-4000**, hammer energy 3700kJ, **pile top flush with sea surface (40.47m)**, no secondary noise mitigation.

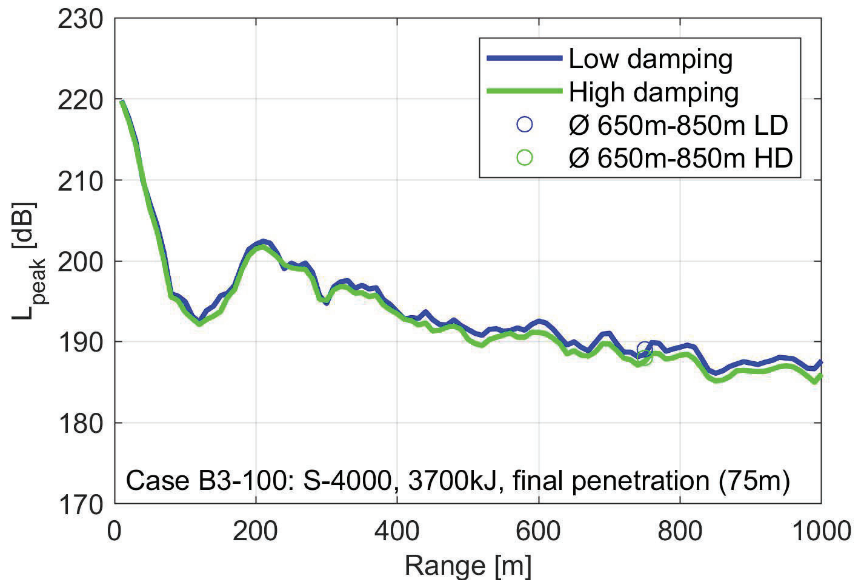

Figure 36: Predicted ***L_{peak}* for case B3-100** in the range up to 1km from the pile for the low and the high soil damping scenario, respectively. **Morgan upper case** pin pile design 5.5m, **IQIP S-4000**, hammer energy 3700kJ, **final penetration depth (75m)**, no secondary noise mitigation.

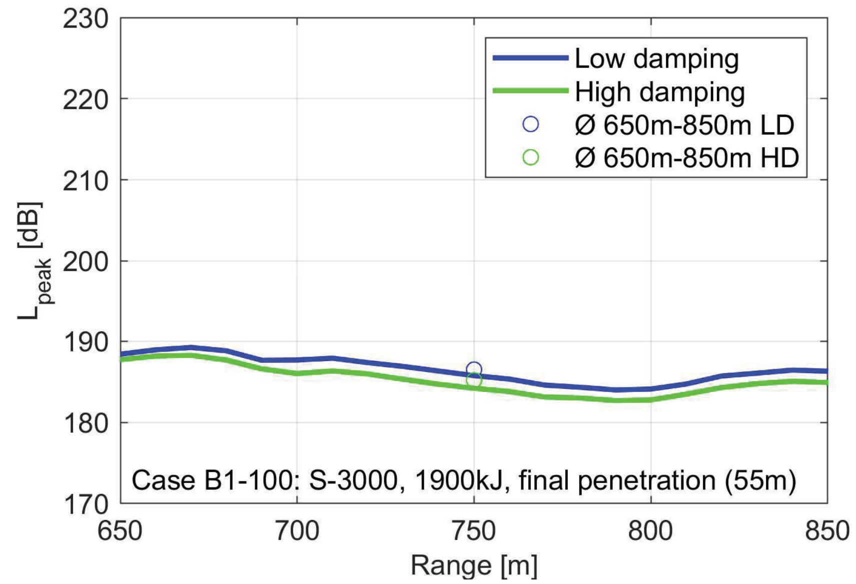

Figure 37: Variation of the predicted ***L_{peak}* for case B1-100** in the range 650m to 850m from the pile for the low and the high soil damping scenario, respectively. **Morgan lower case** pin pile design 3.32m, **IQIP S-3000**, hammer energy 1900kJ, **final penetration depth (55m)**, no secondary noise mitigation.

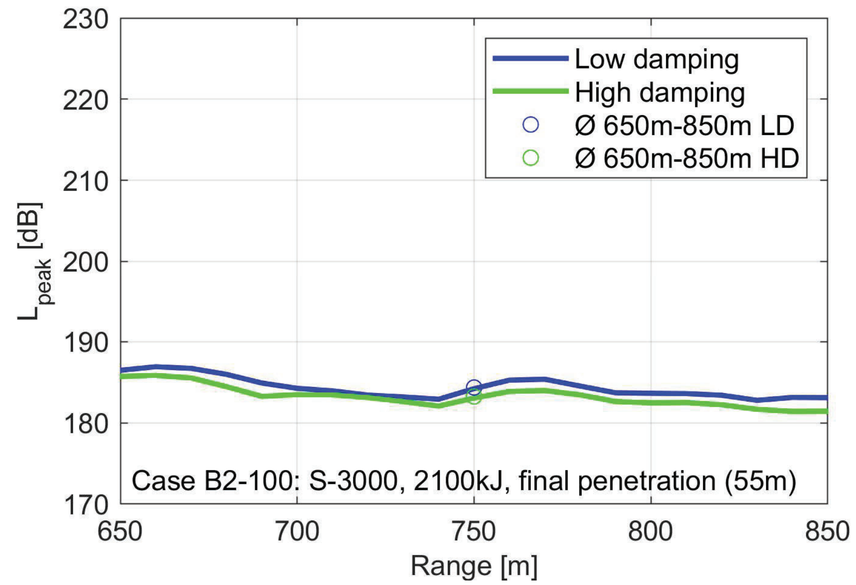

Figure 38: Variation of the predicted ***L_{peak}* for case B2-100** in the range 650m to 850m from the pile for the low and the high soil damping scenario, respectively. **Morgan mid case** pin pile design 4m, **IQIP S-3000**, hammer energy 2100kJ, **final penetration depth (55m)**, no secondary noise mitigation.

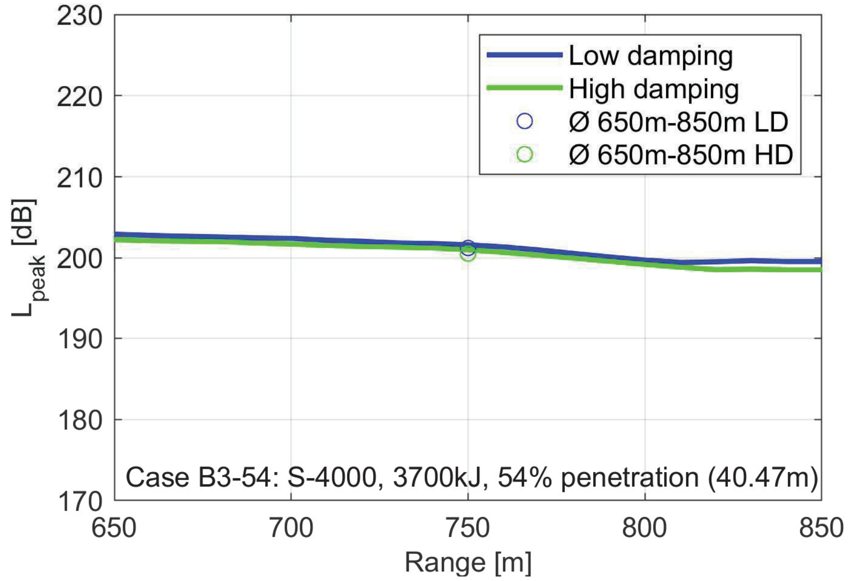

Figure 39: Variation of the predicted L_{peak} **for case B3-54** in the range 650m to 850m from the pile for the low and the high soil damping scenario, respectively. **Morgan upper case** pin pile design 5.5m, **IQIP S-4000**, hammer energy 3700kJ, **pile top flush with sea surface (40.47m)**, no sec. noise mitigation.

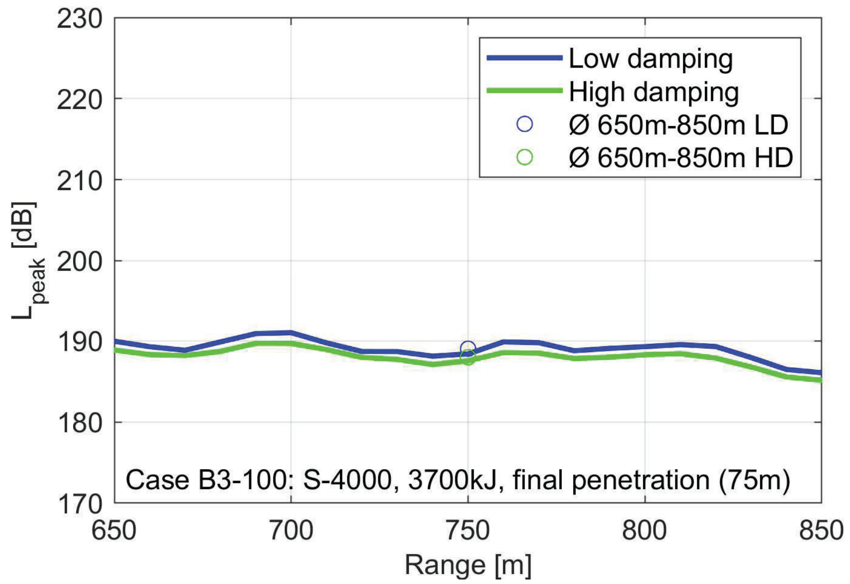

Figure 40: Variation of the predicted L_{peak} **for case B3-100** in the range 650m to 850m from the pile for the low and the high soil damping scenario, respectively. **Morgan upper case** pin pile design 5.5m, **IQIP S-4000**, hammer energy 3700kJ, **final penetration depth (75m)**, no secondary noise mitigation.

7. Results for case C (Mona monopile foundation)

Note: All resultant values given in this chapter are evaluated for a reference height above the seabed of 2m.

Within this Chapter, both the sound exposure levels L_E as well as the peak pressure levels L_{peak} that have been derived by using the FE models for case C are summarized. The investigations are based on the combinations of pile, soil, and hammer excitation as defined in Chap. 4. Based on the previous results for the Morgan monopile foundation (case A), the upper case design has already been identified as the worst case of the three monopile designs with respect to noise emission. Therefore, only the cases C3-50 (intermediate stage of 50% of the final penetration depth) and C3-100 (final penetration depth) with upper case design have been computed for the Mona monopile location.

In addition to the computations with the FE model, virtual source levels at a distance of 1m to the pile axis have been derived by back-calculation of equivalent sound pressure levels and pressure time series using the PE models for the cases B3-50 and B3-100. The corresponding results have been provided to the client in Excel format.

7.1 Sound exposure level L_E

The development of the predicted sound exposure levels L_E in a distance up to 1km to the pile is depicted in Figure 41 to Figure 42. A more detailed view of the range between 650m and 850m is shown in Figure 43 to Figure 44. The corresponding frequency content of the signals is given in Figure 45 to Figure 46

Due to the specific characteristics of the wave guide and corresponding interference effects, the logarithmic decay of the levels with range is only met as a general trend. In practice (both in measurement and simulation), a more or less pronounced oscillation about the decay curve is observed, with dedicated minima and maxima (see Figure 41 to Figure 42). These oscillations contribute significantly to the high variability of the

monitored underwater noise levels, as an exact deployment of the measuring devices at a certain distance to the pile within a few meters is not possible under offshore conditions.

In 750m distance to the pile and 2m above the sea floor, the $L_{E,mean}$ levels (arithmetic mean in the range of 650m to 850m) result to 183.9dB/183.2dB (case C3-50) and 182.9dB/182.0dB (case C3-100) for the low and the high soil damping scenario, respectively. The variations of the L_E in the range of ±100m around the arithmetic mean levels $L_{E,mean}$ for the 750m position are up to about ±0.5dB (see Figure 43 to Figure 44).

A compilation of the predicted levels can be found in Appendix A. An estimation of the effect on the noise levels when changing the hammer energy can be obtained according to Appendix B.

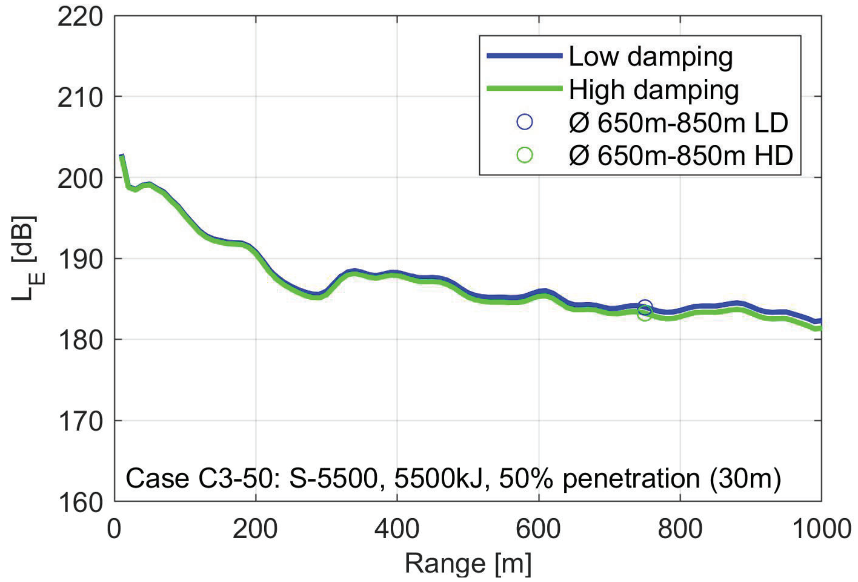

Figure 41: Predicted ***L_E* for case C3-50** in the range up to 1km from the pile for the low and the high soil damping scenario, respectively. **Mona upper case** monopile design 12m/16m, **IQIP S-5500**, hammer energy 5500kJ, **mid penetration depth (30m)**, no secondary noise mitigation.

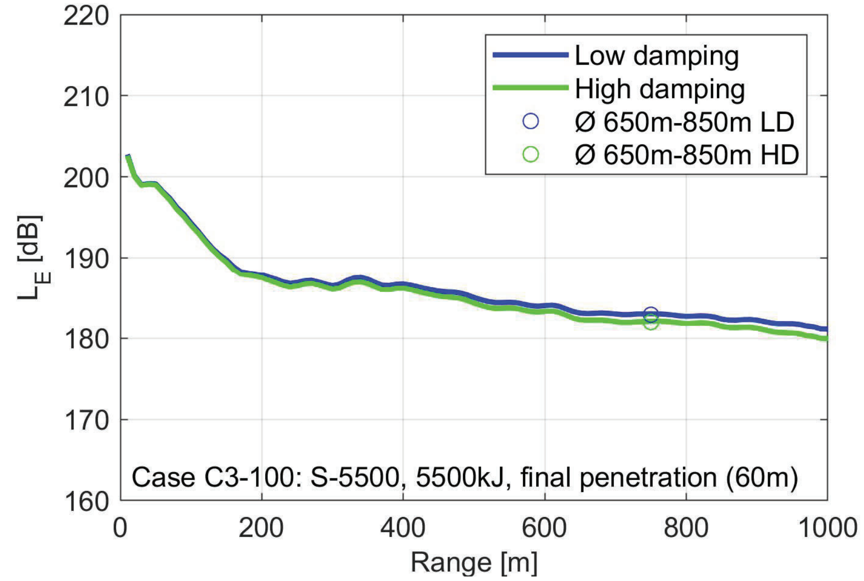

Figure 42: Predicted ***L_E* for case C3-100** in the range up to 1km from the pile for the low and the high soil damping scenario, respectively. **Mona upper case** monopile design 12m/16m, **IQIP S-5500**, hammer energy 5500kJ, **final penetration depth (60m)**, no secondary noise mitigation.

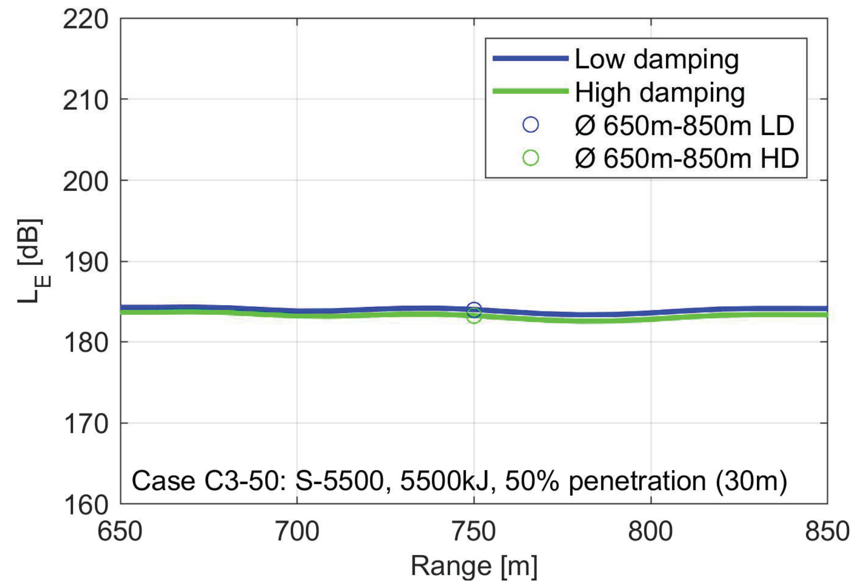

Figure 43: Variation of the predicted ***L_E* for case C3-50** in the range 650m to 850m from the pile for the low and the high soil damping scenario, respectively. **Mona upper case** monopile design 12m/16m, **IQIP S-5500**, hammer energy 5500kJ, **mid penetration depth (30m)**, no secondary noise mitigation.

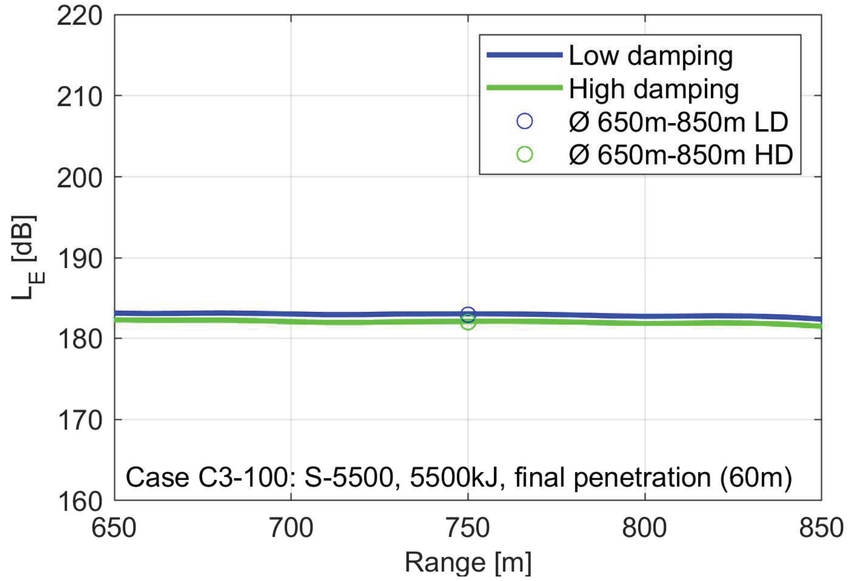

Figure 44: Variation of the predicted ***L_E* for case C3-100** in the range 650m to 850m from the pile for the low and the high soil damping scenario, respectively. **Mona upper case** monopile design 12m/16m, **IQIP S-5500**, hammer energy 5500kJ, **final penetration depth (60m)**, no secondary noise mitigation.

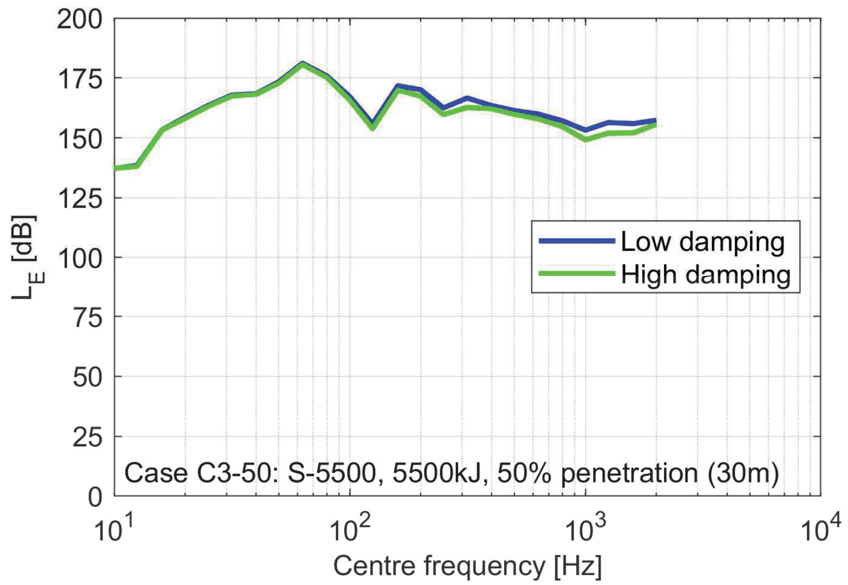

Figure 45: Predicted **spectral *L_E* for case C3-50** at 750m from the pile for the low and the high soil damping scenario, respectively. **Mona upper case** monopile design 12m/16m, **IQIP S-5500**, hammer energy 5500kJ, **mid penetration depth (30m)**, no secondary noise mitigation.

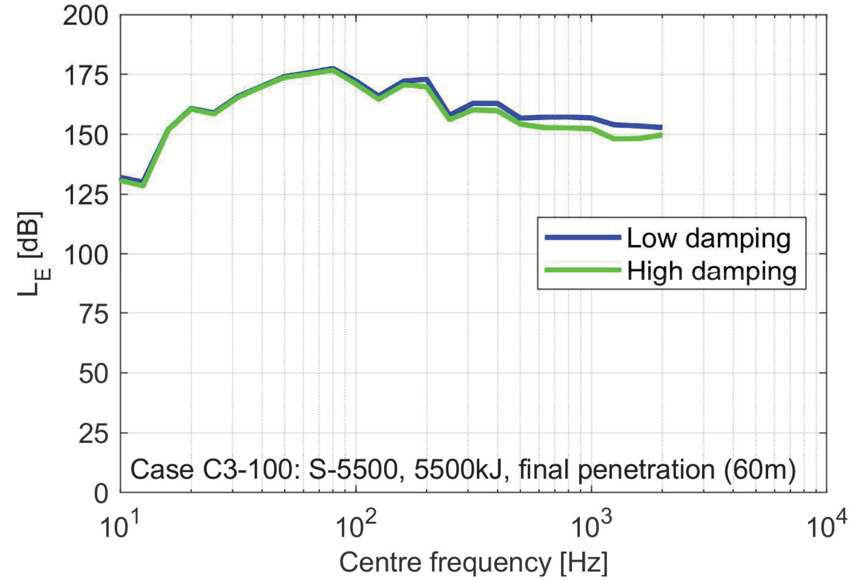

Figure 46: Predicted **spectral *L_E* for case C3-100** at 750m from the pile for the low and the high soil damping scenario, respectively. **Mona upper case** monopile design 12m/16m, **IQIP S-5500**, hammer energy 5500kJ, **final penetration depth (60m)**, no secondary noise mitigation.

7.2 Peak pressure level L_{peak}

For the peak pressure level L_{peak}, similar conclusions can be drawn. The corresponding results for the range up to 1km and the area between 650m to 850m can be found in Figure 47 to Figure 48 and in Figure 49 to Figure 50, respectively.

In 750m distance to the pile and 2m above the sea floor, the $L_{peak,mean}$ levels (arithmetic mean in the range of 650m to 850m) yield values of 201.5dB/200.3dB (case C3-50) and 202.8dB/201.7dB (case C3-100) for the low and the high soil damping scenario, respectively. The variations of the L_{peak} in the range of ±100m around the arithmetic mean levels $L_{peak,mean}$ for the 750m position are up to about -2dB/+1dB (see Figure 49 to Figure 50).

Again, the predicted levels are compiled in Appendix A. An estimation of the effect on the noise levels when changing the hammer energy can be found in Appendix B.

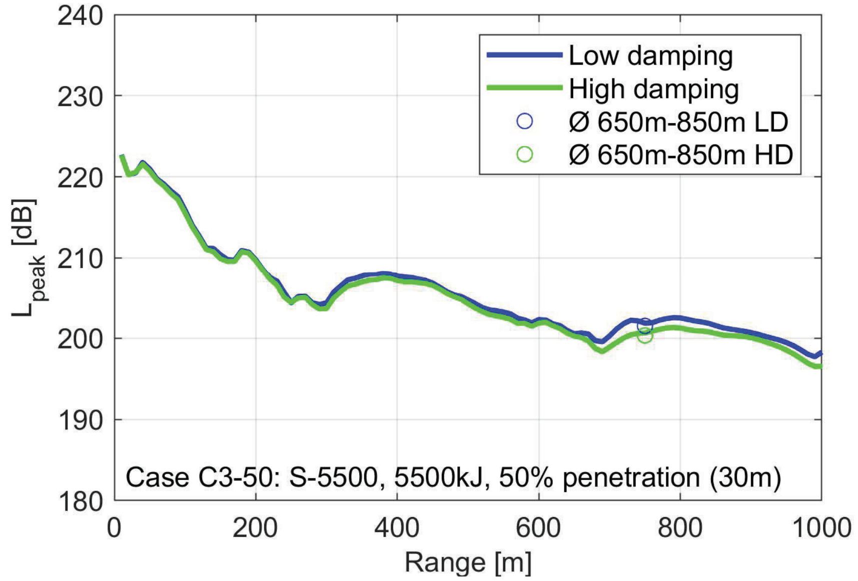

Figure 47: Predicted ***L_{peak}* for case C3-50** in the range up to 1km from the pile for the low and the high soil damping scenario, respectively. **Mona upper case** monopile design 12m/16m, **IQIP S-5500**, hammer energy 5500kJ, **mid penetration depth (30m)**, no secondary noise mitigation.

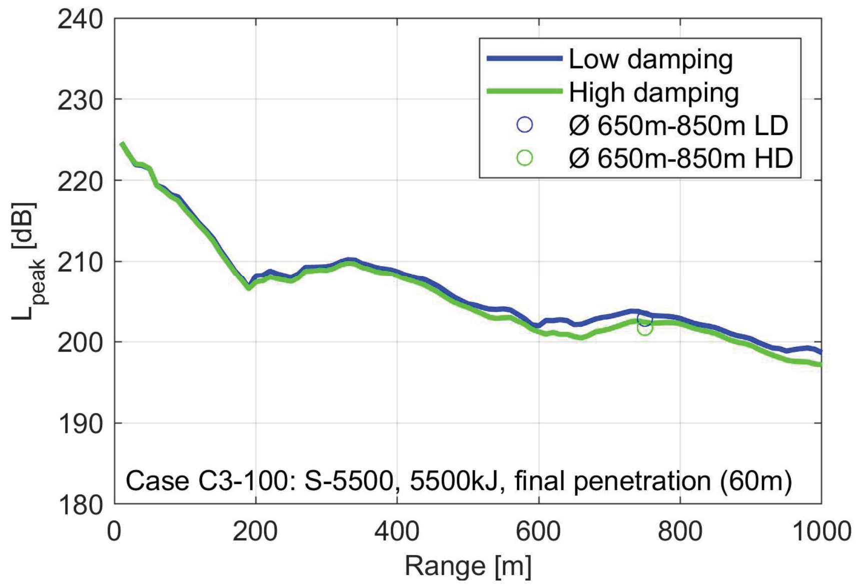

Figure 48: Predicted ***L_{peak}* for case C3-100** in the range up to 1km from the pile for the low and the high soil damping scenario, respectively. **Mona upper case** monopile design 12m/16m, **IQIP S-5500**, hammer energy 5500kJ, **final penetration depth (60m)**, no secondary noise mitigation.

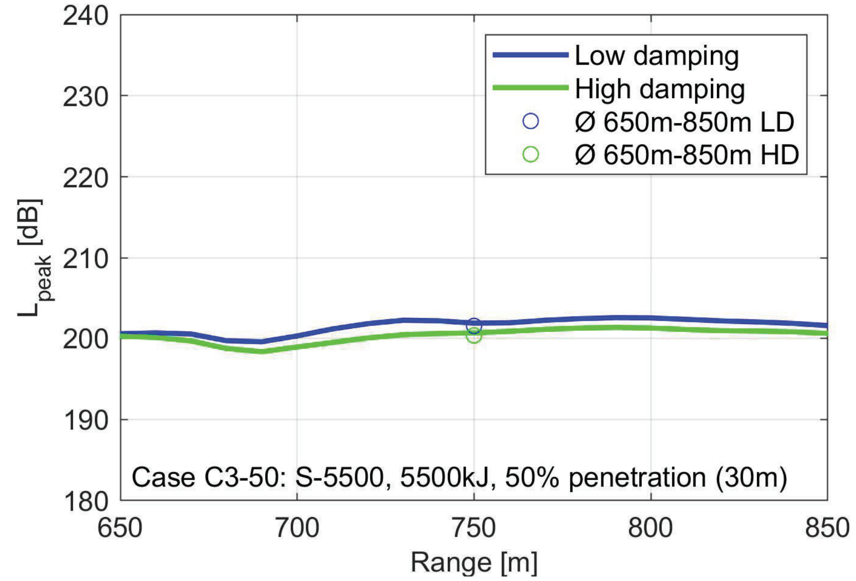

Figure 49: Variation of the predicted ***L_{peak}* for case C3-50** in the range 650m to 850m from the pile for the low and the high soil damping scenario, respectively. **Mona upper case** monopile design 12m/16m, **IQIP S-5500**, hammer energy 5500kJ, **mid penetration depth (30m)**, no secondary noise mitigation.

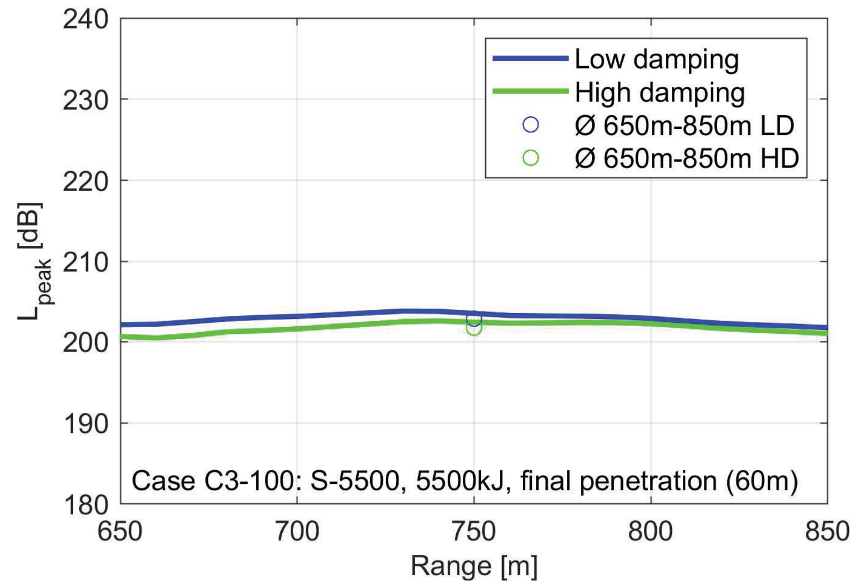

Figure 50: Variation of the predicted ***L_{peak}* for case C3-100** in the range 650m to 850m from the pile for the low and the high soil damping scenario, respectively. **Mona upper case** monopile design 12m/16m, **IQIP S-5500**, hammer energy 5500kJ, **final penetration depth (60m)**, no secondary noise mitigation.

8. Results for case D (Mona pin pile foundation)

Note: All resultant values given in this chapter are evaluated for a reference height above the seabed of 2m.

Within this Chapter, both the sound exposure levels L_E as well as the peak pressure levels L_{peak} that have been derived by using the FE models for case D are summarized. The investigations are based on the combinations of pile, soil, and hammer excitation as defined in Chap. 4. Based on the previous results for the Morgan pin pile foundation (case B), the upper case design has already been identified as the worst case of the three pin pile designs with respect to noise emission. Therefore, only the cases D3-50 (50% of the final penetration depth, where the pile top is flush with the sea surface) and D3-100 (final penetration depth) with upper case design have been computed for the Mona pin pile location.

In addition to the computations with the FE model, virtual source levels at a distance of 1m to the pile axis have been derived by back-calculation of equivalent sound pressure levels and pressure time series using the PE models for the cases D3-50 and D3-100. The corresponding results have been provided to the client in Excel format.

8.1 Sound exposure level L_E

The development of the predicted sound exposure levels L_E in a distance up to 1km to the pile is depicted in Figure 51 to Figure 52. A more detailed view of the range between 650m and 850m is shown in Figure 53 to Figure 54. The corresponding frequency content of the signals is given in Figure 55 to Figure 56

Due to the specific characteristics of the wave guide and corresponding interference effects, the logarithmic decay of the levels with range is only met as a general trend. In practice (both in measurement and simulation), a more or less pronounced oscillation about the decay curve is observed, with dedicated minima and maxima (see Figure 51 to Figure 52). These oscillations contribute significantly to the high variability of the monitored underwater noise levels, as an exact deployment of the measuring devices

at a certain distance to the pile within a few meters is not possible under offshore conditions.

In 750m distance to the pile and 2m above the sea floor, the $L_{E,mean}$ levels (arithmetic mean in the range of 650m to 850m) result to 180.1dB/178.8dB (case D3-50) and 169.9dB/168.4dB (case D3-100) for the low and the high soil damping scenario, respectively. The variations of the L_E in the range of ±100m around the arithmetic mean levels $L_{E,mean}$ for the 750m position are up to about -1.5dB/+1dB (see Figure 53 to Figure 54).

A compilation of the predicted levels can be found in Appendix A. An estimation of the effect on the noise levels when changing the hammer energy can be obtained according to Appendix B.

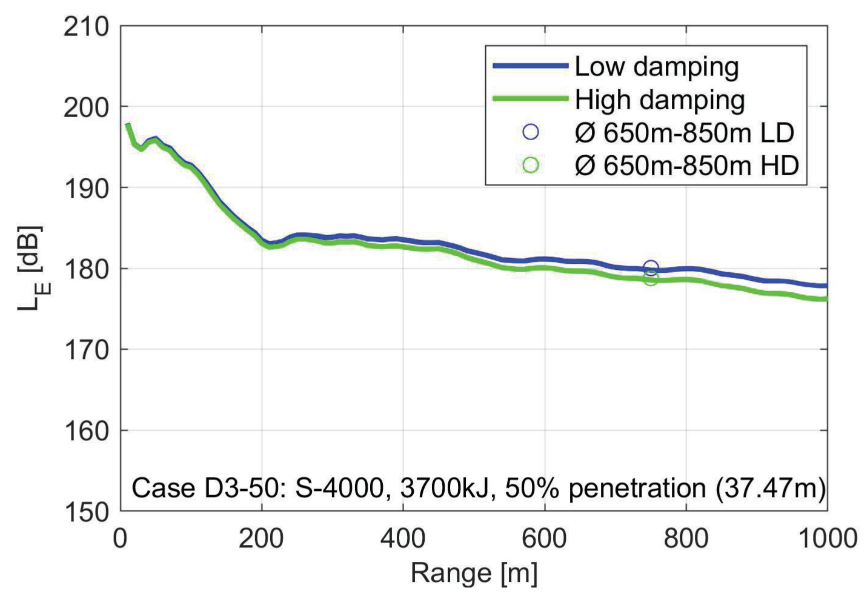

Figure 51: Predicted L_E **for case D3-50** in the range up to 1km from the pile for the low and the high soil damping scenario, respectively. **Mona upper case** pin pile design 5.5m, **IQIP S-4000**, hammer energy 3700kJ, **pile top flush with sea surface (37.47m)**, no secondary noise mitigation.

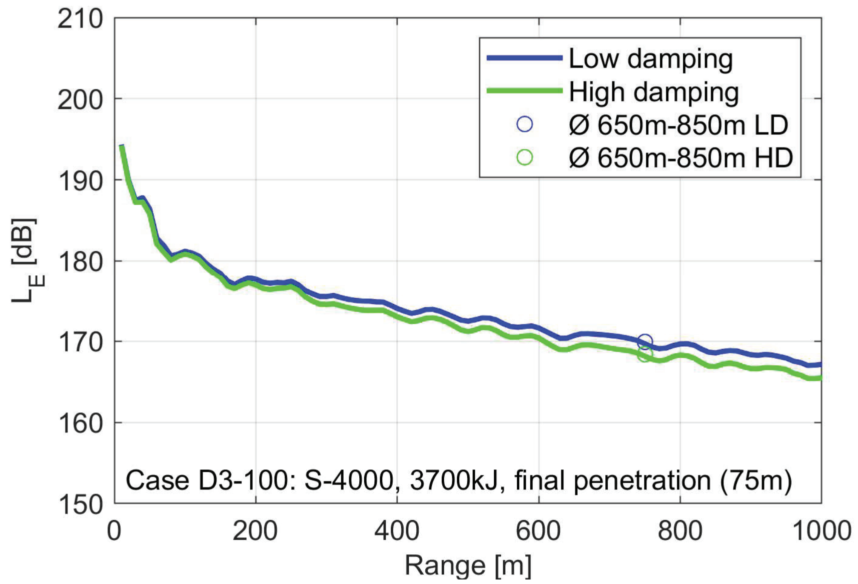

Figure 52: Predicted ***L_E* for case D3-100** in the range up to 1km from the pile for the low and the high soil damping scenario, respectively. **Mona upper case** pin pile design 5.5m, **IQIP S-4000**, hammer energy 3700kJ, **final penetration depth (75m)**, no secondary noise mitigation.

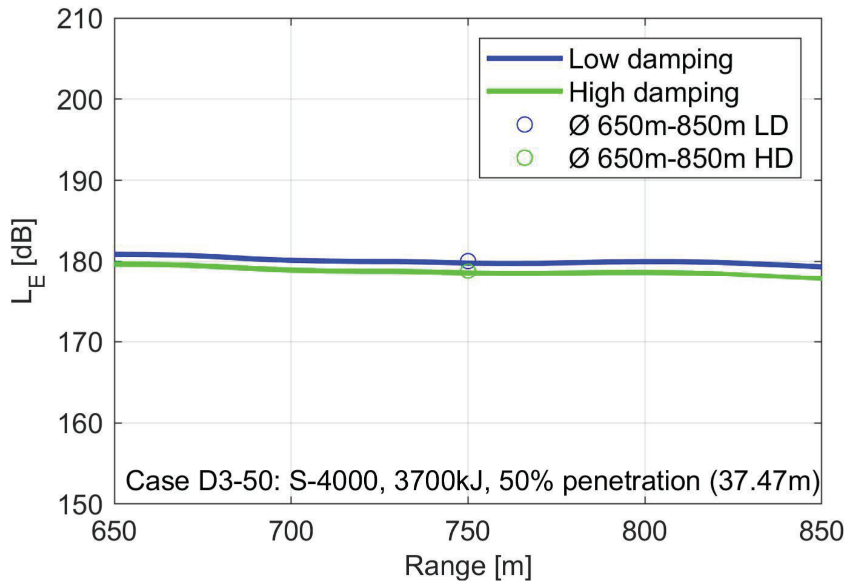

Figure 53: Variation of the predicted ***L_E* for case D3-50** in the range 650m to 850m from the pile for the low and the high soil damping scenario, respectively. **Mona upper case** pin pile design 5.5m, **IQIP S-4000**, hammer energy 3700kJ, **pile top flush with sea surface (37.47m)**, no sec. noise mitigation.

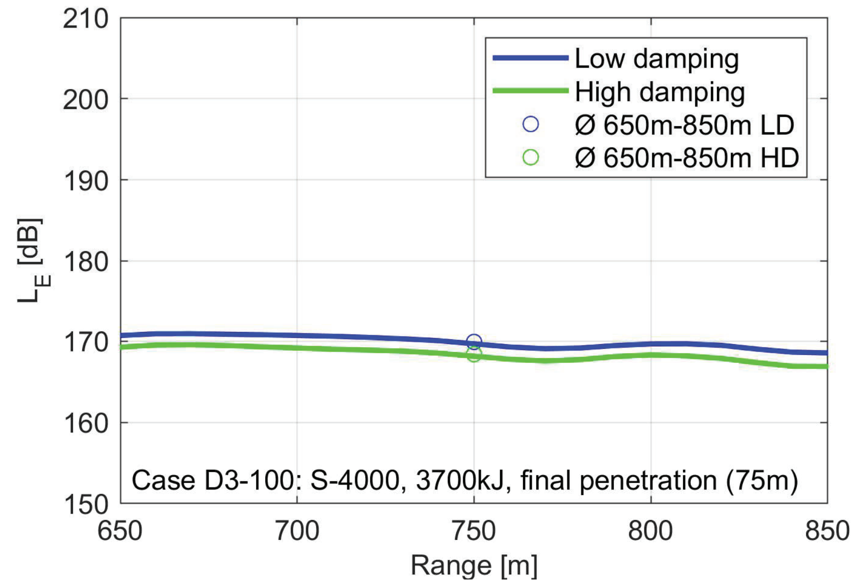

Figure 54: Variation of the predicted ***L_E* for case D3-100** in the range 650m to 850m from the pile for the low and the high soil damping scenario, respectively. **Mona upper case** pin pile design 5.5m, **IQIP S-4000**, hammer energy 3700kJ, **final penetration depth (75m)**, no secondary noise mitigation.

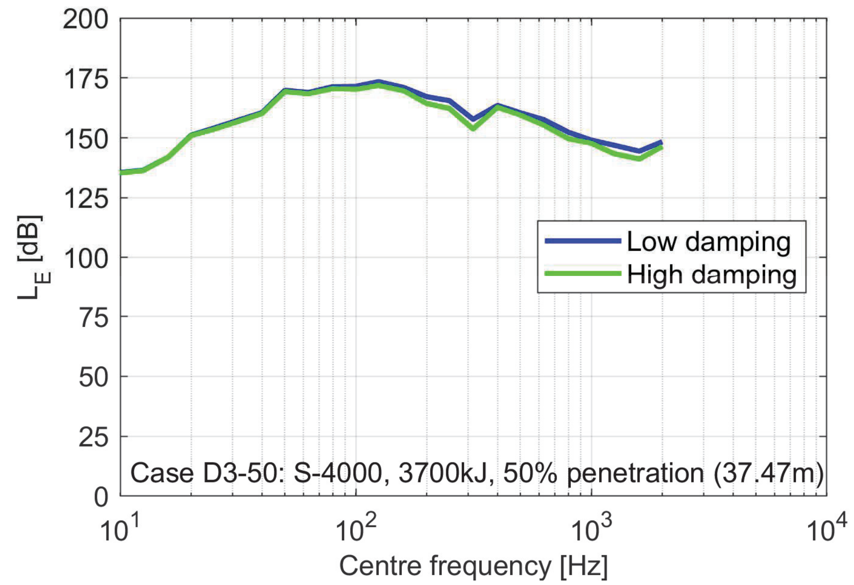

Figure 55: Predicted **spectral *L_E* for case D3-50** at 750m from the pile for the low and the high soil damping scenario, respectively. **Mona upper case** pin pile design 5.5m, **IQIP S-4000**, hammer energy 3700kJ, **pile top flush with sea surface (37.47m)**, no secondary noise mitigation.

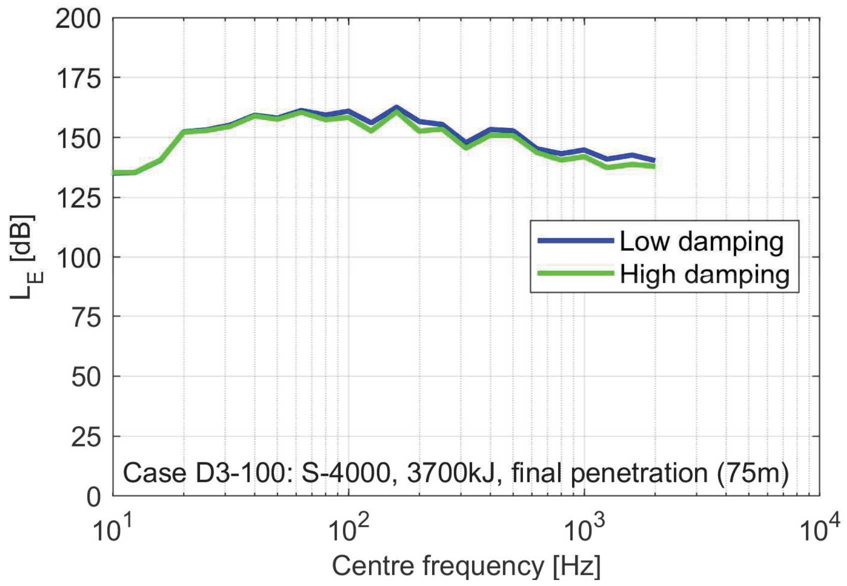

Figure 56: Predicted **spectral L_E for case D3-100** at 750m from the pile for the low and the high soil damping scenario, respectively. **Mona upper case** pin pile design 5.5m, **IQIP S-4000**, hammer energy 3700kJ, **final penetration depth (75m)**, no secondary noise mitigation.

8.2 Peak pressure level L_{peak}

For the peak pressure level L_{peak}, similar conclusions can be drawn. The corresponding results for the range up to 1km and the area between 650m to 850m can be found in Figure 57 to Figure 58 and in Figure 59 to Figure 60, respectively.

In 750m distance to the pile and 2m above the sea floor, the $L_{peak,mean}$ levels (arithmetic mean in the range of 650m to 850m) yield values of 201.1dB/199.4dB (case D3-50) and 188.9dB/187.7dB (case D3-100) for the low and the high soil damping scenario, respectively. The variations of the L_{peak} in the range of ±100m around the arithmetic mean levels $L_{peak,mean}$ for the 750m position are up to about -2.5dB/+3dB (see Figure 59 to Figure 60).

Again, the predicted levels are compiled in Appendix A. An estimation of the effect on the noise levels when changing the hammer energy can be found in Appendix B.

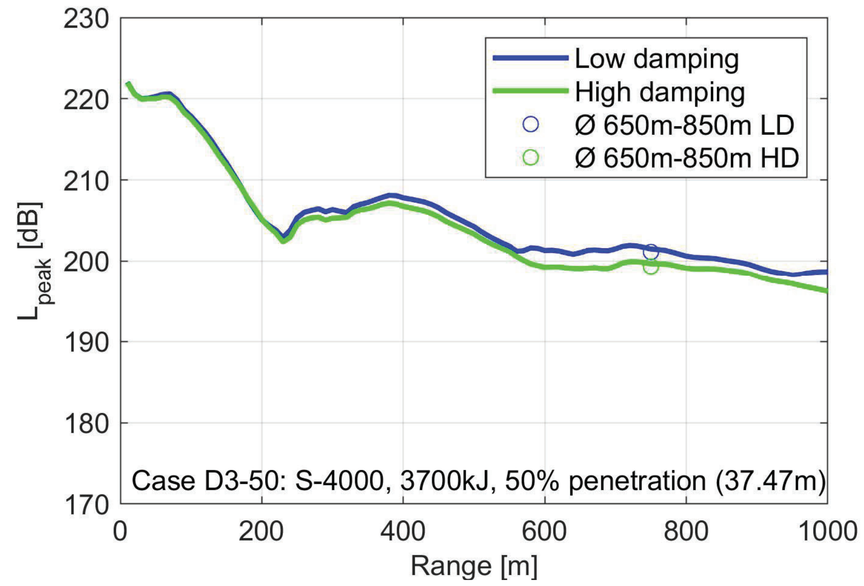

Figure 57: Predicted **L_{peak} for case D3-50** in the range up to 1km from the pile for the low and the high soil damping scenario, respectively. **Mona upper case** pin pile design 5.5m, **IQIP S-4000**, hammer energy 3700kJ, **pile top flush with sea surface (37.47m)**, no secondary noise mitigation.

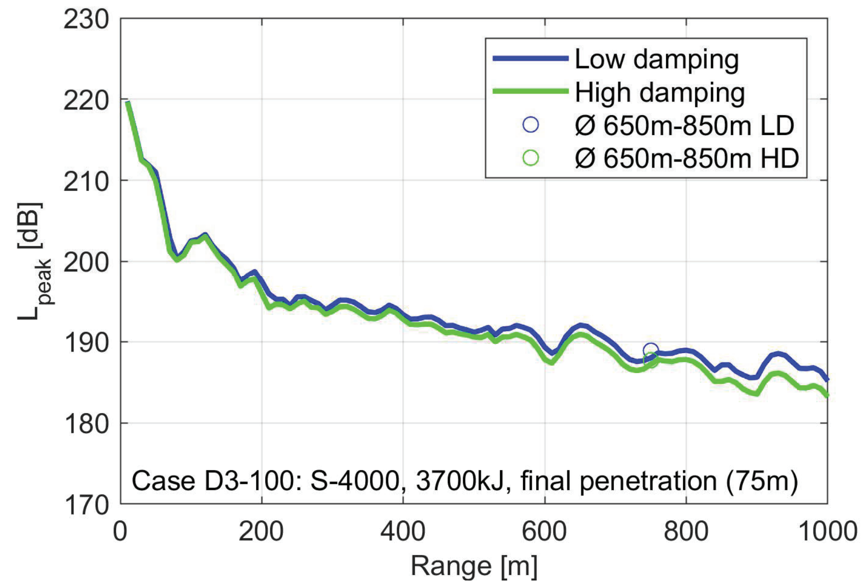

Figure 58: Predicted **L_{peak} for case D3-100** in the range up to 1km from the pile for the low and the high soil damping scenario, respectively. **Mona upper case** pin pile design 5.5m, **IQIP S-4000**, hammer energy 3700kJ, **final penetration depth (75m)**, no secondary noise mitigation.

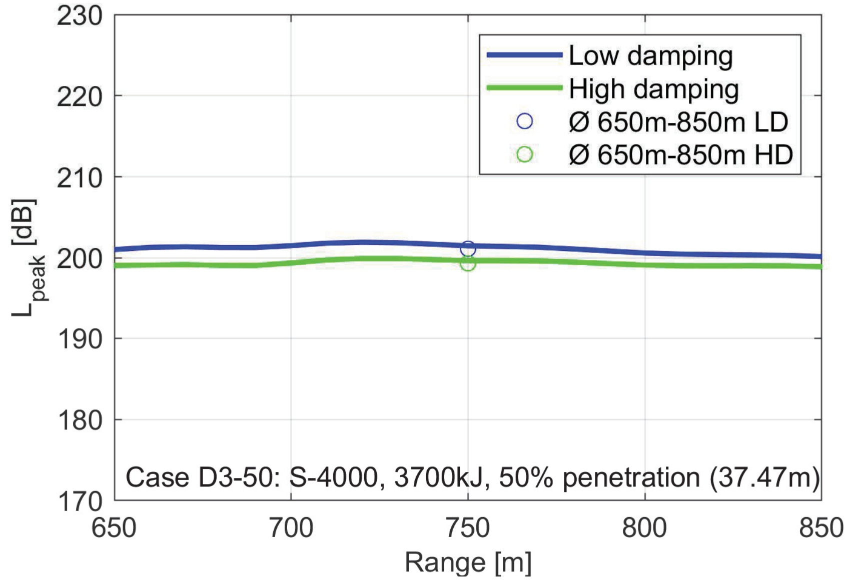

Figure 59: Variation of the predicted ***L_{peak}* for case D3-50** in the range 650m to 850m from the pile for the low and the high soil damping scenario, respectively. **Mona upper case** pin pile design 5.5m, **IQIP S-4000**, hammer energy 3700kJ, **pile top flush with sea surface (37.47m)**, no sec. noise mitigation.

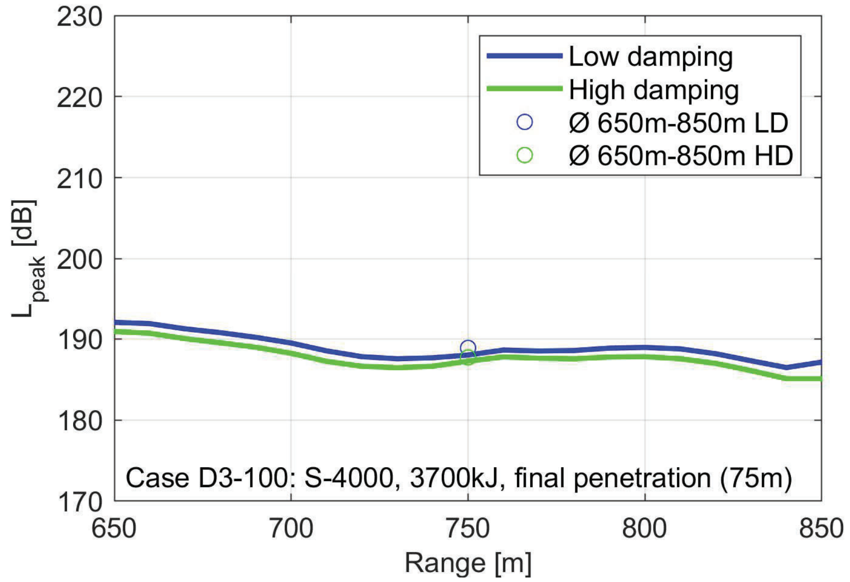

Figure 60: Variation of the predicted ***L_{peak}* for case D3-100** in the range 650m to 850m from the pile for the low and the high soil damping scenario, respectively. **Mona upper case** pin pile design 5.5m, **IQIP S-4000**, hammer energy 3700kJ, **final penetration depth (75m)**, no secondary noise mitigation.

9. Accuracy of the predictions

Computational prediction models require certain simplifications, which directly result from the method being used and are often necessary to achieve acceptable calculation times. The prediction models at hand are based on a comprehensively validated calculation approach as described in Chap. 3 and allow for a detailed consideration of the pile driving relevant processes and parameters. These include, for example, the determination of the hammer excitation on the pile head by means of a separate pre-calculation (in this case carried out by IQIP), the consideration of the interaction between pile and soil, and the implementation of soil layers that transmit both pressure and shear waves allow for a high level of detail. Nevertheless, even with the model at hand it is not possible to take the entire reality into account. Due to the 2D rotational symmetric setup of the FE model, for example, a dedicated 3D topology/bathymetry at the site or asymmetrically designed/deployed noise mitigation systems cannot be considered. Furthermore, not every single physical effect is included, e.g. the possible non-ideal reflection at the water surface due to waves and air bubbles (though, the model uses a conservative estimate, as the considered ideal total reflection results in the highest noise levels).

However, the calculation approach at hand generally provides very reliable results, as the simplifications made have been chosen carefully and validated regularly with measurements from offshore construction. The model used for this study can be seen as one of the most mature and up-to-date models in the field of offshore pile driving.

Besides the above mentioned model simplifications, whose extent can be evaluated sufficiently enough, uncertainties of the input parameters, which are the basis for the simulation, constitute the largest source of prediction inaccuracy. Sometimes, the necessary information is only partly available or does not satisfy the desired quality. Especially, the soil model dimensioning is very challenging. The soil configuration could vary more or less significantly even in the surroundings of a single location and thus change along the propagation path of the acoustic waves in the soil. Further uncertainties occur due to the derivation of the acoustical layering as well as the wave speeds v_p and v_p and the damping parameters from the available survey data.

Therefore, it is explicitly pointed out that, despite of the fact that the calculations have been carried out in all conscience, the simulated results might possibly differ from the sound levels that may be measured during the actual construction. At present it is not possible to give precise information about the general prediction accuracy of pile driving calculation models based on FEM. Nevertheless, the techniques used in this study are considered to be a more robust scientific method of estimating pile sound emissions compared to, for example, using sound emissions measured on other sites as a proxy source. This is particularly important given the large pile dimensions proposed for the Morgan and Mona Offshore Wind Projects where it would be otherwise be necessary to extrapolate data well beyond the currently available measurement data.

10. Summary and conclusions

Novicos GmbH has been commissioned by *Seiche Ltd* to predict the underwater sound emissions to be expected during construction of the Morgan and Mona Offshore Wind Projects, located in the Irish Sea approximately 30km off the coast between Liverpool and the Isle of Man. Both the sound exposure levels (L_E) and the peak pressure levels (L_{peak}) have been evaluated. Furthermore, corresponding spectral source levels have been provided as input for a following marine impact assessment that will be carried out by the client.

For the prediction at hand, FEM models have been generated for several preliminary monopile and pin pile designs for both a typical Morgan and a typical Mona location as requested by the client [25]. The piles are to be driven by an impact hammer. Depending on the pile design, different hammer options have been considered.

All in all, the following cases have been investigated:

Case A (Morgan monopile foundation)

Case A1-100:	Lower case MP, IQIP S-5500 @4500kJ, final penetration
Case A2-100:	Mid case MP, IQIP S-5500 @4700kJ, final penetration
Case A3-50:	Upper case MP, IQIP S-5500 @5500kJ, 50% penetration
Case A3-100:	Upper case MP, IQIP S-5500 @5500kJ, final penetration

Case B (Morgan pin pile foundation)

Case B1-100:	Lower case PP, IQIP S-3000 @1900kJ, final penetration
Case B2-100:	Mid case PP, IQIP S-3000 @2100kJ, final penetration
Case B3-54:	Upper case PP, IQIP S-4000 @3700kJ, flush with sea surface
Case B3-100:	Upper case PP, IQIP S-4000 @3700kJ, final penetration

Case C (Mona monopile foundation)

Case C3-50:	Upper case MP, IQIP S-5500 @5500kJ, 50% penetration
Case C3-100:	Upper case MP, IQIP S-5500 @5500kJ, final penetration

Case D (Mona pin pile foundation)

Case D3-50:	Upper case PP, IQIP S-4000 @3700kJ, flush with sea surface
Case D3-100:	Upper case PP, IQIP S-4000 @3700kJ, final penetration

The model setup is based on the data of the site as provided by the client. Details regarding the model setup can be found in Chap. 4.

In a first step, the cases A1-100, A2-100, and A3-100 for the Morgan monopile foundation have been executed, which consider three different pile designs (lower/mid/upper) at final penetration depth. Based on these results, the upper case has been identified as the worst case of the three pile designs with respect to sound emission. Therefore, an intermediate stage of 50% of the final penetration depth has only been computed for the case A3-50.

The same approach has been chosen for the Morgan pin pile foundation by executing the cases B1-100, B2-100, and B3-100 first. For the identified upper bound design as worst case, an additional intermediate penetration of 54%, at which the pile top is flush with the sea surface at the Morgan location, has been evaluated (case B3-54).

For the Mona location, only the worst case designs for the monopile and the pin pile as identified for the Morgan location have has been considered, so that the cases C3-50, C3-100, D3-50, and D3-100 have been computed.

In addition to the computations with the FE model, virtual source levels at a distance of 1m to the pile axis have been derived by back-calculation of equivalent sound pressure levels and pressure time series using the PE models for the cases A3-50, A3-100, B3-54, B3-100, C3-50, C3-100, D3-50, and D3-100. The corresponding results have been provided to the client in Excel format.

The computations of the underwater noise emission for **case A** yielded the following results:

- At 750m distance from the pile at 2m above the sea floor, the $L_{E,mean}$ levels (arithmetic mean in the range of 650m to 850m) result to 180.8dB/180.1dB (case A1-100), 181.3dB/180.5dB (case A2-100), 183.5dB/183.0dB (case A3-50), and 182.9dB/182.1dB (case A3-100) for the low and the high soil damping scenario, respectively. The corresponding $L_{peak,mean}$ levels (arithmetic mean in the range of 650m to 850m) yield values of 199.2dB/198.6dB (case A1-100), 201.4dB/200.6dB (case A2-100), 201.8dB/201.2dB (case A3-50), and

201.6dB/200.9dB (case A3-100)for the low and the high soil damping scenario, respectively.

- Due to the specific characteristics of the wave guide and corresponding interference effects, the logarithmic decay of the levels with range is only met as a general trend. In practice (both in measurement and simulation), a more or less pronounced oscillation about the decay curve is observed, with dedicated minima and maxima. These oscillations contribute significantly to the high variability of the monitored underwater noise levels, as an exact deployment of the measuring devices at a certain distance to the pile within a few meters is not possible under offshore conditions. The variations of the L_E in the range of ±100m around the arithmetic mean levels $L_{E,mean}$ for the 750m position are up to about -2dB/+1dB, while the L_{peak} show variations up to about -4dB/+3dB around the arithmetic mean levels $L_{peak,mean}$.

The computations of the underwater noise emission for **case B** yielded the following results:

- At 750m distance from the pile at 2m above the sea floor, the $L_{E,mean}$ levels (arithmetic mean in the range of 650m to 850m) result to 165.0dB/163.6dB (case B1-100), 165.9dB/164.6dB (case B2-100), 180.2dB/179.4dB (case B3-54), and 170.5dB/169.4dB (case B3-100) for the low and the high soil damping scenario, respectively. The corresponding $L_{peak,mean}$ levels (arithmetic mean in the range of 650m to 850m) yield values of 186.5dB/185.2dB (case B1-100), 184.4dB/183.2dB (case B2-100), 201.2dB/200.6dB (case B3-54), and 189.0dB/188.0dB (case B3-100) for the low and the high soil damping scenario, respectively.
- The variations of the L_E in the range of ±100m around the arithmetic mean levels $L_{E,mean}$ for the 750m position are up to about -1dB/+1.5dB, while the L_{peak} show variations up to about ±3dB around the arithmetic mean levels $L_{peak,mean}$.

The computations of the underwater noise emission for **case C** yielded the following results:

- At 750m distance from the pile at 2m above the sea floor, the $L_{E,mean}$ levels (arithmetic mean in the range of 650m to 850m) result to 183.9dB/183.2dB (case C3-50) and 182.9dB/182.0dB (case C3-100) for the low and the high soil damping scenario, respectively. The corresponding $L_{peak,mean}$ levels (arithmetic mean in the range of 650m to 850m) yield values of 201.5dB/200.3dB (case C3-50) and 202.8dB/201.7dB (case C3-100) for the low and the high soil damping scenario, respectively.
- The variations of the L_E in the range of ±100m around the arithmetic mean levels $L_{E,mean}$ for the 750m position are up to about ±0.5dB, while the L_{peak} show variations up to about -2dB/+1dB around the arithmetic mean levels $L_{peak,mean}$.

The computations of the underwater noise emission for **case D** yielded the following results:

- At 750m distance from the pile at 2m above the sea floor, the $L_{E,mean}$ levels (arithmetic mean in the range of 650m to 850m) result to 180.1dB/178.8dB (case D3-50) and 169.9dB/168.4dB (case D3-100) for the low and the high soil damping scenario, respectively. The corresponding $L_{peak,mean}$ levels (arithmetic mean in the range of 650m to 850m) yield values of 201.1dB/199.4dB (case D3-50) and 188.9dB/187.7dB (case D3-100) for the low and the high soil damping scenario, respectively.
- The variations of the L_E in the range of ±100m around the arithmetic mean levels $L_{E,mean}$ for the 750m position are up to about -1.5dB/+1dB, while the L_{peak} show variations up to about -2.5dB/+3dB around the arithmetic mean levels $L_{peak,mean}$.

A compilation of the simulation results from the FE model can be found in Appendix A. An estimation of the effect on the noise levels when changing the hammer energy can be obtained according to Appendix B. Note that due to the non-linearity of the interac-

tion between hammer and pile during impact, the accuracy of the approximation decreases with increasing difference between initial hammer energy and new hammer energy of interest.

Beside the results documented in this report, animations of the wave propagation from the FE model both in the sea water and in the soil have been provided to the client for the cases A3-50, A3-100, B3-54, B3-100, C3-50, C3-100, D3-50, and D3-100. These animations help interpreting the results and give a deeper physical insight into the noise propagation. However, the animations are not part of this report.

Please note the following when using the predicted noise levels of this study:

- All computations have been performed at a fixed water column depth. The resulting sound levels may differ for sea levels other than that depth, e.g. due to tides or variations between different pile locations. However, the effect on the sound levels is likely to be small when having only low tidal changes or in case of a fairly consistent water depth across the construction site.
- So far, one Morgan location and one Mona location with preliminary pile designs have been investigated. For design changes of the parameters at these locations or for different locations at the two sites, the noise levels can vary due to the differences in pile design, penetration depth, hammer energy, water depth, and surrounding soil conditions. The two locations and their preliminary design parameters may not be the worst case from an acoustical point of view. Additional investigations for updated design parameters or for other location may be performed, if this uncertainty should be further addressed.
- Uncertainties of the input parameters, which are the basis for the simulation, constitute the largest source of prediction inaccuracy. Especially, the soil model dimensioning is very challenging. The soil configuration could vary more or less significantly even in the surroundings of a single location and thus change along the propagation path of the acoustic waves in the soil. Further uncertainties occur due to the derivation of the acoustical layering as well as the wave speeds v_p and v_p and the damping parameters from the available survey data.

Nevertheless we have used state-of-the-art techniques and best available information to provide a robust estimate on the sound emission, the computed results might therefore possibly differ from the sound levels that may be measured on site during the actual construction.

Literature

[1] OSPAR commission, *Overview of the impacts of anthropogenic underwater sound in the marine environment*, OSPAR publication number 441/2009, 2009

[2] European Parliament, *Directive 2008/56/EC of the European Parliament and of the Council of 17 June 2008: Establishing a framework for community action in the field of marine environmental policy (Marine Strategy Framework Directive)*, 2008

[3] German Federal Maritime and Hydrographic Agency (BSH), *Standard Untersuchung der Auswirkung von Offshore-Windenergieanlagen auf die Meeresumwelt (StUK4)*, October 2013

[4] A. Müller, C. Zerbs, *Offshore-Windparks: Prognosen für Unterwasserschall*, Report by order of the German Federal Maritime and Hydrographic Agency (BSH), 2013

[5] O. von Estorff, K. Heitmann, S. Lippert, T. Lippert, K. Reimann, M. Ruhnau, M. Schwarz, *Unterwasser-Rammschall: Eine Herausforderung bei der Errichtung von Offshore-Windparks und für die numerische Simulation*, Lärmbekämpfung **8**(2), 2013

[6] S. Lippert, T. Lippert, K. Heitmann, O. von Estorff, *Prediction of Underwater Noise and Far Field Propagation due to Pile Driving for Offshore Wind Farms*, Proceedings of the 21st International Conference on Acoustics (ICA), Montréal, Canada, 2013

[7] K. Heitmann, T. Lippert, M. Ruhnau, S. Lippert, O. von Estorff, *Computational Prediction of the Underwater Sound Pressure due to Offshore Pile Driving*, Proceedings of the 21st International Congress on Sound and Vibration (ICSV), Beijing, China, 2014

[8] K. Heitmann, T. Lippert, M. Ruhnau, S. Lippert, O. von Estorff, *Untersuchung des Einfusses der geometrischen Abmessungen eines Monopiles auf den Schalldruckpegel während einer Offshore-Pfahlrammung*, Proceedings of the 40. Jahrestagung für Akustik (DAGA), Oldenburg, Germany, 2014

[9] A. J. Deeks, M. F. Randolph, *Analytical Modelling of Hammer Impact for Pile Driving*, International Journal for Numerical and Analytical Methods in Geomechanics **17**, pp. 279-302, 1993

[10] P. Reinhall, P. Dahl, *Underwater Mach Wave Radiation from Impact Pile Driving: Theory and Observation*, Journal of the Acoustical Society of America **130**(3), pp. 1209-1216, 2011

[11] K. Heitmann, S. Mallapur, T. Lippert, M. Ruhnau, S. Lippert, O. von Estorff, *Numerical Determination of Equivalent Damping Parameters for a Finite Element Model to Predict the Underwater Noise due to Offshore Pile Driving*, Proceedings of the 10th European Congress and Exposition on Noise Control Engineering (EuroNoise 2015), Maastricht, The Netherlands, 2015

[12] M. Milatz, K. Reimann, J. Grabe, *Numerical Simulations of Hydro Sound Emissions due to Offshore Pile Driving*, Proceedings of the 7th International Conference on Offshore Site Investigation and Geotechnics, London, UK, 2012

[13] T. Schossau, K. Heitmann, S. Lippert, O. von Estorff, *Modellierung des IHC Noise Mitigation Screen durch die Verwendung von Materialmodellen höherer Ordnung*, Workshop AK Hydroschall at Hamburg University of Technology TUHH, Hamburg, Germany, 2015

[14] Projekt BORA - Berechnung von Offshore Rammschall (FKZ 0325421), see http://www.tuhh.de/bora.

[15] K. Heitmann, T. Lippert, M. Ruhnau, S. Lippert, O. von Estorff, *Rammschallvorhersage zur dritten Offshore-Messkampagne (OMK3) des BORA-Projektes*, Workshop Schallschutzworkshop 2014 at the German Federal Maritime and Hydrographic Agency (BSH), Hamburg, Germany, 2014

[16] K. Heitmann, M. Ruhnau, T. Lippert, S. Lippert, O. von Estorff, *Numerical Investigation of the Influence of Different Sound Mitigation Systems on the Underwater Sound Pressure Level due to Offshore Pile Driving*, Proceedings of the 22st International Congress on Sound and Vibration (ICSV), Florence, Italy, 2015

[17] S. Lippert, M. Huisman, M. Ruhnau, O. von Estorff, K. van Zandwijk, *Prognosis of Underwater Pile Driving Noise for Submerged Skirt Piles of Jacket Structures*, Proceedings of the 4th International Conference and Exhibition on Underwater Acoustics (UACE 2017), Skiathos, Greece, 2017

[18] K. Heitmann, *Vorhersage des Unterwasserschalls bei Offshore-Rammarbeiten unter Berücksichtigung von Schallminderungsmaßnahmen*, PhD Thesis, Hamburg University of Technology TUHH, Hamburg, Germany 2016

[19] S. Lippert, O. von Estorff, *Offshore Pile Driving Noise: Capability of Numerical Prediction Models and Ways to Consider New Technologies*, Advances in Engineering Materials, Structures and Systems: Innovations, Mechanics and Applications - Proceedings of the 7th International Conference on Structural Engineering, Mechanics and Computation (SEMC 2019), Cape Town, South Africa, 2019

[20] J. von Pein, S. Lippert, O. von Estorff, *Validation of a Finite Element Modelling Approach for Mitigated and Unmitigated Piledriving Noise Prognosis*, Journal of the Acoustical Society of America **149**(3), pp. 1737-1748, 2021

[21] M. D. Collins, E. K. Westwood, *A Higher-Order Energy-Conserving Parabolic Equation for Range-Dependent Ocean Depth, Sound Speed, and Density*, Journal of the Acoustical Society of America **89**(3), pp. 1068-1075, 1991

[22] M. D. Collins, *A Two-Way Parabolic Equation for Acoustic Backscattering in the Ocean*, Journal of the Acoustical Society of America **91**(3), p. 1357, 1992

[23] J. von Pein, E. Klages, S. Lippert, O. von Estorff, *A Hybrid Model for the 3D Computation of Pile Driving Noise*, Proceedings of the OCEANS 2019 Conference, Marseille, France, 2019

[24] F. B. Jensen, W. A. Kuperman, M. B. Porter, H. Schmidt, *Computational Ocean Acoustics*, Springer New York, 2011

[25] IQIP, *Monopile and pin pile designs for Morgan and Mona (lower – mid – upper case)*, MS Excel document “M&M - Pile Cases.xlsx”, provided to Novicos by email on 20.05.2022

[26] IQIP, *Hammer excitation signal for lower case monopile*, MS Excel document “Case 13-S5500-4500kJ - 09_Result_Pile_top_2D-C Geotech diagram-Scaling the velocity”, provided to Novicos by email on 17.06.2022

[27] IQIP, *Hammer excitation signal for mid case monopile*, MS Excel document "Case 14-S5500-4700kJ - 09_Result_Pile_top_2D-C Geotech diagram-Scaling the velocity", provided to Novicos by email on 17.06.2022

[28] IQIP, *Hammer excitation signal for upper case monopile*, MS Excel document "Case 17-S5500-5500kJ - 09_Result_Pile_top_2D-C Geotech diagram-Scaling the velocity", provided to Novicos by email on 17.06.2022

[29] IQIP, *Hammer excitation signal for lower case pin pile*, MS Excel document "Case 18-S3000-1900kJ - 09_Result_Pile_top_2D-C Geotech diagram-Scaling the velocity", provided to Novicos by email on 17.06.2022

[30] IQIP, *Hammer excitation signal for mid case pin pile*, MS Excel document "Case 19-S3000-2100kJ - 09_Result_Pile_top_2D-C Geotech diagram-Scaling the velocity", provided to Novicos by email on 17.06.2022

[31] IQIP, *Hammer excitation signal for upper case pin pile*, MS Excel document "Case 22-S4000-3700kJ - 09_Result_Pile_top_2D-C Geotech diagram-Scaling the velocity", provided to Novicos by email on 17.06.2022

[32] Seiche, *Wave velocities and densities in water column and soil for Morgan and Mona location*, MS Excel document "Geoacoustic model v2.xlsx", provided to Novicos by email on 21.04.2022

Appendix A – Result compilation

In the following, the noise levels that have been computed for the different cases with the FE model are summarized.

A.1 Predicted $L_{E,mean}$ and $L_{peak,mean}$ levels for case A

Table 3: Predicted $L_{E,mean}$ and $L_{peak,mean}$ levels **for case A** in a distance of **750m to the pile** (arithmetic mean in the range of 650m to 850m), 2m above the seabed. **Morgan monopile foundation**, water depth 40m, Morgan soil layering, no secondary noise mitigation. Variabilities in the parentheses are given for the L_E relative to the $L_{E,mean}$ in the range between 650m and 850m distance to the pile.

	Low soil damping scenario		High soil damping scenario	
	$L_{E,mean}$ [dB]	$L_{peak,mean}$ [dB]	$L_{E,mean}$ [dB]	$L_{peak,mean}$ [dB]
Case A1-100: IQIP S-5500 @4500kJ, lower case monopile design 11m/12m, length 104.3m, final penetration (50m)	180.8 (-0.8/+0.9)	199.2 (-0.9/+0.8)	180.1 (-0.7/+0.9)	198.6 (-0.9/+0.7)
Case A2-100: IQIP S-5500 @4700kJ, mid case monopile design 12m/13m, length 114.3m, final penetration (60m)	181.3 (-0.6/+0.3)	201.4 (-2.0/+1.3)	180.5 (-0.7/+0.4)	200.6 (-2.2/+1.3)
Case A3-50: IQIP S-5500 @5500kJ, upper case monopile design 12m/16m, length 114.3m, mid penetration (30m)	183.5 (-1.9/+1.0)	201.8 (-3.8/+2.0)	183.0 (-2.0/+1.0)	201.2 (-3.9/+2.0)
Case A3-100: IQIP S-5500 @5500kJ, upper case monopile design 12m/16m, length 114.3m, final penetration (60m)	182.9 (-1.0/+0.9)	201.6 (-3.3/+2.7)	182.1 (-1.1/+1.0)	200.9 (-3.3/+2.9)

A.2 Predicted $L_{E,mean}$ and $L_{peak,mean}$ levels for case B

Table 4: Predicted $L_{E,mean}$ and $L_{peak,mean}$ levels **for case B** in a distance of **750m to the pile** (arithmetic mean in the range of 650m to 850m), 2m above the seabed. **Morgan pin pile foundation**, water depth 40m, Morgan soil layering, no secondary noise mitigation. Variabilities in the parentheses are given for the L_E relative to the $L_{E,mean}$ in the range between 650m and 850m distance to the pile.

	Low soil damping scenario		High soil damping scenario	
	$L_{E,mean}$ [dB]	$L_{peak,mean}$ [dB]	$L_{E,mean}$ [dB]	$L_{peak,mean}$ [dB]
Case B1-100: IQIP S-3000 @1900kJ, lower case pin pile design 3.32m, length 60.47m, final penetration (55m)	165.0 (-1.0/+1.2)	186.5 (-2.5/+2.7)	163.6 (-0.9/+1.3)	185.2 (-2.5/+3.1)
Case B2-100: IQIP S-3000 @2100kJ, mid case pin pile design 4.00m, length 60.47m, final penetration (55m)	165.9 (-0.7/+0.9)	184.4 (-1.6/+2.6)	164.6 (-0.6/+0.9)	183.2 (-1.8/+2.6)
Case B3-54: IQIP S-4000 @3700kJ, upper case pin pile design 5.50m, length 80.47m, pile top flush (40.47m)	180.2 (-0.5/+1.0)	201.2 (-1.8/+1.7)	179.4 (-0.5/+1.1)	200.6 (-2.0/+1.7)
Case B3-100: IQIP S-4000 @3700kJ, upper case pin pile design 5.50m, length 80.47m, final penetration (75m)	170.5 (-0.9/+0.6)	189.0 (-3.0/+2.0)	169.4 (-1.0/+0.6)	188.0 (-2.8/+1.7)

A.3 Predicted $L_{E,mean}$ and $L_{peak,mean}$ levels for case C

Table 5: Predicted $L_{E,mean}$ and $L_{peak,mean}$ levels **for case C** in a distance of **750m to the pile** (arithmetic mean in the range of 650m to 850m), 2m above the seabed. **Mona monopile foundation**, water depth 43m, Mona soil layering, no secondary noise mitigation. Variabilities in the parentheses are given for the L_E relative to the $L_{E,mean}$ in the range between 650m and 850m distance to the pile.

	Low soil damping scenario		High soil damping scenario	
	$L_{E,mean}$ [dB]	$L_{peak,mean}$ [dB]	$L_{E,mean}$ [dB]	$L_{peak,mean}$ [dB]
Case C3-50: IQIP S-5500 @5500kJ, upper case monopile design 12m/16m, length 114.3m, mid penetration (30m)	183.9 (-0.6/+0.4)	201.5 (-2.0/+1.0)	183.2 (-0.7/+0.5)	200.3 (-2.0/+1.0)
Case C3-100: IQIP S-5500 @5500kJ, upper case monopile design 12m/16m, length 114.3m, final penetration (60m)	182.9 (-0.5/+0.2)	202.8 (-1.1/+0.9)	182.0 (-0.5/+0.3)	201.7 (-1.3/+0.8)

A.4 Predicted $L_{E,mean}$ and $L_{peak,mean}$ levels for case D

Table 6: Predicted $L_{E,mean}$ and $L_{peak,mean}$ levels **for case D** in a distance of **750m to the pile** (arithmetic mean in the range of 650m to 850m), 2m above the seabed. **Mona pin pile foundation**, water depth 43m, Morgan soil layering, no secondary noise mitigation. Variabilities in the parentheses are given for the L_E relative to the $L_{E,mean}$ in the range between 650m and 850m distance to the pile.

	Low soil damping scenario		High soil damping scenario	
	$L_{E,mean}$ [dB]	$L_{peak,mean}$ [dB]	$L_{E,mean}$ [dB]	$L_{peak,mean}$ [dB]
Case D3-50: IQIP S-4000 @3700kJ, upper case pin pile design 5.50m, length 80.47m, pile top flush (37.47m)	180.1 (-0.7/+0.8)	201.1 (-1.0/+0.8)	178.8 (-0.9/+0.9)	199.4 (-0.4/+0.6)

Case D3-100: IQIP S-4000 @3700kJ, upper case pin pile design 5.50m, length 80.47m, final penetration (75m)	169.9 (-1.3/+1.0)	188.9 (-2.4/+3.2)	168.4 (-1.5/+1.2)	187.7 (-2.6/+3.2)

Appendix B – Effect of reduced or increased hammer energy on the noise levels

An estimation of the effect on the noise levels when changing the hammer energy can be obtained according to Table 7. This approximation is based on assuming a fixed relation between hammer energy and noise levels. However, please note that due to the non-linearity of the interaction between hammer and pile during impact, the accuracy of the approximation decreases with increasing difference between initial hammer energy and new hammer energy of interest. Dedicated values of estimated noise levels from scaling for different cases can be found in Table 8 to Table 15.

Table 7: Estimation of the effect on the L_E and L_{peak} levels when reducing or increasing hammer energy. Please note that due to the non-linearity of the interaction between hammer and pile during impact, the accuracy of the approximation decreases with increasing variation of the hammer energy.

	ΔL [dB]
Reduction of hammer energy by a factor of 4 (-75%)	-6.0
Reduction of hammer energy by a factor of 2.86 (-65%)	-4.6
Reduction of hammer energy by a factor of 2 (-50%)	-3.0
Reduction of hammer energy by a factor of 1.54 (-35%)	-1.9
Reduction of hammer energy by a factor of 1.33 (-25%)	-1.2
Increase of hammer energy by a factor of 1.25 (+25%)	+1.0
Increase of hammer energy by a factor of 1.35 (+35%)	+1.3
Increase of hammer energy by a factor of 1.5 (+50%)	+1.8
Increase of hammer energy by a factor of 1.65 (+65%)	+2.2
Increase of hammer energy by a factor of 1.75 (+75%)	+2.4
Increase of hammer energy by a factor of 2 (+100%)	+3.0

Table 8: Predicted $L_{E,mean}$ and $L_{peak,mean}$ levels **for case A3-50** in a distance of **750m to the pile** (arithmetic mean in the range of 650m to 850m), 2m above the seabed for different hammer energies. **Morgan monopile foundation**, water depth 40m, Morgan soil layering, **mid penetration depth (30m)**, no secondary noise mitigation. Please note that due to the non-linearity of the interaction between hammer and pile during impact, the accuracy of the approximation decreases with increasing variation of the hammer energy (**scaling based the results of the FE model for 5500kJ**).

	Low soil damping scenario		High soil damping scenario	
	$L_{E,mean}$ [dB]	$L_{peak,mean}$ [dB]	$L_{E,mean}$ [dB]	$L_{peak,mean}$ [dB]
IQIP S-5500 @400kJ, mid penetration	172.1	190.4	171.6	189.8
IQIP S-5500 @600kJ, mid penetration	173.9	192.1	173.3	191.6
IQIP S-5500 @800kJ, mid penetration	175.1	193.4	174.6	192.8
IQIP S-5500 @1000kJ, mid pen.	176.1	194.3	175.6	193.8
IQIP S-5500 @1200kJ, mid pen.	176.9	195.1	176.4	194.6
IQIP S-5500 @1400kJ, mid pen.	177.5	195.8	177.0	195.3
IQIP S-5500 @1600kJ, mid pen.	178.1	196.4	177.6	195.9
IQIP S-5500 @1800kJ, mid pen.	178.6	196.9	178.1	196.4
IQIP S-5500 @2000kJ, mid pen.	179.1	197.4	178.6	196.8
IQIP S-5500 @2200kJ, mid pen.	179.5	197.8	179.0	197.2
IQIP S-5500 @2400kJ, mid pen.	179.9	198.1	179.4	197.6
IQIP S-5500 @2600kJ, mid pen.	180.2	198.5	179.7	198.0
IQIP S-5500 @2800kJ, mid pen.	180.6	198.8	180.0	198.3
IQIP S-5500 @3000kJ, mid pen.	180.9	199.1	180.3	198.6
IQIP S-5500 @3200kJ, mid pen.	181.1	199.4	180.6	198.9
IQIP S-5500 @3400kJ, mid pen.	181.4	199.7	180.9	199.1
IQIP S-5500 @3600kJ, mid pen.	181.6	199.9	181.1	199.4
IQIP S-5500 @3800kJ, mid pen.	181.9	200.1	181.4	199.6
IQIP S-5500 @4000kJ, mid pen.	182.1	200.4	181.6	199.8
IQIP S-5500 @4200kJ, mid pen.	182.3	200.6	181.8	200.0
IQIP S-5500 @4400kJ, mid pen.	182.5	200.8	182.0	200.2
IQIP S-5500 @4600kJ, mid pen.	182.7	201.0	182.2	200.4
IQIP S-5500 @4800kJ, mid pen.	182.9	201.2	182.4	200.6
IQIP S-5500 @5000kJ, mid pen.	183.1	201.3	182.6	200.8
IQIP S-5500 @5300kJ, mid pen.	183.2	201.5	182.7	201.0
IQIP S-5500 @5400kJ, mid pen.	183.4	201.7	182.9	201.1
IQIP S-5500 @5500kJ, mid pen.	**183.5**	**201.8**	**183.0**	**201.2**

Table 9: Predicted $L_{E,mean}$ and $L_{peak,mean}$ levels **for case A3-100** in a distance of **750m to the pile** (arithmetic mean in the range of 650m to 850m), 2m above the seabed for different hammer energies. **Morgan monopile foundation**, water depth 40m, Morgan soil layering, **final penetration depth (60m)**, no secondary noise mitigation. Please note that due to the non-linearity of the interaction between hammer and pile during impact, the accuracy of the approximation decreases with increasing variation of the hammer energy (**scaling based the results of the FE model for 5500kJ**).

	Low soil damping scenario		High soil damping scenario	
	$L_{E,mean}$ [dB]	$L_{peak,mean}$ [dB]	$L_{E,mean}$ [dB]	$L_{peak,mean}$ [dB]
IQIP S-5500 @400kJ, final penetration	171.5	190.2	170.7	189.6
IQIP S-5500 @600kJ, final penetration	173.3	192.0	172.5	191.3
IQIP S-5500 @800kJ, final penetration	174.5	193.3	173.7	192.6
IQIP S-5500 @1000kJ, final pen.	175.5	194.2	174.7	193.5

IQIP S-5500 @1200kJ, final pen.	176.3	195.0	175.5	194.3
IQIP S-5500 @1400kJ, final pen.	176.9	195.7	176.1	195.0
IQIP S-5500 @1600kJ, final pen.	177.5	196.3	176.7	195.6
IQIP S-5500 @1800kJ, final pen.	178.0	196.8	177.2	196.1
IQIP S-5500 @2000kJ, final pen.	178.5	197.2	177.7	196.5
IQIP S-5500 @2200kJ, final pen.	178.9	197.7	178.1	197.0
IQIP S-5500 @2400kJ, final pen.	179.3	198.0	178.5	197.3
IQIP S-5500 @2600kJ, final pen.	179.6	198.4	178.8	197.7
IQIP S-5500 @2800kJ, final pen.	179.9	198.7	179.2	198.0
IQIP S-5500 @3000kJ, final pen.	180.2	199.0	179.5	198.3
IQIP S-5500 @3200kJ, final pen.	180.5	199.3	179.7	198.6
IQIP S-5500 @3400kJ, final pen.	180.8	199.5	180.0	198.8
IQIP S-5500 @3600kJ, final pen.	181.0	199.8	180.2	199.1
IQIP S-5500 @3800kJ, final pen.	181.3	200.0	180.5	199.3
IQIP S-5500 @4000kJ, final pen.	181.5	200.2	180.7	199.6
IQIP S-5500 @4200kJ, final pen.	181.7	200.5	180.9	199.8
IQIP S-5500 @4400kJ, final pen.	181.9	200.7	181.1	200.0
IQIP S-5500 @4600kJ, final pen.	182.1	200.9	181.3	200.2
IQIP S-5500 @4800kJ, final pen.	182.3	201.0	181.5	200.3
IQIP S-5500 @5000kJ, final pen.	182.5	201.2	181.7	200.5
IQIP S-5500 @5300kJ, final pen.	182.6	201.4	181.8	200.7
IQIP S-5500 @5400kJ, final pen.	182.8	201.5	182.0	200.9
IQIP S-5500 @5500kJ, final pen.	**182.9**	**201.6**	**182.1**	**200.9**

Table 10: Predicted $L_{E,mean}$ and $L_{peak,mean}$ levels **for case B3-54** in a distance of **750m to the pile** (arithmetic mean in the range of 650m to 850m), 2m above the seabed for different hammer energies. **Morgan pin pile foundation**, water depth 40m, Morgan soil layering, **pile top flush with sea surface (40.47m)**, no secondary noise mitigation. Please note that due to the non-linearity of the interaction between hammer and pile during impact, the accuracy of the approximation decreases with increasing variation of the hammer energy (**scaling based the results of the FE model for 3700kJ**).

	Low soil damping scenario		High soil damping scenario	
	$L_{E,mean}$ [dB]	$L_{peak,mean}$ [dB]	$L_{E,mean}$ [dB]	$L_{peak,mean}$ [dB]
IQIP S-4000 @400kJ, pile top flush	170.5	191.6	169.8	190.9
IQIP S-4000 @600kJ, pile top flush	172.3	193.3	171.5	192.7
IQIP S-4000 @800kJ, pile top flush	173.5	194.6	172.8	193.9
IQIP S-4000 @1000kJ, pile top flush	174.5	195.6	173.8	194.9
IQIP S-4000 @1200kJ, pile top flush	175.3	196.3	174.6	195.7
IQIP S-4000 @1400kJ, pile top flush	176.0	197.0	175.2	196.3
IQIP S-4000 @1600kJ, pile top flush	176.5	197.6	175.8	196.9
IQIP S-4000 @1800kJ, pile top flush	177.0	198.1	176.3	197.4
IQIP S-4000 @2000kJ, pile top flush	177.5	198.6	176.8	197.9
IQIP S-4000 @2200kJ, pile top flush	177.9	199.0	177.2	198.3
IQIP S-4000 @2400kJ, pile top flush	178.3	199.4	177.6	198.7
IQIP S-4000 @2600kJ, pile top flush	178.6	199.7	177.9	199.0
IQIP S-4000 @2800kJ, pile top flush	179.0	200.0	178.2	199.3
IQIP S-4000 @3000kJ, pile top flush	179.3	200.3	178.5	199.6
IQIP S-4000 @3200kJ, pile top flush	179.5	200.6	178.8	199.9
IQIP S-4000 @3400kJ, pile top flush	179.8	200.9	179.1	200.2

IQIP S-4000 @3600kJ, pile top flush	180.1	201.1	179.3	200.4
IQIP S-4000 @3700kJ, pile top flush	**180.2**	**201.2**	**179.4**	**200.6**
IQIP S-4000 @3800kJ, pile top flush	180.3	201.4	179.6	200.7
IQIP S-4000 @4000kJ, pile top flush	180.5	201.6	179.8	200.9

Table 11: Predicted $L_{E,mean}$ and $L_{peak,mean}$ levels **for case B3-100** in a distance of **750m to the pile** (arithmetic mean in the range of 650m to 850m), 2m above the seabed for different hammer energies. **Morgan pin pile foundation**, water depth 40m, Morgan soil layering, **final penetration depth (75m)**, no secondary noise mitigation. Please note that due to the non-linearity of the interaction between hammer and pile during impact, the accuracy of the approximation decreases with increasing variation of the hammer energy (**scaling based the results of the FE model for 3700kJ**).

	Low soil damping scenario		High soil damping scenario	
	$L_{E,mean}$ [dB]	$L_{peak,mean}$ [dB]	$L_{E,mean}$ [dB]	$L_{peak,mean}$ [dB]
IQIP S-4000 @400kJ, final penetration	160.8	179.4	159.7	178.3
IQIP S-4000 @600kJ, final penetration	162.6	181.1	161.5	180.1
IQIP S-4000 @800kJ, final penetration	163.8	182.4	162.7	181.3
IQIP S-4000 @1000kJ, final pen.	164.8	183.3	163.7	182.3
IQIP S-4000 @1200kJ, final pen.	165.6	184.1	164.5	183.1
IQIP S-4000 @1400kJ, final pen.	166.2	184.8	165.1	183.8
IQIP S-4000 @1600kJ, final pen.	166.8	185.4	165.7	184.3
IQIP S-4000 @1800kJ, final pen.	167.3	185.9	166.2	184.9
IQIP S-4000 @2000kJ, final pen.	167.8	186.4	166.7	185.3
IQIP S-4000 @2200kJ, final pen.	168.2	186.8	167.1	185.7
IQIP S-4000 @2400kJ, final pen.	168.6	187.1	167.5	186.1

IQIP S-4000 @2600kJ, final pen.	168.9	187.5	167.8	186.4
IQIP S-4000 @2800kJ, final pen.	169.2	187.8	168.1	186.8
IQIP S-4000 @3000kJ, final pen.	169.5	188.1	168.4	187.1
IQIP S-4000 @3200kJ, final pen.	169.8	188.4	168.7	187.3
IQIP S-4000 @3400kJ, final pen.	170.1	188.7	169.0	187.6
IQIP S-4000 @3600kJ, final pen.	170.3	188.9	169.2	187.9
IQIP S-4000 @3700kJ, final pen.	**170.5**	**189.0**	**169.4**	**188.0**
IQIP S-4000 @3800kJ, final pen.	170.6	189.1	169.5	188.1
IQIP S-4000 @4000kJ, final pen.	170.8	189.4	169.7	188.3

Table 12: Predicted $L_{E,mean}$ and $L_{peak,mean}$ levels **for case C3-50** in a distance of **750m to the pile** (arithmetic mean in the range of 650m to 850m), 2m above the seabed for different hammer energies. **Mona monopile foundation**, water depth 43m, Mona soil layering, **mid penetration depth (30m)**, no secondary noise mitigation. Please note that due to the non-linearity of the interaction between hammer and pile during impact, the accuracy of the approximation decreases with increasing variation of the hammer energy (**scaling based the results of the FE model for 5500kJ**).

	Low soil damping scenario		High soil damping scenario	
	$L_{E,mean}$ [dB]	$L_{peak,mean}$ [dB]	$L_{E,mean}$ [dB]	$L_{peak,mean}$ [dB]
IQIP S-5500 @400kJ, mid penetration	172.5	190.1	171.8	189.0
IQIP S-5500 @600kJ, mid penetration	174.3	191.9	173.6	190.7
IQIP S-5500 @800kJ, mid penetration	175.5	193.1	174.8	192.0
IQIP S-5500 @1000kJ, mid pen.	176.5	194.1	175.8	192.9
IQIP S-5500 @1200kJ, mid pen.	177.3	194.9	176.6	193.7
IQIP S-5500 @1400kJ, mid pen.	178.0	195.6	177.3	194.4
IQIP S-5500 @1600kJ, mid pen.	178.5	196.1	177.8	195.0

IQIP S-5500 @1800kJ, mid pen.	179.1	196.7	178.3	195.5
IQIP S-5500 @2000kJ, mid pen.	179.5	197.1	178.8	195.9
IQIP S-5500 @2200kJ, mid pen.	179.9	197.5	179.2	196.4
IQIP S-5500 @2400kJ, mid pen.	180.3	197.9	179.6	196.7
IQIP S-5500 @2600kJ, mid pen.	180.7	198.3	179.9	197.1
IQIP S-5500 @2800kJ, mid pen.	181.0	198.6	180.3	197.4
IQIP S-5500 @3000kJ, mid pen.	181.3	198.9	180.6	197.7
IQIP S-5500 @3200kJ, mid pen.	181.6	199.2	180.8	198.0
IQIP S-5500 @3400kJ, mid pen.	181.8	199.4	181.1	198.3
IQIP S-5500 @3600kJ, mid pen.	182.1	199.7	181.4	198.5
IQIP S-5500 @3800kJ, mid pen.	182.3	199.9	181.6	198.7
IQIP S-5500 @4000kJ, mid pen.	182.5	200.1	181.8	199.0
IQIP S-5500 @4200kJ, mid pen.	182.7	200.3	182.0	199.2
IQIP S-5500 @4400kJ, mid pen.	182.9	200.5	182.2	199.4
IQIP S-5500 @4600kJ, mid pen.	183.1	200.7	182.4	199.6
IQIP S-5500 @4800kJ, mid pen.	183.3	200.9	182.6	199.7
IQIP S-5500 @5000kJ, mid pen.	183.5	201.1	182.8	199.9
IQIP S-5500 @5300kJ, mid pen.	183.7	201.3	183.0	200.1
IQIP S-5500 @5400kJ, mid pen.	183.8	201.4	183.1	200.3
IQIP S-5500 @5500kJ, mid pen.	**183.9**	**201.5**	**183.2**	**200.3**

Report no. 22-121-128-01-02 (Rev. 02)

Table 13: Predicted $L_{E,mean}$ and $L_{peak,mean}$ levels **for case C3-100** in a distance of **750m to the pile** (arithmetic mean in the range of 650m to 850m), 2m above the seabed for different hammer energies. **Mona monopile foundation**, water depth 43m, Mona soil layering, **final penetration depth (60m)**, no secondary noise mitigation. Please note that due to the non-linearity of the interaction between hammer and pile during impact, the accuracy of the approximation decreases with increasing variation of the hammer energy (**scaling based the results of the FE model for 5500kJ**).

	Low soil damping scenario		High soil damping scenario	
	$L_{E,mean}$ [dB]	$L_{peak,mean}$ [dB]	$L_{E,mean}$ [dB]	$L_{peak,mean}$ [dB]
IQIP S-5500 @400kJ, final penetration	171.5	191.4	170.6	190.3
IQIP S-5500 @600kJ, final penetration	173.3	193.2	172.4	192.1
IQIP S-5500 @800kJ, final penetration	174.5	194.5	173.6	193.3
IQIP S-5500 @1000kJ, final pen.	175.5	195.4	174.6	194.3
IQIP S-5500 @1200kJ, final pen.	176.3	196.2	175.4	195.1
IQIP S-5500 @1400kJ, final pen.	176.9	196.9	176.0	195.8
IQIP S-5500 @1600kJ, final pen.	177.5	197.5	176.6	196.4
IQIP S-5500 @1800kJ, final pen.	178.0	198.0	177.1	196.9
IQIP S-5500 @2000kJ, final pen.	178.5	198.4	177.6	197.3
IQIP S-5500 @2200kJ, final pen.	178.9	198.8	178.0	197.7
IQIP S-5500 @2400kJ, final pen.	179.3	199.2	178.4	198.1
IQIP S-5500 @2600kJ, final pen.	179.6	199.6	178.7	198.5
IQIP S-5500 @2800kJ, final pen.	179.9	199.9	179.1	198.8
IQIP S-5500 @3000kJ, final pen.	180.2	200.2	179.4	199.1
IQIP S-5500 @3200kJ, final pen.	180.5	200.5	179.6	199.4
IQIP S-5500 @3400kJ, final pen.	180.8	200.7	179.9	199.6

IQIP S-5500 @3600kJ, final pen.	181.0	201.0	180.1	199.9
IQIP S-5500 @3800kJ, final pen.	181.3	201.2	180.4	200.1
IQIP S-5500 @4000kJ, final pen.	181.5	201.4	180.6	200.3
IQIP S-5500 @4200kJ, final pen.	181.7	201.7	180.8	200.6
IQIP S-5500 @4400kJ, final pen.	181.9	201.9	181.0	200.8
IQIP S-5500 @4600kJ, final pen.	182.1	202.1	181.2	200.9
IQIP S-5500 @4800kJ, final pen.	182.3	202.2	181.4	201.1
IQIP S-5500 @5000kJ, final pen.	182.5	202.4	181.6	201.3
IQIP S-5500 @5300kJ, final pen.	182.6	202.6	181.7	201.5
IQIP S-5500 @5400kJ, final pen.	182.8	202.7	181.9	201.6
IQIP S-5500 @5500kJ, final pen.	**182.9**	**202.8**	**182.0**	**201.7**

Table 14: Predicted ***$L_{E,mean}$*** and ***$L_{peak,mean}$*** levels **for case D3-50** in a distance of **750m to the pile** (arithmetic mean in the range of 650m to 850m), 2m above the seabed for different hammer energies. **Mona pin pile foundation**, water depth 43m, Mona soil layering, **pile top flush with sea surface (37.47m)**, no secondary noise mitigation. Please note that due to the non-linearity of the interaction between hammer and pile during impact, the accuracy of the approximation decreases with increasing variation of the hammer energy (**scaling based the results of the FE model for 3700kJ**).

	Low soil damping scenario		High soil damping scenario	
	$L_{E,mean}$ [dB]	$L_{peak,mean}$ [dB]	$L_{E,mean}$ [dB]	$L_{peak,mean}$ [dB]
IQIP S-4000 @400kJ, pile top flush	170.4	191.5	169.1	189.7
IQIP S-4000 @600kJ, pile top flush	172.2	193.2	170.9	191.5
IQIP S-4000 @800kJ, pile top flush	173.4	194.5	172.1	192.7
IQIP S-4000 @1000kJ, pile top flush	174.4	195.5	173.1	193.7
IQIP S-4000 @1200kJ, pile top flush	175.2	196.2	173.9	194.5
IQIP S-4000 @1400kJ, pile top flush	175.8	196.9	174.5	195.1
IQIP S-4000 @1600kJ, pile top flush	176.4	197.5	175.1	195.7
IQIP S-4000 @1800kJ, pile top flush	176.9	198.0	175.6	196.2
IQIP S-4000 @2000kJ, pile top flush	177.4	198.5	176.1	196.7
IQIP S-4000 @2200kJ, pile top flush	177.8	198.9	176.5	197.1
IQIP S-4000 @2400kJ, pile top flush	178.2	199.3	176.9	197.5
IQIP S-4000 @2600kJ, pile top flush	178.5	199.6	177.2	197.8
IQIP S-4000 @2800kJ, pile top flush	178.8	199.9	177.6	198.1
IQIP S-4000 @3000kJ, pile top flush	179.1	200.2	177.9	198.4
IQIP S-4000 @3200kJ, pile top flush	179.4	200.5	178.1	198.7
IQIP S-4000 @3400kJ, pile top flush	179.7	200.8	178.4	199.0
IQIP S-4000 @3600kJ, pile top flush	179.9	201.0	178.6	199.2
IQIP S-4000 @3700kJ, pile top flush	**180.1**	**201.1**	**178.8**	**199.4**
IQIP S-4000 @3800kJ, pile top flush	180.2	201.3	178.9	199.5
IQIP S-4000 @4000kJ, pile top flush	180.4	201.5	179.1	199.7

Table 15: Predicted $L_{E,mean}$ and $L_{peak,mean}$ levels **for case D3-100** in a distance of **750m to the pile** (arithmetic mean in the range of 650m to 850m), 2m above the seabed for different hammer energies. **Mona pin pile foundation**, water depth 43m, Mona soil layering, **final penetration depth (75m)**, no secondary noise mitigation. Please note that due to the non-linearity of the interaction between hammer and pile during impact, the accuracy of the approximation decreases with increasing variation of the hammer energy (**scaling based the results of the FE model for 3700kJ**).

	Low soil damping scenario		High soil damping scenario	
	$L_{E,mean}$ [dB]	$L_{peak,mean}$ [dB]	$L_{E,mean}$ [dB]	$L_{peak,mean}$ [dB]
IQIP S-4000 @400kJ, final penetration	160.2	179.2	158.7	178.0
IQIP S-4000 @600kJ, final penetration	162.0	181.0	160.5	179.8
IQIP S-4000 @800kJ, final penetration	163.3	182.2	161.7	181.1
IQIP S-4000 @1000kJ, final pen.	164.2	183.2	162.7	182.0
IQIP S-4000 @1200kJ, final pen.	165.0	184.0	163.5	182.8
IQIP S-4000 @1400kJ, final pen.	165.7	184.7	164.2	183.5
IQIP S-4000 @1600kJ, final pen.	166.3	185.2	164.8	184.1
IQIP S-4000 @1800kJ, final pen.	166.8	185.8	165.3	184.6
IQIP S-4000 @2000kJ, final pen.	167.2	186.2	165.7	185.0
IQIP S-4000 @2200kJ, final pen.	167.6	186.6	166.1	185.4
IQIP S-4000 @2400kJ, final pen.	168.0	187.0	166.5	185.8
IQIP S-4000 @2600kJ, final pen.	168.4	187.3	166.9	186.2
IQIP S-4000 @2800kJ, final pen.	168.7	187.7	167.2	186.5
IQIP S-4000 @3000kJ, final pen.	169.0	188.0	167.5	186.8
IQIP S-4000 @3200kJ, final pen.	169.3	188.3	167.8	187.1
IQIP S-4000 @3400kJ, final pen.	169.5	188.5	168.0	187.3
IQIP S-4000 @3600kJ, final pen.	169.8	188.8	168.3	187.6
IQIP S-4000 @3700kJ, final pen.	**169.9**	**188.9**	**168.4**	**187.7**
IQIP S-4000 @3800kJ, final pen.	170.0	189.0	168.5	187.8
IQIP S-4000 @4000kJ, final pen.	170.2	189.2	168.7	188.0

Appendix C – Detailed monopile geometries

In the following, the detailed pile geometries of the monopile designs that the FE models are based on are compiled.

Table 16: Pile geometry for monopile design 1 (lower case) according to [25].

Segment length [mm]	Wall thickness [mm]	OD top [mm]	OD bottom [mm]
3030	186	11000	11000
4130	152	11000	11000
3600	138	11000	11000
3200	134	11000	11000
3150	115	11000	11000
3575	110	11000	11500
3575	104	11500	12000
3575	104	12000	12000
4200	104	12000	12000
4200	103	12000	12000
4200	106	12000	12000
4200	117	12000	12000
4200	132	12000	12000
4116	155	12000	12000
4200	136	12000	12000
4200	130	12000	12000
4200	130	12000	12000
4200	127	12000	12000
4200	120	12000	12000
4200	103	12000	12000
3400	92	12000	12000
3400	92	12000	12000
3400	92	12000	12000
3200	92	12000	12000
3200	92	12000	12000
3200	92	12000	12000
3149	100	12000	12000
3200	134	12000	12000

Table 17: Pile geometry for monopile design 2 (mid case) according to [25].

Segment length [mm]	Wall thickness [mm]	OD top [mm]	OD bottom [mm]
3030	196	12000	12000
4130	162	12000	12000
3600	148	12000	12000
3200	144	12000	12000
3150	125	12000	12000
3575	120	12000	12500
3575	114	12500	13000
3575	114	13000	13000
4200	114	13000	13000
4200	113	13000	13000

4200	116	13000	13000
4200	127	13000	13000
4200	142	13000	13000
4116	165	13000	13000
4200	146	13000	13000
4200	140	13000	13000
4200	140	13000	13000
4200	137	13000	13000
4200	129	13000	13000
4200	113	13000	13000
3400	102	13000	13000
3400	102	13000	13000
3400	102	13000	13000
3400	102	13000	13000
3400	102	13000	13000
3200	102	13000	13000
3200	102	13000	13000
3200	102	13000	13000
3200	102	13000	13000
3149	110	13000	13000
3200	144	13000	13000

Table 18: Pile geometry for monopile design 3 (upper case) according to [25].

Segment length [mm]	Wall thickness [mm]	OD top [mm]	OD bottom [mm]
3030	196	12000	12000
4130	170	12000	12000
3600	160	12000	12000
3200	157	12000	12000
3150	142	12000	12000
4200	138	12000	12587
4200	134	12587	13175
4200	134	13175	13762
4200	134	13726	14350
4200	134	14350	14937
4200	134	14937	15524
3415	144	15524	16000
3110	155	16000	16000
4116	172	16000	16000
4200	158	16000	16000
4200	154	16000	16000
4200	154	16000	16000
4200	152	16000	16000
4200	146	16000	16000
4200	133	16000	16000
3400	125	16000	16000

3400	125	16000	16000
3400	125	16000	16000
3400	125	16000	16000
3400	125	16000	16000
3200	125	16000	16000
3200	125	16000	16000
3200	125	16000	16000
3200	125	16000	16000
3149	131	16000	16000
3200	157	16000	16000

Appendix D – Revision history

The following revisions have been issued:

- Report no. 22-121-128-01-01 (Rev. 01), August 25, 2022
- Report no. 22-121-128-01-02 (Rev. 02), September 01, 2022:
    - Incorporation of different changes based on feedback from Seiche